DETECTING SIGNALS OF CLIMATIC SHIFTS AND LAND USE CHANGE FROM PRECIPITATION AND RIVER DISCHARGE VARIATIONS: THE WHANGANUI AND WAIKATO CATCHMENTS

A thesis

submitted in partial fulfilment

of the requirements for the degree

of

Master of Science in Earth Sciences

at

The University of Waikato

by

Ying Qiao

THE UNIVERSITY OF
WAIKATO
Te Whare Wānanga o Waikato

The University of Waikato

2012

Abstract

The Whanganui and Waikato river catchments have somewhat different degrees of exposure to the westerly wind systems. It is of interest to determine whether the two regions have similar times of occurrence of any concurrent shifts in river discharge and rainfall, with particular reference to mean value changes. Concurrent rainfall and runoff shifts are indicative of climatic variation but catchment land use changes (which will influence only discharge change) have also been occurring in both catchments, particularly with respect to forest planting or forest clearance. This thesis gives a summary of both climatic and land use change effects within the two catchments. If it happens that both catchments have similar climatic change-points then the data can be combined to provide a more robust framework for future water right specifications in both regions. Also, any similar responses to land use change may enable some degree of anticipation as to how future land use changes might lead to similar discharge responses.

Change-points in river and rainfall time series flows were determined by an objective approach to detect breaks of slope in cumulative mass plots. Using repeated least squares fitting of piecewise linear segments, time points of maximum difference are determined as measured by the minimum least-squares in 2-segment fitting. Randomisation of time ordering of the original data was then employed to check that changes in the cumulative plots were statistically significant. Many significant but minor shifts were detected but a number of the shifts shown evidently in the rainfall and runoff cumulative mass plots. A set of change-points due to land management impacts were identified as discharge changes in the absence of concurrent rainfall changes. Rainfall-runoff linear relationship changes associate with changes in discharge time series.

Change-points in rainfall and runoff times were detected at 44 flow gauges and 59 rainfall sites. There is some indication of a degree of natural geographic grouping with spatial correlation of times of discharge change. The times of the detected changes tend to cluster, with similar times for the same sign of change toward either greater or lower values of rainfall and discharge. The alternation of positive

and negative signs is interesting as it was found 1981 and 1998 were times of negative shifts, while 1988 and 1994/1995 were times of positive shifts. Almost over the whole Waikato and Whanganui region, the changes in rainfall and runoff appears to relate to El Nino and La Nino events, which is of practical interest for water right considerations. The driver of the shifts in rainfall pattern was found to be the changes in high rainfall events, which can change the rainfall-runoff linear relationship in some areas.

The land use component of some of the shifts was evaluated also and found only in 10 of the 44 flow gauges. The type of the land-use can be categorized into three groups: hydropower diversion, flood control system and afforestation. Within the study catchments, the impact of hydropower diversion is more significant than the other two types. With regards to the Whanganui catchments, the operation of the Tongariro power scheme from 1973 decreased low-flow by 89% in the Wahkapapa River and around 42% and 26% of the flow in the Whanganui River at Pariaka and Te Maire respectively. In the Whanganui catchments, the impact of farmland and native forest on river discharge was compared and farmland in the Ongarue catchment reduced flow much more than the native forest in the upper Whanganui catchment. The relationship of the high flow (Q90) in the two catchments is quite close to the ratio relationship of the catchment area, however, the relation of the low flows in the two catchments is fairly different and exceeds much more than the 0.75 ratio relationship of the catchment area.

Acknowledgements

Firstly, I am thankful to my supervisor, Associate Professor Earl Bardsley for his encouragement throughout my research. Thank you so much Earl for your advice and comments on my thesis.

I would also like to extend my gratitude to Genesis Energy for funding me by means of the Whanganui River Enhancement Trust Scholarship. I sincerely thank Neil Jelley for being my liaison with Genesis Energy, and for making good comments on my research direction and quick response to my e-mails. I also acknowledge Joanne from the scholarships office for your encouragement and provision of the process and rules of scholarships.

I acknowledge the Broad Memorial Fund which was very helpful and invaluable for the field work of my search. Thanks to the Department of Earth and Ocean Sciences, the University of Waikato and the New Zealand Hydrological Society, for providing some funds to attend the 2011 and 2012 New Zealand hydrology conference. The experience in the conference is valuable for me to widen my views on hydrology and meet the excellent hydrologists from New Zealand.

I also sincerely thank Dr Ganqing Xu, for his friendly teaching and helping on using the GIS software. Thanks to Bevan Jenkins from Waikato Regional Council for providing the information of the Waikato region that I need for this research.

I would also like to thank my family for understanding when I was too busy to call them, and for all your support and quiet encouragement. Thanks to Weitao, for your encouragement for my research, your concern and help for my daily life. Especially, I would like to give my special thanks to my friends, Varvara, David and Yanwei, for telling me the useful information for this research, and specially for your visit to make me feel not lonely.

Lastly, I offer my regards and blessings to all of those who supported me in any respect during the completion of the research.

Table of Contents

List of Figures

List of Tables

Chapter 1 – Introduction

1.1 Background

Climatic variation on the scale of decades appears to alternate between extended periods of similar characteristics, with brief, relatively sudden changes to slightly different climatic regimes. In addition, changes in catchment land use may also result in transitions to different downstream discharge mode in terms of both water quality and quantity. The changes arising from both climatic and land use effects are not necessarily dramatic but can have significance in terms of modifying river flow characteristics. The Whanganui and Waikato river catchments have different degrees of exposure to the westerly wind systems and it is of scientific interest to discover whether the two regions have similar or different times of shift towards different stable periods of river flow regimes driven by climatic factors. Land use changes have also been occurring in both catchments, particularly with respect to the consequences of forest planting or forest clearance. The aim of this thesis is to quantify the importance of both climatic and land use change effects and identify both common and different aspects of these two factors in the respective catchments. The study aims to analyse the available data base of main river and tributary discharge records in both catchments to identify years of change-points in river discharge behaviour, and then determine which changes are related to upstream land management changes and which to climatic shifts. If it happens that both the Whanganui and Waikato catchments contain regions with similar climatic change-points then the data of those regions can be combined to provide a more robust framework for future water right specifications in both regions. In the same way, any similar responses to land use change should enable some degree of anticipation as to how land use changes in the Whanganui catchment might impact on the catchment in the future. This thesis gives a selective overview of some results to date.

The upper Waikato catchment and the upper Whanganui catchment are located in the central of North Island. As noted by Westmacott and Burn (1997) and Labat *et al.* (2004), streamflow is an integrated response on a drainage basin area to

meteorology, geographical features, and human activity in spatial and temporal dimensions. Any change in the basin is likely to modify basin discharge in some way. To identify changes caused by climate or non-climatic factors, the relevant recordings should desirably be indicative of the whole catchments. Longer record periods give greater possibility for change detection.

1.2 Objectives of Study

The primary objective of this thesis is to locate change-points in selected river discharge time series and relate these to either change in rainfall modes or the impact of upstream land management change. Any rainfall made changes are then referenced to the climate change effects over the two regions, noting regions of similar climatic response. The goals will be achieved through:

- Develop a statistical method to detect change-points in a time series (river discharge or precipitation) and detect signals of land-use change and climatic change from river discharge and rainfall variations.
- Detect any change-points in precipitation time series within the upper Wanganui catchments and Waikato catchments. Then analyse the climate change effects on precipitation over the two regions, noting regions of similar climatic response. Finally relate the precipitation variation to the Pacific Ocean circulation patterns such as La Nina and El Nino periods.
- Determine any change-points in river discharge series within the upper Whanganui catchments and the Waikato catchments, and relate this to either change in rainfall modes or the impact of upstream land management changes. For the change-points driven by the rainfall modes, characterise and compare the nature of river and tributary flows for different stable time periods (not impacted by climatic or land management changes). Establish the relative importance of different types of land use change for those change points identified as land-use-related.
- Specifically analyse the degree of Tongoriro Power Scheme's impact on the lower reaches of the Whanganui River discharge.

1.3 Methodology

The required rainfall and discharge data sets were provided by the Waikato Regional Council, and Genesis Energy. The methodology applied for each specific research goal is described below.

1. Climatic shifts will be reflected in concurrent rainfall changes for different gauges. On the other hand, river discharge variation could reflect climate change or upstream changes in land use. Even under stable conditions, the relationship between rainfall and runoff is complicated and may be impacted by various factors including wind, temperature, water usage, and topography. However, a land use change should be reflected in a discharge change without concurrent change in rainfall. For the purpose of detecting signals of land use change and climatic change from river discharge and rainfall variation, a standard graphical approach was adopted with changes detected as breaks of slope in cumulative mass plots and double mass plots of rainfall and runoff. Constant gradients between breaks reflect a stable mean value over the period concerned, and the extent of the gradient difference before and after a break reflects the magnitude of any change (Gao et al., 2011; Searcy and Hardison, 1960). Rainfall-runoff double mass plots are of particular value as change in slope denotes a shift in the rainfall-runoff relation, as might be caused by land use change, for example. One issue which arises with such graphical interpretation is the problem of subjectivity in determining which evident breaks of slope are real and not simple minor random chance effects. To this end, permutation testing was employed to check the statistical significance of slope changes.
2. It is anticipated that climatic change effects will be of regional extent (compared to more catchment-specific land use change effects) and regions of similar climatic response will be identified as those regions will have similar change-points times. The times of climatic change-points will be compared to changes in the Pacific Ocean

circulation patterns such as La Nina and El Nino periods. This will be a preliminary evaluation only and it may or may not prove possible to discover causal linkages.

3. The set of change points due to land management impacts will be identified as discharge changes in the absence of concurrent rainfall changes. For the stable time periods, flow duration curves and average monthly mean discharge curves will be constructed for each time period to quantify the difference between different periods of stability. The times of land use related change points in discharge will be related back to the nature and magnitude of the land use change type upstream of the sites concerned.

1.4 Thesis Outline

This thesis is organised by chapters.

Chapter 2 characterizes the study area and geology, climate, land use characteristics.

Chapter 3 reviews relevant literature associated with the detection of climate and land use change as well as the modern methodologies for change-point detection in time series.

Chapter 4 describes the available data regarding precipitation and streamflow in both Waikato and Wanganui regions.

Chapter 5 involves the change of data time scale, such as from daily to monthly, a preliminary analysis with respect to the rainfall spatial correlation analysis as well as serial correlation analysis and the chosen rainfall runoff gauge pairs.

Chapter 6 develops a piecewise linear regression technique to detect change points in a time series. Methods of detecting signals of climatic shifts and land use changes from discharge and precipitation time series is briefly described.

Chapter 7 presents the result of the change-point detection analysis from precipitation and river discharge time series and identifies the regions with similar times of change. A comparison between the El Nino and La Nino years and the times of change in precipitation is also made. The impact of climate variability on precipitation is then estimated.

Chapter 8 presents the results of change-point detection from river discharge series and the results of estimation of signals of land use changes in river discharge.

Chapter 9 carries out a specific study within the upper Wanganui River catchments with respect to the comparison of the impact of forest and agriculture on river discharge.

Chapter 10 presents conclusions and recommendations.

Chapter 2 –Study Region

2.1. Introduction

This chapter presents a brief overview of the geomorphology, climate, hydrology and land use situation in the Waikato and Whanganui catchments. The information of land use change within the study region is described.

2.2. Geomorphology

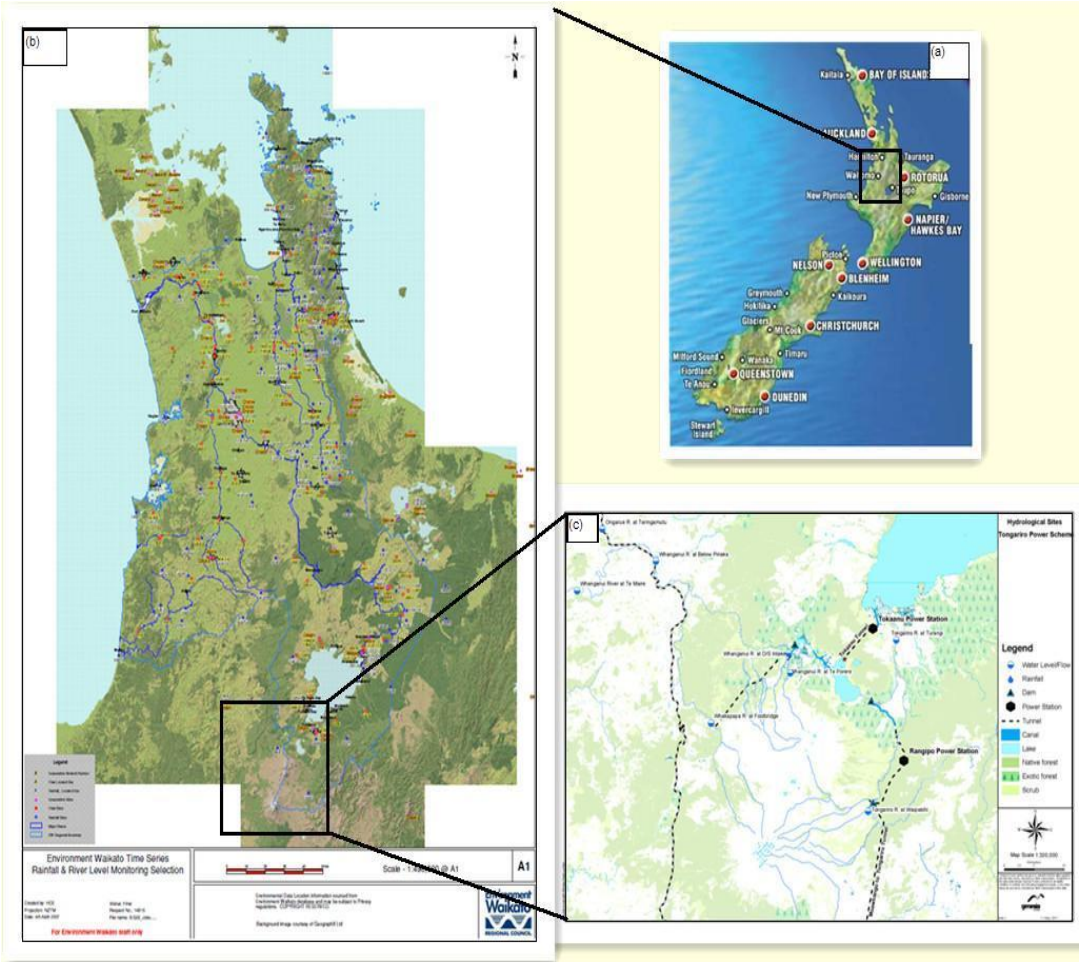

Figure 2.1: Location of the study region within New Zealand (a), Waikato catchments (b) and part of the Whanganui catchments (c). (b) and (c) show a detailed view of the location of the streamflow and precipitation gauges in Waikato Region and part of Whanganui catchments (Source: Waikato Regional Council and Genesis Energy)

The study areas include the Waikato region and part of the Whanganui region. The Waikato region is ranked as the fourth largest region in New Zealand and is

located in the North Island (Figure 2.1). It covers an area of 25,000 km² and has a population of 409,300 (June 2010 estimate). It is bounded by Auckland on the north, Bay of Plenty on the east, Hawke's Bay on the south-east, Manawatu-Wanganui and Taranaki in the south. The region includes coastal areas, flat floodplains, rolling hills, mountain ranges and steep volcanoes. According to the Waikato Regional Council, the Waikato Region is characterised by four different landscapes: Taupo Volcanic Zone, Waikato Lowlands and Hauraki Plains, Western and Central Hill Country, and Eastern Ranges**.**

The Whanganui catchments in this study are located in the upper Whanganui river catchment which belongs to the Manawatu-Wanganui region. It is to the south-west of Lake Taupo and covers some of the various catchments affected by the Tongariro Power scheme.

2.3 Climate

2.3.1 Waikato region

The Waikato region is exposed to the west and south-west wind system from the Tasman Sea. It is characterized by humid summer and mild winter conditions. Because no location is more than 80 km from the ocean, the temperatures are quite regulated. The maximum temperatures in winter are 12-15^{o}C. However, in summer with maximum temperatures of 25-28^{o}C, there is a potential for drought occurring one year in ten. Winter storms with strong winds and heavy rain are quite common in this area. The special geographic position and character result in rapidly changing weather. Average annual rainfall in Waikato region is 1250 mm. Figure 2.2 shows the distribution of annual average precipitation and wind speed and direction within the Waikato region. The three typical areas of high rainfall (shown as darker blue) are the Coromandel Peninsula area, Waitomo/Kawhia area and the alpine area. In the sheltered and elevated inland areas, extremes of hot and cold are common. The areas marked in pale blue in Figure 2.2 are typical sheltered areas with low rainfall. They are Taupo, Reporoa Valley, Hauraki Plains and the lower Waikato lowlands. These lower areas experience many frosts and fog events under anti-cyclonic conditions.

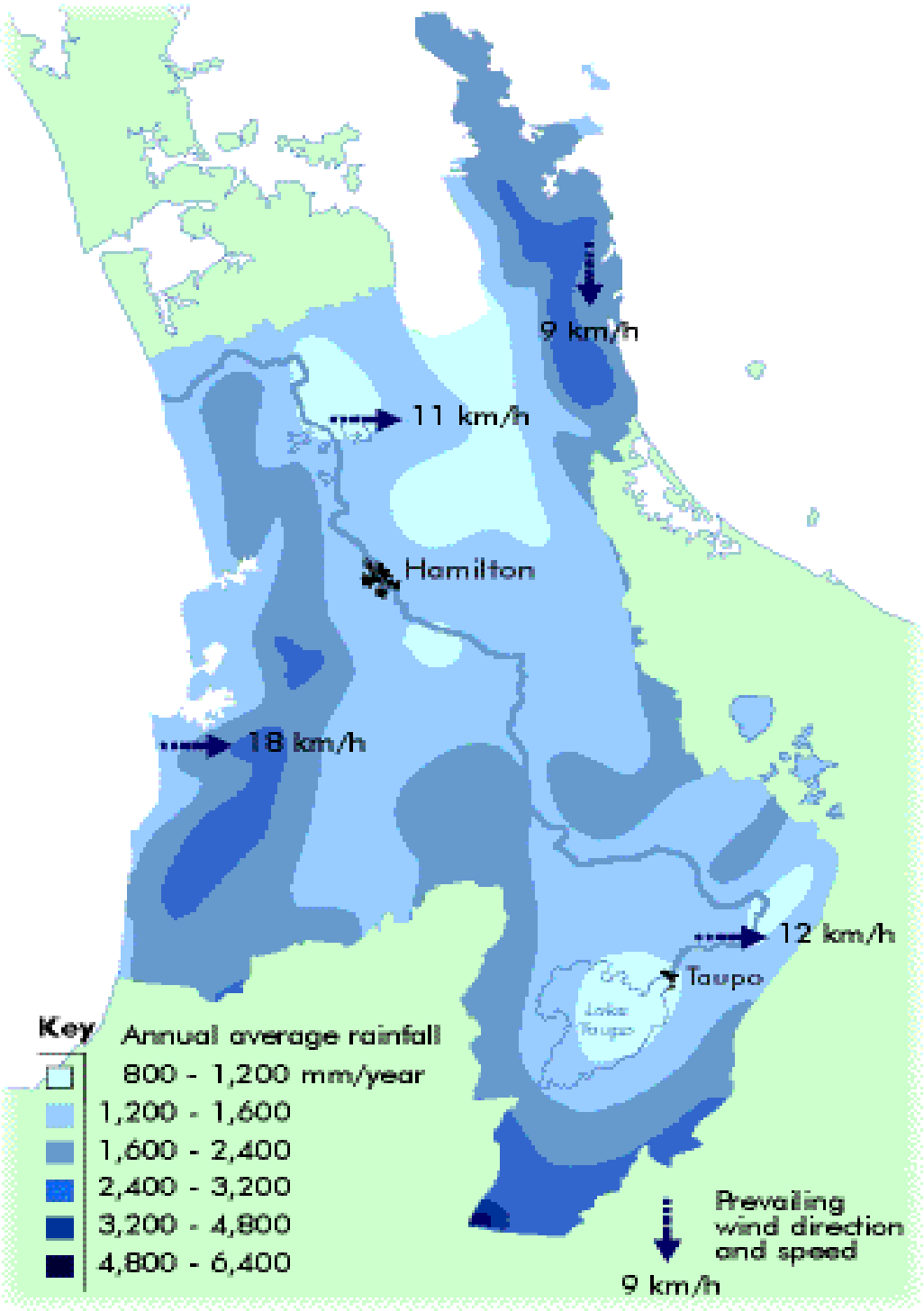

Figure 2.2: Distribution of annual average precipitation and wind speed and direction within the Waikato region. (Source: Waikato Regional Council)

2.3.2 Whanganui region

The Manawatu-Whanganui region is windy because of its exposure to distributed weather systems from the Tasman Sea. However, the region has relatively few climate extremes with warm summers and mild winters. Frost occurs inland during clear calm conditions in winter. Annual sunshine hours average about 2000 hours. Typical summer daytime maximum air temperatures range from 19°C to 24°C, seldom exceeding 30°C and winter daytime maximum air temperatures range from10°C to 14°C. Table 2.1 shows the climate data for the Whanganui Region. Annual rainfall in Whanganui region is 882 mm with high rainfall in winter and low rainfall in summer.

Table 2-1: Monthly and annual mean high and low temperature, and rainfall in the Whanganui region. (Source: NIWA Climate Data)

Month	Jan	Feb	Mar	Apr	Ma	Jun	Jul	Aug	Sep	Oct	Nov	Dec	Year
Average high °C (°F)	22.4	22.7	21.3	18.8	16	14	13	13.8	15.3	17	18.8	20.7	17.8
	-72.3	-73	-70	-66	-61	-57	-56	-56.8	-60	-63	-66	-69	-64
Average low °C (°F)	14	14	12.9	10.6	8.5	6.5	5.6	6.2	8	9.6	10.9	12.8	10
	-57	-57	-55	-51	-47	-44	-42	-43.2	-46	-49	-52	-55	-50
Precipitation mm (inches)	62	65	68	71	81	82	88	70	72	81	74	70	882
	-2.44	-2.6	-2.7	-2.8	-3	-3.2	-3.5	-2.76	-2.8	-3.2	-2.9	-2.8	-35

2.4 Hydrology

2.4.1 Waikato region

The Waikato region has more than 100 lakes, 20 large rivers and 1,420 small river systems and around 1,150 km of coastline. The region includes the Waikato, Waihou, Piako, Awakino and Mokau river catchments. Due to the large river systems, large areas of lack of vegetation cover, high rainfall and low lying flood plains, flooding is frequent. The areas at risk include Coromandel, characterized by its short steep catchments, Hauraki Plains along the Waihou and Piako River system, farmland adjacent to the Waipa River, lower Waikato River and the

southern end of Lake Taupo (shown in Figure 2.3). The groundwater resource is abundant, making up about 90 percentage of the region's freshwater resource.

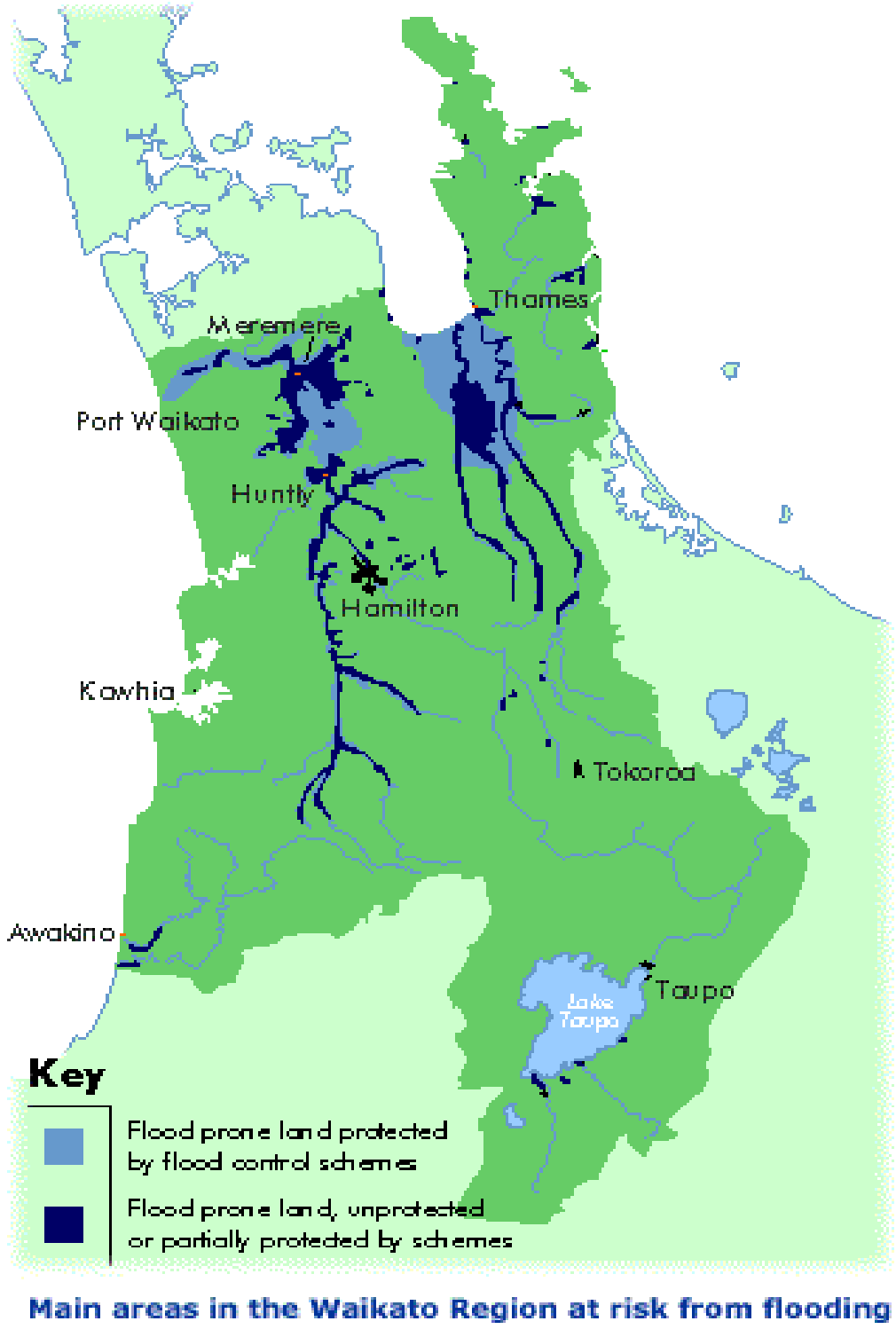

Figure 2.3: Main areas in the Waikato region at risk from flooding. (Source: Waikato Regional Council)

2.4.2 Whanganui catchment

The rivers located in the Whanganui catchment and included in this study are the Tongariro River, the Whanganui River, the Whakapapa River which is a tributary of Whanganui River, and the Ongarue River.

The Tongariro River originates from numerous tributaries that flow off the surrounding hill ranges and mountains, such as Mount Ruapehu, and then flow north to Turangi, before reaching Lake Taupo. The minimum flow of the Tongariro River ranges from approximately 16 m^3s^{-1} to 21 m^3s^{-1}.

The Ongarue River and the Whakapapa River are two tributaries of the Whanganui River. The former starts from the Hauhungaroa Range northwest of Lake Taupo and flows west then south, passing through the town of Taumarunui before reaching the Whanganui River. The source of the Whakapapa River is the Mount Ruapehu. Before merging with the Whanganui River, it flows in the western slopes of the mountain through Owhango.

The Whanganui River draining most of the inland region west of Lake Taupo is the longest navigable river in New Zealand and the second longest river in the North Island. It also holds cultural and spiritual values for Maori.

2.5 Land Use

2.5.1 Land cover in the Waikato region

In the Waikato region, urban area accounts for only 1 % of the region. The major productive land uses are pastoral farming and plantation forestry, making up 58 % and 12 % of the region respectively. Indigenous vegetation (including forests, wetlands and grasslands) covers 28 %. Figure 2.4 shows the main land cover in the whole Waikato region. About 56 % of the area is pastoral farming. On the Coromandel peninsula, the western fringes and the south east of the region marked with deeper green in Figure 2.4, there are large areas of planted forest and indigenous vegetation (Collins, 2002). The broad floodplain of the Waikato River,

which lies to the east of the coastal hills, is largely pastoral farmland. The middle and upper reaches of the Waikato River are used for hydroelectricity generation.

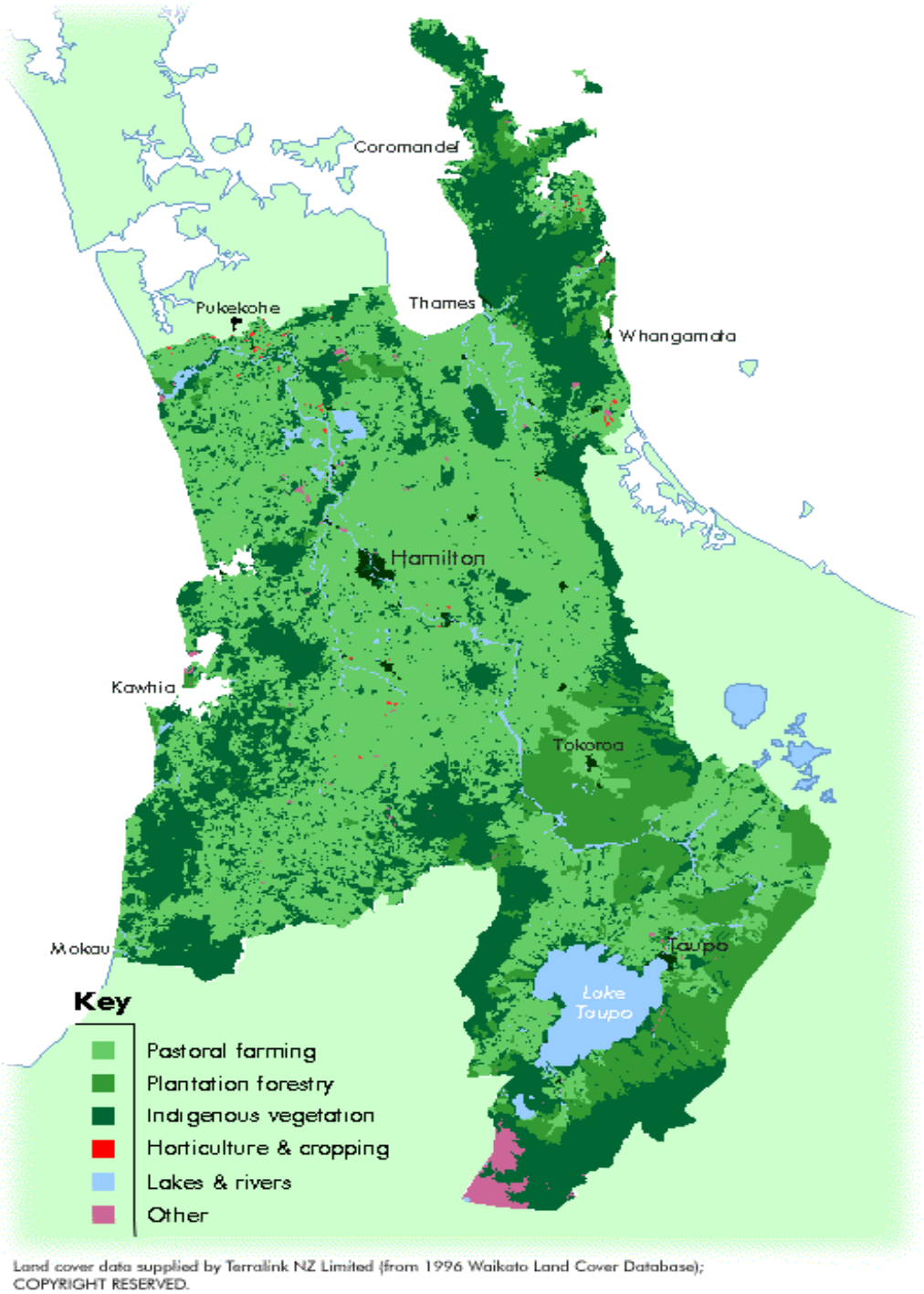

Figure 2.4: Main land cover in the whole Waikato region. (Source: Waikato Regional Council)

2.5.2 Land cover in the Whanganui region

The Whanganui region was covered by forest around 1250-1300 AD when no humans had settled in NZ. After the Maori had settled, forests had been cleared by fire. Before the Europeans arrived, most of the region was bush-covered. In the nineteenth century, deforestation, burn-offs of timber and scrub and large scale drainage combined with overgrazing resulted in environmental degradation. In the middle reaches of the Ongarue River which arises in the Pureora Forest, farmland has been established for decades. The upper reaches of the Whanganui River go through the beautiful native forest.

2.5.3 Power stations in Waikato region and part of Whanganui catchments

In the Waikato region, nine power stations have been developed along the Waikato River to meet demand for electricity. In the Whanganui catchments, the influence of the two hydro-power schemes on streamflow is also considered in this study. This section reviews the power stations within the study area.

2.5.3.1 Power stations on the Waikato River

Nine power stations have been built along the Waikato River from the Taupo Gates where water from out of Taupo lake flows to the Waikato hydropower system. The location of each station is shown in Figure 2.5.

Aratiatia power station, built in 1964, is located 14 kilometres downstream of Lake Taupo. The downstream power station, Ohakuri opened in 1961, is located five kilometres upstream of the Atiamuri Dam which channels water from Lake Ohakuri to the Waikato River.

Atiamuri power station, which takes water from the Ohakuri upstream station, is located near Lake Atiamuri. It was built in 1958, and it is operated by Mighty River Power. The Whakamaru power station is located in Lake Whakamaru, and opened in 1949.

The Maraetai power station near Mangakino was opened in 1953. This power station has two powerhouses; Maraetai I, Maraetai II. The water of Maraetai I is directed from the front of the Maraetai Dam (Lake Maraetai) and the water of

Maraetai II is from the downstream of Maraetai I, and then flows back into the Waikato River.

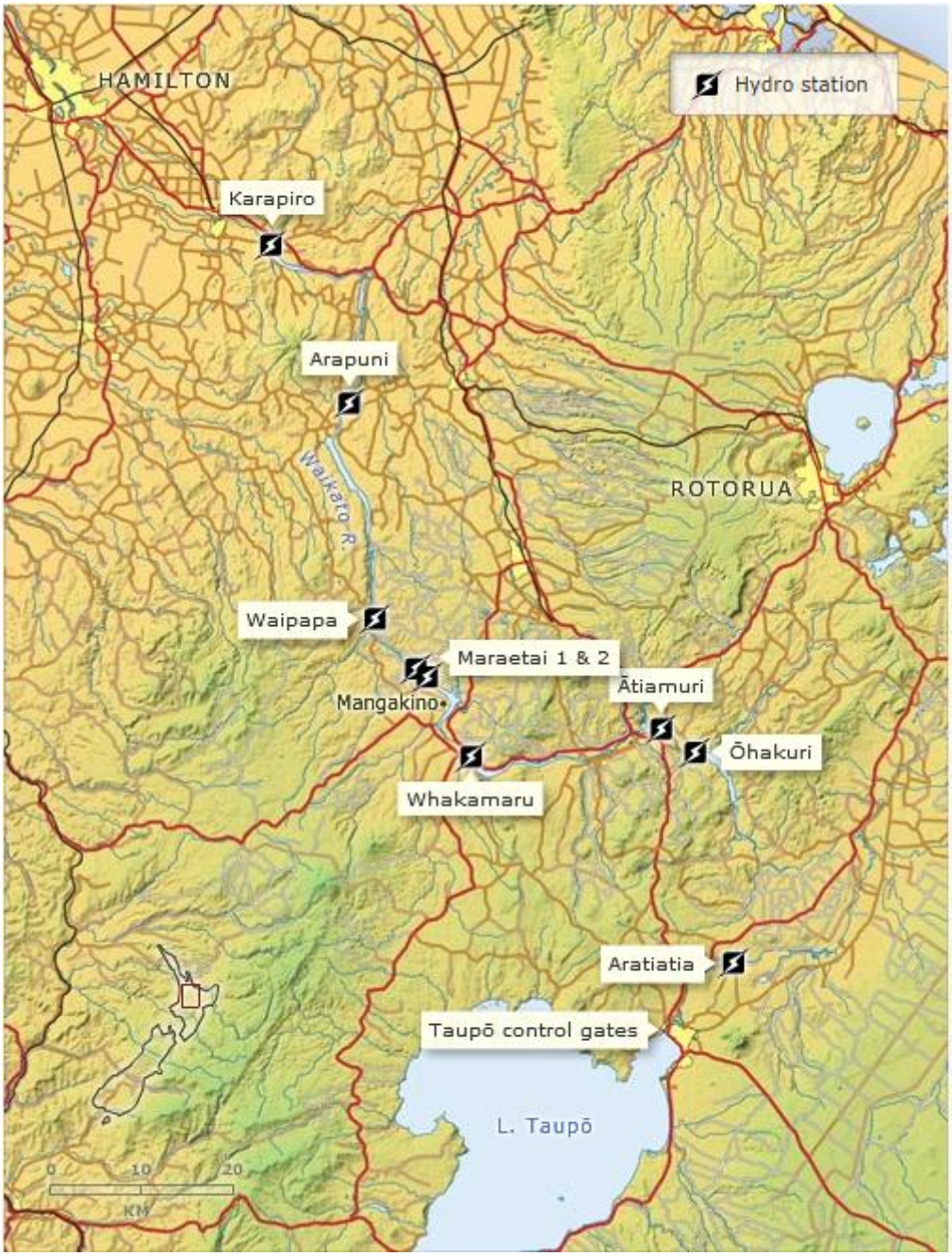

Figure 2.5: Waikato River hydropower system. (Source: http://www.teara.govt.nz/en/waikato-region/10/4)

Waipapa power station is the smallest power station on the Waikato River. The function of this power station is to supplement other upstream and downstream stations during periods of heavy demand.

Arapuni power station, located on Lake Arapuni, is the first government built hydro-electric station on the Waikato River and was completed in 1929.
Karapiro power station is located 188 kilometres downstream of Lake Taupo in the Waikato River, and was opened in 1948. The water of Karapiro power station from Lake Karapiro runs through the penstocks, then the water flows back into the Waikato River nearly 30 kilometres upstream from Hamilton City.

2.5.3.2 Power stations in the Whanganui catchments

In the study area of the Whanganui catchments, the Tongariro Power Scheme shown in (Figure 2.6) run by Genesis Energy is operated via the Rangipo and Tokaanu power stations. The scheme taps a catchment area of more than 2600 sq. km. The Tongariro Power Scheme partly takes water from the Whanganui headwaters and discharges the water into Lake Taupo. The Tokaanu Power Station is located at the base of Mount Tihia, near the township of Turangi. It was opened in 1973. The Rangipo power station is located on the Eastern Division of the scheme, on the upper Tongariro River of central North Island. It was opened in 1983. The Tongariro power scheme system includes the Eastern Division which diverts the Whangaehu River to Rangipo Dam, the Tongariro Division which draws water from Rangipo Dam to Lake Rotoaira, the Western Division which channels water from Whakapapa River to Lake Rotoaira and the Rotoaira Division which channels the water in Lake Rotoaira to Lake Taupo.

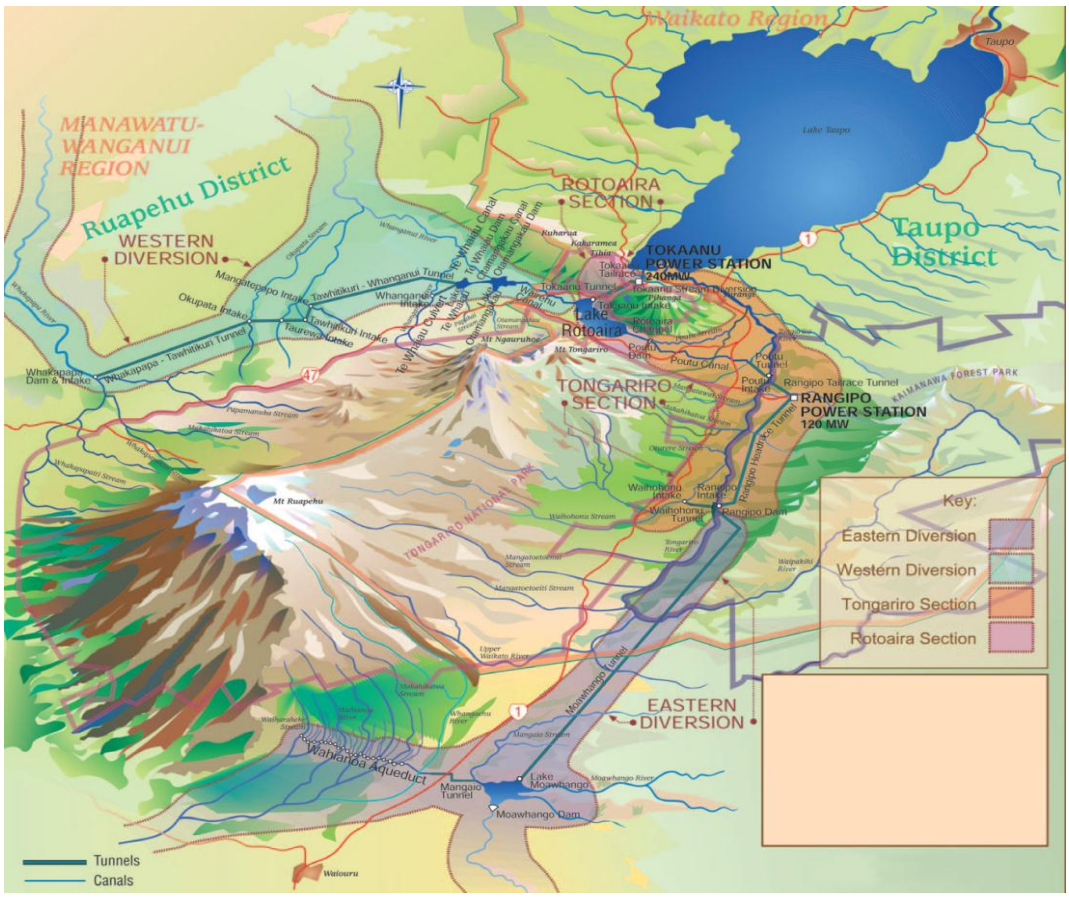

Figure 2.6: Overview of the Tongariro Power Scheme. (Source: Genesis Energy)

Chapter 3 - Literature Review

3.1 Introduction

This chapter firstly gives an overview of the climate variation and characteristics in New Zealand. Beyond that, the impact of climate variation as well as land use change on hydrology is reviewed. The findings of previous studies related to the detection of climate variation and land use change from precipitation and river discharge series is described. Following that, the theoretical definition of change points as well as techniques for change points detection are reviewed.

3.2 Literature Review of Climate Characteristics in New Zealand

New Zealand is located in the mid-latitude zone (Mullan et al., 2001) and the climate variation is complex and mainly driven by the El Nino-Southern Oscillation (ENSO) phenomenon and the Inter-decadal Pacific Oscillation (IPO). New Zealand has various climate regions (Figure 3.1) separated by the mountain chains which hinder the prevailing westerly winds from southwest (NIWA, 2001). Overall, the western areas are much wetter than the eastern area in the North Island and eastern and inland areas in the south island (Mullan et al., 2001). This section will briefly describe the rainfall, temperature variation with respect to different spatial areas of New Zealand as well as the observed climate changes in New Zealand.

3.2.1 Rainfall and temperature

Overall, over most areas of New Zealand, annual rainfall ranges from 600 to 1500 mm. Over the northern and central area of New Zealand, the wet season is winter, while in the south of New Zealand, winter has the least rainfall. The driest areas in the North Island include the Hawke's Bay, the Wairarapa and the coastal Manawatu, in the South Island include the central and southern Otago and south Canterbury (Mullan et al., 2001). In the climate zone of central North Island, due to the south and east high country's shelter, there is less wind. Therefore, summer is warm and dry with temperatures ranging from 21°C to 26°C and winter is cool with daytime maximum temperatures ranging from 10°C to 14°C. Over the whole

of New Zealand, mean annual temperature varies from 10°C in the far south to 16°C in the far north (NIWA, 2001). Although, extreme temperatures may occur in the central North Island and central Otago areas, it is less common in the whole New Zealand compared to the continental areas (Mullan et al., 2001).

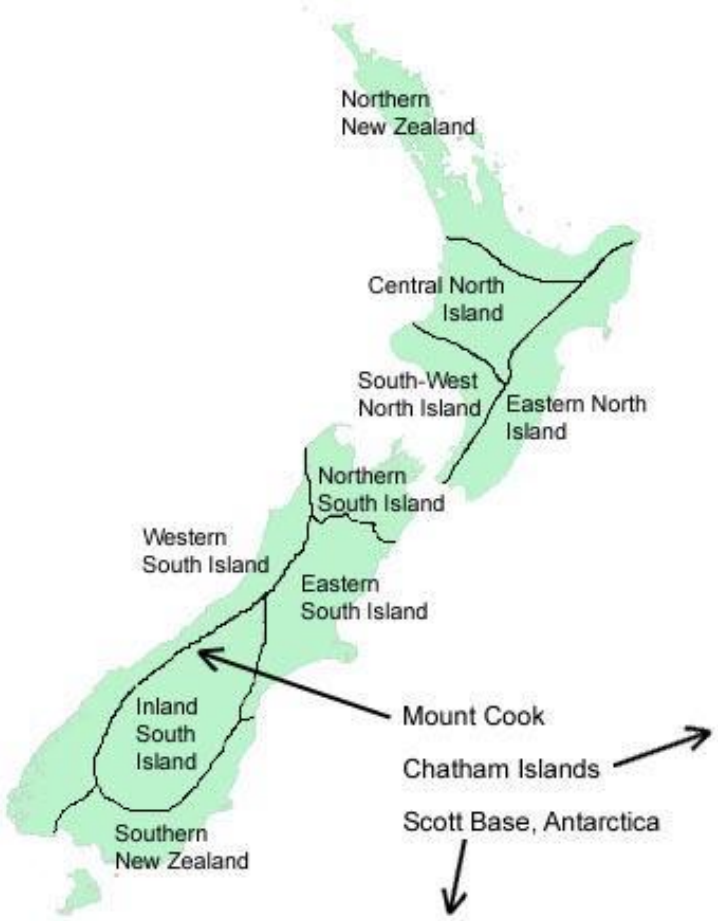

Figure 3.1: NZ climate zones (Source: http://www.niwa.co.nz/node/98757)

3.2.2 Observed climate variations

Climate change can lead to higher or lower temperatures, flooding and impact on water resources, human health, biodiversity, build environment and even transport. Generally, the global climate changed has negatively impacted on the whole earth and some specific regions. The climate change can be largely responsible for changes such as extreme events like flood or drought rather than changes in the

long term mean (Ministry for the Environment, 2008). Focusing on New Zealand, agriculture is the largest sector of the tradable economy, and agriculture will be directly influenced by climate change, rainfall, air fall, temperature change as well as more extreme weather events. Moreover, the change of rainfall patterns will directly influence local agriculture, such as higher rainfall in the west of country and decrease in many eastern regions. It is important to note that climate change may have a significant impact on the South Island, because most of the electricity supply is based on hydro-electricity in the South Island. A number of studies had been noting that in the mid-1970s the climate showed an obvious shift over the Pacific (Gong and Ho, 2002). According to Levi (2008), there are some other studies relating to the time series of climate-related variables discovered a sudden change in around the mid-1980s. However, the shifts in climate regime may vary slightly due to the climate system of different climate-related variables. Moreover, the length of record applied for the study may also impact the results (Gong and Ho, 2002).

3.2.2.1 El Nino and La Nina

McFadgen (2001) points out that EI Nino can impact on New Zealand's climate by producing more rain in the west and drought in the east, as well as leading to the more southerly and colder winter weather. Take the identified climate shift 1977 for an example. The EI Nino event which happened in 1977 lead to climate being 10 percent wetter in the west and south of South Island and 10 percent drier in the north and east of the North Island (NIWA, 2005). When an EI Nino occurs in New Zealand, in most of northern and eastern regions, the weather will be wetter, and in southern and western areas the weather will be drier (Lorrey et al., 2007). Also, during an El Nino period, there will be more winds from the south in winter, bringing colder conditions to both the island and the surrounding ocean and then reducing the temperature in both islands. The precipitation will be increased during EI Nino. Ummenhofer et al. (2009) point out that the whole New Zealand climate had become drier over the period from 1979 to 2006 due to the EI Nino effects.

La Nina events also play an important role in impacting New Zealand's climate variability. During La Nina periods, rainfall will be increased in the north-east part of the North Island and reduced in the south and south-west of the South Island.

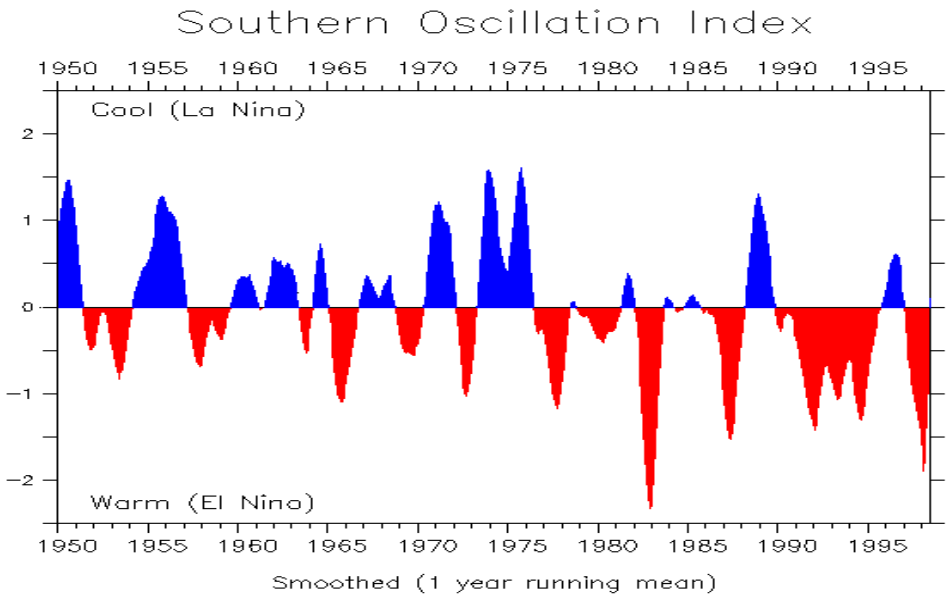

Figure 3.2: El Niño and La Nina years (Source: http://faculty.washington.edu/kessler/index.html)

Figure 3.2 indicates the El Nino has occurred more frequently than La Nina from 1980. The extreme strong El Nino events in the recent three decades happened in around 1982, and in 1997-1998. In 1986-1987, 1991-1992, El Nino was less strong. The comparatively stronger La Nina events over the recent three decades happened in 1988-1989, and in around 1995.

3.2.2.2 Temperature

Studies show that global mean surface temperatures have improved by 0.6°C and temperature of New Zealand increased 0.8°C between the decades 1941-1950 and 1981-1990 for the North Island, and 0.7 °C for the South Island (Mullan et al., 2001). In New Zealand, the 1980s and the individual 1998 and 1999 were warmer periods than the previous decades (Mullan et al., 2001).

3.2.2.3 Rainfall

Mullanet al. (2001) quantified the heavy rainfall intensity at 22 locations over New Zealand for the period 1950-1996 and found in the west and south of the South Island and in the west of the North Island, the 95 % daily rainfall amount has increased from 5 to 15 % respectively.

Over the period 1950 to 1994, 1975 has an obvious shift in rainfall pattern (NIWA, 2005). In the period 1951 to 1975, rainfall increased in the north of the North Island, especially in autumn and decreased in the south east of the South Island particularly in the summer season. The reason for the change is that there was an increase in the east and north east airflow over New Zealand (NIWA, 2005), while, after 1975, there were several strong El Nino events leading to annual rainfall being reduced in the north of the North Island and increased in the South Island excluding the east (NIWA, 2005).

3.3. Impacts of Climatic Variation and Land Use Change

Briefly, climate change is a result of both the natural change and the anthropogenic change (Feng et al., 2010). With the aggravation of pollution, the increase in population and other factors, climate change leading to changes in hydrological systems globally is inevitable and verifiable. According to NASA (2011), the potential future effects of global climate change include more frequent wildfires, longer periods of drought in some regions and an increase in the number, duration and intensity of tropical storms. The effect of climate variation on hydrological system includes the amount and distribution of precipitation, the amount of river catchment discharge; by extension, climate change can alter the frequency and intensity of flood and drought, and the quantity and quality of freshwater resources (Xu et al., 2010).

Land use change will impact hydrology processes such as surface runoff, baseflow, infiltration and groundwater recharge (Lin et al., 2007). Urbanization has a large effect on flood flows by increasing storm runoff and decreasing storage times. The alternation of vegetation type can alter mean annual flow as

well as the variability of annual flow (Brown et al., 2005). For instance, afforestation will reduce annual runoff of the area, but, deforestation can increase the local annual runoff; the landscape with established trees has lower water yield compared with those with short vegetation (Chescheir et al., 2009), the replacement of forests by shallow rooted vegetation is expected to increase runoff. Within a catchment, the higher percentage change in land cover leads to greater change in water yield. Figure 3.3 shows the changes in water yield as a result of change in land cover (Brown et al., 2005). Different types of vegetation and percentage change in forest cover both influence the amount of change in water yield. For example, compared to scrub, deforestation of eucalyptus leads to larger difference in water yield and high percentage change in land cover also leads to larger difference in water yield.

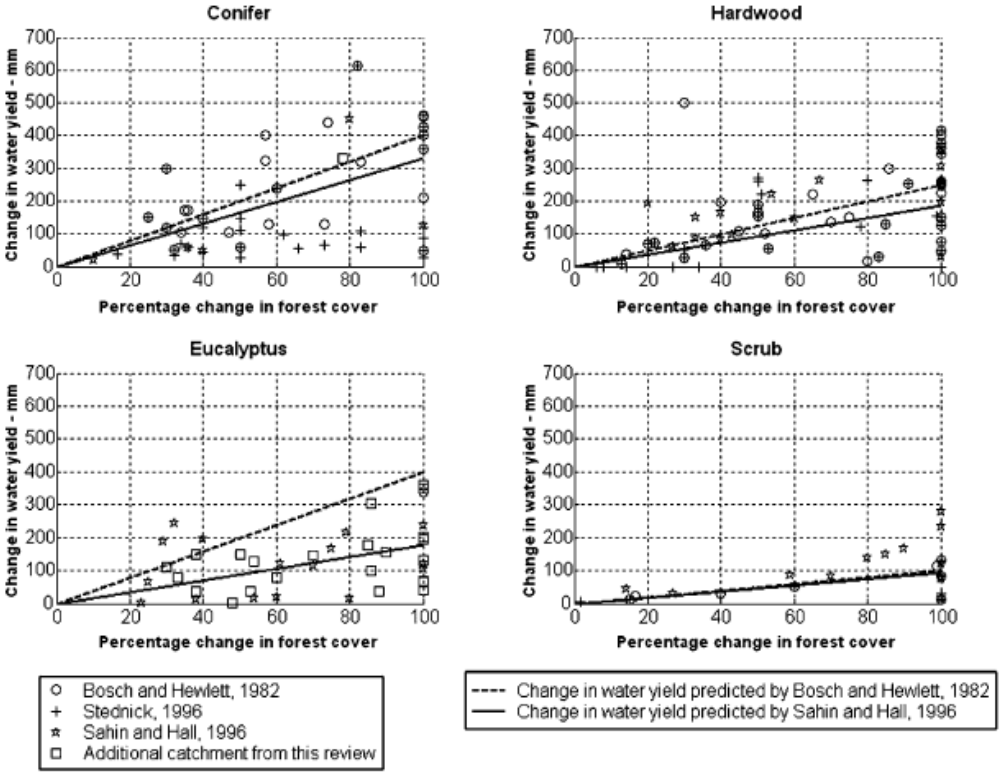

Figure 3.3: Water yield changes as a result of changes in vegetation cover from Bosch and Hewlett (1982), Sahin and Hall (1996) and Stednick (1996). Results from Bosch and Hewlett and Stednick represent the maximum increase in the first five years after treatment for deforestation, regrowth and forest conversion experiments or maximum change in water yield for afforestation experiments. The results from Salin and Hall are the average increases in water yield in the first five years after treatment. (Source: Brown et al., 2005.)

There exist many studies on the impact of vegetation shift on water yield. Chescheir et al. (2009) quantified the impact of afforestation from pasture to pine on hydrology through a paired catchments study. They concluded afforestation increases both evapotranspiration (ET) and infiltration, leading to a 28 % reduction of total water yield in the first year after the pre-treatment period and reduction on storm flow and peakflow rate respectively. Pereira et al. (2009) applied a linear regression analysis to identify the relationship between land use conversion from forest to pasture and silviculture in water yield during dry season. The authors' conclusion indicates that during the dry seasons at Atibainha watershed, Brazil, there exists a water yield decrease which is considered as resulting from the main factors of deforestation rates and land use conversion to silviculture and pasture.

The major reason for the difference resulting from vegetation alternation is the plants evapotranspiration. Generally, trees have larger leaf area making more interception and higher aerodynamic roughness above canopy (Davie and Fahey, 2005). However, when studying the relationship between ET and rainfall of various types of vegetation, other factors that influence the catchment water yield such as soil water capacity resulting from seasonal interactions, and infiltration should be considered as well.

The impact of vegetation change on water yield is greatest in high rainfall areas or during wet periods, however, in dry area/periods, the impact is comparatively small. The changes in the hydrological process because of land use changes also have significant seasonal implications (Brown et al., 2005). Although the understanding of impact of vegetation change on mean annual water yield is well advanced, the impact of land use variation on daily, monthly and seasonal water yield is not well understood (Brown et al., 2005). Compared with the response time of streamflow following deforestation, it takes longer time for the trees to reach equilibrium water use following afforestation (Brown et al., 2005). Also, according to Brown et al., deforestation can increase flood volume and flood peaks, reforestation increase low flows, but this effect is variable with respect to some special years or seasons.

The impact of land use change on streamflow is relatively small compared with that of climate variability which can also veil the land use effect on streamflow (Kim et al., 2009). In practice, it is difficult to gather the data or information on land use, therefore the land use impact cannot be accurately detected. Moreover, the high quality streamflow or other variables data without errors for study is required for land use effect analysis, because the errors may hide the impact of land use change (Kim et al., 2009). For better planning and managing water resource, it is crucial to separate the impact of land use change on hydrology processes from the impact of climate change.

3.4 Detection of Climate Variation and Land Use Change

In previous studies, the emphasis regarding detecting climate change has been on the analysis of temperature variability, atmospheric circulation pattern, precipitation and streamflow. Kiely (1999) detected climate changes in Ireland from precipitation, streamflow and North Atlantic Oscillation (NAO) index and found that Ireland experienced the same upward change after 1975 of all the three time series.

The impact of land use often leads to the alternation of landscape pattern (Lin et al., 2007). Recently, landscape metrics, which is an appropriate tool for land use planning and designing, have been applied to quantify landscape patterns (Lin et al., 2007). According to Lin et al. (2007) the models used for land use change effect detection can be classified into stochastic models, optimization models, dynamic process-based simulation models and empirical models. Until now, various approaches have been developed to simulate the pattern and impact of land use change (Lin et al., 2007). Paired catchments approaches that compare two catchments under conditions of the same climatic conditions but different land use are widely used for their merit of reducing the impact of climate change in hydrology. Kim et al. (2009) incorporate a combined method to isolate the land use change effect on streamflow from climate variability effect. They applied data analysis techniques to detect the temporal and spatial variation in streamflow and a lumped conceptual rainfall-runoff model to evaluate the predictive error and consistency of catchment response. Flow duration curves (FDCs) are widely used

to describe and analyse the impacts of vegetation variation on flow regime (Brown et al., 2005).

Generally speaking, river discharge is the integrated result of climatic factors such as precipitation and evaporation, the local area water resource, water usage and catchment characteristics. River discharge to ocean can also influence the oceanic circulation patterns. Moreover, uncertainties still exist not only in climate projections but also in the simulation of hydrological responses to climate perturbations (Xu et al., 2010). Therefore, detecting climatic shifts and land use change from river discharge data variation is a complex study (Kundzwicz and Robson, 2004). The site selection and data/information collection should be carefully considered. A paired catchment approach, time series analysis and hydrological modelling are three main groups of methods developed to detect climate and land use change effect on hydrology (Li et al., 2009).

Changnon and Demissie (1996) detect the changes in streamflow and floods resulting from climate fluctuations and land use drainage changes by using paired rural catchments and paired urbanized catchments. Li et al. (2009) applied a physically-based distributed hydrological model SWAT (soil and water assessment tools) to study the impact of climate and land use change effect on hydrology. Cuo et al. (2009) used a spatially distributed hydrological model to assess land cover change and temperature variability impact on the hydrology of the Puget Sound basin, in North America.

To study changes in hydrological time series, exploratory data analysis (EDA) involves using graphs to explore, understand and present data is a key component of the analysis (Kundzwicz and Robson, 2004). It can highlight the important features of the data and is helpful for the statistical tests which can confirm the change is significant by telling the independence or statistical distribution of data. The commonly applied graphs include histograms and normal probability plots, time series plots, autocorrelation plots, scatter plots and smoothing curves (Kundzwicz and Robson, 2004).

The main steps of a statistical analysis of change involve deciding the type of the

series/variable to test; deciding the types of change which are of interest (step-change or gradual change); checking the data assumption; selecting a statistical test; evaluating significance levels; and investigating and interpreting results (Kundzwicz and Robson (2004).

Each method has its disadvantages. For instance, the paired catchments approach can only applied to the small catchments, the time series analysis lacks physical mechanism as it can only analyse the hydrological signals of environmental change (Liu et al., 2010).

3.5 Theoretical Background of Change Point Detection

3.5.1 Time series with change points

Time series is a data set collected in time order. A change point in a time series is defined as a point along a distribution of values where the characteristics of the values before and after the point are statistically different. For instance, there is a time series $\{y_1, y_2, \ldots y_n\}$,it is assumed a change point happens in position k ($1 \leq k \leq n$), then the change point will separate the whole time series into two segments which are significantly various in some statistical characteristics. Of course, in reality, within a time series, there exists more than one change point (multiple change points).

Therefore, the task for change point detection is testing the most probable temporal position of the points (one or more) and then the statistics of the variation of the change points. Change point problems exist widely in various fields including econometrics, finance, biology, agronomy and hydrology. A number of approaches for change point detection have been developed. In hydrological processes, the change in a river flow series can be caused by numerous factors: e.g. climate variability and change, human activities such as land use in the catchment, vegetation growth, large scale water resource development projects, river regulations, and change in water withdrawal. Under such influences, the hydrological time series can change gradually (a trend), abruptly (a step-change) or in a more complex form (Kundzwicz and Robson,

2004). Therefore, detecting whether there are any changes in the time series or not, then analysing the origin of the change are essential for both water resources development and utilization and land use management.

3.5.2 Type of the series/variable

The types of hydrological or climate time series such as streamflow time series, precipitation time series, temperature time series applied for change point detection are various and depend on the study interest. Generally, the time scales of streamflow or precipitation time series include daily, monthly, annual, seasonal, or monthly average, the de-seasonalised time series, annual maxima, annual minima.

Jiang et al. (2011) transfer the daily precipitation, potential evapotranspiration (PET) and runoff into annual to quantify the effects of climate variability and human activities on runoff from Laohahe basin in northern China by using Mann-Kendall trend test, Pettitt test and Double Cumulative Curves methods. They also applied the average monthly variables between the natural period and the human-induced period to analyse the intra-annual variability. Tabari and Talaee (2011) transform the monthly precipitation series to annual and seasonal precipitation series to study the variability of precipitation over Iran. Changnon and Demissie (1996) use the existing annual streamflow and precipitation series to detect changes in streamflow and floods under climate fluctuations and changes of land-use drainage.

3.5.3 Missing data

Missing data commonly exist in environmental time series. This may have various causes: natural hazards, the failure of equipment, errors in measurement (Kalteh and Hjorth, 2009). For some particular studies, especially those which have a high demand for good quality datasets, it is necessary to consider some robust methods to fill in the missing data. At present, there are many approaches for treating the missing data. Using case deletion and the mean value of the sample to fill in data gaps are two traditional approaches (Lo et al., 2010). Newer approaches include

applying a nearby similar gauge station data information and regression methods such as simple substitution, parametric regression, ranked regression and Theil method (Lo et al., 2010). More recently, the multiple imputation method has also become available (Lo et al., 2010).

However, blindly implementing infilling missing data is not desirable. The proportion of missing data within a time series is always considered to decide whether the time series can be used for the study analysis or not. For example, the flow gauge stations with more than 10 percentage of missing data were discarded from Chiew and McMahon's (1993) study.

3.6 Techniques for Change Point Detection

Up to now, a number of statistical or non-statistical approaches have been developed. The application of the graphical techniques combined with some of the statistical techniques is efficient.

3.6.1 Graphical techniques

In hydrology, it is quite helpful for analysing change with the help of graphs such as histograms and normal probability plots, double mass plots, time series plots, autocorrelation plots, scatter plots and smoothing curves. This process could be considered as an essential component of the statistical tests. The most commonly used graphs for detecting changes from streamflow time series are described in the following section.

Flow mass curves (Accumulated mass)

Flow mass curves are plots of cumulative discharge in the vertical axis against time in the horizontal axis. Different from hydrograph that plots Q (discharge rate) vs t, flow mass curve is an integral of hydrograph (Subramanya, 2008). The flow volume is cumulated as:

$V = \int_{t_0}^{t} Q\, dt$ Subramanya (2008) Eq. 1

Figure 3.5 is a typical mass curve showing standardised cumulative runoff. The application of mass curves is much wider, ranging from meteorological variables such as precipitation, temperature, and El Nino to hydrological variables including runoff, sediment discharge. In the ordinate of the curve, the units of the variables depend on the study objectives and the available data being analysed such as m^3s^{-1} or m^3. Sometimes, because of the largely cumulative values, it is convenient to combine 10 to the nth power (10^n) with the normal unit m^3s^{-1} for the unit of cumulative discharge. In Figure 3.5, the horizontal ordinate is the chronological time series in unit of year. The units can be expanded to month, week or day. If the starting point and the last point of a flow mass curve can be connected by a straight line, the slope of straight line represents the average discharge over the entire study period (Subramanya, 2008).

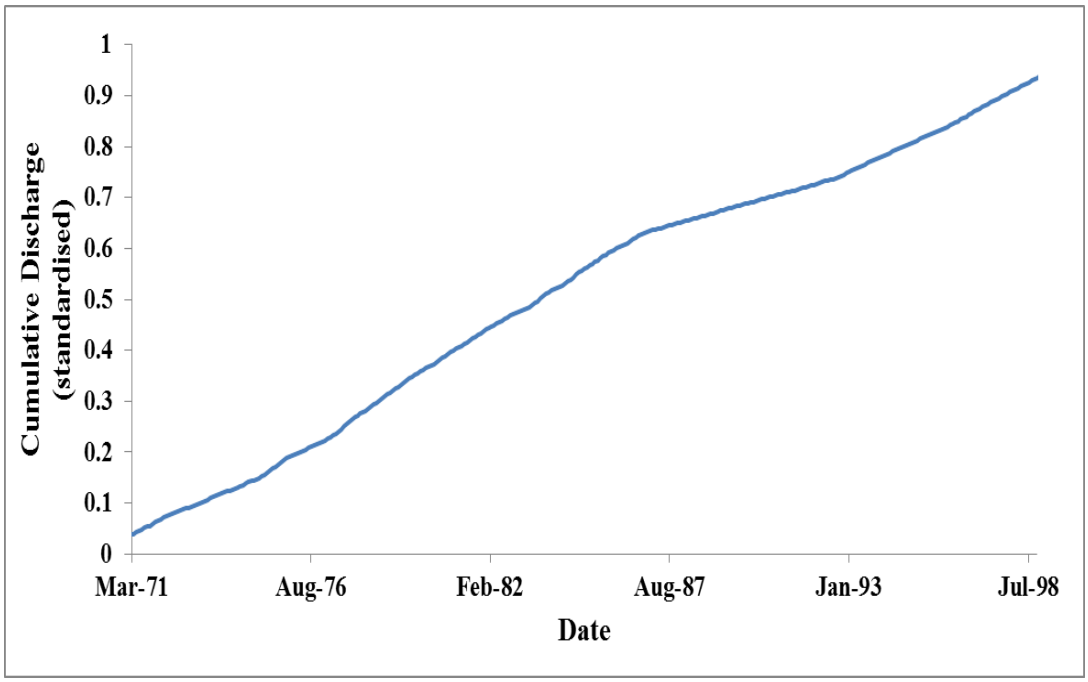

Figure 3.4: River discharge cumulative mass curves

Double mass curves

Double mass curve (DMC) is a simple, visual and practical method, which is widely applied to check the consistency and the long term trend of hydrological data (Gao et al., 2011). In the DMC, the cumulative of one quantity is plotted against the cumulative of another quantity during the same period. So long as the

relation between the two variables is unchanged, the curve will exhibit a straight line. In contrast, a changed relation will cause a break in the slope (Gao et al., 2011; Searcy and Hardison, 1960). The difference in the slope of before and after a change point indicates the degree of change in the relationship. DMC plays a role in smoothing a given time series and suppressing random elements in a time series, providing the main changes of the time series (Gao et al., 2011).

A change in the gradient of a DMC may infer that the characteristics of either of the variables have changed. Further study should indicate the reason for the change. In hydrology, the precipitation-runoff DMC method is widely used, combining with other methods to quantify the effect of climate variability or human activities on hydrology. For example, Jiang et al. (2011) applied the precipitation-runoff DMC to detect an abrupt change point reflecting the effect of human activities on runoff in 1979. Gao et al. (2011) plotted DMCs of precipitation vs. runoff and precipitation vs. sediment during 1957-2008 in the middle reaches of the Yellow River in China and found cumulative streamflow and sediment discharge decreased by 17.8 % and 28 % respectively compared to the period before the transition years. These changes were mainly caused by human activities.

Residual mass curves

A residual mass curve is a plot of cumulative residual against time. Within a time series X_i $(i = 1\ to\ N)$, the cumulative residual is computed by first subtracting each individual variable value X_i from a referenced value to obtain the residuals and second by cumulating the residuals (Searcy and Hardison, 1960). The referenced value varies in different studies. For mass curves, a residual mass curve can be used to represent cumulative departures from the mean. Taking Searcy and Hardison (1960) as an example, they calculated residuals by subtracting the computed runoff from the measured runoff. In hydrology and climatology, residual mass curves can effectively detect the variabilities or homogeneities of a time series. They can magnify the minor breaks that may be hidden in smooth double mass curves (Searcy and Hardison, 1960). Briefly, the characteristics of the residual mass curve incorporate magnifying the difference

between two variables and indicating the breaks in mass curves or double mass curves through the maximum or minimum points in residual mass curves (Searcy and Hardison).

3.6.2 Statistical techniques

There are many techniques that can be applied for trend/change point analysis and each of them has its own assumptions and can be used for a particular case. The traditional approaches include the maximum likelihood estimation, Bayesian and time series methods, and the newer ones range from phase randomization to smoothing techniques and so on (Kundzwicz and Robson, 2004).

3.6.2.1 Nonparametric (distribution-free) test methods

The nonparametric methods are based on the assumption that the random variables are independent and identically distributed. However, they do not require any assumption about the data distribution. These methods are seldom affected by some anomalous values (Feng et al., 2010) and are more adapted to cases when the data seriously departs from normality rather than the cases of normally distributed data (Radziejewski et al., 2010).

The typically traditional nonparametric methods for change detection are the running t-test method, Cramer method, Le Paga method, Yamamoto method, Mann-Kendall method, and Pettitt method (Feng et al., 2010). The first four methods are suitable for the detection of the change of a time series mean value, but, the latter two are suitable for the change trends detection of time series (Feng et al., 2010). Among them, Mann-Kendall test is the most commonly applied method for its robustness for both non-normally distributed and censored data (Gao et al., 2011).

Kundzwicz and Robson (2004) also give a brief summary of the tests for both step change and trend change. For step change, the tests include Pettitt's test, Mann-Whitney test, CUSUM test, Kruskal-Wallis test, cumulative deviation tests and Student's t-test, and for trend change, tests range from the rank-based Spearman's rho and Mann-Kendall tests to linear regression tests.

Ranked-based tests, tests using a normal scores transformation and using resampling approaches, all belong to distribution-free testing (Kundzwicz and Robson, 2004).

Ranked-based tests

The rank-based tests use the ranks of the data instead of using the raw data (Kundzwicz and Robson, 2004). For example, for a dataset of X_i $(i = 1\ to\ n)$, each data has its rth smallest or largest rank, the tests will use the r values for statistical analysis. According to Derryberry et al. (2010), rank-based tests are some of the most powerful non-parametric methods. They are robust and simple to use and they can perform as powerful as parametric approaches when the assumptions of parametric approaches are met (Kundzwicz and Robson, 2004; Derryberry et al., 2010). Typical rank-based tests incorporate Pettitt's test, Mann-Whitney test, Mann-Kendall tests and CUSUM test.

Resampling approaches

Resampling approaches can be categorized into three types: bootstrapping, permutation and jack-knifing. When compare bootstrapping and permutation, the former is more flexible and can be applied in a wide range of circumstances; however, the latter is more powerful (Kundzwicz and Robson, 2004). For hydrological data, resampling methods are quite powerful not only because they require only few assumptions about the data, but also because they are applicable to a wide range of data type (Kundzwicz and Robson, 2004).

- *Bootstrap*

Every original data series can randomly generate numerous random samples with a different number of data values. In bootstrap methods, a new data series is created by repeatedly sampling with replacement from the random samples from the original series. The number of values for each new series is same as that of the original series. Therefore, each data value may be used more than once or not at all in a new series.

- *Permutation*

Instead of replacement, permutation methods just re-order the data values within a same data series to generate resamples (new series) in a way that is consistent with the null hypothesis of the test. As a result, each data value in the original series can only be used once in each new re-sampled series.

To carry out a permutation test, the procedures below must be followed:

1. Compute the statistics for the original data under the null hypothesis;
2. Permute the data series many times and re-calculate the statistics each time; and
3. Compare the original statistics to the generated test statistic values to get the P-value.

For both bootstrap and permutation methods, a number of re-samples is needed for the tests. Theoretically, the larger the number, the more accurate the significance level (e.g. 1%, 5%) can be generated (Kundzwicz and Robson, 2004). However, because for each data series with n data values, there are n! permutaions, it is practical to randomly select some possible permutations (Kundzwicz and Robson). For example, there are K re-samples and the test statistic for each of them has been calculated. The original test statistic for the Null hypothesis is S. To obtain the significance of the result S, comparion is carried out among S and the test statistics for each generated re-sample and derive m values not exceeding S are derived, then the probability of not exceeding S is

$$p = m/K. \qquad \text{Eq. 2}$$

In reality, the river discharge data are strongly correlated, especially in daily scales. However, this character cannot satisfy the assumption of normality or independence, typically in parametric and non-parametric tests. That is why not only parametric tests but also non-parametric tests are problematic for river flow analysis (Radziejewski et al., 2010). Now, many people are promoting the use of a randomization test because it is a more intuitive approach to assessing evidence compared to t-test and can be applied to cases where the two samples t-test is not

valid. Permutation tests that use the randomly generated data series for statistical analysis are just special case of randomization tests. Radziejewski et al. (2010) developed a method, phase randomization technique, which has potential applicability to hydrological data. They use phase randomization to generate the series with the same autocorrelation and then apply a bootstrapping approach to compare the result of each test with those obtained from other series.

A large number of studies are made to detect change points by using the non-parametric methods which are thought robust. For example, Kiely (1999) used the non-parametric Mann-Whitney-Pettitt test to identify the change point in the precipitation time series to study climate change in Ireland. In the analysis, the time series was considered as two samples which were parted by the change point. The means of the two samples were hypothetically equal. The significance probability for a change point was computed to find out the most significant change point. Ha and Ha (2006) applied the Pettitt test for its advantages of application of a remarkably stable distribution as well as providing a robust change point test resistant to outliers. In their study, they estimate the change point for the mean annual and monthly precipitation from 1771 to 2000 and suggest that the climate in the pre-modern era was more fluctuating and abnormal than that in the modern. They also detected that the major abrupt climate change happened in the late Changma period (August to September). Tabari and Talaee (2011) detected trends of annual and seasonal precipitation using Mann-Kendall test, Sen's slope estimator and linear regression method over the period of 1966 to 2005 in Iran and found decreasing annual precipitation trend of 60 percent of the stations, with an especially significant decreasing trend in northwest Iran.

For seasonal variability, they found spring and winter precipitations were mostly decreasing. Jiang et al. (2011) quantify the effects of climate variability and human activities on runoff from Laohahe basin in northern China by using Mann-Kendall trend test, Pettitt test and Double Cumulative Curves methods. Changnon and Demissie (1996) detect changes in streamflow and floods under climate fluctuations and changes of land-use drainage using a three-step statistical analysis. They firstly fit a linear regression for annual flow, peakflow, precipitation, peak precipitation time series and then apply the non-parametric

Kendall Rank correlation test to determine the correlation coefficients and their significance for all of the four data sets. They use a linear regression method to analyse annual flow against precipitation and annual peakflow against peak precipitation and finally calculate the flows due to precipitation or land use drainage.

3.6.2.2 Parametric test methods

The parametric tests assume the distribution of the data (Ha and Ha, 2006) and often require the data are of normal probability distribution (Liu et al., 2010). Although, the parametric tests are known for their less robust function, some studies choose them for their efficient performance. For example, Liu et al. (2010) use the cumulative sum (CUSUME) analysis to estimate the change points and finally, segment the entire flood season into multiple sub-seasons. Galeano (2007) developed a cumulative sum statistic approach to test the presence of a change point. In the study, after detecting a change point using the segmentation algorithm proposed, the author splits the data into segments and tests change in each step which overcomes the limitation of multiple change point testing.

The maximum likelihood ratio test is another type of parametric test and has been used widely (Ha and Ha E, 2006). However, the test also encounters a problem caused by the endpoint. Spurious change points can be caused by some events near the beginning or end of a sample time series (Galeano, 2007).

3.6.2.3 Bayesian methods

Bayesian methods have been widely employed to detect shifts/change points in the mean level of time series in hydrological literature (Perreault et al., 2000). Tripathi and Govindaraju (2009) also detect the abrupt changes in the rainfall and temperature pattern by employing a Bayesian method.

Bayesian methods differ by identifying the parameters of a model as random variables rather than fixed values (Perreault et al., 1999). The main merit of the Bayesian approach is the locations of the change point and amplitudes posteriors are of interest to quantify the amount of uncertainty introduced by correcting in-

homogeneities. It also gives an objective and coherent decision theory to decide on the number of change points and on their positions (Hannart and Naveau, 2009). Most of the Bayesian approaches are based on a single shifting model and the main difference among them is the prior distributions specified to represent the other unknown parameters such as mean before and after the mean and amount of change and variance of the observation (Perreault et al., 1999). Perreault et al.(1999) concentrated on a single shift in the mean level of precipitation and runoff time series. However, Bayesian methods are widely known for their high complexity.

3.6.2.4 Wavelet analysis

Wavelet analysis has attracted attention and has been successfully used in the field of signal processing such as in geophysics and meteorology. For instance, it can be used to identify coherent convective storm structures and characterize their temporal variability or can be used to analyse localized variations within geophysical time series including climatic indices (Coulibaly and Burn, 2004). In hydrological analysis, wavelet analysis has also been applied owing to its wide range of possible dominant frequencies, such as examining rainfall-runoff relationship and characterizing streamflow time series (Coulibaly and Burn, 2004).

Compared to Fourier transformation, wavelet analysis is scale independent (Coulibaly and Burn, 2004) and can provide more accurately localized and quantified temporal and frequency information, like a change point with its particular shape of a time series curve (Lee and Yamamoto, 1994; Wang and Cai, 2010). The algorithms for wavelet methods are efficient which makes their computation speed high (Wang and Cai, 2010). However, limitations of wavelet method do exist. According to Feng et al. (2010) wavelets decompose a time series curve into various components that correspond to different fixed frequency bands. Therefore, it is subjective to choose the wavelet bases and decomposition scales and this method needs to be further improved (Feng et al., 2010). The theory and applications of wavelet analysis have been by presented by numerous published articles, for instance in Lee and Yamamoto (1994).

In the detection of change points, the wavelet methods are quite efficient because of their sensitivity to singularities such like jumps and sharp cusps of a curve (Wang and Cai, 2010). Massei et al. (2009) identified the variability of streamflow time series in the Mississippi river from 1934 to 1998 by using Morlet wavelet for its good basic frequency resolution. Coulibaly and Burn (2004) also adopted continuous wavelet transformation to recognize variability in annual Canadian streamflow and study the links between the results and climate variability.

3.7 Summary and Conclusion

When comparing the impact of climate variation and land use change, the former influenced streamflow more significantly than the latter. Thus, separation of the impact of the two factors on streamflow should be made which can provide information on climate complexity and land use management.

A number of articles have been published on the perspective of detection of climate change and land use variation. The techniques for detection, to some extent, have been developed to the mature phase. However, limitations still exist; for instance, traditional techniques for climate change detection are statistical based methods which do not take the dynamic process into account, therefore, developing a new method combining statistics with dynamics is important to achieve accurate results (Feng et al., 2010). With respect to global warming, climate observation series have displayed some more complex characters. Therefore, it is also essential to improve and perfect the theory and methods for climate change detection which needs further studied (Feng et al., 2010).

3.8 Prospects

A shift in development which reflects where things change from quantitative to qualitative commonly exists in the area of natural processes as well as the area of social economy. In hydrology, as the impact of human activity on nature is more serious as time is going on, detecting change has drawn attention of many hydrologists globally. Numerous methods can be applied to detect changes, each

of them preferred by specific researchers. Therefore, there is neither any organic unification of theories nor any methods that have been approved widely with advantages of widespread applicability and high accuracy.

Chapter 4 – Data Sources

4.1 Introduction

To detect changes from hydrological records, the primary issue that should be considered is data availability. Long-period records will give more information on change. High quality data can also benefit accuracy of the results. Therefore, understanding whether data sets contain missing data is particularly important. In this study, there is a large amount of available data including both precipitation and runoff. The data sets were from all over the Waikato region and part of the north Whanganui region. Rainfall and river inflow data of Waikato region were obtained from Waikato Regional Council. Rainfall and river inflow data of the Whanganui part was available from Genesis Energy. The time scale of the data is daily, which has been converted to appropriate time scales as described in the next chapter.

4.2 Rainfall and River Discharge in the Waikato Region

59 rain gauges and 46 streamflow recorders based on a daily scale were available for this study. The data contain the flow and rainfall gauged over four main rivers: Waikato, Waipa, Waihou and Piako, and three smaller rivers Tairua, Awakino, Mokau and their tributaries within the Waikato region. The streamflow data was recorded in cubic meters per second (m^3s^{-1}), and the rainfall data was recorded in millimetres (mm).The amount of daily flow ranges from the 500 m^3day^{-1} of the main rivers to the less than 1 m^3day^{-1} of the small streams. The lengths of the records vary from the minimum 12 years to the maximum 80 years, pre-1900 to 2007. The blue rhombuses shown in Figure 4.1 represent the locations of the rain gauges with available data, the location of the red triangles shown in Figure 4.1 shows the flow sites with available records. The details including site name, river name, start date, end date, years of records and data quality (percentage of missing data) for each rainfall and runoff recorders are summarized in Appendix A-a and A-b. The digital map of the Waikato region is in Appendix H.

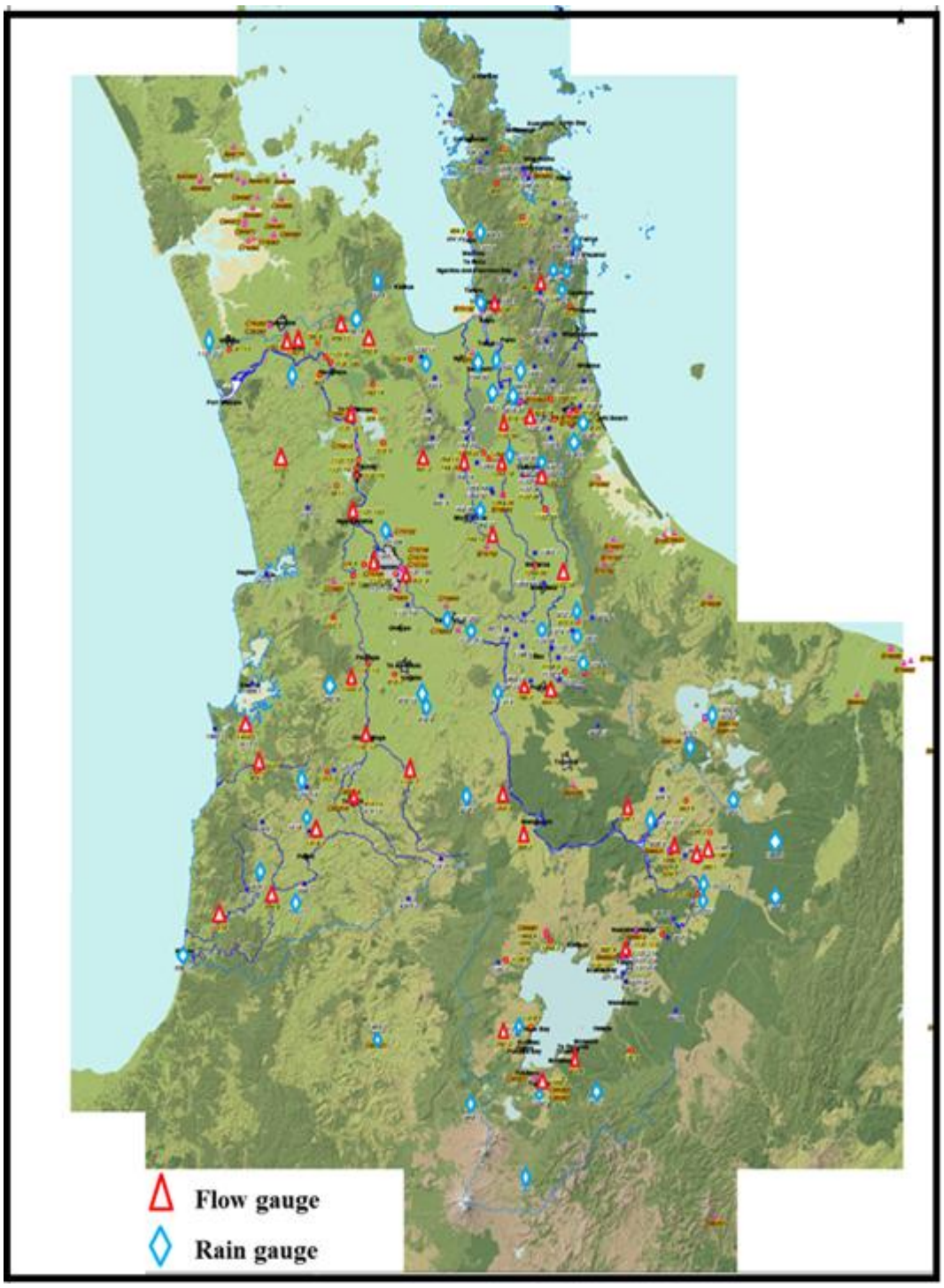

Figure 4.1: Locations of rainfall and river discharge gauges utilised. (Source: Waikato Regional Council)

4.3 Rainfall and River Discharge in the Whanganui Region

In the Whanganui catchments, four rainfall and eight flow data sets along the Whanganui River, the Tongarito River, the Kuratau River, the Whakapapa River

and the Ongarue River were provided by Genesis Energy. The unit of streamflow data was cubic meters per second (m^3s^{-1}), while the unit of rainfall data was millimetres (mm). The flow data sets are quite good for this study because of their long records and no missing data. The flow data of the Whanganui river at Te Porere, the Whanganui river at D/S intake, the Whanganui river at Below Piriaka, the Whanganui river at Te Maire, the Ongarue river at Taringamutu, the Whakapapa river at Footbridge, the Tongariro river at Waipakihi and the Tongariro river at Turangi are available from 1966, 2004, 1970, 1962, 1962, 1959, 1960 and 1957 respectively to April 2011. Due to the short length of records, the data gauged in the Whanganui River at D/S intake was not used in this study.

Of the four rainfall data sets (Whanganui river at Te Porere, Whanganui river at Below Piriaka, Ongarue river at Taringamutu, Tongariro river at Waipakihi), the Waipakihi gauge site has the longest period records from 1989 to 2011. However, due to this study needing a longer period record to detect change points, none of the four rainfall time series were considered in this study. The rainfall data in the Waikato region that cover the study site in the Whanganui part includes the sites located in Mangatoetoe and Hatchery, Tongariro River as well as the gauge sites at Taumarunui and Te Porere, Whanganui River (Figure 4.2). The first two data series start from 1929 and 1987 and finish at 2004 and 2007 respectively. The last two start from 1962 and, and finish at 2002 and 2004 respectively. Therefore, these four time series are applied for the analysis in the Whanganui part. Figure 4.2 shows the locations of the rainfall and runoff gauge stations in the Whanganui catchments. A summary of data characteristics of the gauged rainfall and flow and applied in this study is shown in Appendix A-c and A-d.

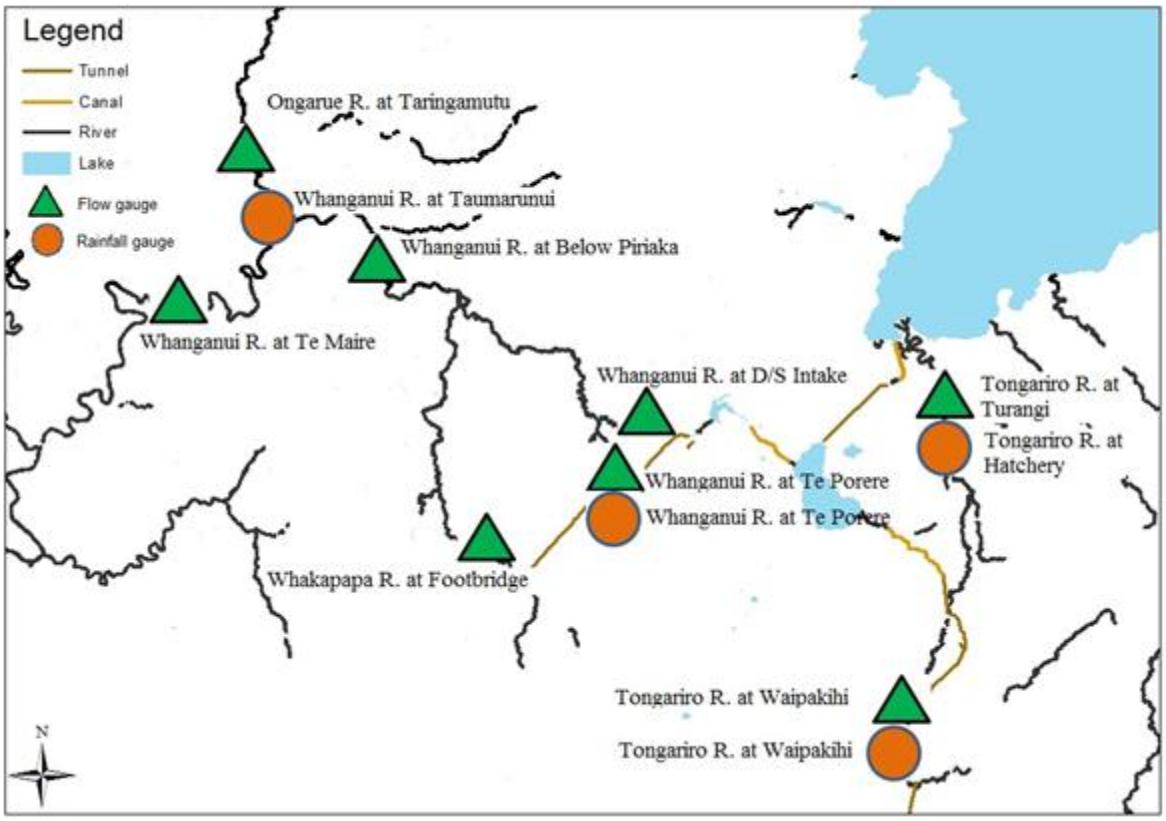

Figure 4.2: Northern portion of the Tongariro Power Scheme showing locations of utilised rainfall and river discharge gauges.

Chapter 5 –Preliminary Analysis

5.1 Introduction

The length and data quality for the records are variable. To avoid the impact of missing data and too large amount of data, the time scale of the data applied to this thesis was primarily determined as monthly which reduced the high variability of daily data.

It is of interest to discover the similarity or difference of rainfall characteristics in different sites. A brief literature review relating to the study of spatial and temporal rainfall variability is given, followed by the rainfall spatial correlation analysis in the study area of this thesis.

Serial correlation analysis with respect to all of the available rainfall and runoff time series was carried out to investigate whether the data variables in each series are randomly distributed. The lag-n correlation scatterplots are created as plotting the last N-n observations against the first N-n observations. N is the sample size (total number of month). In this study, both the rainfall lag-1 and runoff lag-12 serial correlation were analysed to check if such series (lag-1 rainfall and lag-12 streamflow) are random. The results can justify calculating the monthly averages using the $\partial/\sqrt{\mathrm{N}}$ errors to have the confidence limits about the monthly mean values.

Finally, each runoff gauge was paired by a representative rain gauge or the average of several representative rainfall gauges in the upstream river catchment.

5.2 Transforming the Available Data from Daily to Monthly

The objective of this thesis is to detect changes from the hydrological and meteorological data. Various reasons such as equipment failure, natural hazards, error in measurements or faults in data acquisition lead to missing data (Kalteh and Hjorth, 2009). It is essential to check the quality of the data set for each gauge station and discover methods to interpolate the missing data. The software that will be used for the later change point detection can generate an accurate result

with a good quality time series. Therefore, treating the missing data is primarily important for this study. To avoid the appearance of too many "noises" of missing data, the daily mean streamflow was transformed into monthly mean flow and the daily precipitation time series was transformed into cumulated monthly rainfall for all of the available data.

In this thesis, a traditional linear methodology for treating missing data is proposed. A VBA macro is created for this task. The main procedures are:

- Sum: Total the daily values for each month.
- Average: Divide the monthly total of the daily values by the number of non-missing values to get the average.
- Monthly: multiply the average daily values to monthly total by the number of absolute days of each month (rainfall dataset only).

Let us consider a daily time series X_i (i=1 to n). The time series is first divided by the macros into a number of segments representing different months for different years. For each month, there are m (m= 0 to N) days with observed data. N represents the total days of that month. If m is larger than 25, then the macro will scale and give the monthly data through the equations below:

$$(x+a)^n = (\sum_{i=1}^{m} X_i)/\mathrm{m} \qquad \text{Eq.3}$$

$$(x+a)^n = ((\sum_{i=1}^{m} X_i)/\mathrm{m}) * \mathrm{N} \qquad \text{Eq. 4}$$

If m is no more than 25, then the VBA macro will determine the monthly data for that month as missing.

In both Waikato and Whanganui study areas, the available streamflow datasets based on daily and in units of m^3s^{-1} were converted into monthly mean flow through Equation (3). The available rainfall datasets based on daily and in units of millimetre (mm) were converted into total monthly rainfall through Equation (4). The step of interpolating missing data in both of the two conversions is on the basis of considering the days with available data within a month. The quality of

the datasets is improved but not much due to most of the missing data exists in succession which leads to more than 25 days missing in a month.

5.3 Monthly Rainfall Spatial Correlations

5.3.1 An interpretation of spatial and temporal rainfall variability

Surface runoff is closely related to the spatial and temporal variability of rainfall (Sen and Habib, 2001). The rainfall process which decides the hydrological cycle is complexly driven by meteorological phenomena (Sen and Habib, 2001). Before studying the rainfall runoff relationship, knowing the rainfall characteristics in an area is helpful for the precision of the results. For each runoff gauge site, the rainfall that can explain the amount of runoff in the gauged site is received rainfall by the upstream watershed. Because it is difficult to collect enough data within a catchment, comparing the rainfall gauges above the target runoff gauge can be helpful for reducing the errors caused by limited data availability. The degree of correlation between two rainfall gauges gives a good explanation of how similar the meteorological and topographical features driving the two gauge stations are (Berndtsson, 1987). Generally, two nearby rainfall gauges may exhibit a positive correlation. However, sometimes, they may have some degree of negative correlation in the interrelationships (Sen and Habib, 2001) which occurs randomly. Therefore, the study of rainfall similarities within a catchment is nessary.

The temporal rainfall variability will change as the change in the data time scale (Berndtsson, 1987). Figure 5.1 showing the rainfall gauges correlation-distance pattern and how correlation coefficients change when daily data is cumulated in monthly and yearly periods is discovered by Berndtsson (1987). Through his study, on the basis of yearly data, the rain gauges are highly correlated even though the distance between two gauges increases to 300-400 km. For monthly data, the paired stations are less correlated than yearly data and the high correlation happens within 50-100 km distance. However, for daily data, even rain gauge stations 10 km apart are not well correlated. The correlation-distance pattern tends to be smoothed when the data are in large time scale, for instance, in yearly time scale, the rain gauges at different locations are highly correlated.

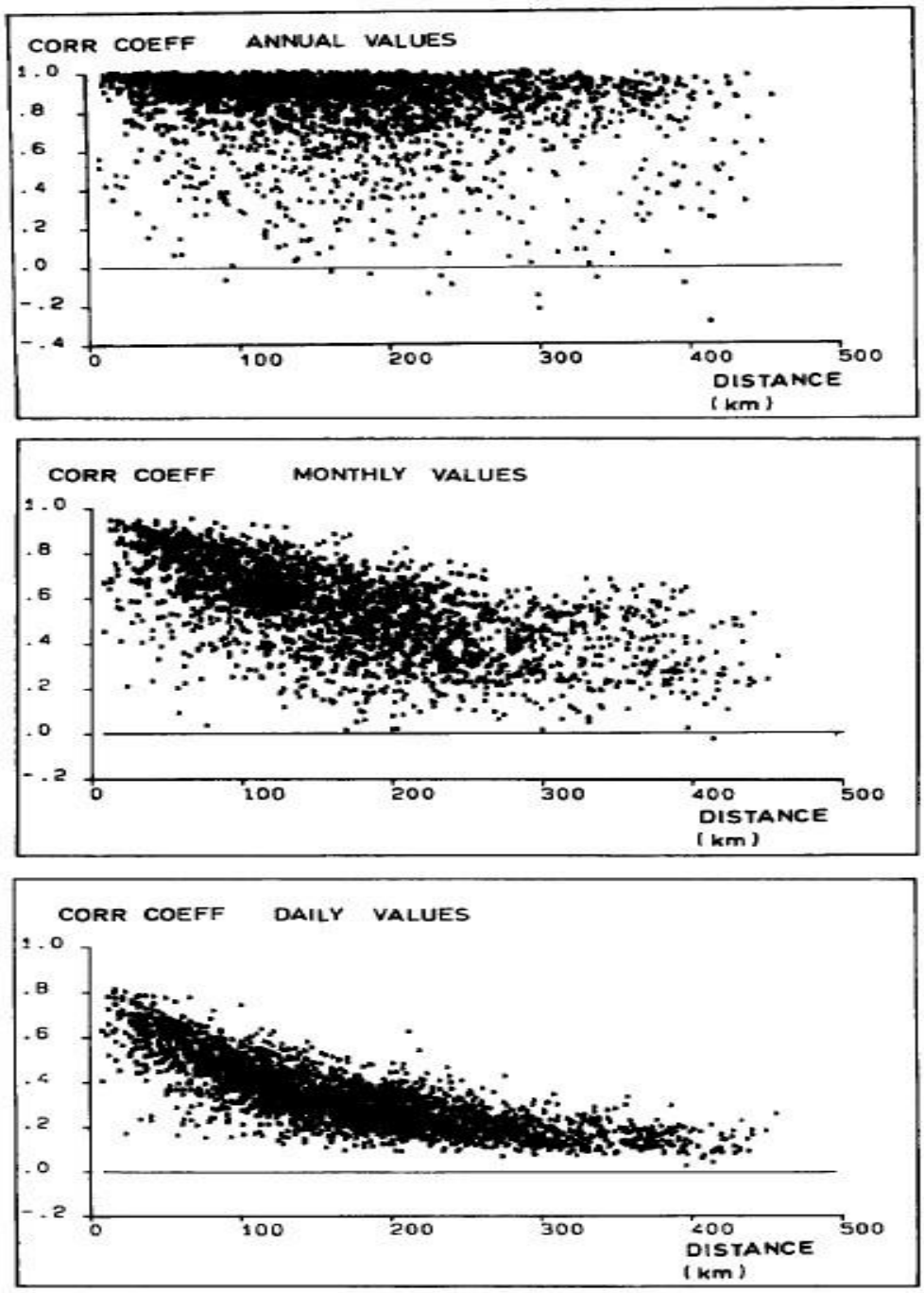

Figure 5.1: Lag-zero cross-correlation coefficients for yearly, monthly and daily data vs. interstation distance (67 stations, 1979-83). (Source: Berndtsson, 1987))

5.3.2 Identification of the spatial rainfall variability in the study area

The climate over the Waikato regions varies on the basis of the influence of the adjacent ocean, large lakes and wind. Within the Waikato region, the spatial

distribution of rainfall gauges is not homogeneous, with a large number of stations in the north-east, an even distribution in the middle and lower south area, with a sparse distribution in the north-west.

The data applied to estimate the spatial rainfall variability are the monthly rainfall records. 57 gauges which differ from each other on the basis of length of record and locations were selected for the study. Contemporary correlation between two gauges was analysed giving a value of the linear correlation coefficient R^2. The distance between the two gauges is given in the units of 1 km. Theoretically, with 57 rainfall gauges considered in this study, there will be 57*(57/2) times correlation. Considering the correlation coefficient is more accurate with more data, a threshold of five years overlapping period was determined. Therefore, every two stations selected at different location should overlap by at least 5*12 monthly data. A threshold of 100 km for the distance between two gauges was also specified. In the north-east area of Waikato region, there is a large concentration of rainfall gauges. To avoid too many scatter points concentrated in a same area in the figure, some typical pairs only were considered. Finally, 445 rain gauge pair observations were selected.

The paired gauges and their distance, correlation coefficient, start time, end time and total months of records are summarized in Appendix A-e. Figure 5.2 is a scatter-plot showing the change of correlation among the 445 paired rain gauge stations with distance. The maximum distance between two gauges is 100 km and the minimum distance is 2 km.

It can be seen that there is a slightly decreasing pattern in correlation coefficients with increasing distance (Figure 5.2). The highest correlation R^2 equals to 0.845 occurs on the distance equals to 2 km, but the lowest correlation R^2 equals to 0.125 occurs on the distance equals 88 km. However, it also should be highlighted that even with around 100 km distance between only two rain gauges, some of them are highly correlated, and even within 20km distance some are poorly correlated. In the scatter plot (Figure 5.2), three areas can be recognized as abnormal from the correlation-distance pattern. They are the points in the area

circled by red line (A), in the area below the red line in the left of the plot (B) and in the area above the red line in the right side of the scatter plot (C).

A: the correlation coefficients of two stations within 20 km are comparatively lower ranges from 0.4 to 0.65;

B: the correlation coefficients of two stations within 40 km are extremely low ranges from approximately 0.15 to 0.4;

C: the correlation coefficients of two stations within 60 to 100 km are extremely high ranges from approximately 0.6 to 0.8.

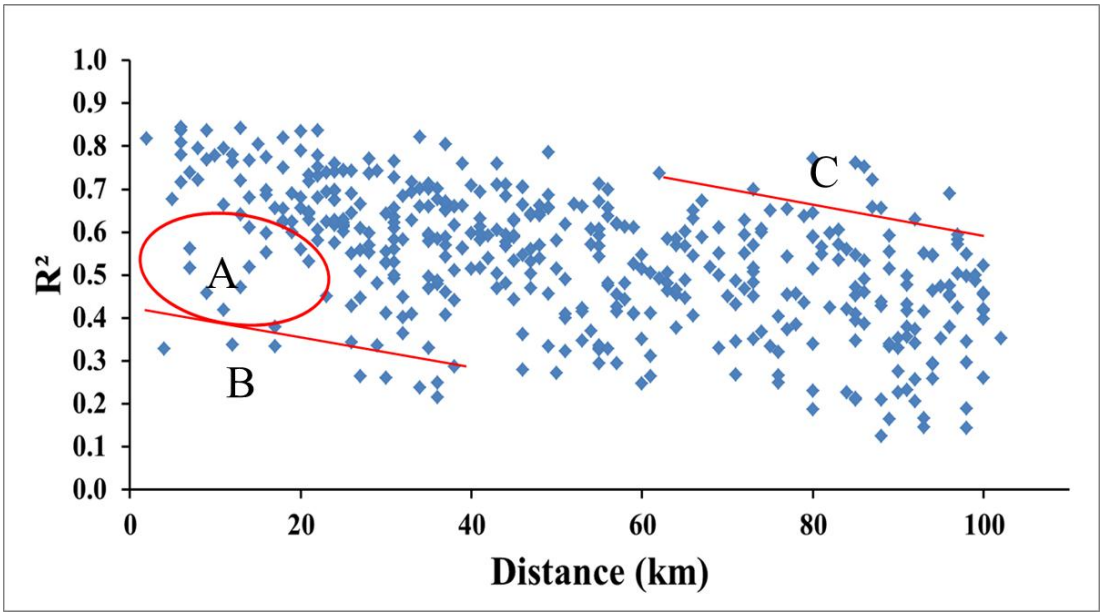

Figure 5.2: Correlation coefficients for monthly rainfall data vs. interstation distance (fifty-seven stations).

This implies that the climatology of the stations employed to produce the point in area A, B and C are driven by some factor differing from the other area. These abnormal correlation points were then linked to local correlation structure as shown in Figures 5.3, 5.4 and 5.5. It is clear that in the north-east part of Waikato region, spatial correlation is low even within short distances less than 40 km. The local factor that causes this spatial pattern is probably the variation of coastal influence. In the south middle of Waikato region, the correlation is comparably high with long distances of more than 60 km, this may be because the rainfall

pattern in the middle of the Waikato region is stable caused by similar factors such as wind. However, although the correlation coefficients are higher than others in the same distance level, the correlation is still not big enough to make sure the south middle of Waikato is a homogeneous rainfall area.

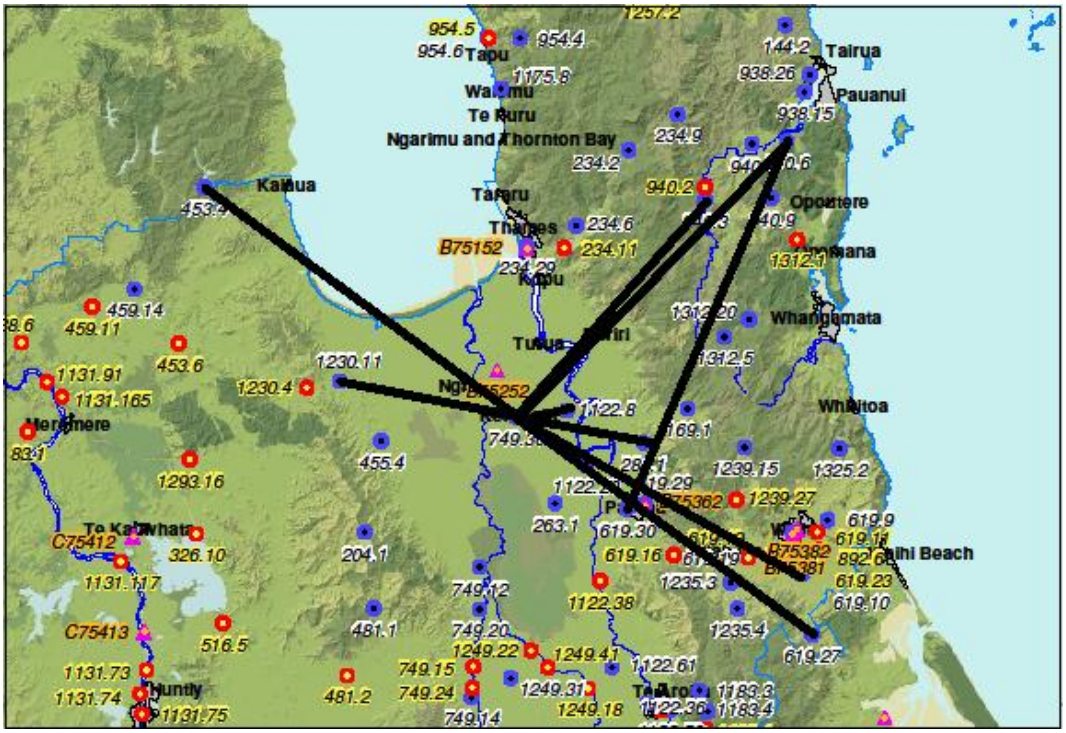

Figure 5.3: Correlation linkage for monthly rainfall data with distance < 40 km and correlation coefficients range from 0.2 to 0.35.

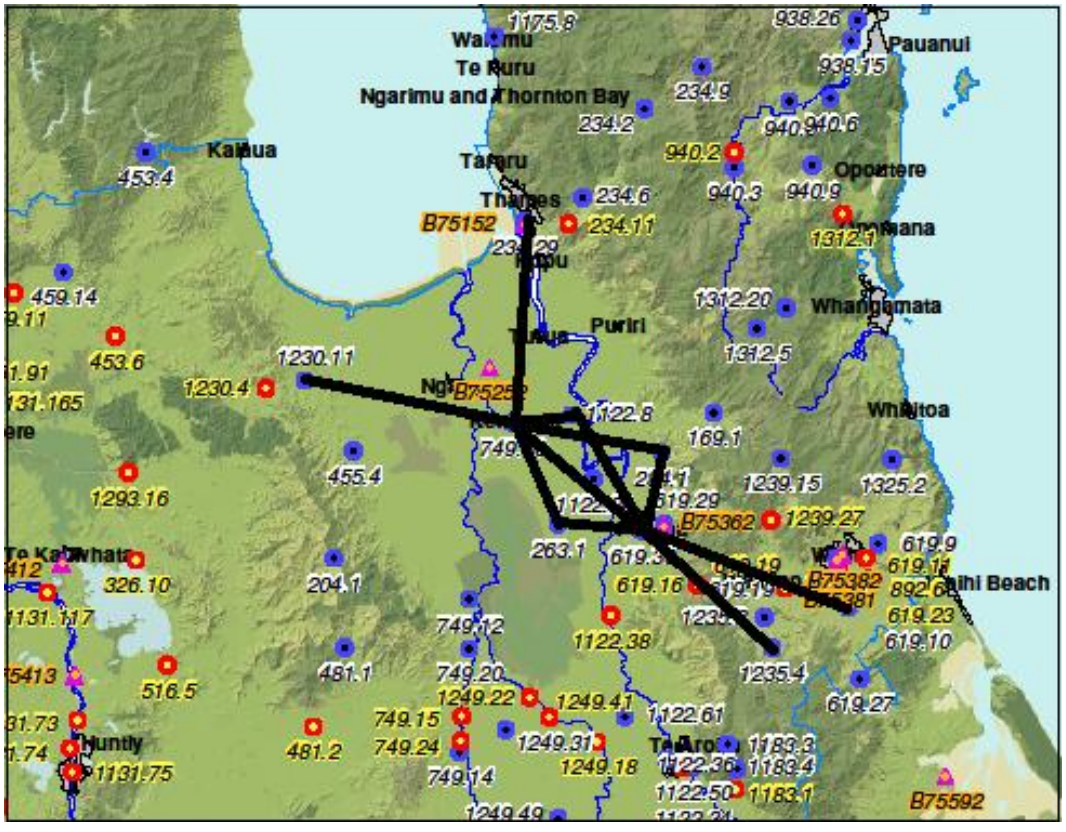

Figure 5.4: Correlation linkage for monthly rainfall data with distance < 20 km and correlation coefficients range from 0.3 to 0.6.

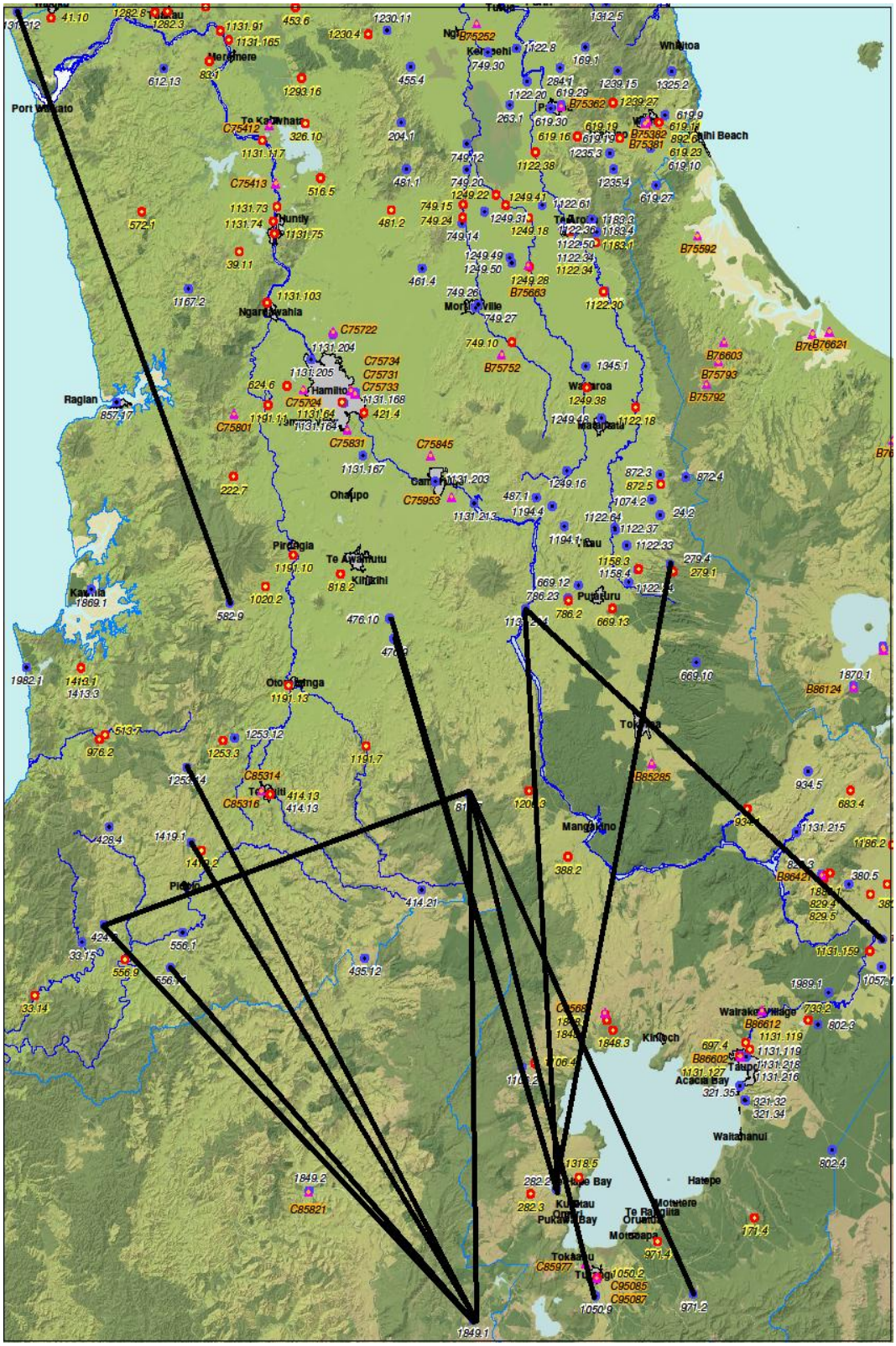

Figure 5.5: Correlation linkage for monthly rainfall data with distance > 60 km and correlation coefficients range from 0.55 to 0.77.

5.4 Serial Correlation

Some statistical analysis is based on the assumption that data in a time series is independent, while in most hydrological series, the data points are not independent which may lead to the inaccurate statistical results. For example, in a high baseflow river discharge series, seasonality is one of the important conditions that drive the persistence of dataset. To characterize the persistence of both precipitation and streamflow series, the serial correlation (lag-1) of each time series was calculated. It should be noted that a lower value of the correlation coefficient shows a lack of the serial correlation, suggesting each value in the dataset is independent of the previous one. The lag-1 and lag-12 correlation coefficient was calculated for each time series and a check made as to whether the calculated value was statistically significant with respect to the critical value defined as $r_{.95}$ which equals to $0 \pm 2/\sqrt{N}$. If the calculated r is within this range, then the null hypothesis of no serial correlation is accepted at 95% level.

For each monthly rainfall data set, the lag-1 correlation analysis was studied to determine whether the data points within a time series are independent or not. For each series, the last N-1 months (N is the sample size) observations were correlated with the first N-1 months' observations giving the results of r^2 (summarized in Appendix A-f) as well as the 95 % threshold level of correlation $r^2_{.95}$.

All of the 58 precipitation time series are random at 95 % significance level because the serial (lag-1) r^2 is less than the 95 % confidence interval $r^2_{.95}$ for each respective series.

For the river discharge time series, the serial correlation analysis of each individual month (lag-12 serial correlation analysis) was carried out on each discharge time series. From the results (Appendix A-f), the lag-12 analysis of all of the 45 streamflow gauges was found to be independent at 95 % significance level.

In conclusion, both the lag-1 rainfall series and lag-12 streamflow series show no serial correlation at 95% significant level.

5.5 Identification of the Paired Rainfall and Runoff Gauges

Before estimating a rainfall-runoff relationship, the paired rainfall runoff gauges must be carefully selected for fair comparison. Theoretically, the rainfall that can pair a flow gauge is the integrated rainfall from the whole catchment above the flow gauge. However, as the number of rain gauges is limited, a study on selecting a representative rainfall gauge to pair a flow gauge within a same river catchment should be carried out. In the smaller catchments, for each flow gauge if there is no rainfall gauge upstream, the nearest rainfall gauge is selected to pair. However, in a large river catchment, for a flow gauge, the best rainfall gauges used to pair it should be the average rainfall of those located in the upstream. If the rainfall information within the catchment is not available, the rainfall gauge located in the middle of the catchment is the best choice. Moreover, from the study in section 5.3, the rainfall gauges within 40 km distance have higher correlation. Therefore, a distance of more than 40 km of a rainfall gauge from the studied flow gauges was not considered. Also, the correlations of some rainfall gauges near Coromandel are poor even over a short distance. Therefore, the flow gauges in that area are carefully paired with the nearest rainfall gauges.

The situation of there being more than one or two rainfall gauges being suitable to pair with the flow gauge could occur. In this case, a study on the similarities of some nearby rainfall gauges which are all representative will be carried out. The simplest method is comparing plots of one rainfall gauge time series and another rainfall gauge time series. A theoretical 1:1 line on the plot indicates the two gauge stations have a strong fit, equalling each other. If the two gauges have a good fit, then aiming to reduce the random errors, the two rainfall gauges are averaged. In practice, it should also be noted for a long period flow time series, a rainfall time series selected to pair it should overlap as long as possible to the target flow time series.

Finally, each rainfall gauge that can pair a given flow is carefully selected. Appendix A-g gives a summary of the reasons to select the rainfall gauge among all and details of the pairs including period, distance, river catchment and site names. Among the 44 flow gauges in both Waikato and Whanganui regions, 24 are paired by using the nearest rainfall gauge because there are no rainfall gauges in the upstream area, 14 are paired by applying the nearest only one upstream rainfall gauge. However, the remaining 6 are characterised by having more than one rainfall gauge upstream.

5.6 Conclusion

Conversion the data time scale from daily to monthly is helpful for enhancing accuracy and detecting change-points. From the rainfall spatial correlation analysis, within the study area, the monthly rainfall does not vary greatly with distance. Since the correlation coefficient of the lag-1 rainfall and lag-12 runoff serial analysis is less than the 95 % confidence interval, it is concluded that the rainfall time series and the streamflow flow time series for each month can be treated as an independent sequence of observations. The paired rainfall runoff gauges will be utilized for rainfall runoff relationship analysis.

Chapter 6 –Methodology

6.1 Introduction

Climatic shifts will be reflected in concurrent rainfall changes over a broad area. On the other hand, river discharge variation could reflect either climate shifts or upstream changes in land use. Even under stable conditions, the relationship between rainfall and runoff is complicated and may be impacted by various factors including wind, temperature, water usage, and topography. However, a land use change impacting on hydrology should be reflected by a discharge change without a concurrent change in rainfall.

This chapter outlines the methodology used here to detect shifts from rainfall and runoff time series. Briefly, through a piecewise least square linear regression analysis, change points in long term rainfall and runoff time series are detected. A permutation test is then utilized to ensure any shifts detected are significantly better than random chance. VBA models are developed for all of the analysis.

Approximate time series change as the mean values for different periods change obviously (Figure 6.1). The converting of a normal time series (Figure 6.1) to the cumulative mass plot (Figure 6.2) can change the form of change-points' existence. The change points detected from the cumulative mass plots are characterised as shifts with stable periods before and after. In other words, if a cumulative mass plot presents a straight line, no change-point can be detected, otherwise, the breaks in the slope of the cumulative mass plot are detected as change-points.

6.2 Graphical Methodology

For the purpose of detecting signals of land use change and climatic change from river discharge and rainfall variation, a standard graphical approach is adopted with changes detected as breaks of slope in cumulative mass plots and double mass plots, with specific reference to rainfall and runoff. Figure 6.1 is a typical hydrograph with two abrupt change points in around 1973 and 1983. The average monthly mean discharge values for each stable period separated by the change

points vary greatly. If converting the hydrograph to the cumulative discharge plot (Figure 6.2), it is obvious that the change points in the hydrograph will present in the form of the breaks in the slope of the cumulative plot. Therefore, the method for change point detection was finally designed for the purpose of detecting the break-points in the cumulative mass plots.

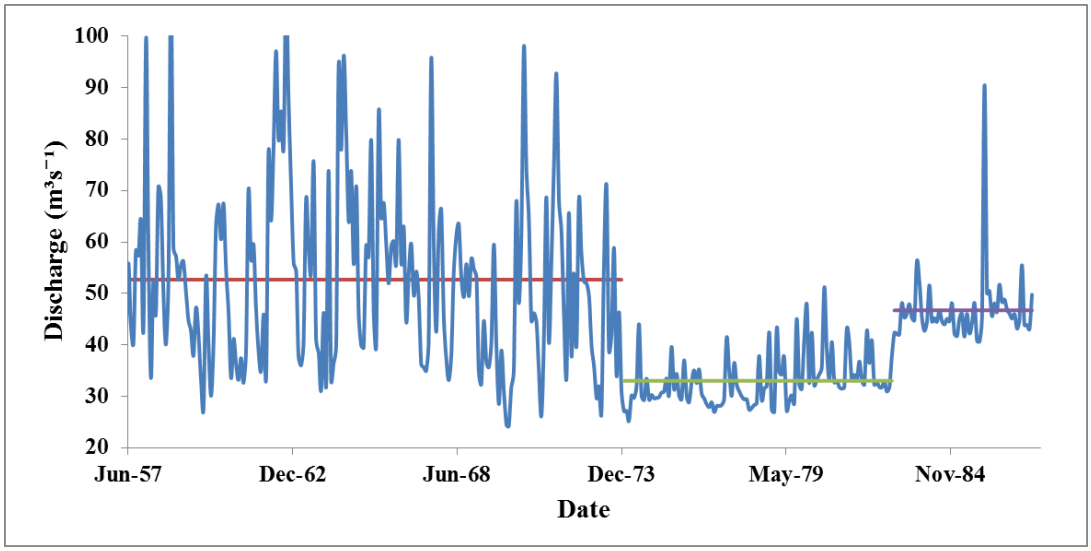

Figure 6.1: An example of a discharge monthly mean time series with two change points

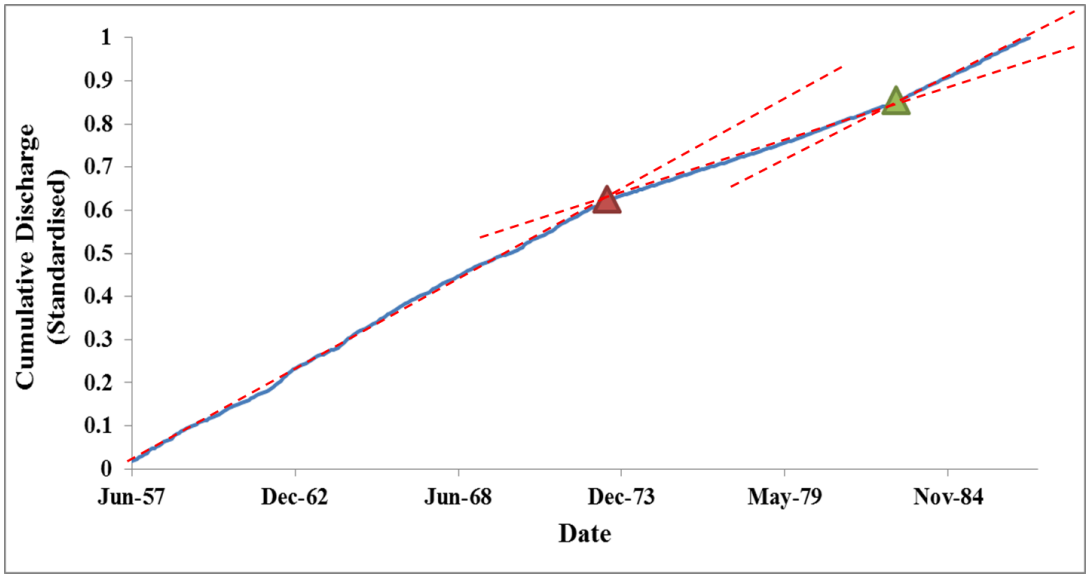

Figure 6.2: Cumulative discharge mass plot

To a good first approximation, constant gradients between breaks reflects a stable mean value over the period concerned, and the extent of the gradient difference before and after a break reflects the magnitude of the change (Gao et al., 2011;

Searcy and Hardison, 1960). Rainfall-runoff double mass plots are of particular value as a change in slope denotes a shift in the rainfall-runoff relation, as might be caused by land use change, for example.

6.3 Statistical Methodology

The task of detecting change points in a time series is carried out here as detecting break-points in the slope of the cumulative mass curves. Any missing data in rainfall or flow time series may introduce artefacts. Therefore, in this study, the segments with missing data have been discarded from the time series. To avoid over-detecting potential change points, a determination of a threshold value of the distance between two change points is specified. In this study, a threshold value equal to 3-years was determined. Therefore, for the monthly data records, the minimum length between two change points contains at least 36 data points.

6.3.1 Piecewise least-squares regression (LSR) approach

A simple linear regression line shows the linear relationship between two variables and explains how one variable responds to another variable's change. To estimate the break-points in the observations, a least squares approach is the most commonly used method and easy to implement. This approach minimizes the square sum of the vertical deviations from each data point to a piecewise line fitted to the data.

For the cumulated data series of two variables X ($x_1, x_2, \dots\dots, x_n$) and Y ($y_1, y_2, \dots\dots, y_n$), the linear regression line is determined as $f(x) = a + bx$ to which gives the least square error:

$$\sum_{i=1}^{n} \mathrm{e_i} = \sum_{i=1}^{n} (\mathrm{y_i} - f(x_i))^2 \qquad \text{Eq. 5}$$

The coefficients intercept a and slope b therefore can be obtained through Eq.6 and Eq.7:

$$\mathrm{a} = \frac{\sum \mathrm{y_i}}{n} - b * \frac{\sum \mathrm{x_i}}{n} \qquad \text{Eq. 6}$$

$$b = \frac{\sum x_i y_i - \frac{\sum x_i * \sum y_i}{n}}{\sum (x_i^2) - \frac{(\sum x_i)^2}{n}} \qquad \text{Eq. 7}$$

Where $\sum$ ... stands for $\sum_{i=1}^{n}$ ...

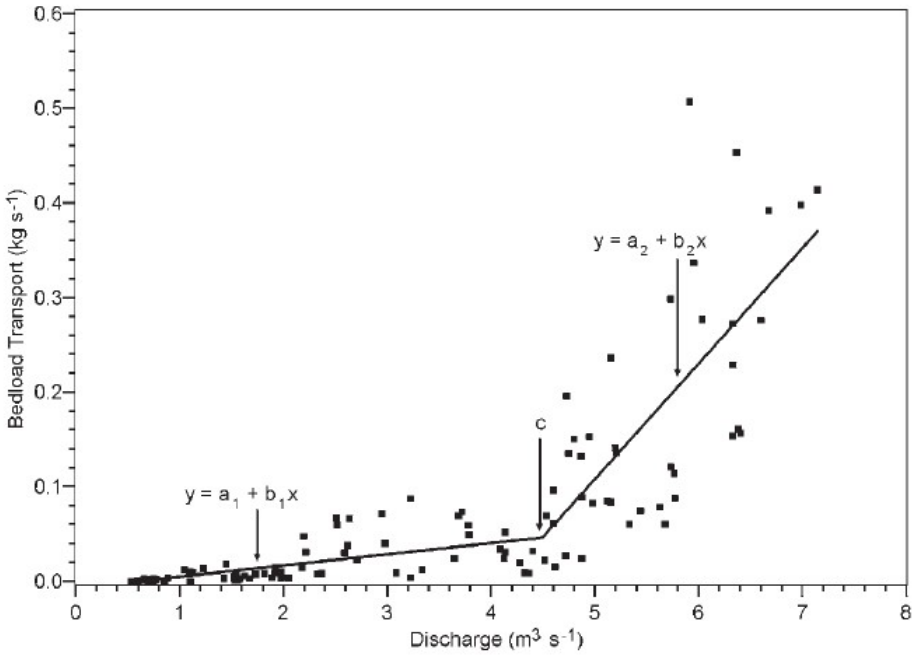

Figure 6.3: Example of a piecewise regression fit between discharge and bedload transport data collected at St. Louis Creek Site 2, Fraser Experimental Forest (Source: Ryan and Porth, 2007).

The data point c ranked as t-th of the data series separates the line into two segments with the corresponding regression lines $f_1(x_i) = a_1 + b_1 x_i$ where $i \leq t$ and $f_2(x_i) = a_2 + b_2 x_i$ where $i > t$ (Figure 6.3).

The four coefficients a_1, b_1, a_2, b_2 are calculated by Eq. 8-11:

$$a_1 = \frac{\sum y_i}{n} - b_1 * \frac{\sum x_i}{n} \qquad \text{Eq. 8}$$

$$b_1 = \frac{\sum x_i y_i - \frac{\sum x_i * \sum y_i}{t}}{\sum (x_i^2) - \frac{(\sum x_i)^2}{t}} \qquad \text{Eq. 9}$$

Where $\sum$ ... stands for $\sum_{i=1}^{c}$ ...

$$a_2 = \frac{\sum y_i}{n} - b_2 * \frac{\sum x_i}{n} \qquad \text{Eq. 10}$$

$$b_2 = \frac{\sum x_i y_i - \frac{\sum x_i * \sum y_i}{n-t}}{\sum (x_i{}^2) - \frac{(\sum x_i)^2}{n-t}} \qquad \text{Eq. 11}$$

Where $\sum$ ... stands for $\sum_{i=c+1}^{n}$ ...

Finally, for a data point x_c, the sum of square errors can be calculated through Eq. 12:

$$\sum_{i=1}^{n} e_i = \sum_{i=1}^{c} \left(y_i - f_1(x_i)\right)^2 + \sum_{i=c+1}^{n} \left(y_i - f_2(x_i)\right)^2 \qquad \text{Eq. 12}$$

With regards to a time series with n data, any data point except the first and last can be a change point, and the total sum of least square errors for the two segments before and after can be calculated. The point which gives the minimum sum of least square errors (Eq.13) among all of the data points will be selected as a change point, to be statistically tested (described in section 6.3.2).

$$\min \sum_{i=1}^{n} e_i = \min\left(\sum_{i=1}^{c} (y_i - f_1(x_i))^2 + \sum_{i=c+1}^{n} (y_i - f_2(x_i))^2 \right) \qquad \text{Eq. 13}$$

In this study, a sequential least squares method of fitting piecewise linear segments was carried out to detect multiple change points. The method works as first a change point is detected which separates the whole given time series into two segments. After that, each segment is treated as an entirety and then analysed to find the change points within each segment; this is carried out repeatedly to identify all potential change points.

6.3.2 A significance test for change-points

One issue which arises with graphical interpretation is the problem of subjectivity in determining which evident breaks of slope are real and not minor random chance effects. To this end, permutation testing was employed (described below) to check statistical significance of slope changes.

Permutation test of significance of changes in slope

The permutation test randomly reorders data-points in the original data series for statistical inference. Each data point from the original data series appears only once in each new generated data set. Then a calculation is made to find the number of times the test statistic from the permuted variables is better than the statistic from the original test.

In this study, the test statistic (E) which equals to $\min \sum_{i=1}^{n} e_i$ in Equation 13 is the piecewise total sum of least square errors given by a change point.

The procedure of permutation test is:

1. Define the null hypothesis is the magnitude of the E value is not different to that which could have arisen by random chance.
2. Randomly create a new data set consisting of the raw data with random reordering.
3. Calculate the test statistic *E'* for all of the possible break-points of the new data set and compare them to *E* to check if they are smaller.
4. Repeat procedures 2 and 3 1000 times.
5. If the original test statistic *E* is bettered by more than 5% of the *E'* under randomisation, then the null hypothesis is accepted at the 0.05 level. Otherwise, the null hypothesis is rejected at 5% level (The p-value is the fraction of permuted tests which are more significant than or as significant as the original test).

The permutation test determines whether randomly reordering the data might result in smaller sum of squares. If more than 5 % of the new minimum sum of least squares values are less than the original minimum sum of least squares, then the change point is deemed not significant at the 0.05 level.

6.4 Detecting Signals of Land Use Change and Climate Variation from Rainfall and Runoff Variation

Using the LSR method, the change point times in rainfall and river flows are determined. Many significant but minor shifts with less than 10 percent change in mean value were detected. To determine the type of signals, the large breaks (with large percentage change in mean) were considered. Briefly, the set of change points due to land management impacts are identified as change in rainfall runoff relationship. However, the set of discharge change points due to climate shifts are associated with concurrent rainfall changes.

6.5 Additional Graphical Analysis

Through change points detection, the rainfall, runoff and rainfall-runoff series are divided into several series segments with different characteristics. For runoff series, each divided segment may be recognized as a natural period series, or a land use shift period series. For rainfall series, the segment division is on the basis of climate variation. The goal is to identify how rainfall, runoff and their relationship changes and identifying the causes. Thus, to interpret the changes of either variable in spatial and temporal areas, various methods may be incorporated such as graphs, maps, and statistical techniques.

Percentage change in mean

In a time series, to compare the magnitude of change before and after a change point, percentage increase or decrease in mean are measured. It is the most basic way to compare the segment before and after a change point.

In theory, suppose a single change happens in a long tern time series, the mean value of the initial part series is X_1, and the mean of the later series segment is X_2. The percent change, D%, is calculated as the standard relation:

$$D\% = 100 * \frac{X_2 - X_1}{X_1} \qquad \text{Eq. 14}$$

Standard error of the mean

Standard error of the mean (SEM) is used to summarize the likely accuracy of the sample mean as compared with the population mean. SEM reflects the distribution of sample means and gives a measure of how well a sample represents the population. The smaller the standard error, the less the spread and the more likely it is that any sample mean is close to the population mean. In other words, when the sample is representative, the standard error will be small. It is calculated through the following formula:

$$StErr = \frac{\sigma}{\sqrt{n}} \qquad \text{Eq. 15}$$

Where $StErr$ (SE) is standard error of the sample mean,

σ is the standard deviation of the sample,

n is the size of the sample.

For a normal distribution of sample means, there is a 95 percent chance that a sample mean lies within around two standard errors of the true mean. The equations below calculate the 95 percentage confidence intervals:

$$\text{Upper 95\% Limit} = X_i + StErr * 1.96 \qquad \text{Eq. 16}$$

$$\text{Lower 95\% Limit} = X_i - StErr * 1.96 \qquad \text{Eq. 17}$$

where X_i is the sample mean,

Within a time series, SE is calculated for each segment separated by the change points. Each of the SE will have an error bar showing the 95 percent confidence intervals. It should be noted that for each two adjacent SE bars, if they present non-overlapping error bands, the corresponding change date will be confirmed as a significant change.

Temporal distribution of shifts

The graph showing the temporal location of change points in all of the time series is created. The positive shifts are marked by positive signs and the negative shifts are marked by negative signs.

Spatial distribution of shifts (spatial correlation maps)

Maps were created for displaying the spatial distribution of shifts for each variable. Sites with a similar important change year are marked. These maps assist in identifying whether any spatial patterns dominated in a specific region. Moreover, when comparing the maps of different variables, the relationship of the variables may be interpreted.

Histogram for the rainfall time series

Histograms were employed to show how the distribution of total rainfall events changes before and after the shift.

Average monthly rainfall/mean runoff plots

These plots summarize the variation of rainfall/runoff by month. The series separated by change points were plotted together for each data set. It will be clear to see how rainfall/runoff changes by month, how rainfall/runoff changes for each month after the detected change year as well as rainfall/runoff in which month changes more than other months.

Flow duration curves (FDC)

FDC is a plot of discharge in daily, monthly or yearly scale against the percentage of time that discharge was equalled or exceeded. It provides a comprehensive view of the runoff variability and represents the relationship between magnitude and frequency of streamflow (Vogel and Fennessey, 1995). In this study, month-based FDCs for each gauge for the period before and after the change points are plotted. Any significant change in the climate or land use will lead to a difference between the FDCs for the periods before and after each change point.

Rainfall/runoff scatter diagrams

Comparison of rainfall/runoff relationship before and after each change point can be achieved by rainfall runoff scatter diagrams. The linear regression of the two datasets provides an R-square which shows how well the two variables are linealy correlated.

6.6 Conclusion

In summary, the piecewise linear regression method gives convenient and automated detection of change points in rainfall or runoff cumulative plots. For the determination of signals of climate variation and land use changes, change points with larger percentage change in mean are considered. The graphical interpretation methods vary for the investigation of the difference between stable periods separated by various types of change points (driven by land use or climate variation).

Chapter 7– Rainfall/Runoff Variations

7.1 Introduction

Small climatic transitions from one climatic mode to another were checked by seeking possible change points in rainfall time series. Rainfall change points can indicate climatic variations, particularly if the effect is repeated over a number of sites over a wide area. In this chapter, rainfall shifts are first analysed. It is emphasized that the research focus here is on relatively short term transitions from one climatic mode to another, as opposed to any overall trend over a long period of time that might be associated, for example, with climate change resulting from global warming. The spatial trend analysis maps were utilized to study the distribution of a rainfall shifts over the whole study area. Additionally, a further investigation of the difference of each stable rainfall period separated by four evident change years (1981, 1988, 1994/5 and 1998) have been analysed through average monthly rainfall value diagrams as well as the rainfall histograms showing the distribution of total rainfall events.

River discharge shifts could derive from either a climatic shift, and/or a change in catchment land use. Discharge shift with concurrent rainfall shift is evidence for a change in climate regime, particularly if the effect is repeated over a number of sites over a wide area. For the spatial studies, river discharge shifts in 10 specific gauges are analysed in this chapter. The rainfall-runoff relationship for different stable periods separated by change-points are analysed through rainfall runoff scatter plots, flow duration curves and average mean monthly discharge diagrams.

7.2 Shifts in Mean Rainfall

Analysis for possible change points in rainfall time series was carried out with respect to data from 59 gauge sites in the Waikato and Whanganui catchments (Figure 7.1). A listing of rainfall sites used is given in Appendix A-a and A-c.

For the purposes of this investigation, a break point was deemed to be any change of slope in the cumulative plots, statistically significant at the 0.05 level (see Chapter 6). Sometimes the detected shift, while significant in the statistical sense,

involved only small changes in the before/after mean values. However, this does represent climatic information and aids the possible identification of concurrent shifts in the same direction (positive or negative) over the whole or part of the study region. The significant rainfall change-points detected by the least square regression method is presented in Appendix B-a.

Interestingly, the detected rainfall changes tend to cluster in time, with similar times for the same sign of change. That is over space toward a dominance of either greater or lower values of rainfall (Figure 7.1). Given the rain gauge sites are widely distributed, the clustering of signs in Figure 7.1 indicates spatial correlation of shifts in rainfall, consistent with temporary shifts in weather patterns to different modes. The implication here is that such widespread rainfall shifts should also be evident in corresponding discharge shifts, discussed in the next section.

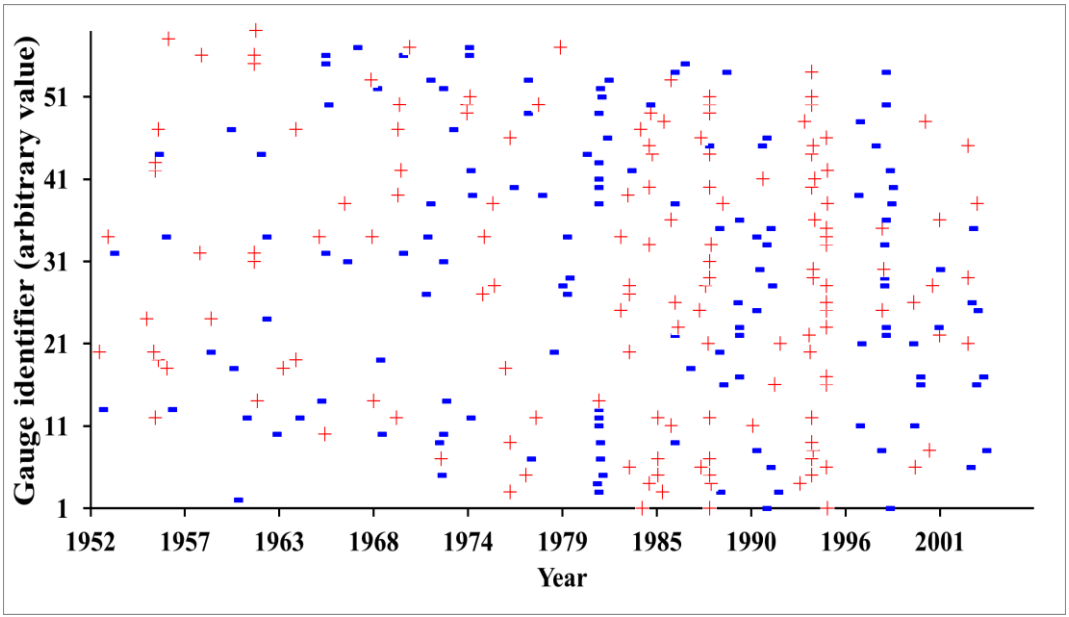

Figure 7.1: Times of statistically significant (p = 0.05) rainfall transitions in the 59 gauges analysed. Red crosses denote transition to increased rainfall; blue dashes denote shifts to lower rainfall.

With respect timing, it is evident from Figure 7.1 that there is a regional transition to higher rainfalls within the periods 1975-77, 1983-88, and 1993-96, with one toward lesser rainfall in the intervening periods.

The low density of the markers in the left of Figure 7.1 is a data availability effect because many rain gauges were not emplaced until after 1970. In contrast, the density of recent markers (to the right of the plot) is higher. Therefore, trend shifts after, say, 1975 are more visible. However, in reality it is likely that rainfall shifts occurred with similar intensity in the earlier period.

Not all rain gauge sites showed statistically significant concurrent changes, and there is some spatial variability as well. However, there is a strong preponderance for the statistically significant changes to be of common sign in any one time period. For example for the change 1981, of the 37 analysed rain gauges operational, 17 statistically significant shifts were detected and of those 16 were a shift to less rainfall. For the 43 gauges analysed, for 1988, 20 exhibited significant shifts in that year, 15 of which were in the direction of increased rainfall. For the 41 rain gauges analysed, for 1994/5, 31 of them showed significant change points in 1994/5, all of which indicates shifts to more rainfall. For the change year 1998, among the 35 rain gauges analysed, 16 demonstrated significant changes in that year, 13 of which were in the direction of decreased rainfall.

On average for the whole study region, comparing the average monthly rainfall in consecutive stable periods indicates average monthly rainfall decreased 12.3% in 1981, increased 14.8% in 1988, increased 13.5% in 1994 and decreased 12.7% in 1998.

Figures 7.2-7.5 show plots of the signs of change of rainfall for selected periods of evident change, together with the magnitude of the changes in percentage terms.

Figure 7.2 shows gauge stations with a decreasing change in 1981. From the distribution of the downward arrows, it is evident that the 1981 shift happened over the whole study area except the Coromandel coastal areas. In contrast to the change in 1981, an increasing shift happened in 1988 and the spatial pattern is shown in Figure 7.3. The homogenous increasing rainfall in 1988 distributed mainly in the south of the study area as well as the coastal area in Coromandel. Interestingly, all five gauges showing a change in the opposite direction were in a small geographical area in the northern Hauraki plains and southern Coromandel

(Figure 7.3) which may because of a local lee effect. In 1994 and 1995, the increased rainfall distributed over the whole study area as shown in Figure 7.4. The change year 1998 was decreasing rainfall distributed mainly in the middle, middle-east and north of Coromandel area of Waikato region. However, two gauges showing the opposite direction are located in the northern Hauraki plains, southern Coromandel and the east of the Ruapehu volcano (Figure 7.5).

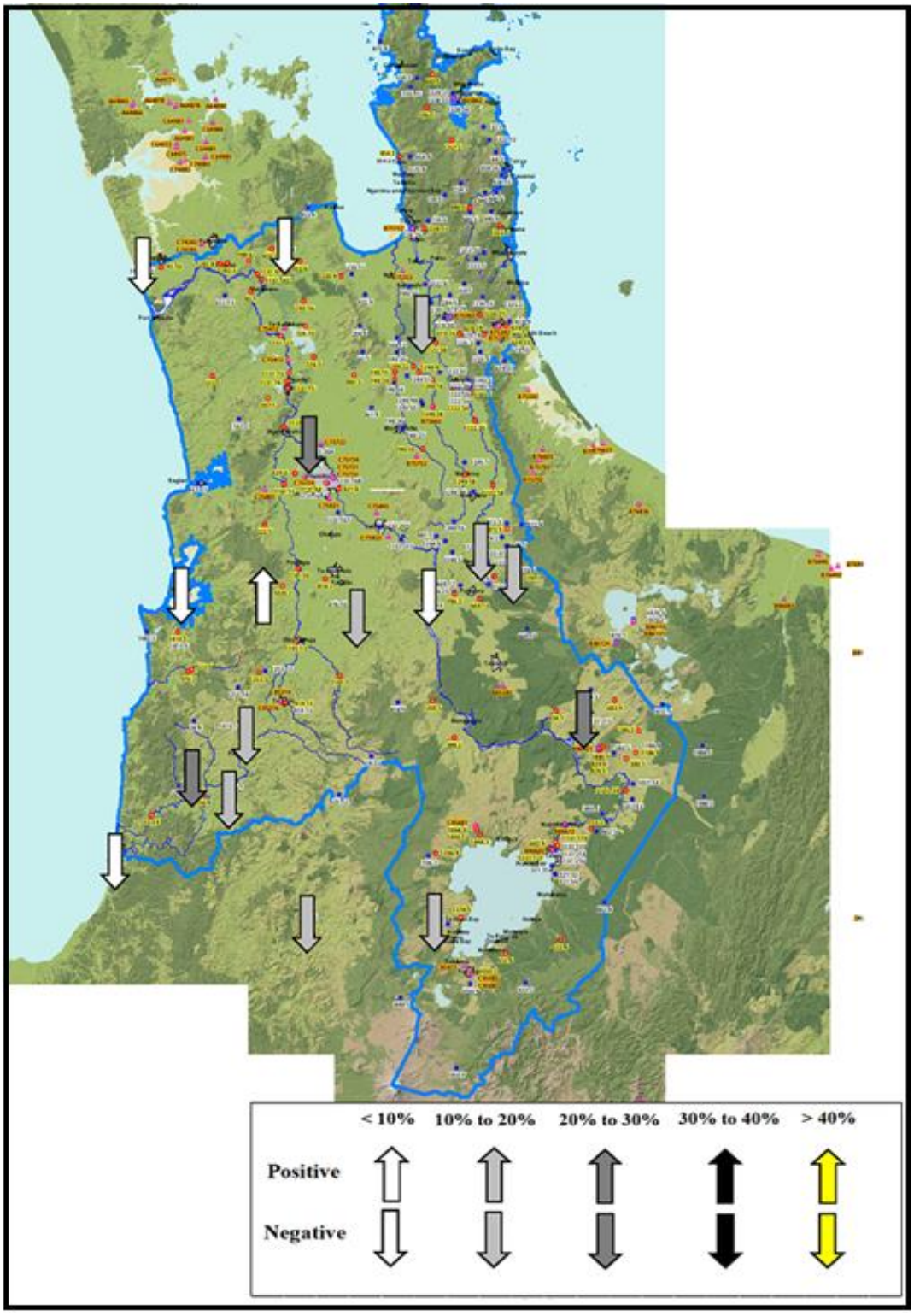

Figure 7.2: Rainfall shift directions and shift magnitudes for 1981 break-points

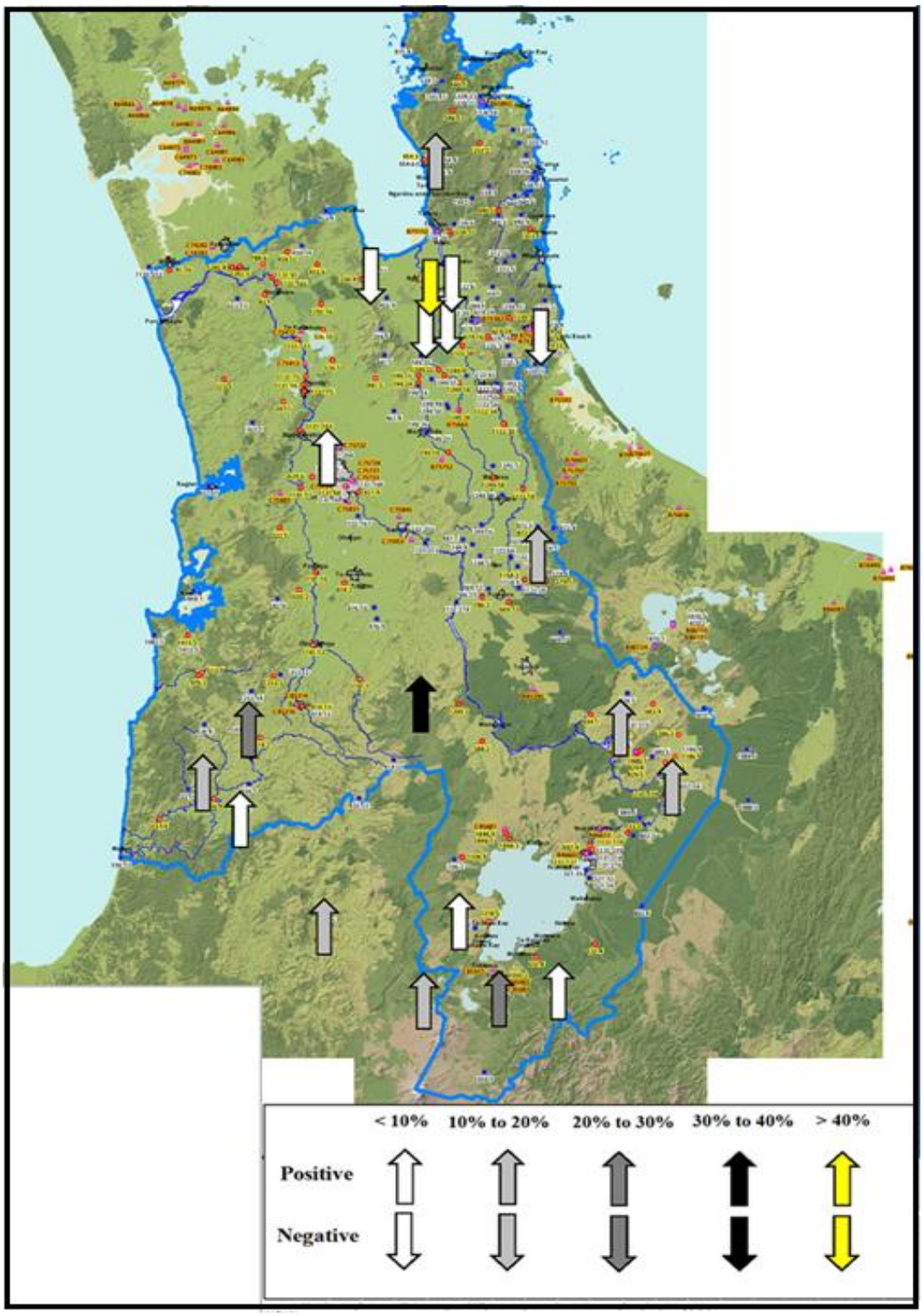

Figure 7.3: Rainfall shift directions and shift magnitudes for 1988 break-points

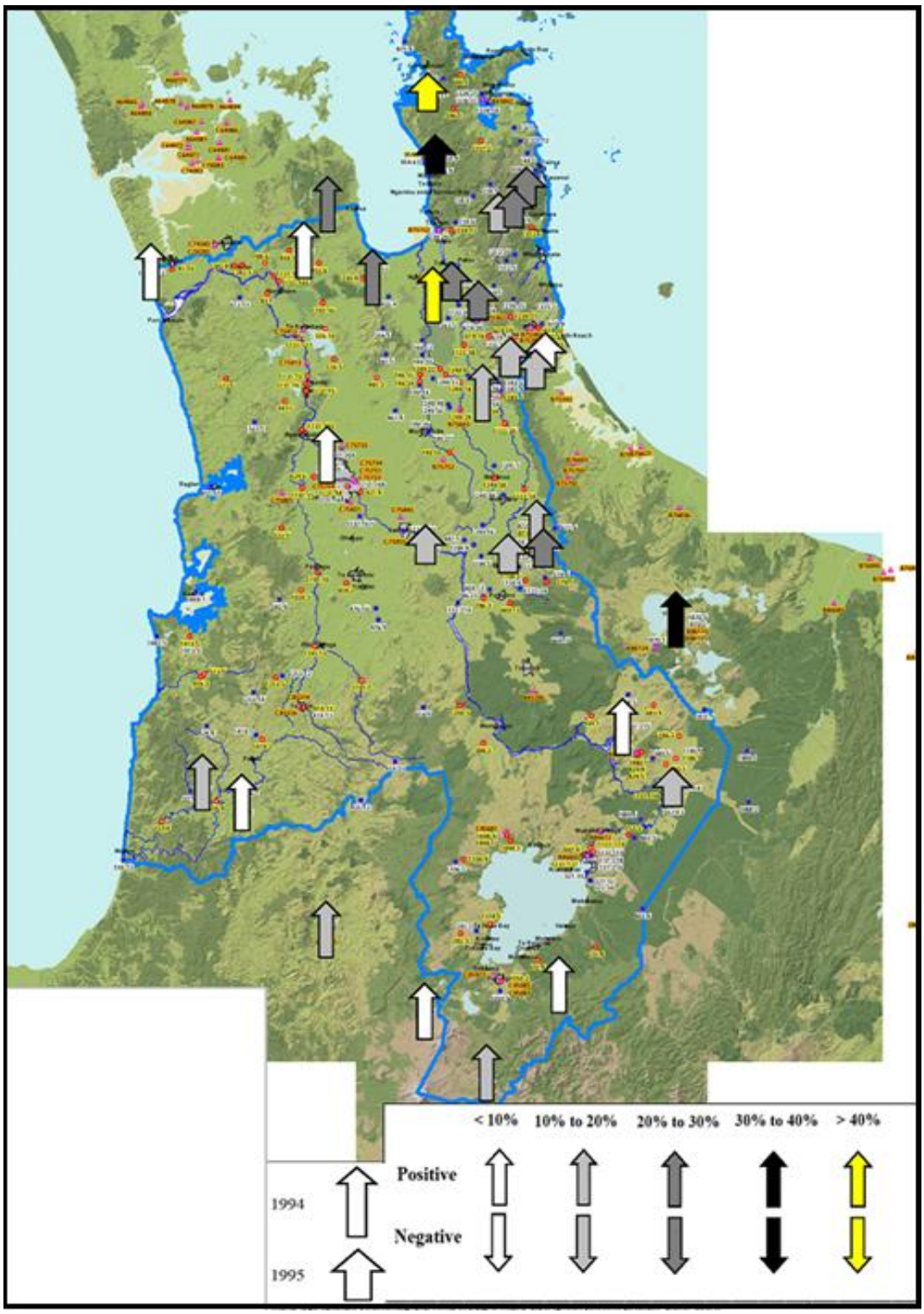

Figure 7.4: Rainfall shift directions and shift magnitudes for 1994/5 break-points

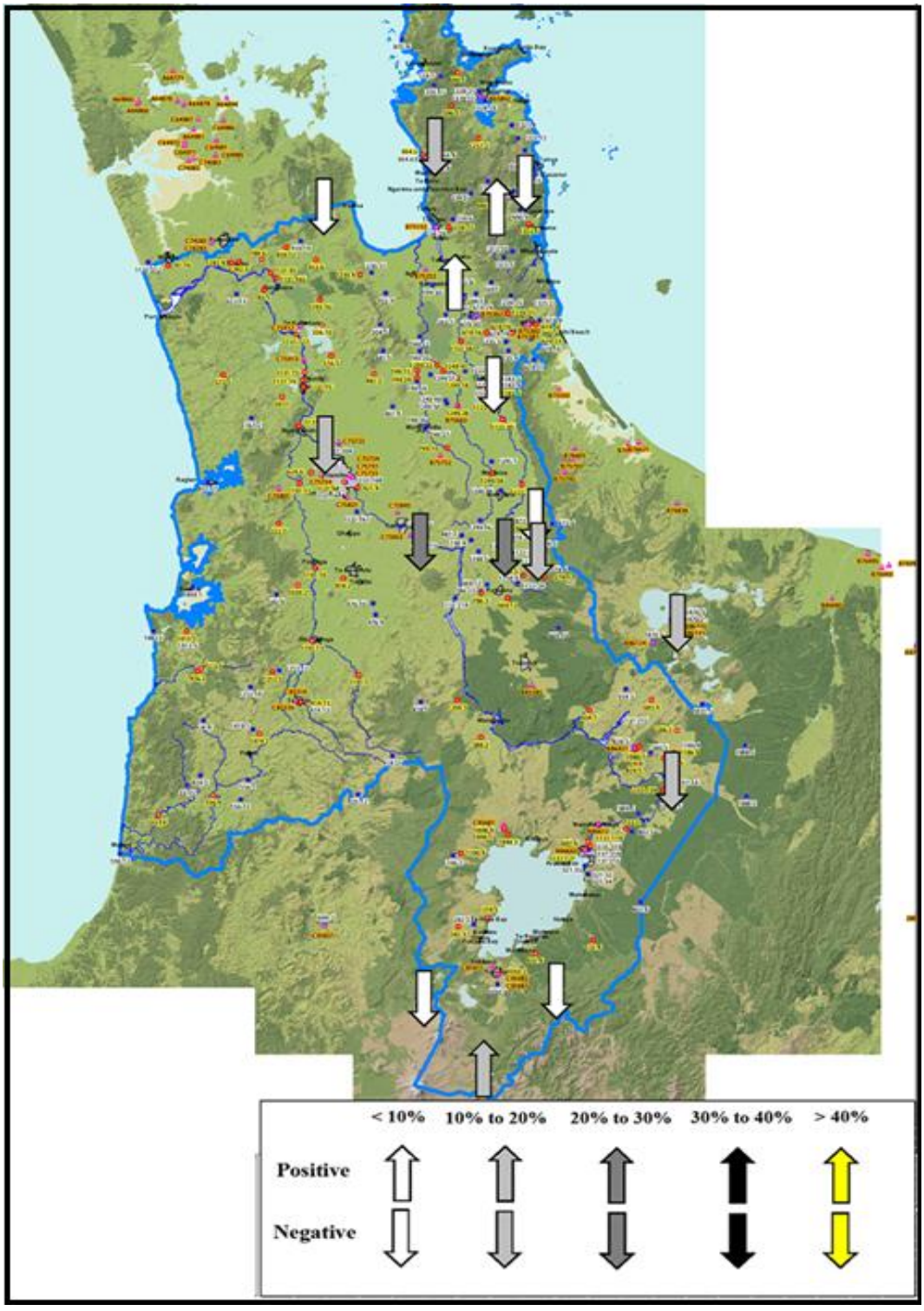

Figure 7.5: Rainfall shift directions and shift magnitudes for 1998 break-points

7.3 Investigation of Differences of Rainfall Characteristics over Various Stable Periods

The shifts in rainfall from one period to the next are not necessarily consistent over all rainfall magnitudes. Sometimes the change is driven by changes in particular rainfall frequencies and not others. Moreover, sometimes the important difference may happen in some particular months of the year. To future investigate the difference of rainfall among various stable periods separated by change-points, rainfall histograms and the rainfall monthly variability were utilized. This is helpful for calculating whether any particular factor contributes to the differences. The four notable change years, 1981, 1988, 1994/5 and 1998, were selected for further analysis. In this section the study period began in 1975 and finished in 2002. The transition periods separated by the four change years 1981, 1988, 1994/5 and 1998 were determined as the stable periods. Therefore, the rain time series containing any one of the change years were selected for the comparison analysis.

In total, 16 rain gauges indicated significant shift to decreased rainfall in 1981, 15 rain gauges showed significant increase in 1988, 31 gauges increased significantly in 1994/5 and 13 gauges decreased significantly in 1998.

7.3.1 Comparison of rainfall events in each stable period using histograms

Rainfall histograms were created for the different stable periods 1975 - 1981 and 1981 - 1988 using rainfall from 16 rain gauge sites where significantly decreased rainfall in 1981 was detected (Appendix C-a). The change year 1988 were detected from 15 rainfall time series, the rainfall histograms for the stable periods 1981 to 1988 and 1988 to 1994 were plotted (Appendix C-b). At 31 rain gauges, the rainfall pattern significantly increased in 1994/5. The histograms for the stable periods 1988 to 1994/5 and 1994/5 to 1998 were compared (Appendix C-c). At 13 gauges, rainfall decreased significantly in 1998, and the histograms for the stable periods 1994/5 to 1998 and 1998 to 2002 were created (Appendix C-d).

Comparing all the rainfall histograms for the stable period before and after the respective change years, there are some key components in common. For the change year 1981 (Appendix C-a), the reduction of rainfall for the period 1981 to 1988 was particularly obvious for the range of high rainfall events. For the stable periods before and after 1988 and 1994/5 (Appendix C-b, c), the increased rainfall for the later period was mainly due to the occurrence of high rainfall events that were not present in the former period. From Appendix C-d, the pattern of extreme monthly rainfall for the period after 1998 is different to the period prior with less extreme rainfall events after 1998 compared with the period before.

One of the rain gauges which changed in all of the four selected obvious years is shown here as an example. Figures 7.6- 7.9 illustrate such changes by magnitude for Taumarunui rainfall (gauge site: Whanganui River at Taumarunui).

To conclude, there is a common feature in that the key differences between the different stable periods before and after the selected change years were mainly the high or low frequency of the extreme rainfall events.

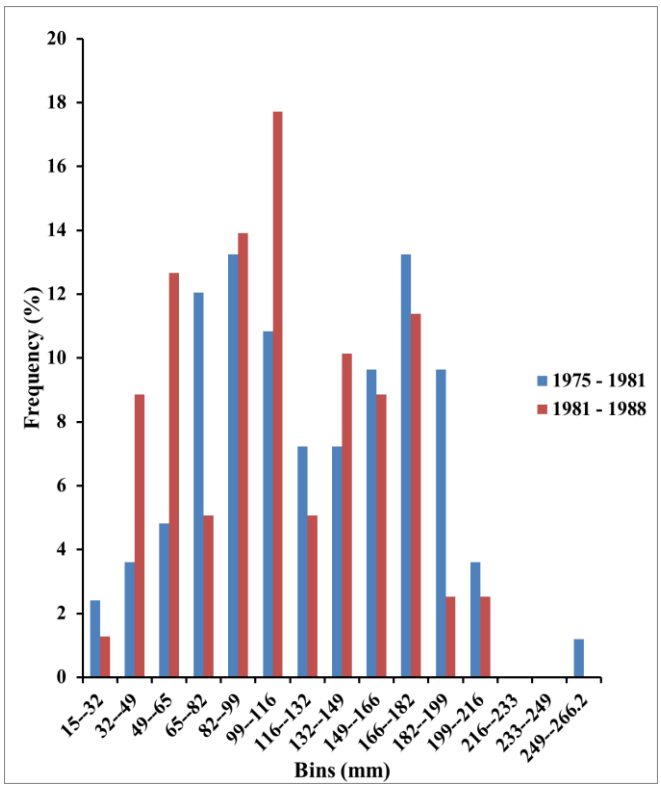

Figure 7.6: Rainfall histograms for the different stable periods before and after 1981 (Whanganui River at Taumarunui)

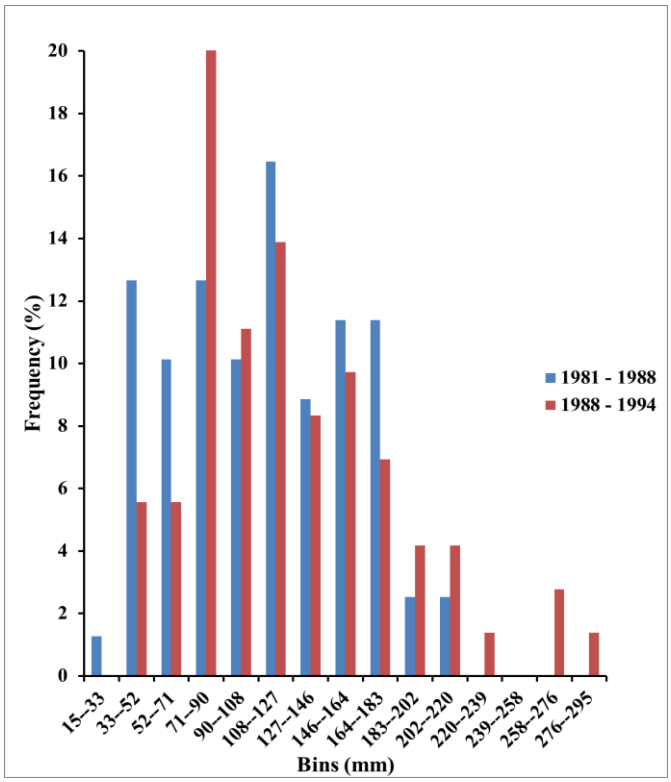

Figure 7.7: Rainfall histograms for the different stable periods before and after 1988 (Whanganui River at Taumarunui)

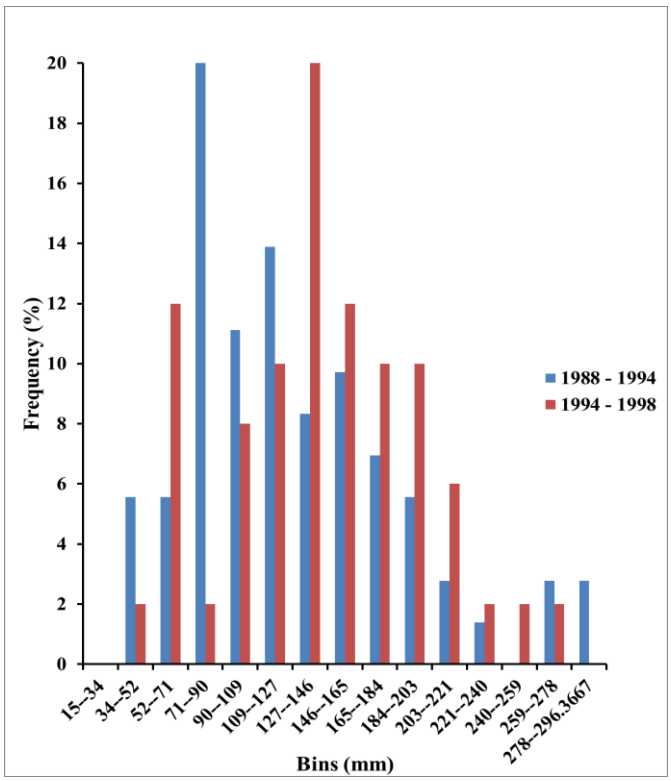

Figure 7.8: Rainfall histograms for the different stable periods before and after 1994 (Whanganui River at Taumarunui)

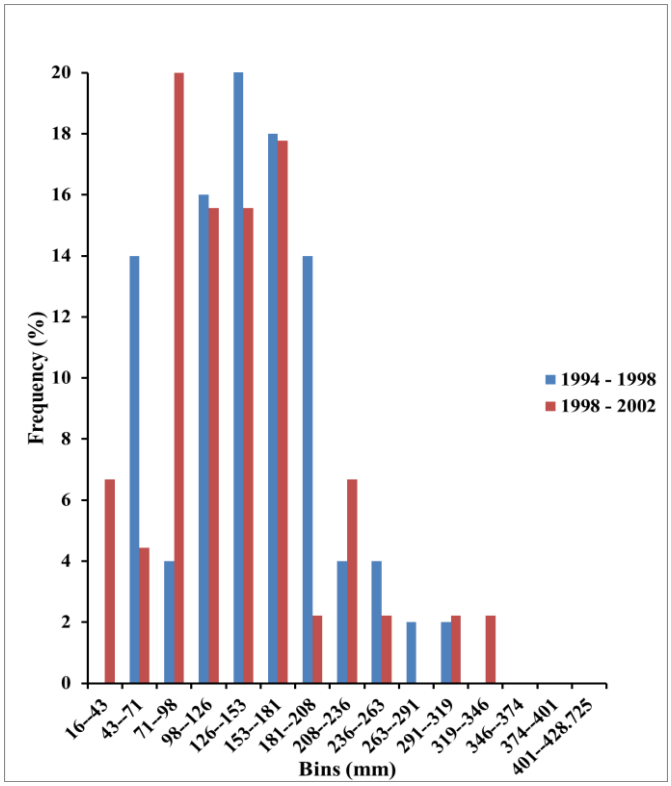

Figure 7.9: Rainfall histograms for the different stable periods before and after 1998 (Whanganui River at Taumarunui)

7.3.2 Comparison of each stable period rainfall characteristics using average monthly rainfall variability

As discussed in Chapter 5.4, the monthly rainfall data for all of the series of 59 gauges are independent with poor r^2 less than the threshold of 95 % confidence. For this reason, for each individual month, the two standard errors which represent 95 % confidence intervals for each individual month were initially calculated. The average monthly rainfall for each stable period was then plotted, together with the two standard errors of the mean for the selected rain gauges. For each month, if the error bars of different periods overlap, this represents the difference is not significant, otherwise, it is significant.

Similar to the period comparison in section 7.3.1, the average monthly rainfall for the periods before and after 1981, 1988, 1994/5 and 1998 for the selected gauges were analysed as shown in Appendix D-a, b, c and d.

The average monthly rainfall curves showed an obvious seasonal pattern with more rainfall in the winter season and less rainfall in the summer season. When focusing on the identification of the common features of the figures, it was found that the most noticeable change from the selected change year is the significant increase or decrease in rainfall in the peak rainfall months, although some of the figures showed little difference. From the distribution of the errors, the differences between the two stable periods before and after the change years were found to be significant in June to August. In other words, the winter season significantly drove the difference in rainfall over the various stable periods. This result coincided with the conclusion drawn from section 7.3.1, that the factor leading to the notable difference over different period at each gauge site is the variability of high rainfall events (winter season). Comparing the four change years (1981, 1988, 1994/5 and 1998), the changes in winter rainfall for the change years 1981 and 1988 were much more significant than those for the other two change years. The difference of monthly rainfall for the period before and after 1994/5 is small with no particularly significant increase over the 12 months. For the change year 1998, except the significant change in winter months, some of the gauges also experienced significant reduction in February or March.

Figures 7.10- 7.13 illustrate an example of such changes by month for rainfall in Taumarunui and Te Porere (gauge site: Whanganui River at Taumarunui, Whanganui River at Te Porere).

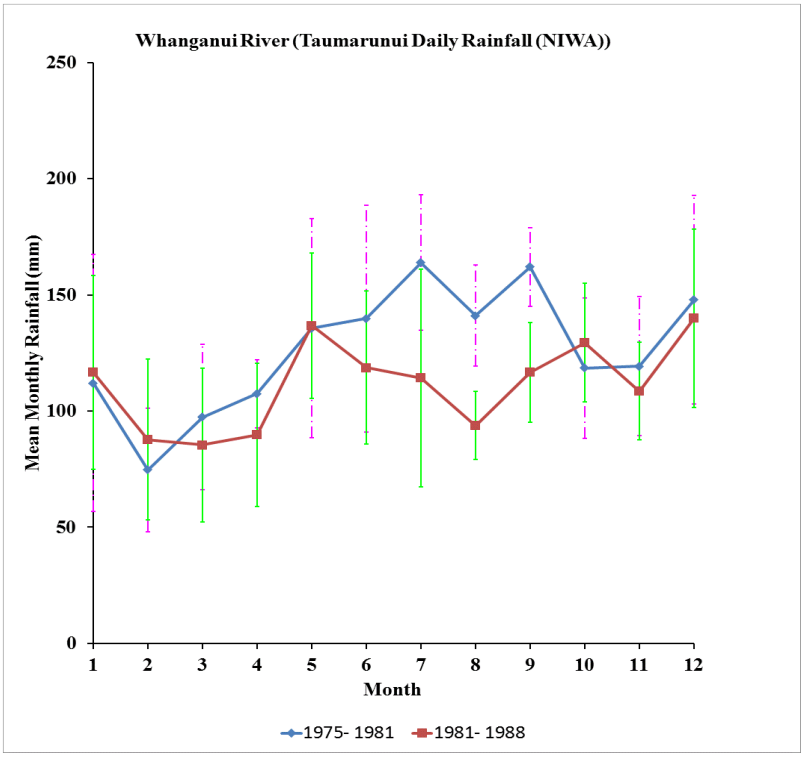

Figure 7.10: Average monthly rainfall for the stable period before and after 1981 (Whanganui River at Taumarunui)

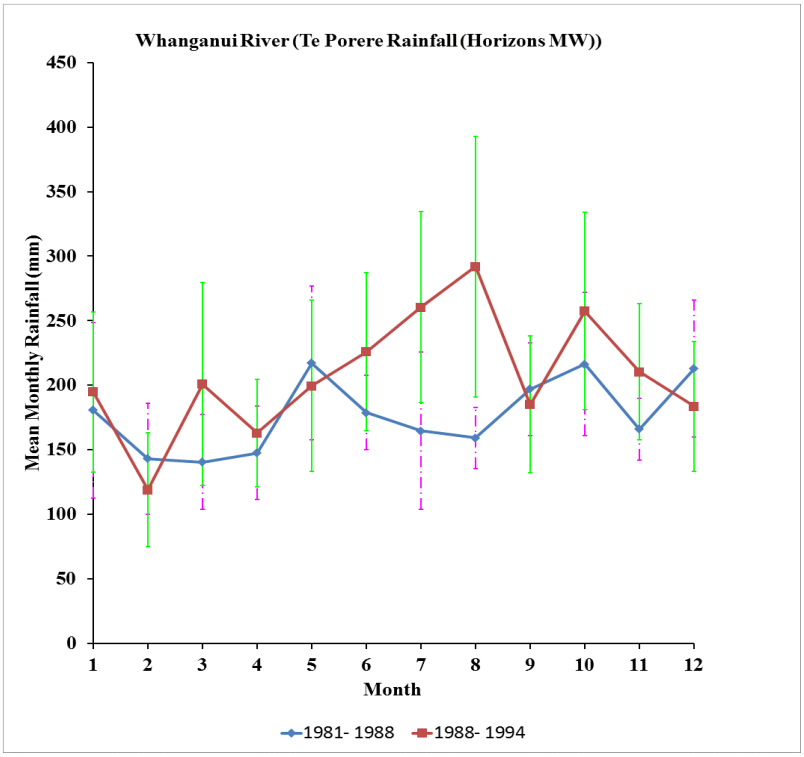

Figure 7.11: Average monthly rainfall for the stable period before and after 1988 (Whanganui River at Te Porere)

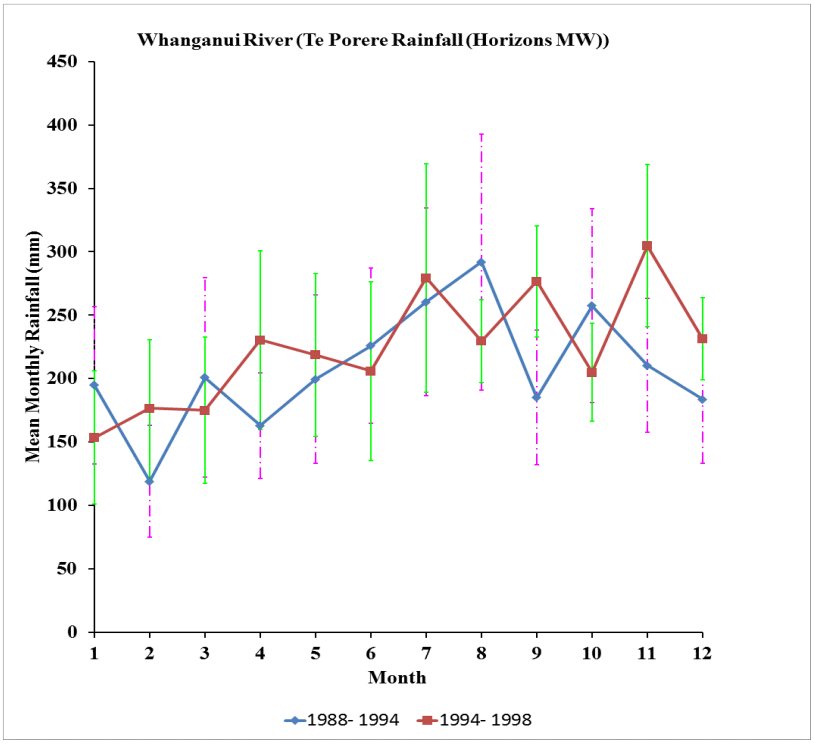

Figure 7.12: Average monthly rainfall for the stable period before and after 1994 (Whanganui River at Te Porere)

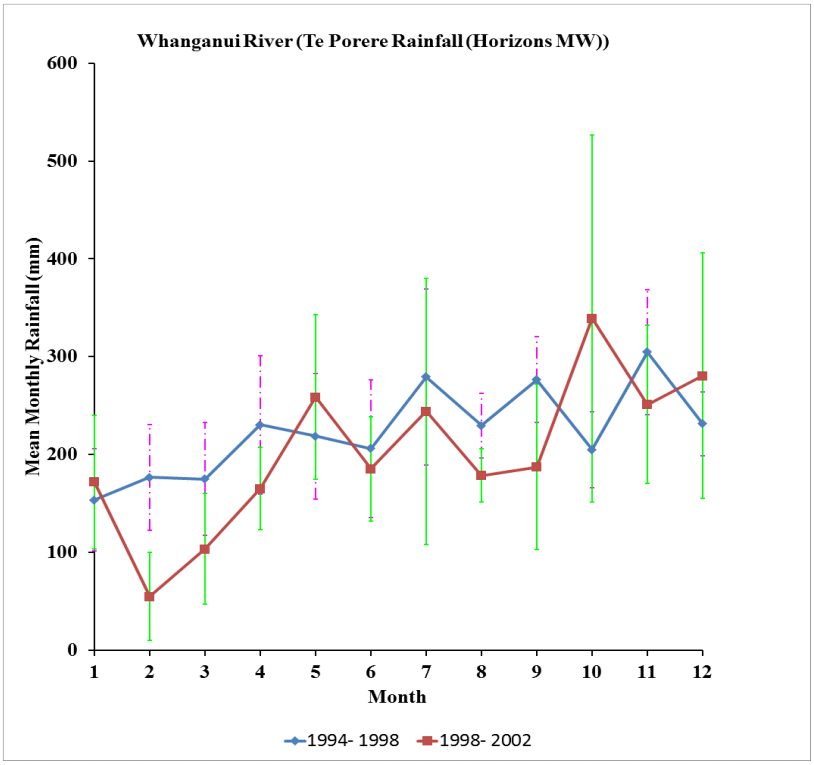

Figure 7.13: Average monthly rainfall for the stable period before and after 1998 (Whanganui River at Te Porere)

7.4 River Discharge Shifts

River discharge shifts could derive either from a climatic shift, or a change in catchment land use under a constant climatic regime. It is useful to find whether there are concurrent change points in runoff time series, and associated shifts in rainfall which give strong evidence for a change in flow regime driven by a shift in rainfall regime, particularly if the effect is repeated over a number of sites over a wide area.

River discharge significant break-points ($p<0.05$) were detected at 44 flow gauges sites (Appendix B-b). The mean values as well as the percentage change in the mean for the stable periods before and after the detected change years are calculated (Appendix B-c). An alternation between positive and negative changes is evident (Figure 7.14), reflecting the corresponding rainfall shifts shown in Figure 7.1. Transitions in the earlier part of the record are not so evident due to a smaller number of operational flow gauges. The times of the detected changes tend to cluster, with similar times for the same sign of change toward either greater or lower values of discharge (Figure 7.14). Compared to the rainfall time series, the temporal trend distribution in flow time series is more apparent with less noise. It is worth noticing that the plotted sign breaks are not independent as there is spatial correlation of flow and sometimes multiple recording sites on the same river. However, the alternation of positive and negative signs is interesting with data from an extensive region being of practical interest for water right considerations.

The clustering is clearer with the increase of data sites from the later 1970s. It can be seen that from 1975 to 2000 there were two apparent decreasing changes. One is the decreasing shift in the mean monthly flow that happened over most of the rain gauge recorders around 1981 and 1998. While within 1981 to 1998, there were several plus uniform shifts, separated by a lesser decline trend in 1990. Mean monthly flow increased in the period 1982 to 1988 with apparent shift in 1988, and from 1989 to 1992 there was a downward shift in rainfall pattern; 1994 is an evident increasing shift. These uniform shifts in river flow time series which

correspond to the shifts in rainfall series suggest it has the most chance of river flow being impacted by rainfall directly.

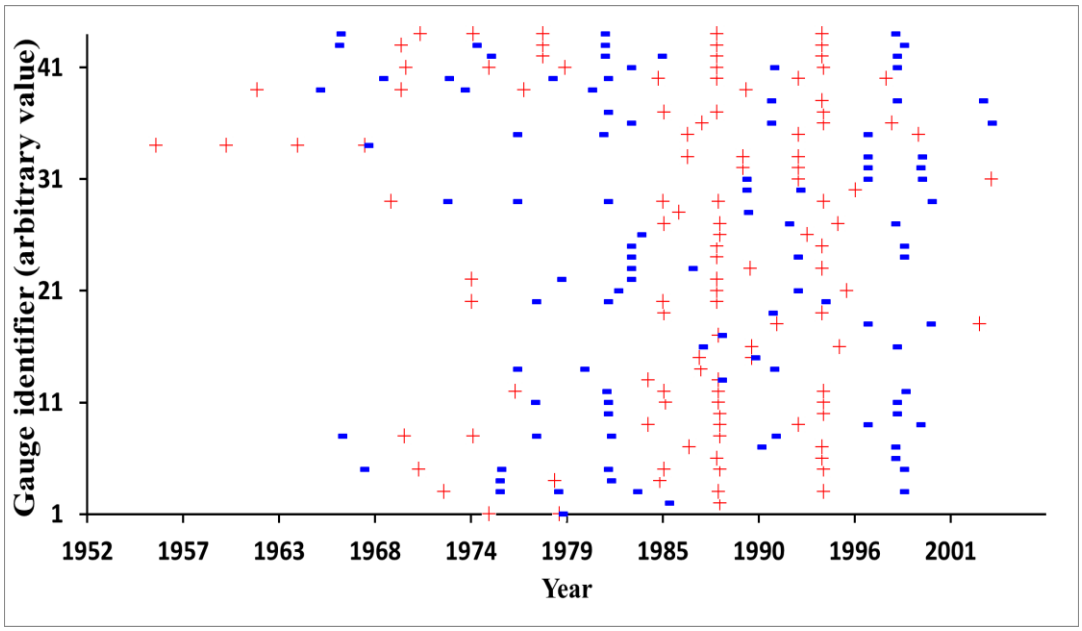

Figure 7.14: Statistically significant (p = 0.05) river discharge transitions in the 44 flow gauge sites analysed. Red crosses denote transition to increased discharge; blue dashes denote shifts to lower discharge.

Similar to rainfall, not all discharge gauge sites showed statistically significant concurrent changes, and there is some spatial variability as well. However, there is a preponderance for statistically significant changes to have a common sign in any one time period. For example, for the change year 1981, of the 18 analysed operational runoff gauges, 13 statistically significant shifts were detected and all of them were a shift to less runoff. For the 38 gauges analysed for 1988, 25 exhibited significant shifts in that year, all of which were in the direction of increased runoff. For the 32 rain gauges analysed, 22 of them showed significant change points in 1994/5, 21 of which indicated shifts to higher runoff. For the change year 1998, among the total 26 rain gauges analysed, 18 demonstrated significant changes in that year, 16 of which were in the direction of decreased runoff.

On average for the whole study region, comparing the average monthly mean discharge in consecutive stable periods indicates average monthly mean discharge decreased 21.5% in 1981, increased 35.7% in 1988, increased 20.2% in 1994 and

decreased 16.6% in 1998. Figures 7.15-7.18 show plots of the sign of change of discharge for selected periods of evident change, together with the magnitude of the changes in percentage terms.

The flow gauges exhibiting a change for a given change year were then identified on a map to check any evident spatial pattern in the trend concerned. Figure 7.15 plots all the flow gauge stations showing a decreasing shift in 1981. From the spatial distribution of downward arrows, the 1981 decreasing shift in river discharge evidently had a focus in the lower and upper-middle of Waikato region. In contrast, the 1988 shift toward increasing discharge occurred over almost the whole study region except Coromandel (Figure 7.16). In 1994 and 1995, river discharges increased for all sites (Figure 7.17). The shift to decreased discharge in 1998 also encompassed the whole Waikato region and the north of the Whanganui region (Figure 7.18).

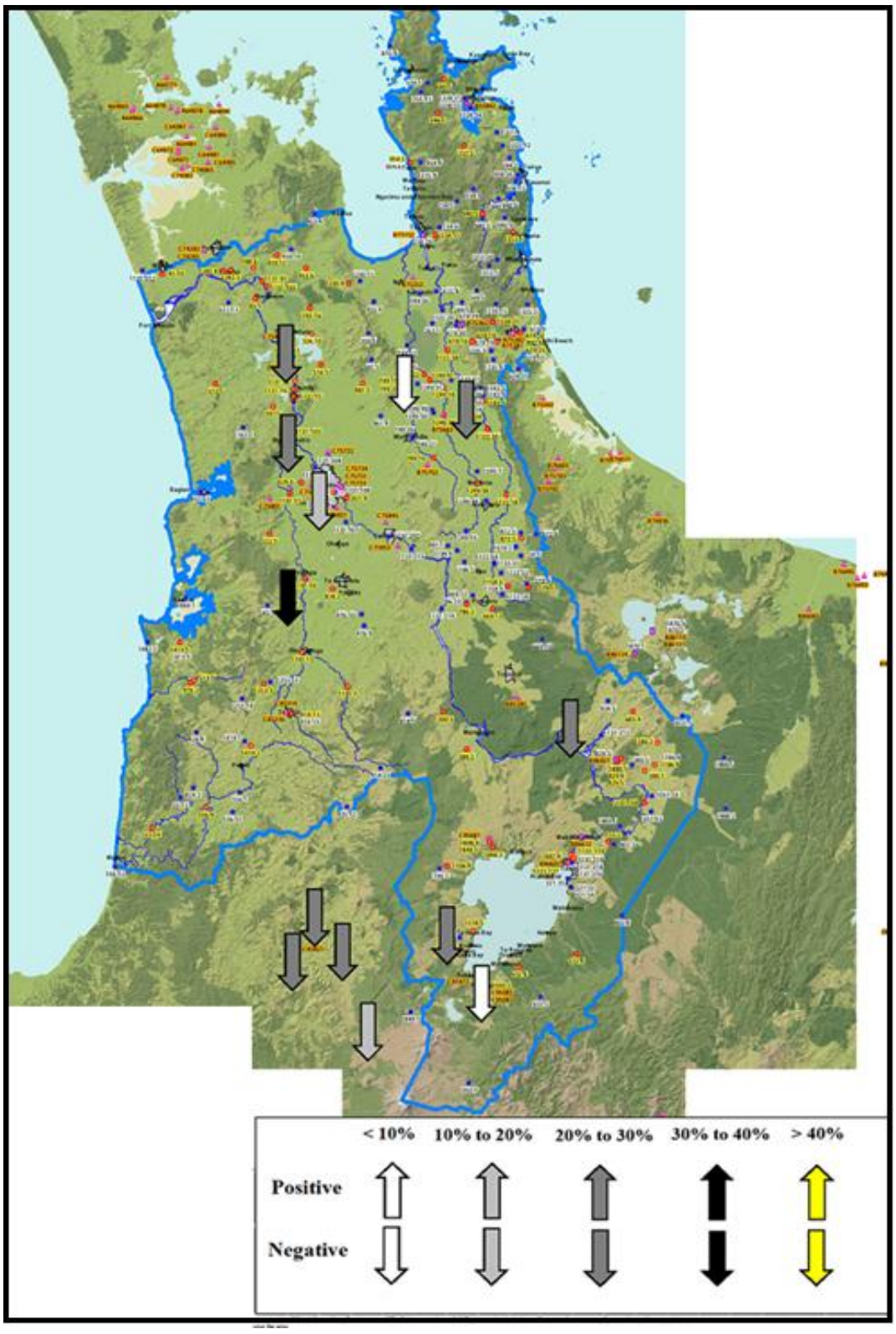

Figure 7.15: Mean discharge shift directions and shift magnitudes for 1981 break-points

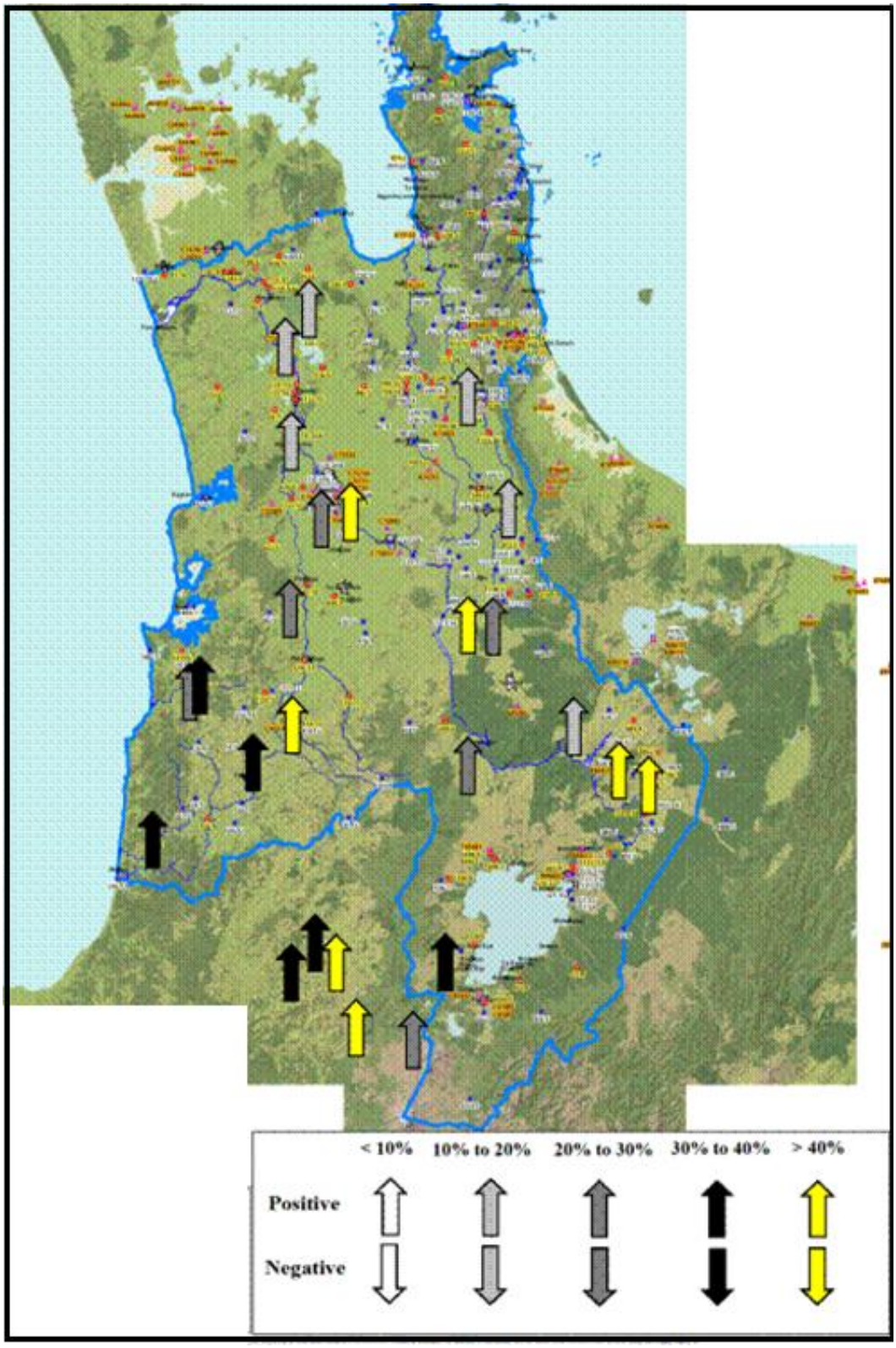

Figure 7.16: Mean discharge shift directions and shift magnitudes for 1988 break points

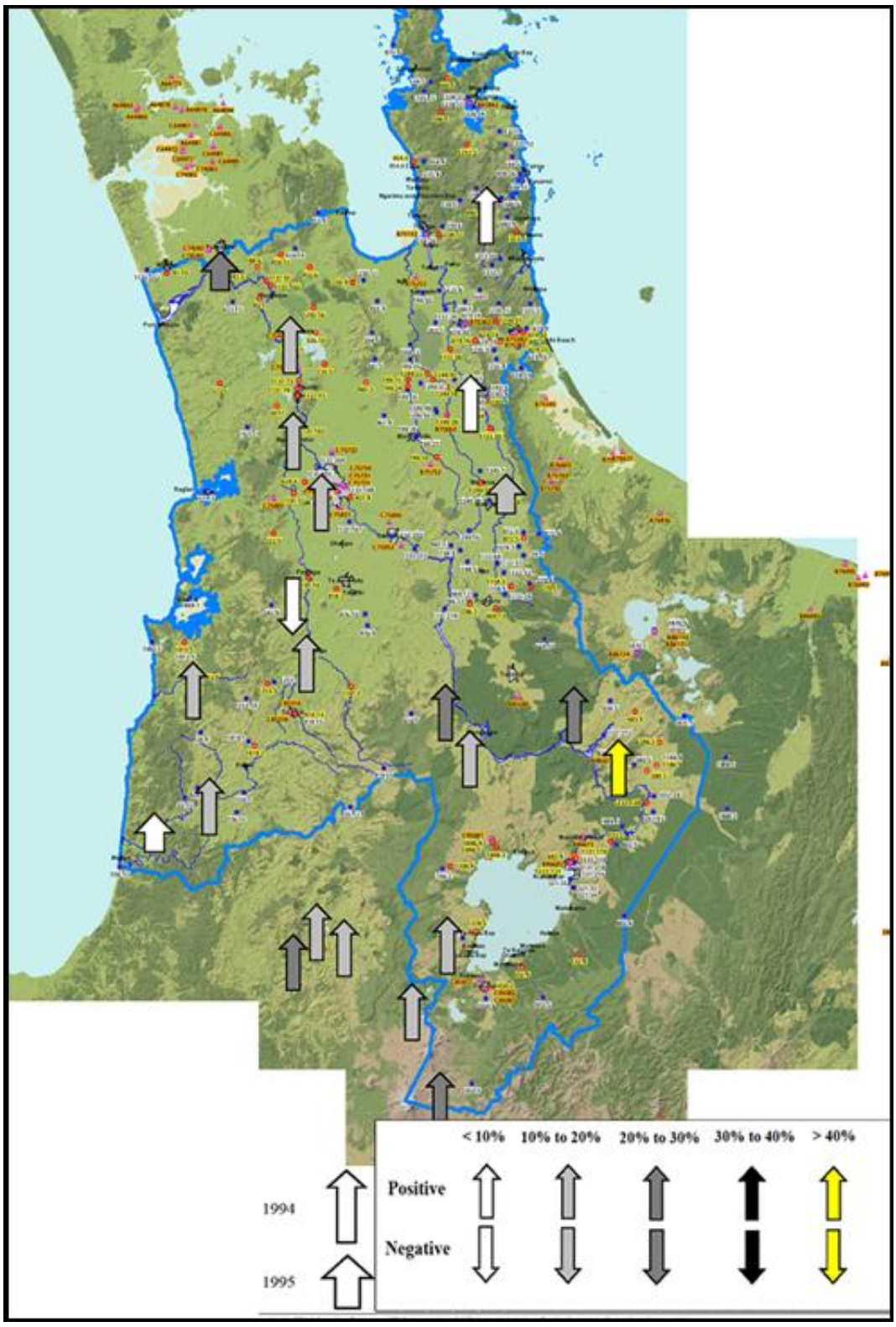

Figure 7.17: Mean discharge shift directions and shift magnitudes for 1994/5 break-points

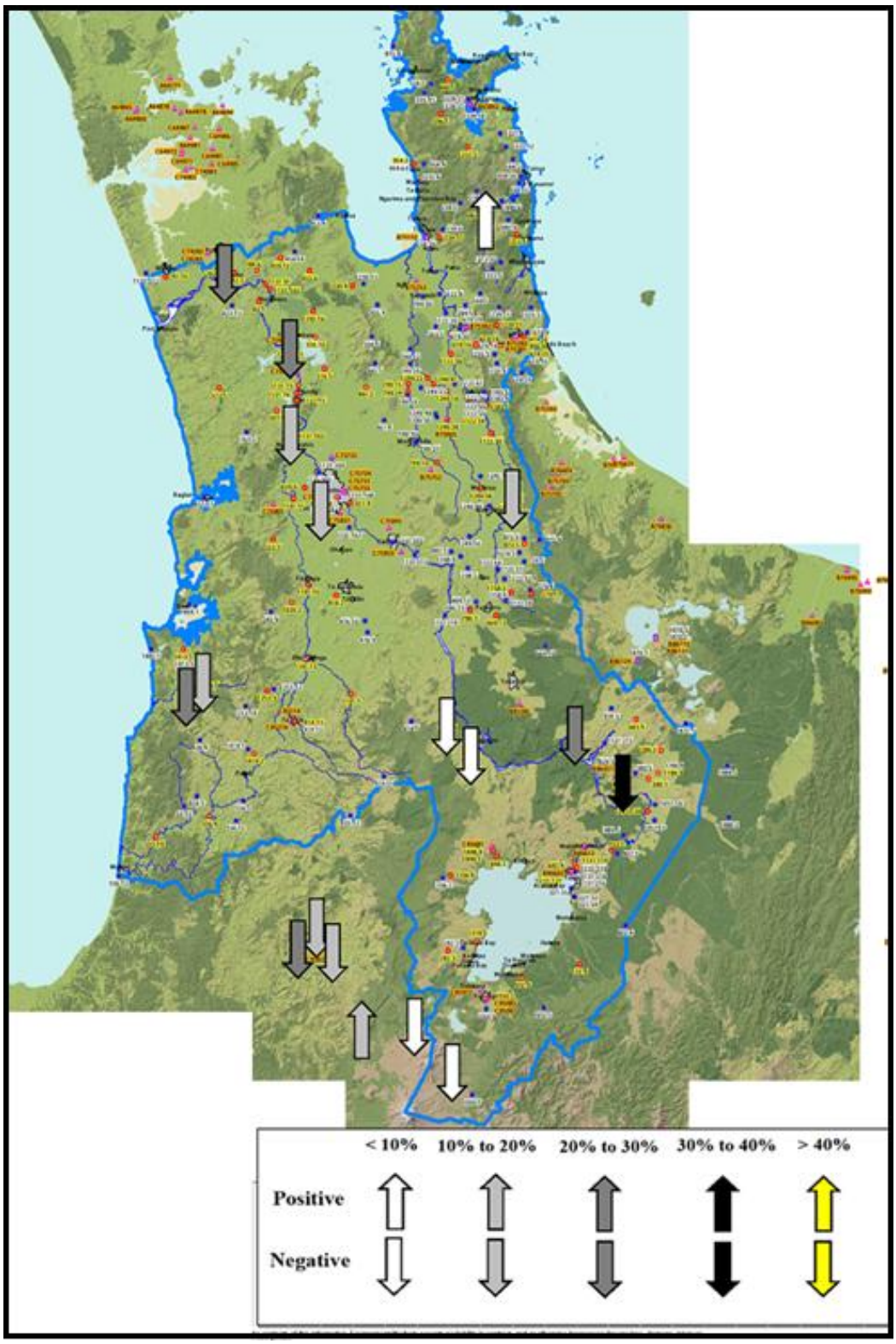

Figure 7.18: Mean discharge shift directions and shift magnitudes for 1998 break-points

7.5 Investigation of the Differences of River Discharge Characteristics over Various Stable Periods

The shifts in runoff from one period to the next are not necessarily consistent over all runoff magnitudes. From section 7.3, high rainfall frequencies lead to the changes in rainfall. The changes in rainfall and runoff regimes are similar (section 7.2 and 7.4) which emphasizes that the changes in flow regime were driven by the shifts in rainfall regime. The investigation of the river discharge differences in various stable periods can explain how flow responses to the changes in rainfall characteristic and the degree of the rainfall regimes drove the flow regimes. Moreover, sometimes the important difference in discharge may happen in some particular months.

The four notable change years, 1981, 1988, 1994/5 and 1998, are selected for investigation. Similarly to the analysis for rainfall variations, the selected study period started in 1975 and finished in 2002. In total, 13 discharge gauges indicated significant decrease shift in 1981, 25 gauges showed significant increase change in 1988, 21 gauges increased significantly in 1994/5 and 16 gauges decreased significantly in 1998.

7.5.1 Comparison of each stable period rainfall event using flow duration curves

To illustrate the influence of the climatic shifts in 1981, 1988, 1994/1995 and 1998, flow duration curves were constructed for the corresponding intervening stable periods (Appendix E-a, b, c and d). It should be noted that not all of the selected flow gauges were impacted only by climate variation, some of them being under the influence of both climate variation and land use change. Therefore, this comparison seeks to discover the regulation changes in river flow characteristics under climate variations.

Comparing the flow duration curves for each gauge site, the main climatic-driven variations evidently impact medium and high flows, with little change in the lower flows for most of the flow gauges (Appendix E-a, b, c and d).

The Tongariro Power Scheme does not impact on streamflow in the Ongarue River. The multi-year variation of streamflow at this site appears dominated by climatic fluctuations with obvious impact on high and median flow but little impact on low flow (Figure 7.19).

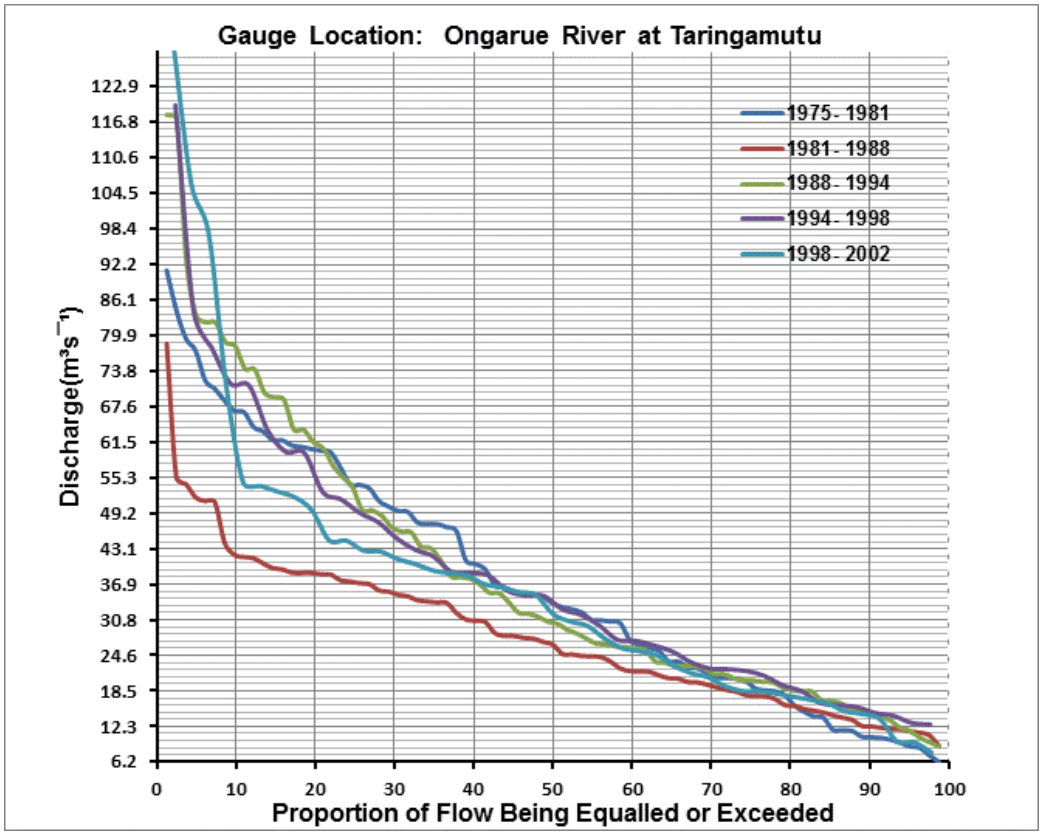

Figure 7.19: Flow duration curves for the Ongarue River at Taringamutu

7.5.2 Comparison of each stable period rainfall event using average monthly mean discharge variability

In Appendix F-a, b, c and d, the average monthly mean discharge curves are presented for the flow gauges with the change years 1981, 1988, 1994/5 and 1998 for the intervening periods.

The key common features of the graphs were the comparably greater differences of monthly mean river discharge in winter and early spring months than those in the other months. For some gauges, the difference was significant for all of the

months and especially large in the peak flow months; however, for some gauges the difference was small and not in significant level even when the difference was comparably higher in peak flow months than others. This may be driven by the size of the rivers or the upstream land use affecting the nature of the runoff. However, from the main regulations of the changes, it can be inferred that the river discharge process closely corresponded to the rainfall regimes driven by the climate variations and the main affect was in high flow months.

Figure 7.20 indicates the changes of monthly mean discharge for the period before and after 1981 for Taringamutu rainfall (gauge site: Ongarue River at Taringamutu).

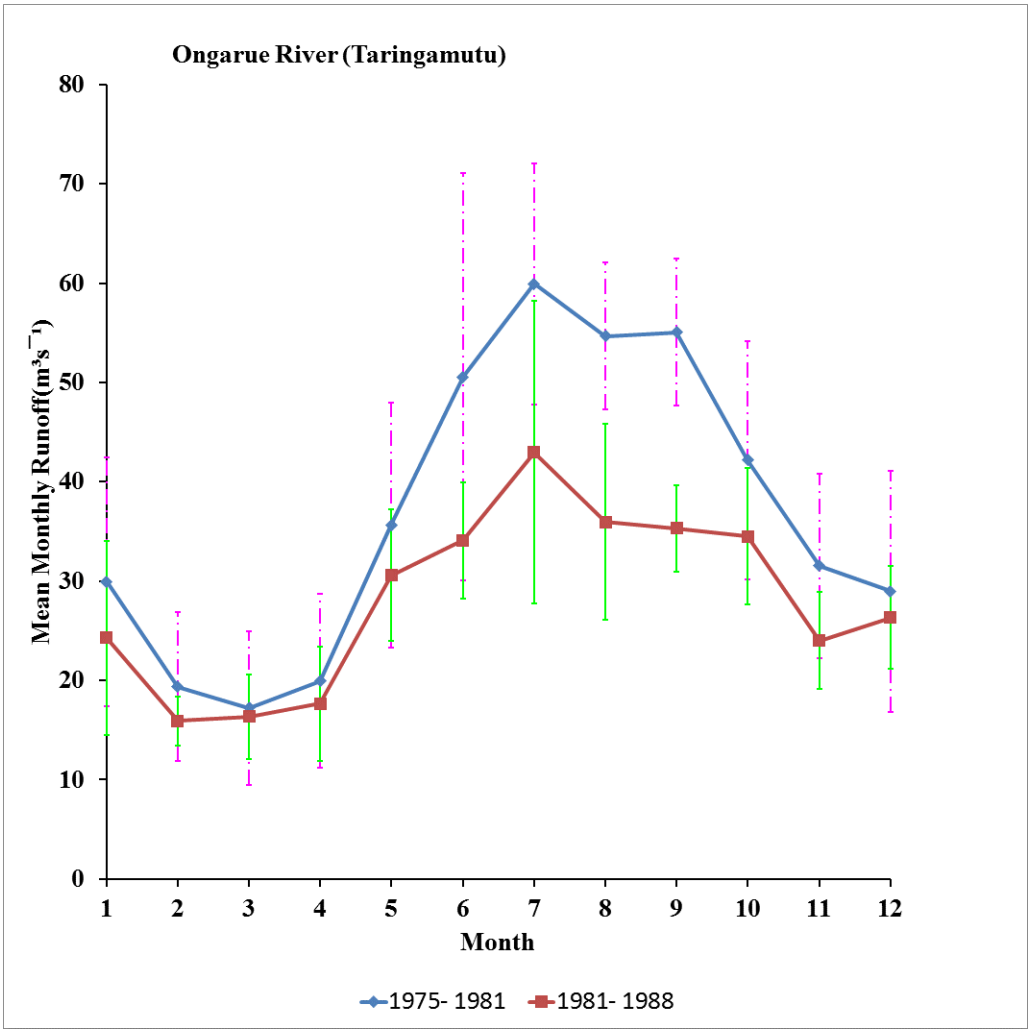

Figure 7.20: Average monthly mean discharge for the stable period before and after 1981 (Ongarue River at Taringamutu)

7.6 Special Cases of Changed Rainfall Runoff Relationship Due to Climate Variation

Among the 44 flow gauge sites, 34 flow gauges were not detect signals of upstream land use change which means the change points in the flow time series also exist in the rainfall time series. However, with respect to the rainfall runoff relationship, the 34 flow gauges can be categorised into two groups: one is where there is a rainfall-runoff relationship change concurrent with the rainfall and runoff change, the other is the rainfall runoff relationship does not change although the rainfall and runoff change concurrently.

Regarding the first category, two possibilities may explain the changed rainfall runoff relationship: one is the rainfall-runoff change from change in rainfall characteristics (rainfall nature influencing evaporation); the other is that the land use shift happened before study period (e.g. forest growth)). This section focuses on the second category with a total of 10 gauges (Figure 7.21) where no land use change happened upstream of the gauge location within the specific study period among the 34 flow gauges. The change of times discussed in this section for the 10 gauges are statistically significant.

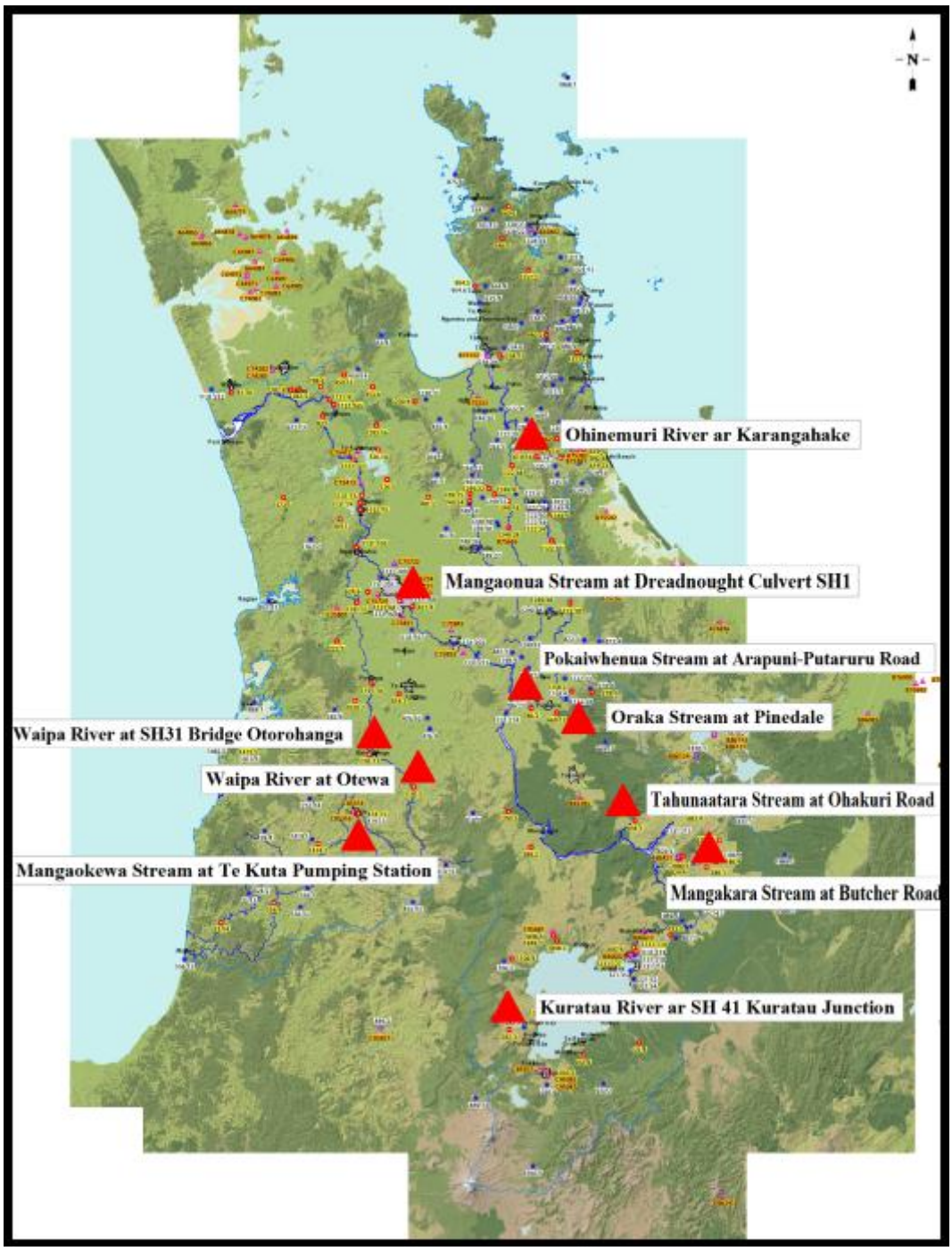

Figure 7.21: Location of the runoff gauges showing the rainfall-runoff nonlinear relationship

7.6.1 Ten specific discharge gauges

Mangakara Stream at Butcher Road

From the discharge time series gauged in the Mangakara Stream at Butcher Road (Figure 7.21) (average monthly mean discharge 0.3 m^3s^{-1}), the flow cumulative mass plot (Figure 7.22) is almost straight before 1988 with the anticipated abrupt change of slope representing an approximately 27.6 percent increase in the monthly mean flow. The 1988 break point in the slope of rainfall cumulative mass plot (Figure 7.23) for the Torepatutahi Stream at Sylvan Lodge is also evident. The break point in 1988 in streamflow series happened concurrently with the change point 1988 in the rainfall pattern with same increasing shift. The rainfall runoff double mass plot (Figure 7.24) also presents a clear change in 1988.

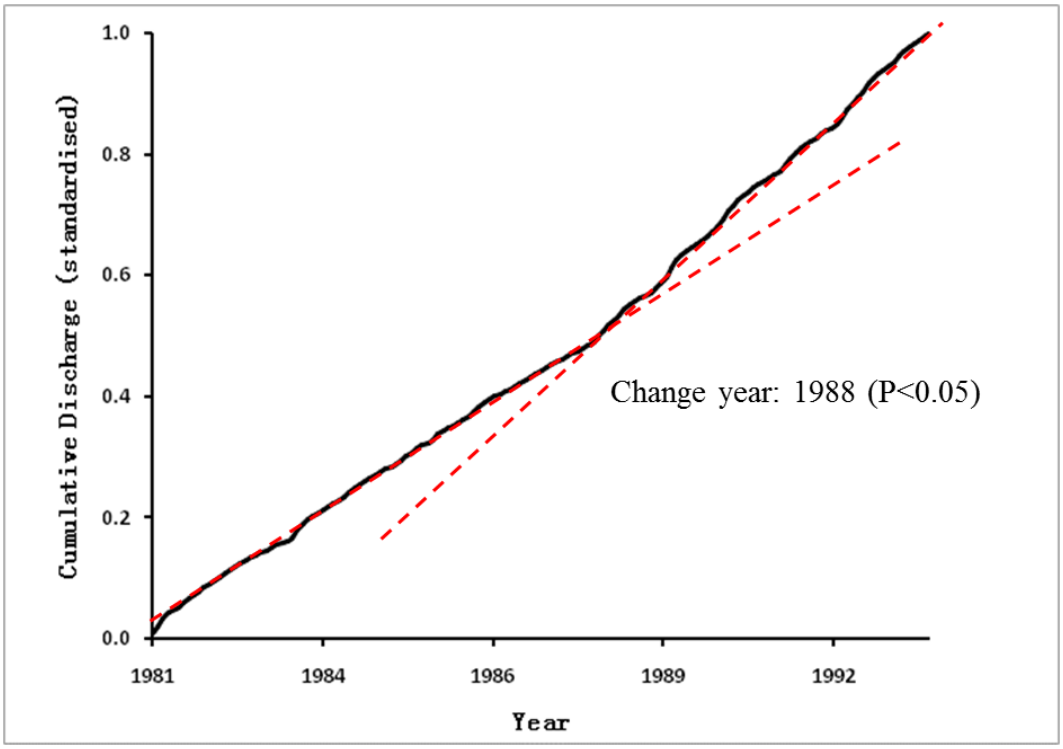

Figure 7.22: Cumulative mass plot of monthly mean runoff at Butcher Road, Mangakara Stream

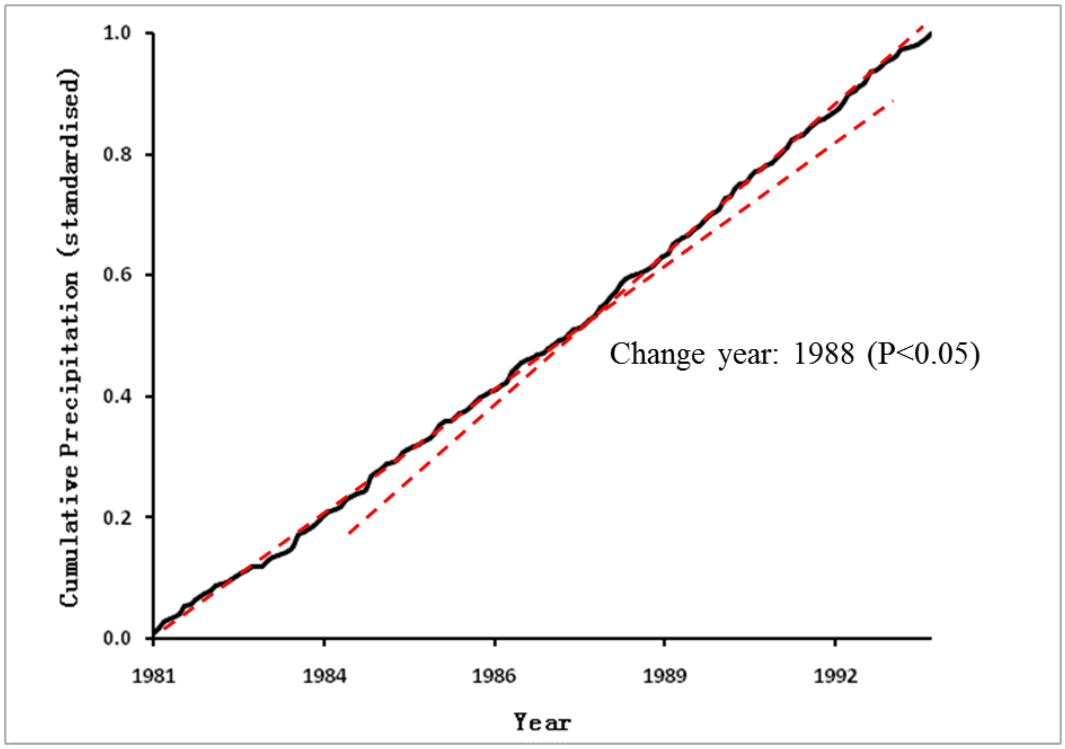

Figure 7.23: Cumulative mass plot of monthly precipitation at Sylvan Lodge, Torepatutahi Stream

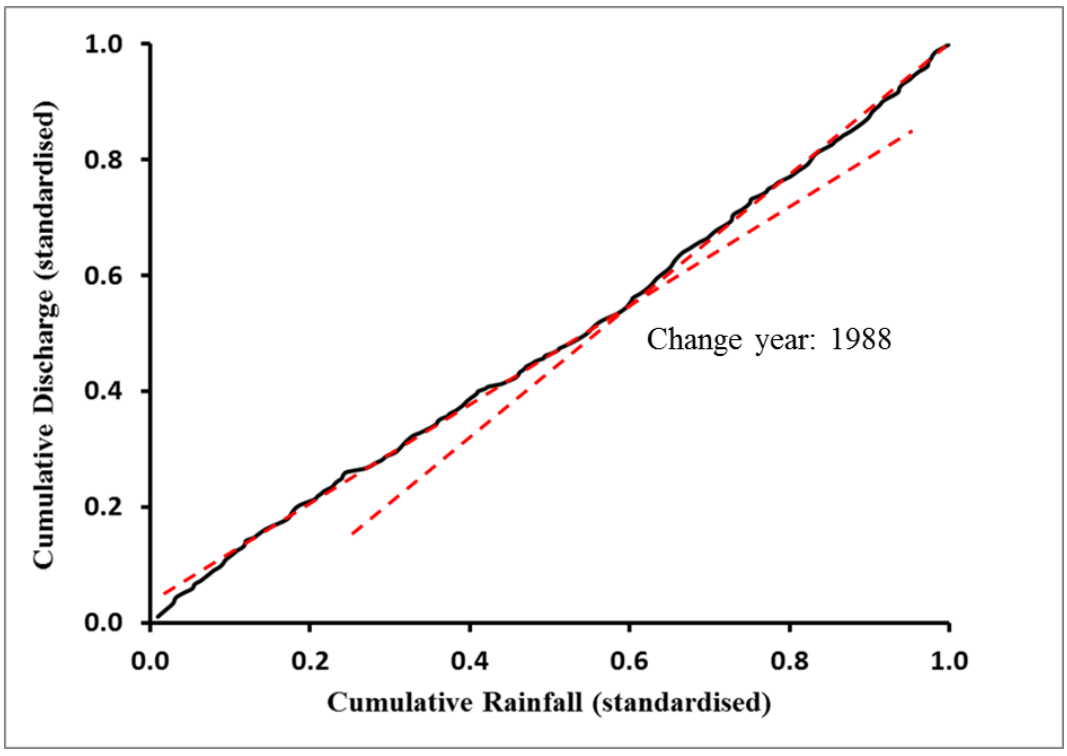

Figure 7.24: Double mass plot of monthly precipitation at Sylvan Lodge, Torepatutahi Stream and monthly mean runoff at Butcher Road, Mangakara Stream

Tahunaatara Stream at Ohakuri Road

Tahunaatara Stream (Figure 7.21) is characterized as a stream with around 4.63 m^3s^{-1} mean monthly flow. Over the study period 1964 to 2003, the break point at 1981 is clear in both the flow cumulative mass plot (Figure 7.25) and the rainfall (gauged at Ngakuru, Waikato River) cumulative mass plot (Figure 7.26) though less evident due to the increase in the later years. Again, there is an evident change point in the rainfall runoff double mass plot (Figure 7.27) which is the 1981.

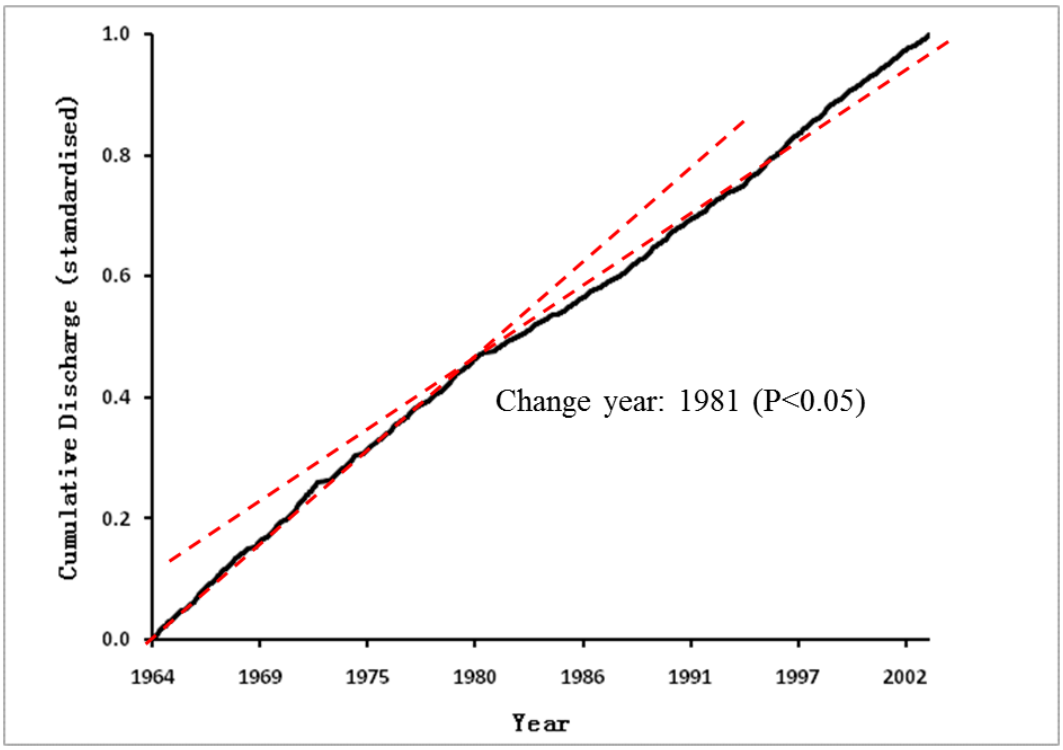

Figure 7.25: Cumulative mass plot of monthly mean runoff at Ohakuri Road, Tahunaatara Stream

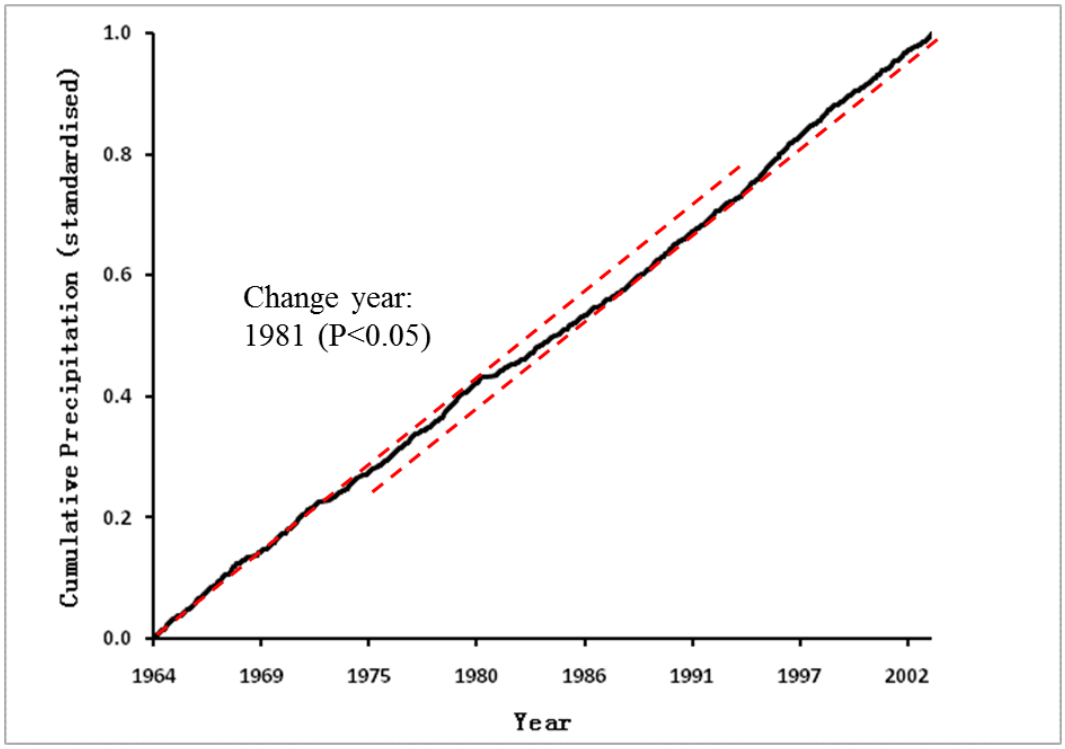

Figure 7.26: Cumulative mass plot of monthly precipitation at Ngakuru, Waikato River

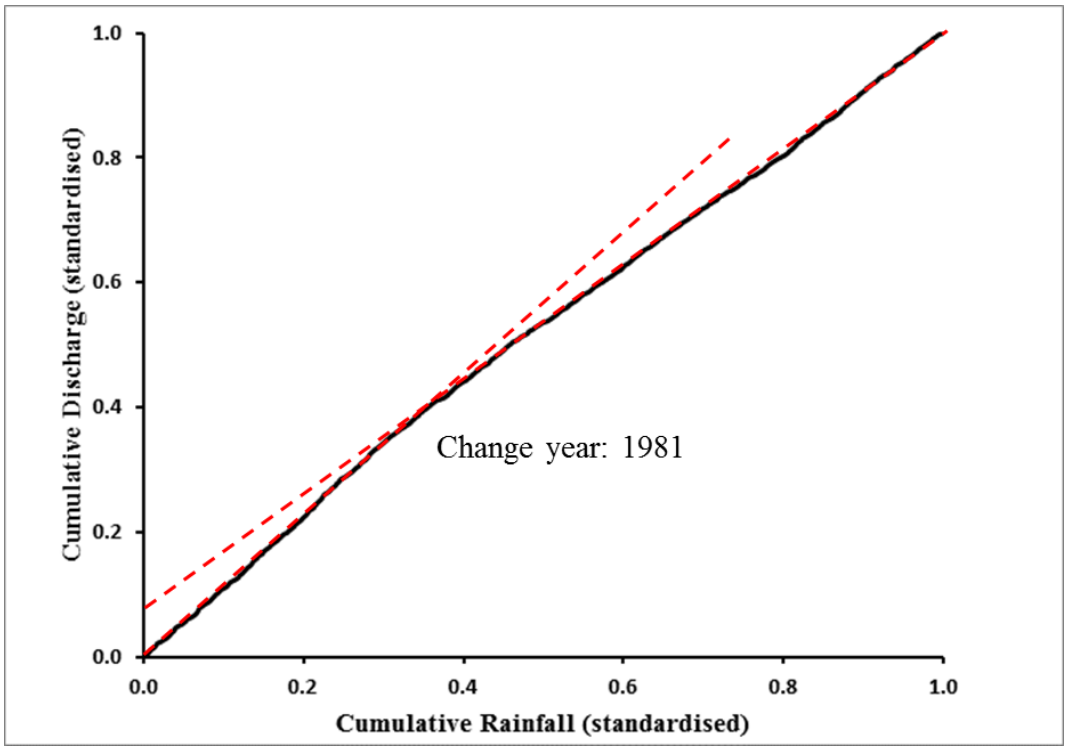

Figure 7.27: Double mass plot of monthly precipitation at Ngakuru, Waikato River and monthly mean runoff at Ohakuri Road, Tahunaatara Stream

Pokaiwhenua Stream at Arapuni-Putaruru Road

Pokaiwhenua Stream (Figure 7.21) that joins Waikato River in Lake Karapiro has an average monthly mean flow of 5.2 m^3s^{-1} in Pokaiwhenua Stream at Arapuni-Putaruru Road (Figure 7.21) from 1963 to 1994. For the flow time series gauged, the break points 1982 and 1988 are evident (Figure 7.28). The two change points are shown in the rainfall (gauged in Arapuni Power Station, Waikato River) cumulative mass plot (Figure 7.29). However, the rainfall runoff double mass plot also indicates the same change points as shown in Figure 7.30.

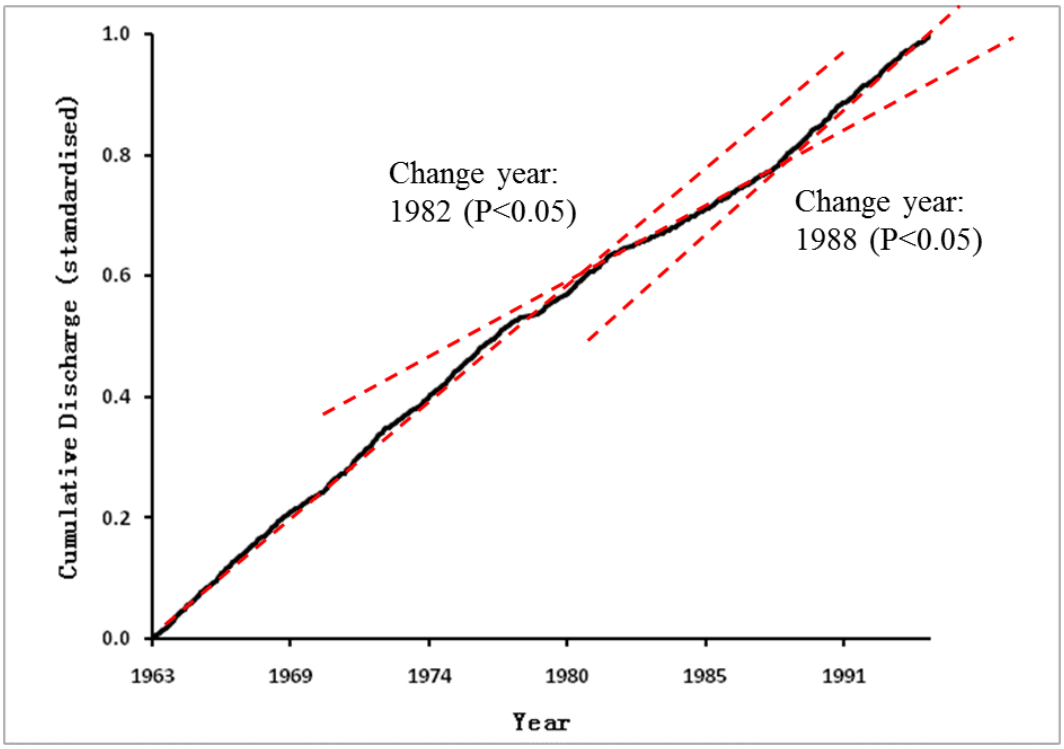

Figure 7.28: Cumulative mass plot of monthly mean runoff at Arapuni-Putaruru Road, Pokaiwhenua Stream

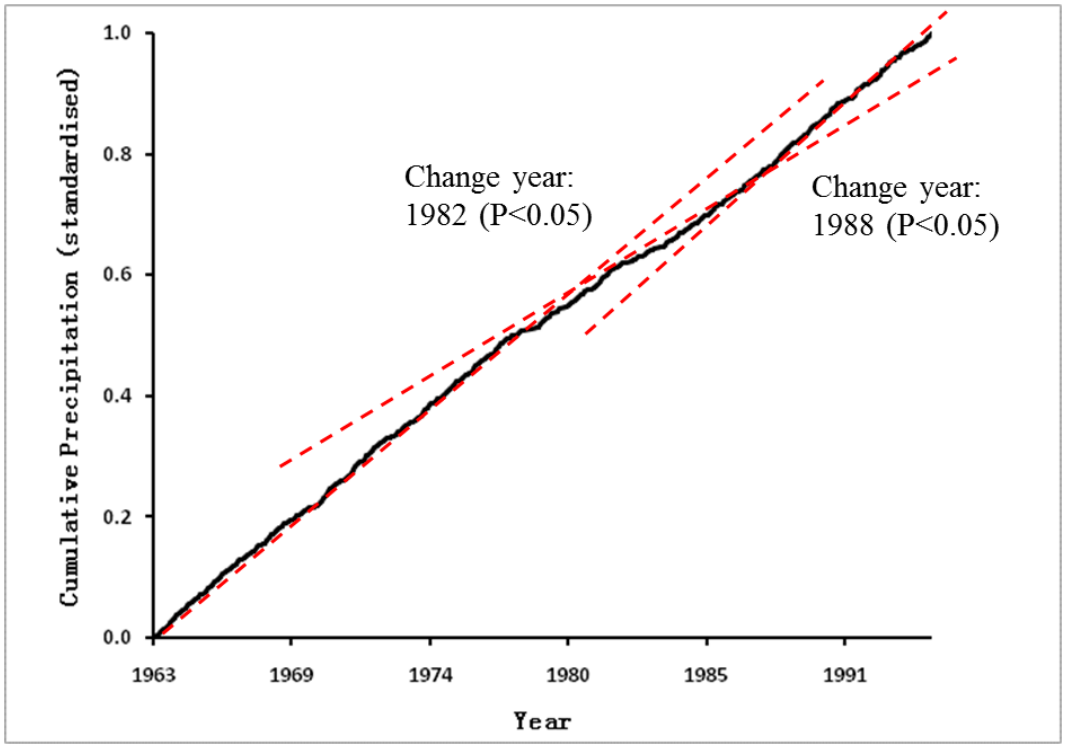

Figure 7.29: Cumulative mass plot of monthly precipitation at Arapuni Power Station, Waikato River

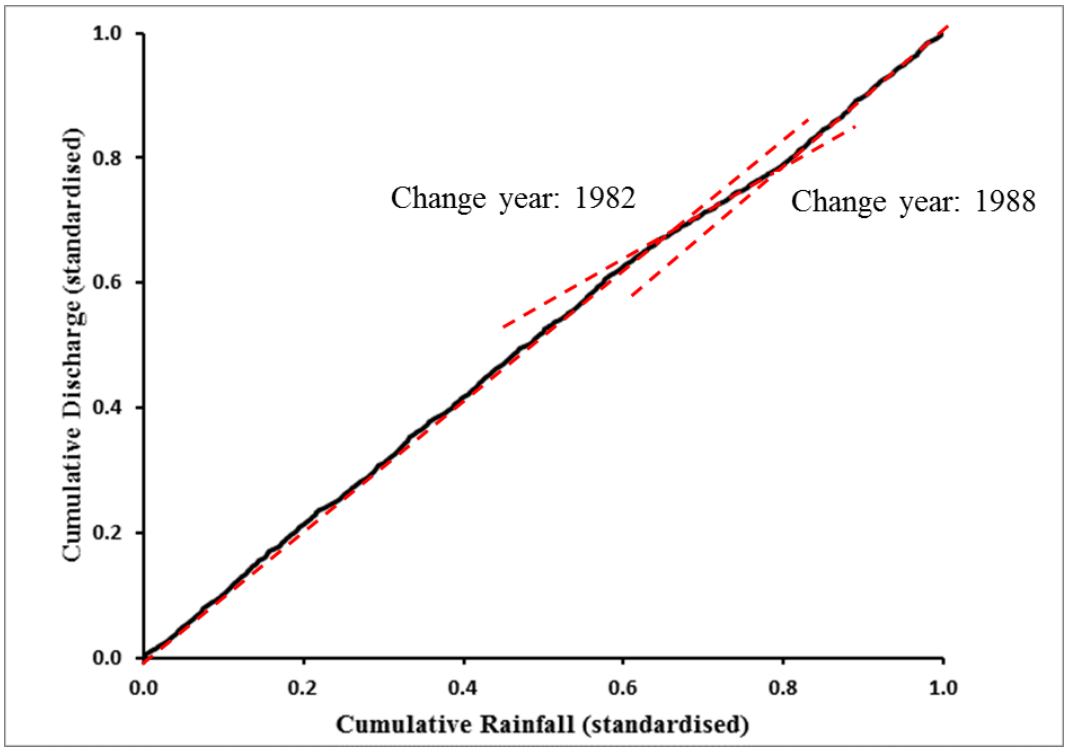

Figure 7.30: Double mass plot of monthly precipitation at Arapuni Power Station, Waikato River and monthly mean runoff at Arapuni-Putaruru Road, Pokaiwhenua Stream

Mangaonua Stream at Dreadnought Culvert SH1

Mangaonua Stream, located in the eastern area of Hamilton city (Figure 7.21) is a tributary of the Waikato River with average monthly mean flow of 2.1 m^3s^{-1} from 1980 to 2003. The break points 1988 and 1996 are evident not only in the flow cumulative mass plot (Figure 7.31) and the rainfall (gauged at Horsham Downs 2, Waikato River) cumulative mass plot (Figure 7.32), but also in the rainfall runoff double mass plot (Figure 7.33). Although the two change points shown in the rainfall cumulative mass plot are not as obvious as shown in the flow cumulative mass plot, they are detected by the least squares regression method and lead to a larger percentage change in mean monthly rainfall than the other change points.

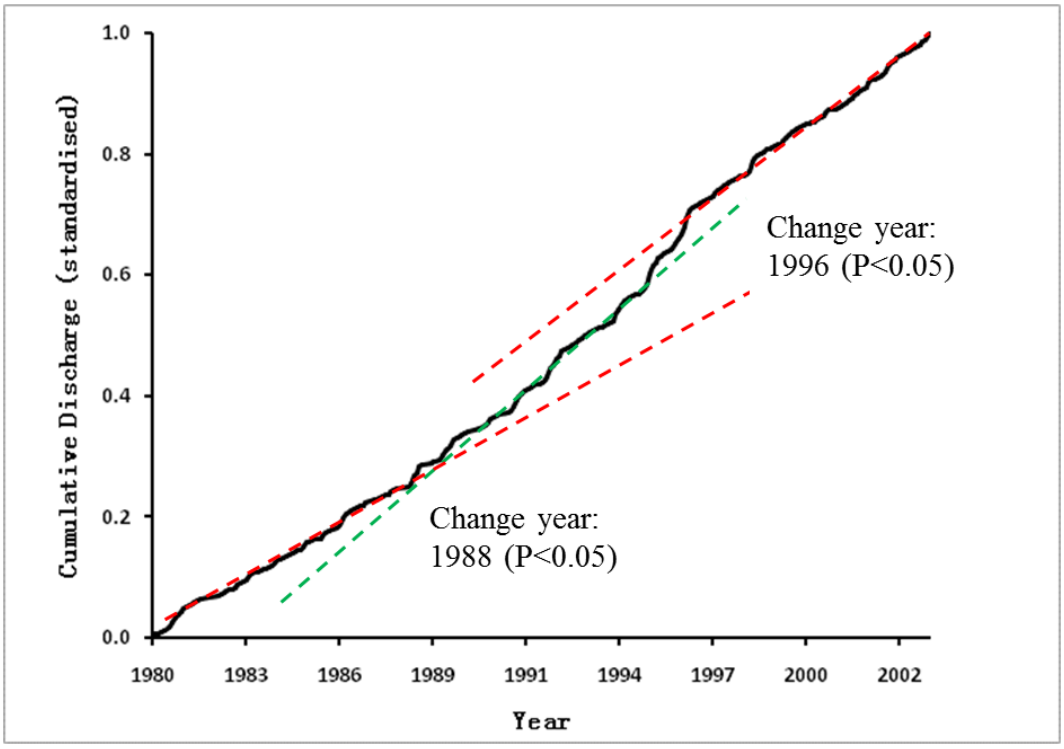

Figure 7.31: Cumulative mass plot of monthly mean runoff at Dreadnought Culvert SH1, Mangaonua Stream

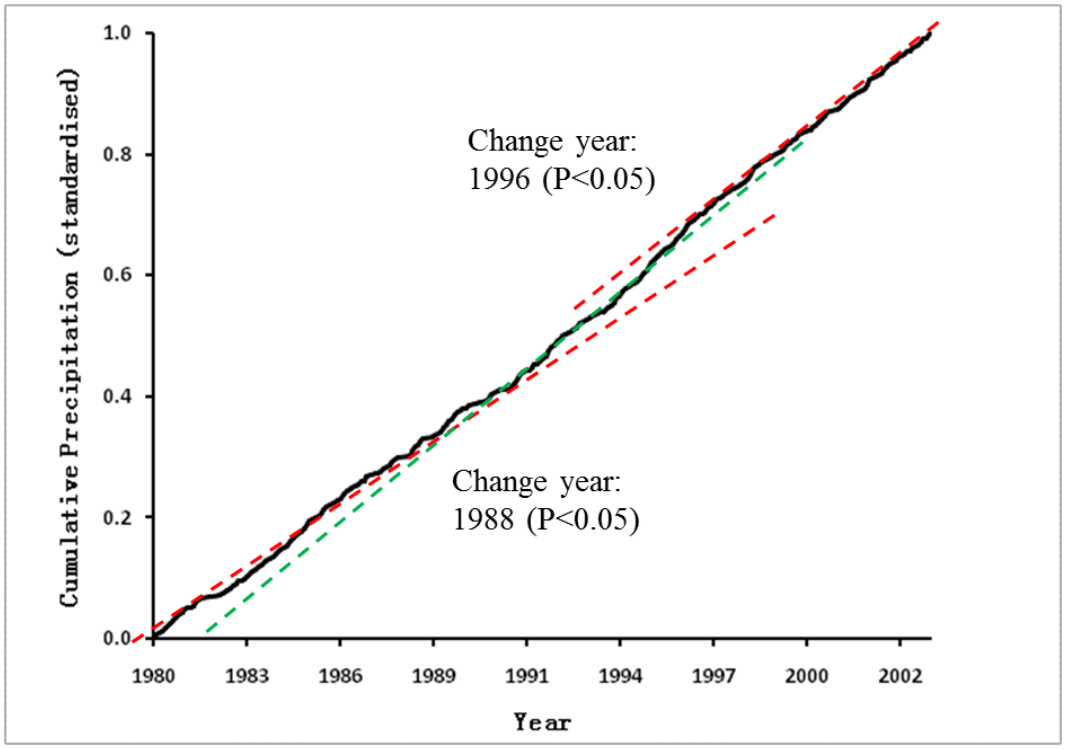

Figure 7.32: Cumulative mass plot of monthly precipitation at Horsham Downs 2, Waikato River

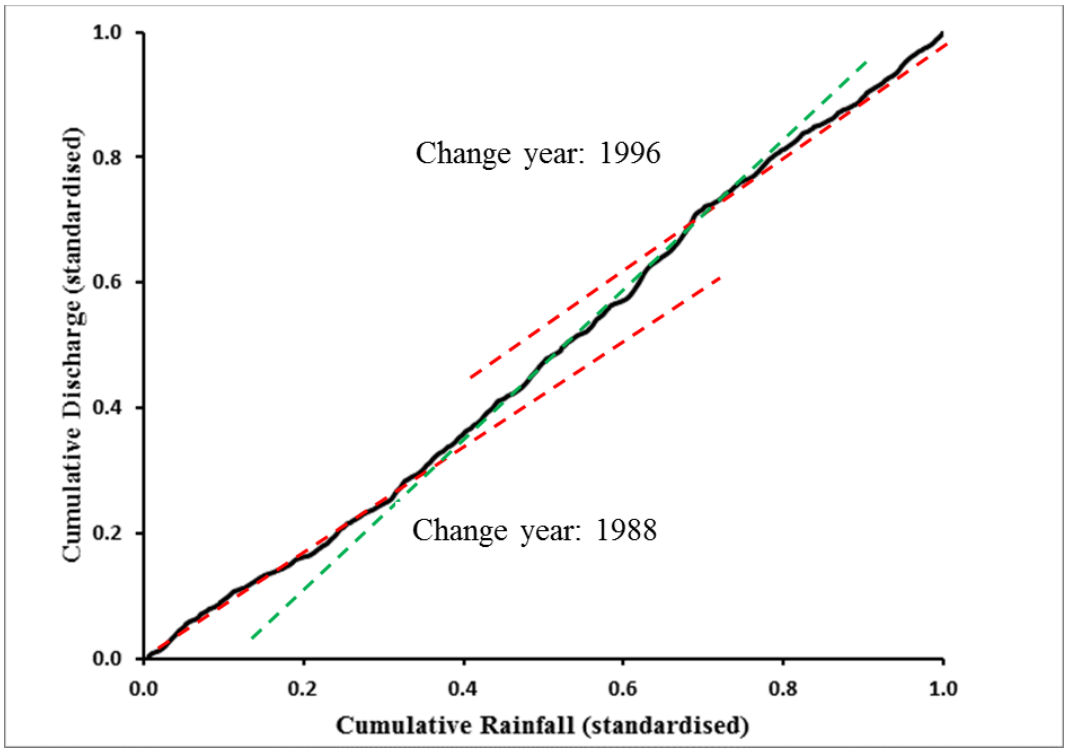

Figure 7.33: Double mass plot of monthly precipitation at Horsham Downs 2, Waikato River and monthly mean runoff at Dreadnought Culvert SH1,Mangaonua Stream

Waipa River at Otewa

In the Waipa River at Otewa (Figure 7.21), the average monthly mean flow was 12.8 m^3s^{-1} from 1985 to 2007. In the flow cumulative mass plot (Figure 7.34), a break point in 1996 is evident, after which the average monthly mean flow decreased around 26 percent. The change point in 1996 is also clear in the rainfall (gauged at Ngaroma, Puniu River) mass plot (Figure 7.35). Therefore, the flow mass plot and the rainfall mass plot show concurrent times of changes indicating no signal of land use shifts happening in the upstream over the study period. However, the rainfall runoff double mass plot also presents a change in 1996 as shown in Figure 7.36.

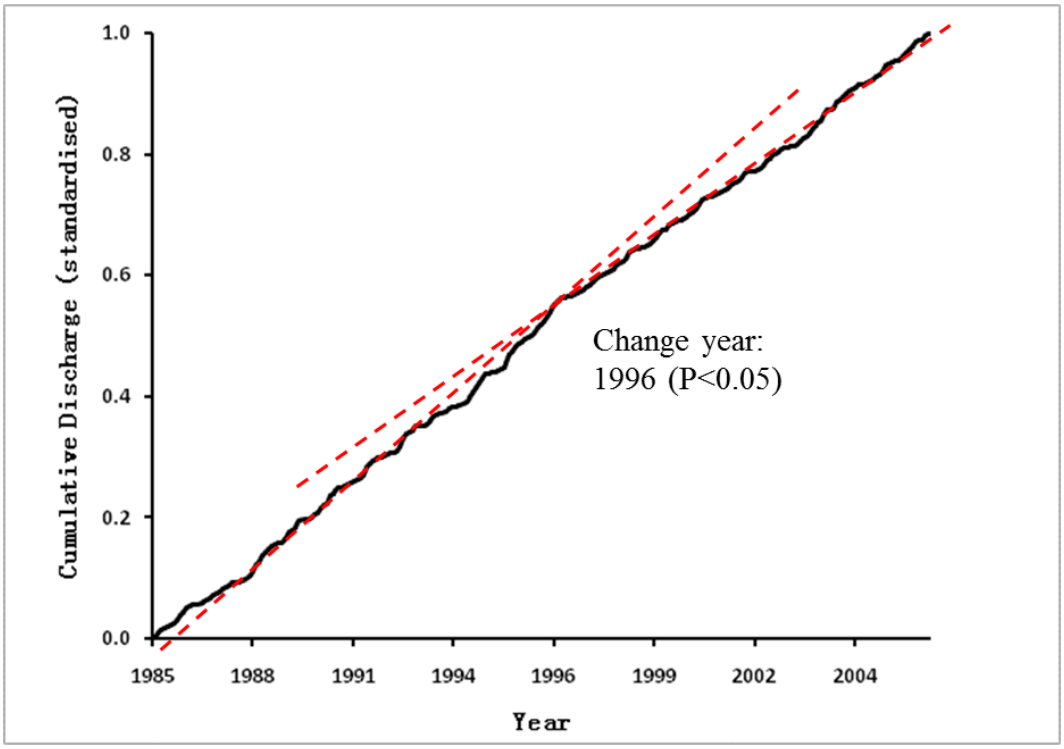

Figure 7.34: Cumulative mass plot of monthly mean runoff at Otewa Waipa River

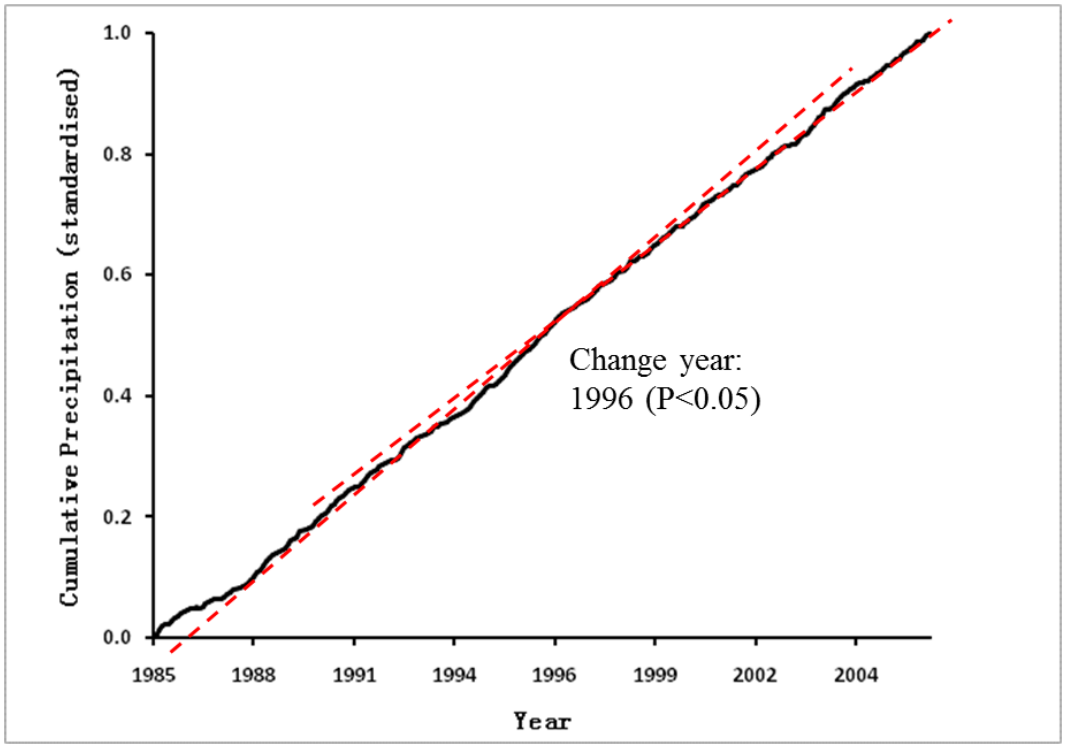

Figure 7.35: Cumulative mass plot of monthly precipitation at Ngaroma, Puniu River

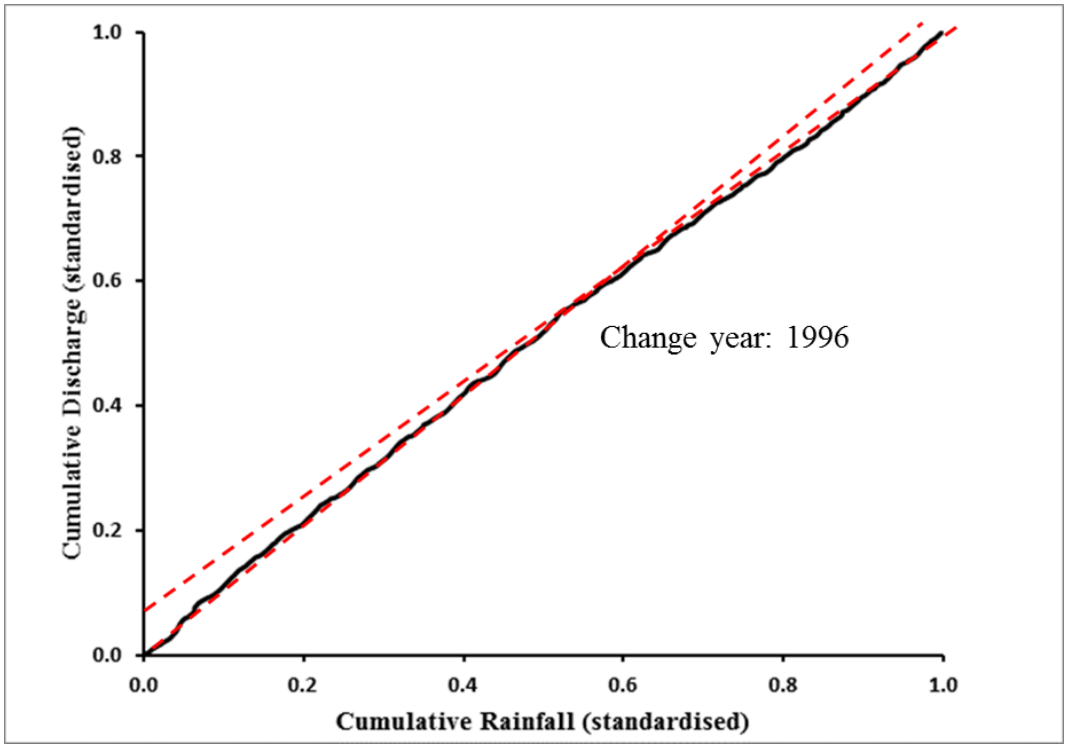

Figure 7.36: Double mass plot of monthly precipitation at Ngaroma, Puniu River and monthly mean runoff at Otewa, Waipa River

Waipa River at SH31 Bridge Otorohanga

In Waipa River at SH31 Bridge Otorohanga (Figure 7.21), the average monthly mean flow was 30.1 m^3s^{-1} from 1981 to 1999. The break point in 1988 is clear in the flow cumulative mass plot (Figure 7.37) and the rainfall (gauged in Ngutunui Stream at Ngutunui) cumulative mass plot (Figure 7.38).The rainfall runoff double mass plot (Figure 7.39) indicates rainfall and runoff relationship was approximately uniform for the whole period but there is a small change point of inflexion in 1988.

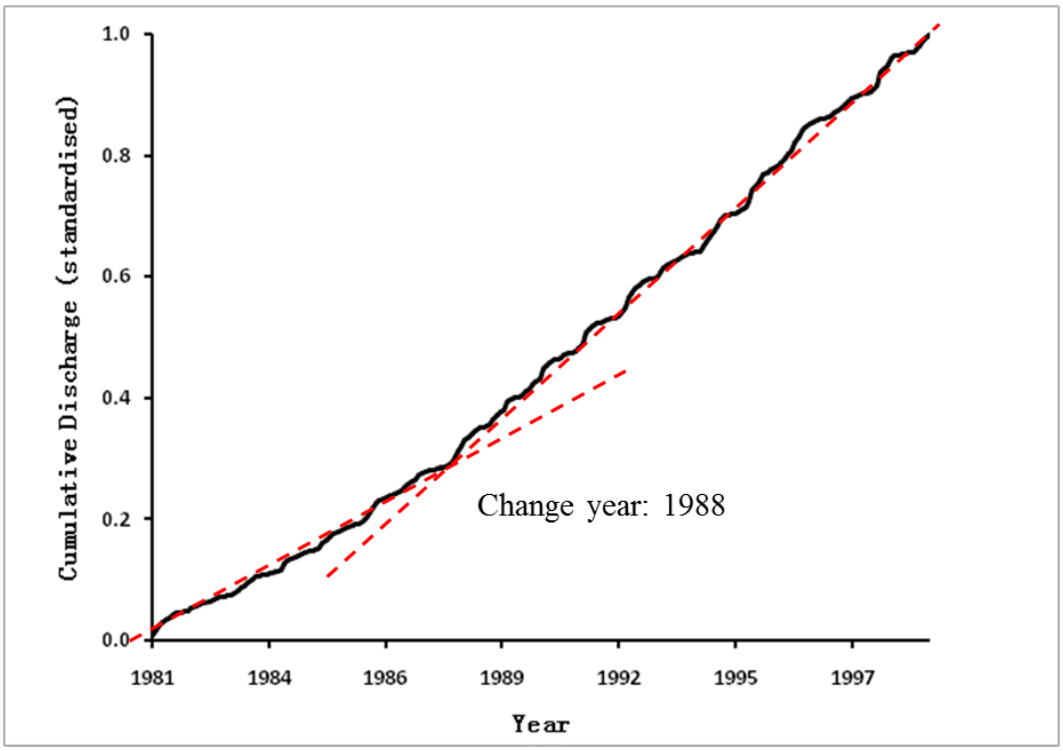

Figure 7.37: Cumulative mass plot of monthly mean runoff at SH31 Bridge Otorohanga, Waipa River

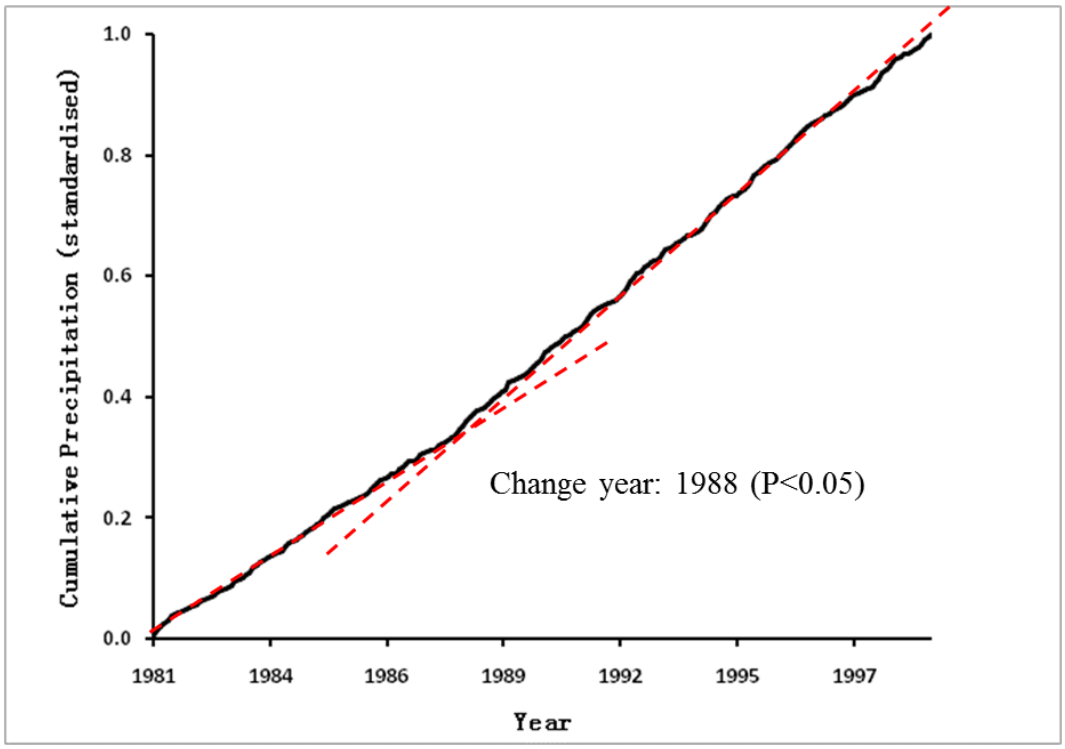

Figure 7.38: Cumulative mass plot of monthly precipitation at Ngutunui, Ngutunui stream

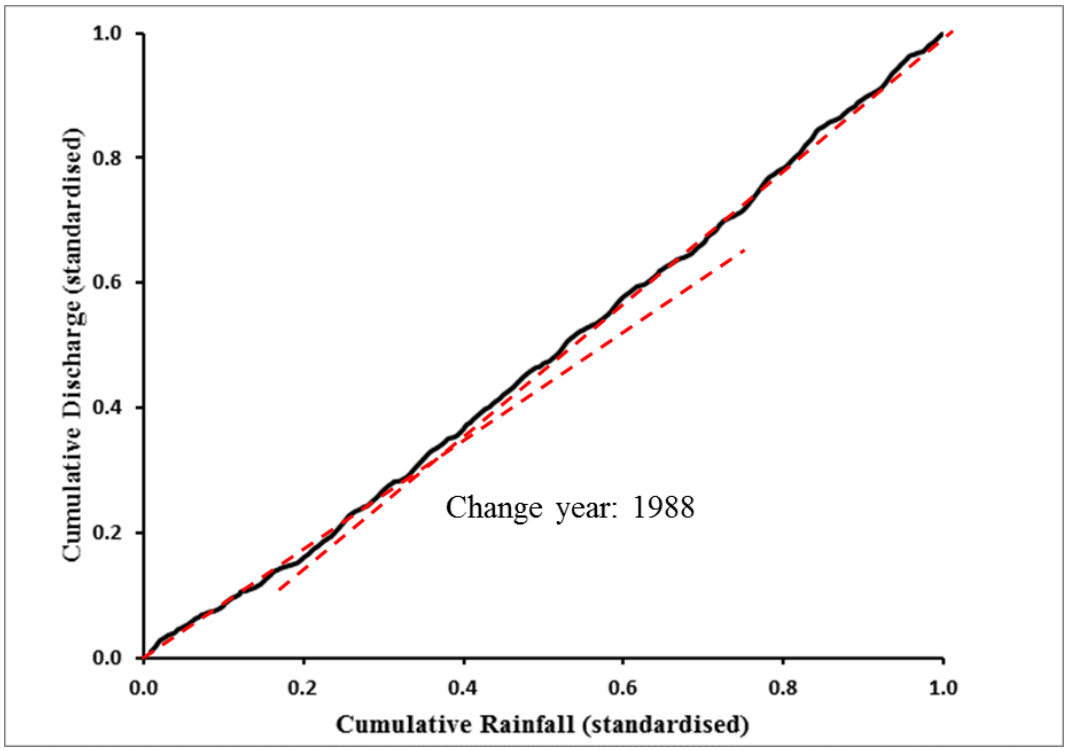

Figure 7.39: Double mass plot of monthly precipitation at Ngutunui, Ngutunui stream and monthly mean runoff at SH31 Bridge Otorohanga, Waipa River

Oraka Stream at Pinedale

In Oraka Stream at Pinedale (Figure 7.21), the average monthly mean flow was 2.8 m^3s^{-1} from 1979 to 1996. For the flow cumulative mass plot (Figure 7.40), the break point in 1988 is evident with around 28 percent change in the mean. In the monthly precipitation (Figure 7.41) (gauged in Kuhatahi Stream at Kuhatahi) cumulative mass plot, the 1988 change point is also clear. The rainfall runoff double mass plot (Figure 7.42) indicates rainfall and runoff relationship changed in 1988.

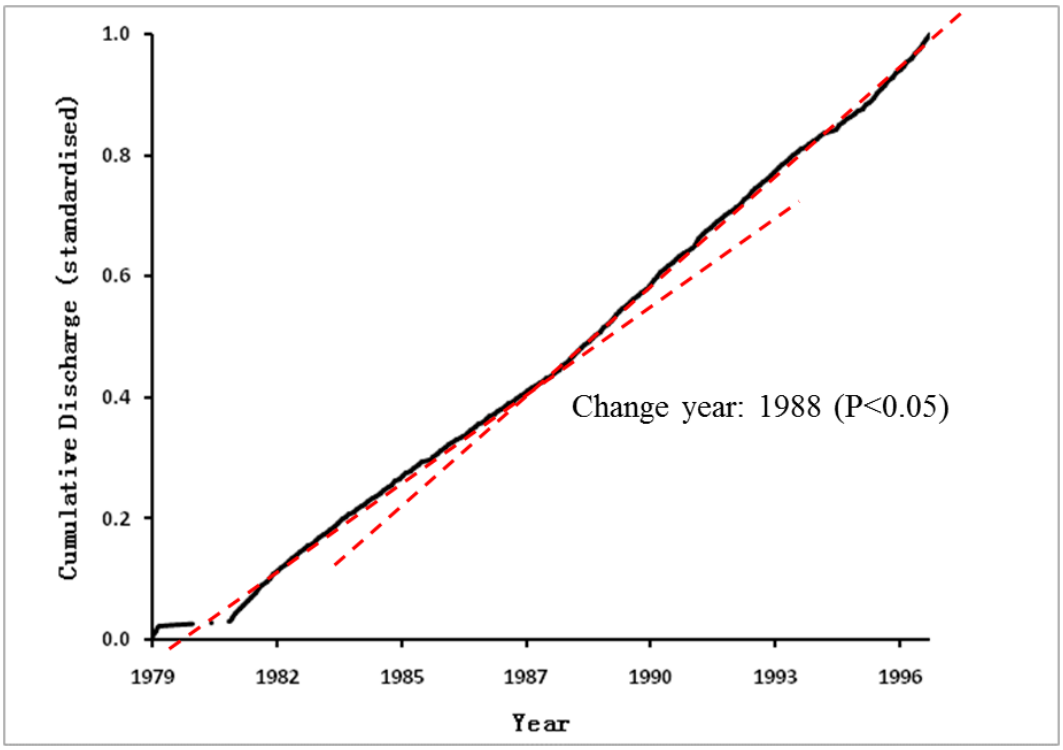

Figure 7.40: Cumulative mass plot of monthly mean runoff at Pinedale, Oraka Stream

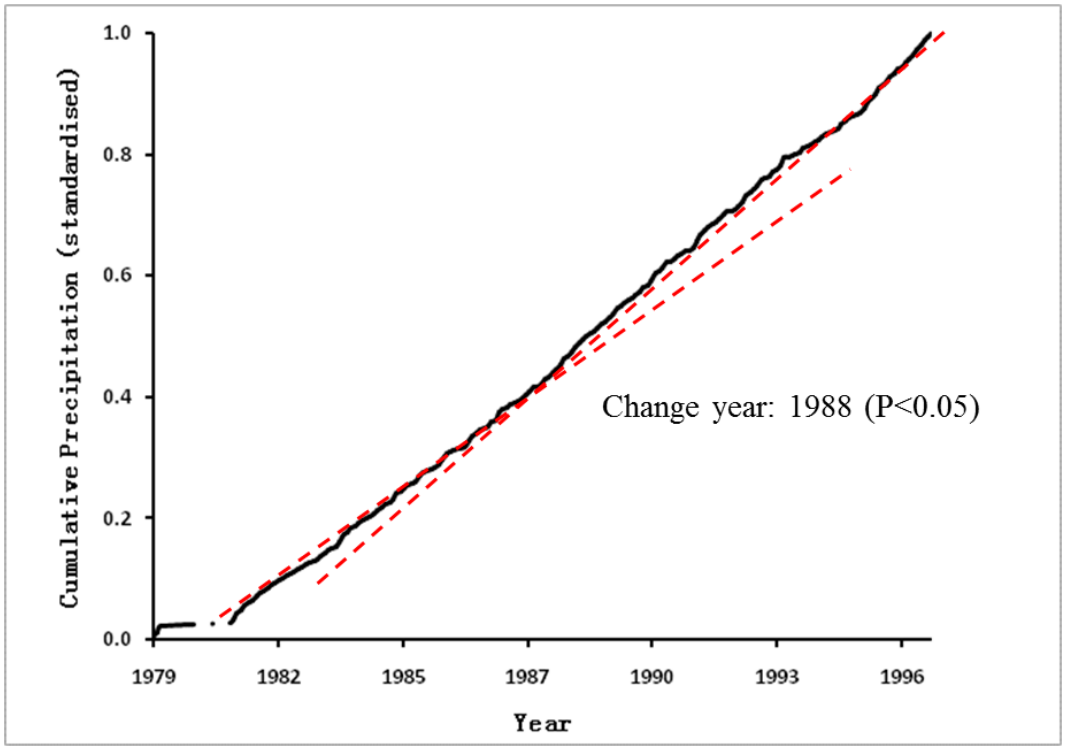

Figure 7.41: Cumulative mass plot of monthly precipitation at Kuhatahi, Kuhatahi Stream

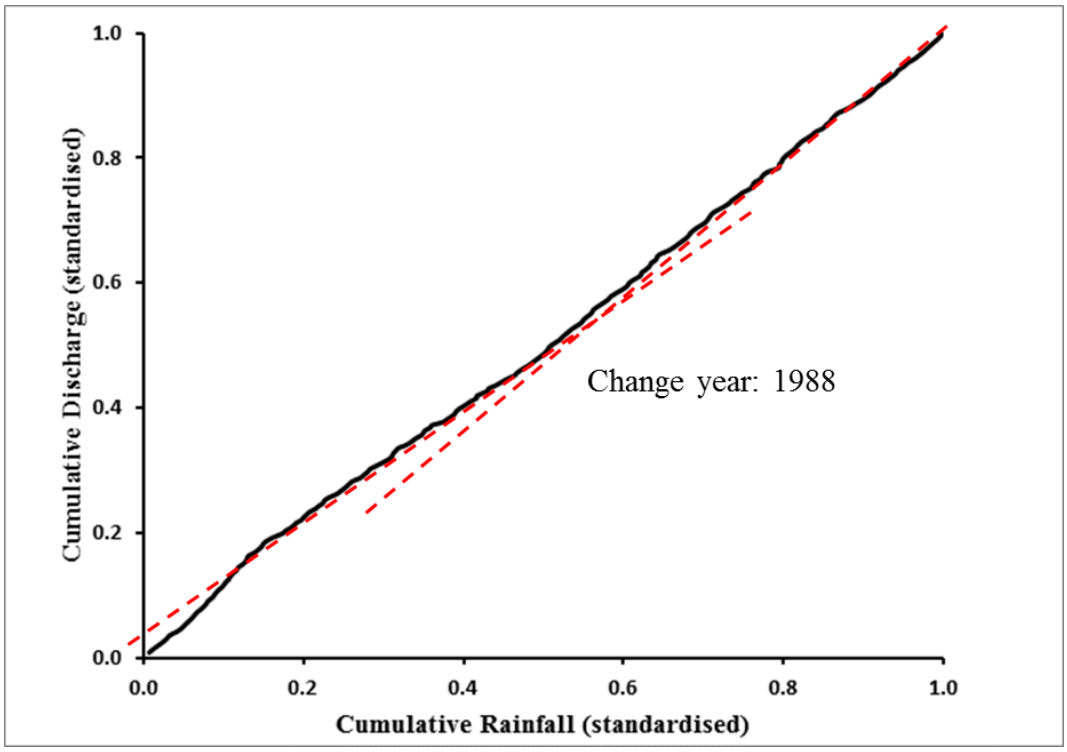

Figure 7.42: Double mass plot of monthly precipitation at Kuhatahi, Kuhatahi Stream and monthly mean runoff at Pinedale, Oraka Stream

Ohinemuri River at Karangahake

In the Ohinemuri River at Karangahake (Figure 7.21), the average monthly mean flow was 11.59 m^3s^{-1} over 1985 to 1999. In the flow cumulative mass plot (Figure 7.43), the break point in 1989 is clear with around 38 percent change in the mean. The break in 1989 is also evident in the average monthly precipitation recorded in Ohinemuri River at Woodlands Road, Waihi and Waitawheta River at Waitawheta cumulative mass plot (Figure 7.44). The rainfall-runoff double mass plot (Figure 7.45) shows an evident change in the slope in 1989 also.

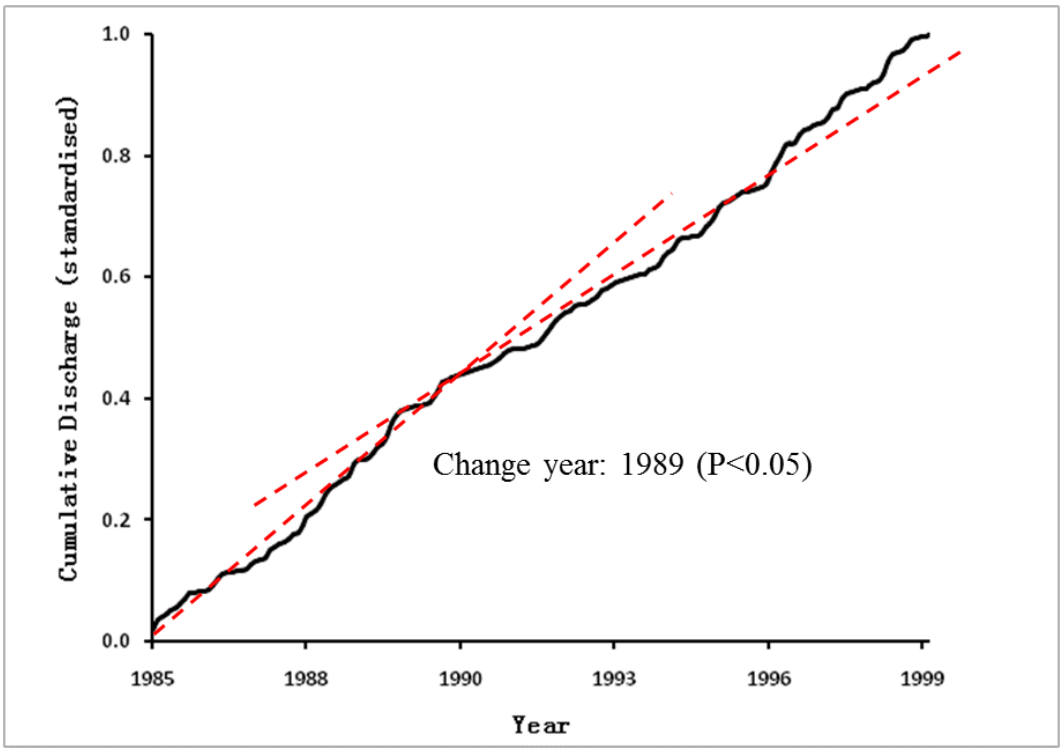

Figure 7.43: Cumulative mass plot of monthly mean runoff at Karangahake, Ohinemuri River

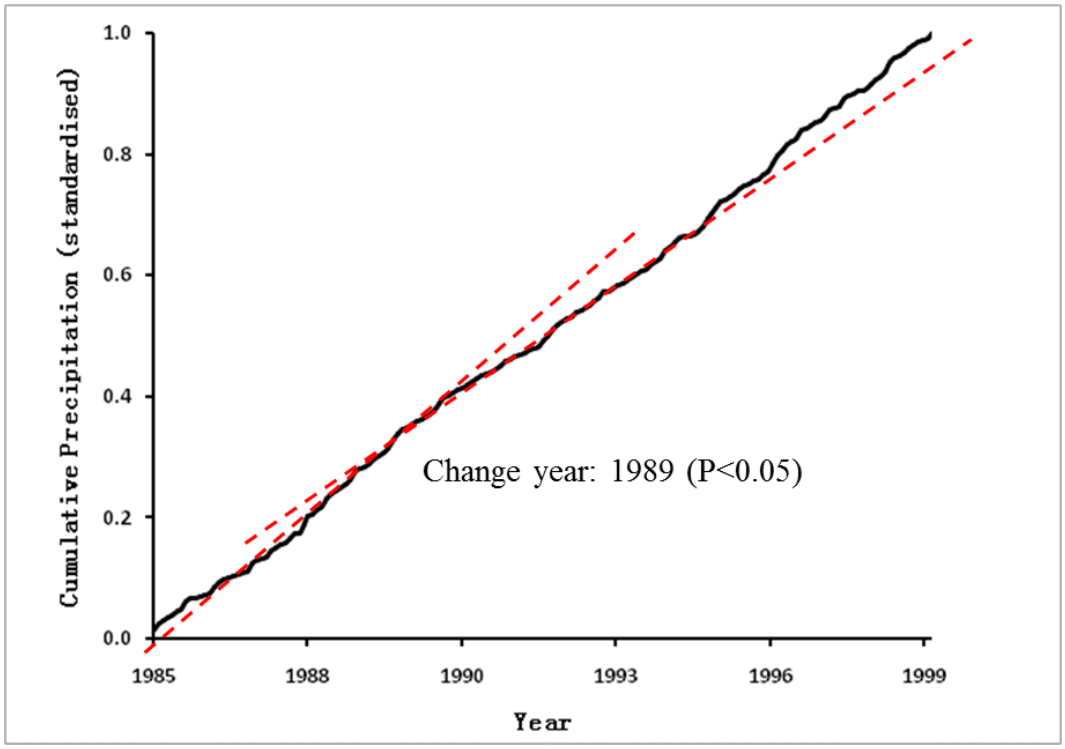

Figure 7.44: Cumulative mass plot of average monthly precipitation at Woodlands Road Waihi, Ohinemuri River and Waitawheta, Waitawheta River

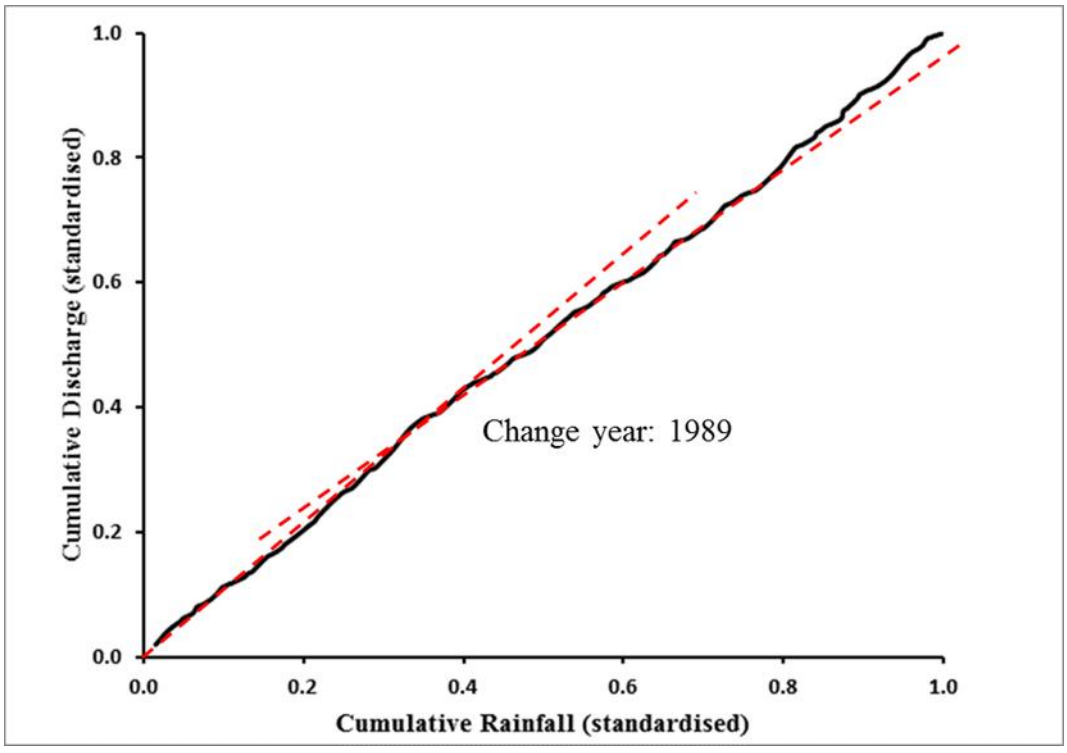

Figure 7.45: Double mass plot of monthly precipitation at Woodlands Road, Waihi, Ohinemuri River and Waitawheta, Waitawheta River and monthly mean runoff at Karangahake, Ohinemuri River

Kuratau River at SH41 Kuratau Junction

In Kuratau River at SH41 Kuratau Junction (Figure 7.21), the average monthly mean flow was 115.04 m^3s^{-1} from 1978 to 1997. In the flow cumulative mass plot (Figure 7.46), the break in 1988 is evident with 39 percent change in the mean value for the period before and after. The change point 1988 is also clear in the monthly precipitation (recorded in Kuratau River at Power Station) cumulative mass plot (Figure 7.47). The change point 1988 is also shown in the rainfall runoff double mass plot (Figure 7.48).

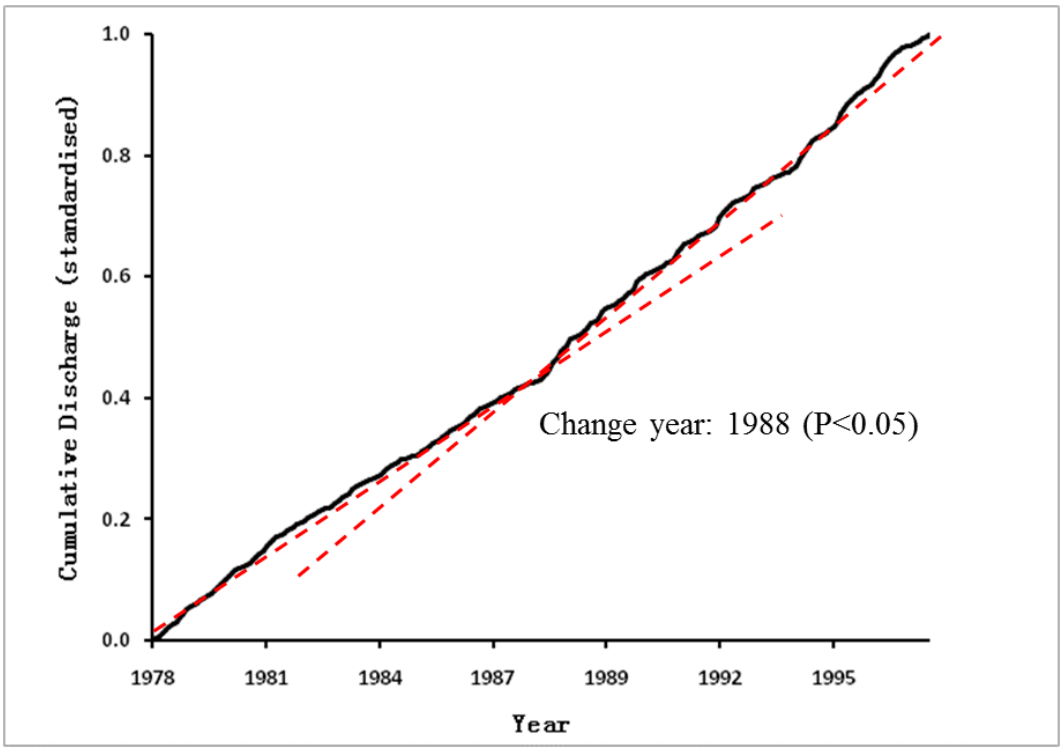

Figure 7.46: Cumulative mass plot of monthly mean runoff atSH41 Kuratau Junction, Kuratau River

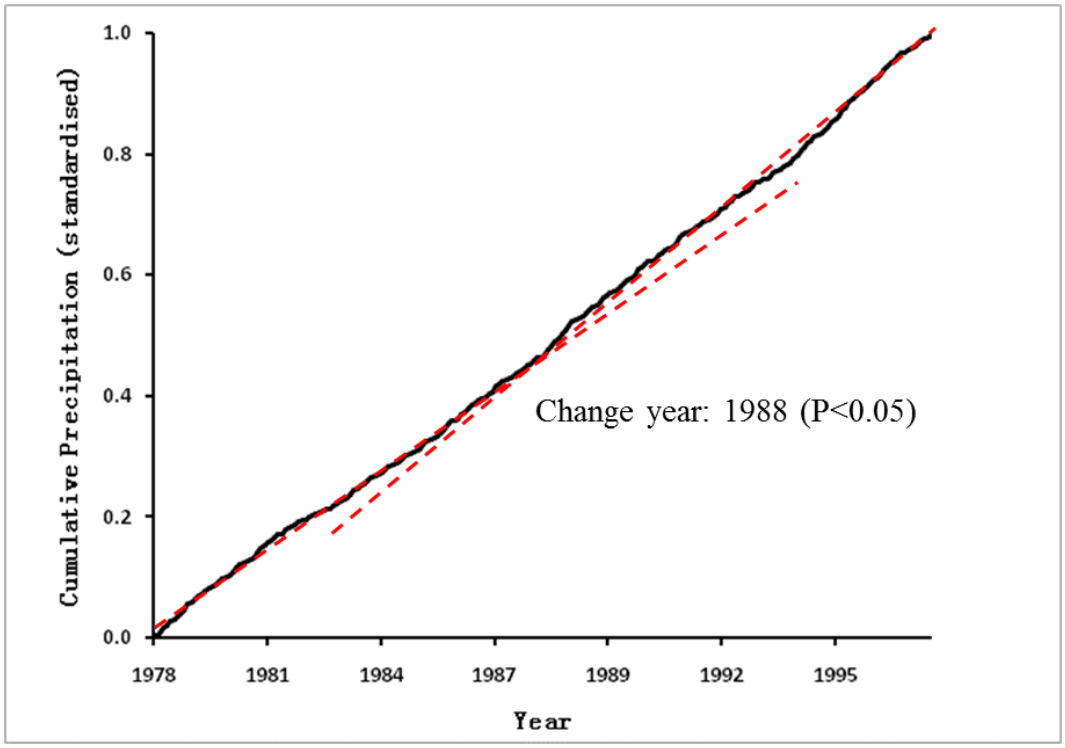

Figure 7.47: Cumulative mass plot of monthly precipitation at Power Station, Kuratau River

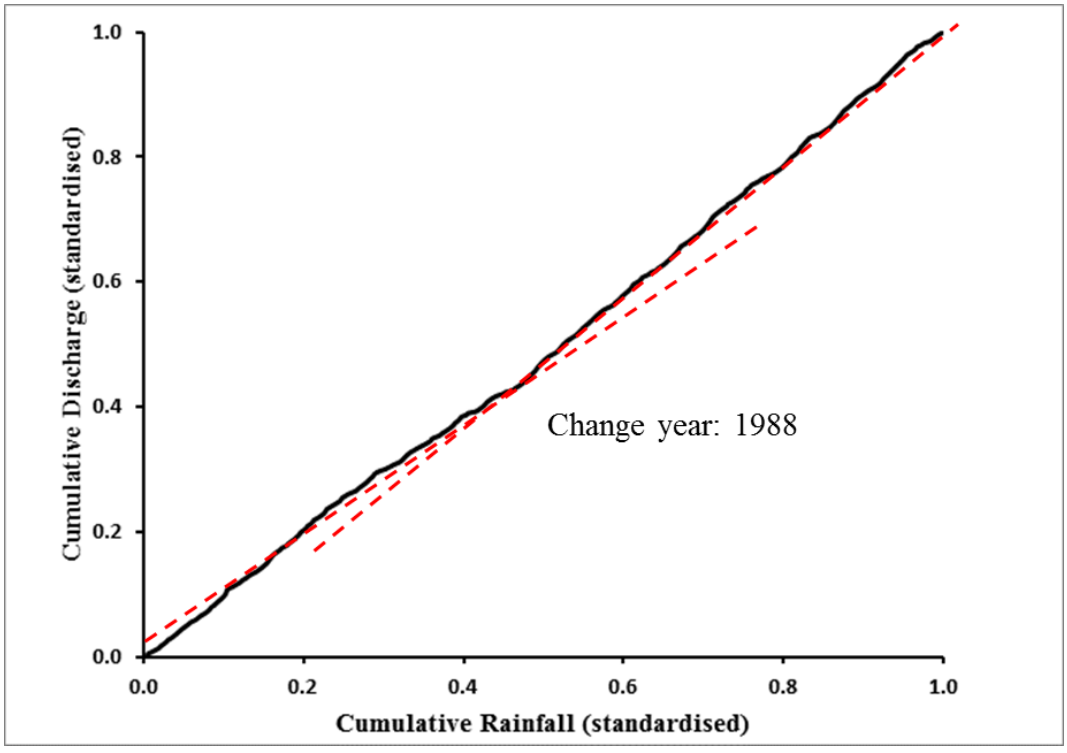

Figure 7.48: Double mass plot of monthly precipitation at Power Station, Kuratau River and monthly mean runoff at SH41 Kuratau Junction, Kuratau River

Mangaokewa Stream at Te Kuiti Pumping Station

In Mangaokewa Stream at Te Kuiti Pumping Station (Figure 7.21), the average monthly mean flow was 5.17 m^3s^{-1} from 1983 to 1993. In the flow time series, the 1988 break points are clear (Figure 7.49) and after 1988 the average monthly mean flow increased by around 45 percent. In the rainfall (gauged in Mangakowhai at Airstrip) cumulative mass plot (Figure 7.50), the 1988 change point is also evident. Therefore, the change points in the flow mass plot which showed with the occurrence of the same changes in rainfall time series indicated no land use shifts happened upstream over the study period. The rainfall runoff DMC (Figure 7.51) indicates rainfall and runoff relationship was uniform separately for each period before and after 1988.

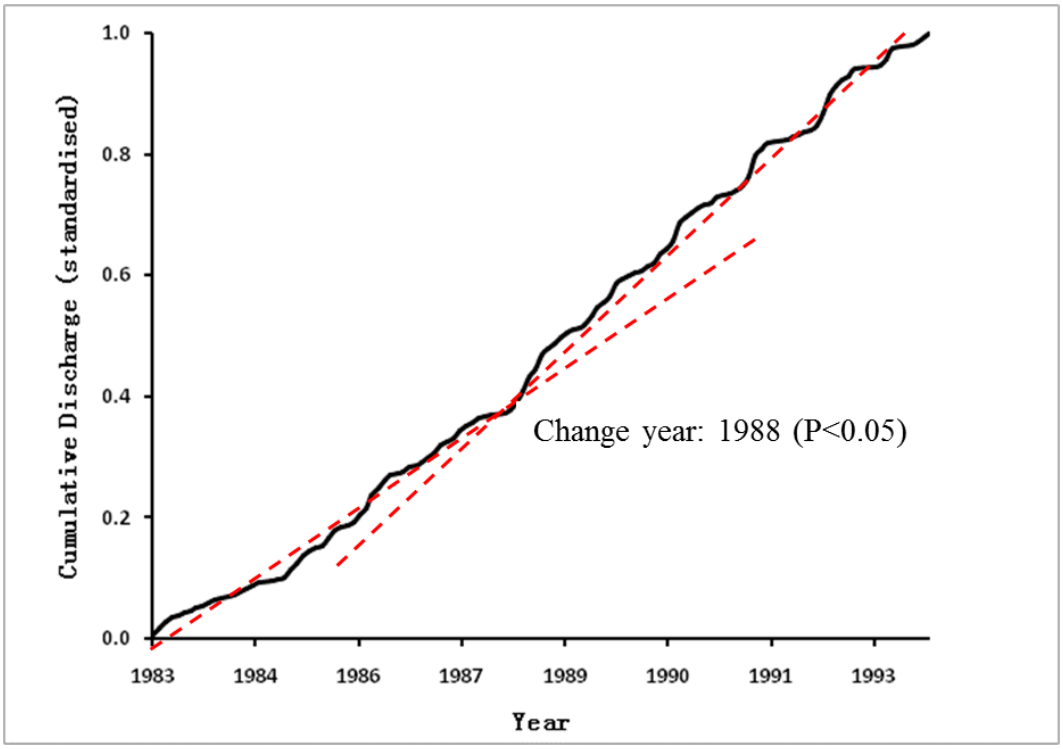

Figure 7.49: Cumulative mass plot of monthly mean runoff at Te Kuiti Pumping Station, Mangaokewa Stream

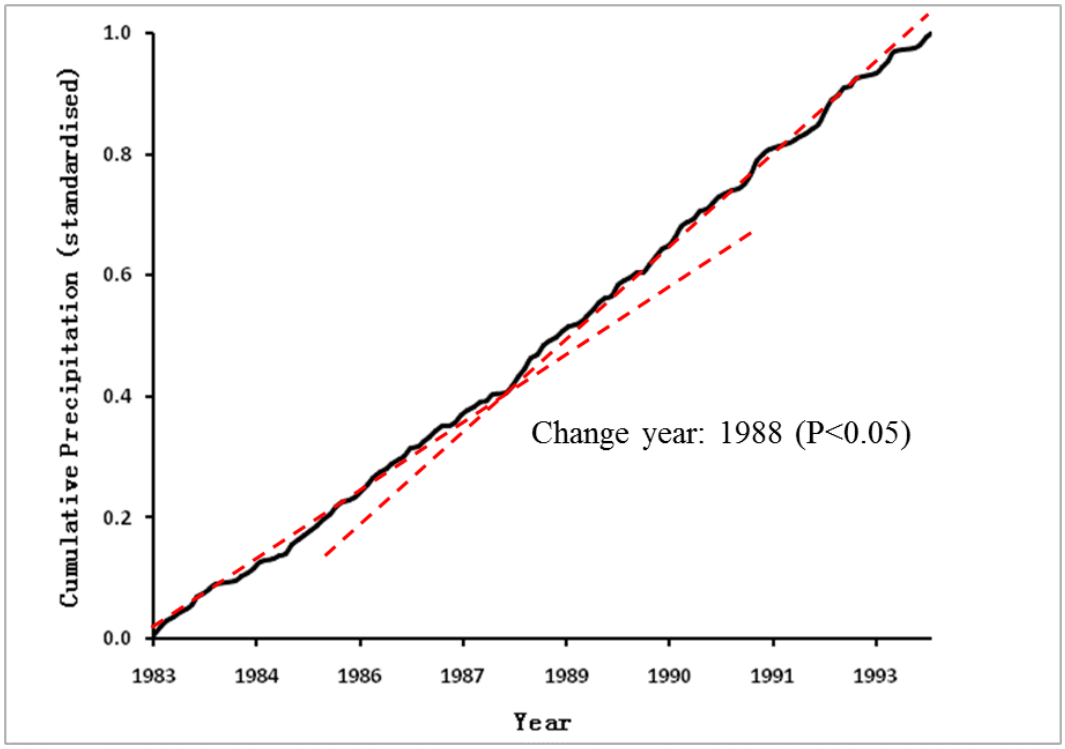

Figure 7.50: Cumulative mass plot of monthly precipitation at Mangakowhai at Airstrip

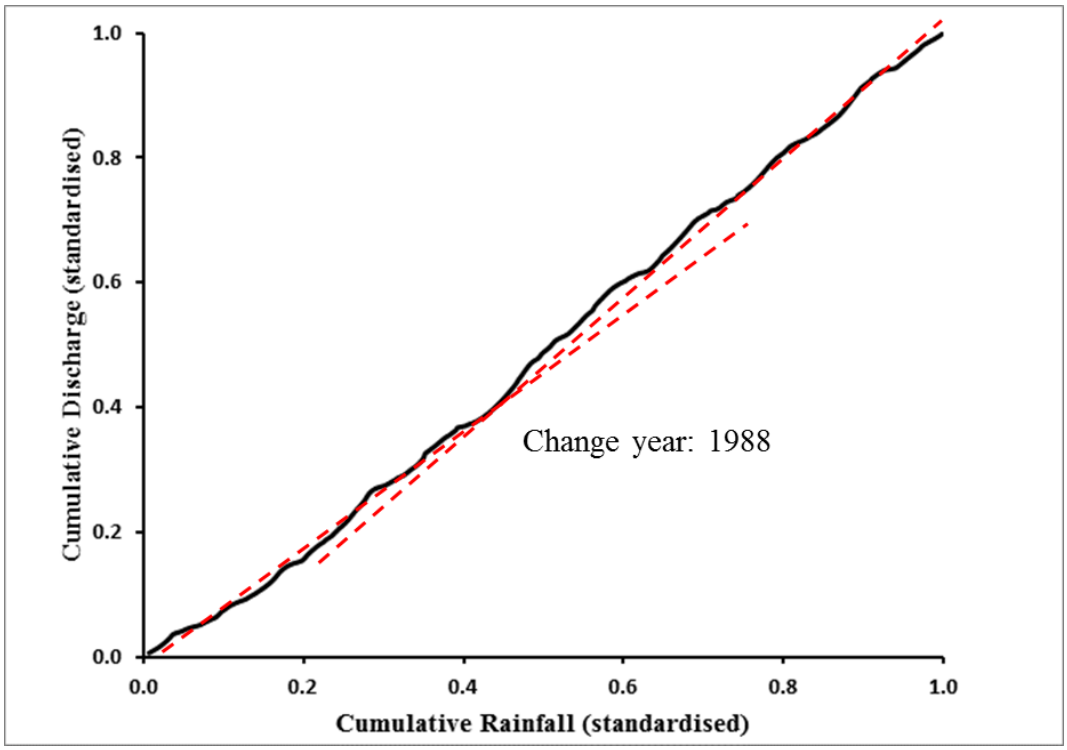

Figure 7.51: Double mass plot of monthly precipitation at Mangakowhai at Airstrip and monthly mean runoff at Te Kuiti Pumping Station, Mangaokewa Stream

In summary, there is a common feature of the 10 special cases: the rainfall-runoff linear relationship changed with the shifts in the rainfall and runoff time series. Some of the double mass plots may be roughly recognized as a straight line by ignoring the departure points in an interval. However, with respect to the percentage change in the mean value for the period before and after a change point, some breaks in the slope of the double mass plot are credible.

Considering the reasons for the changed rainfall-runoff relationship, there are many possibilities. The rainfall-runoff relationship can be easily affected by any even tiny changes in either the component of rainfall or runoff. The changes in the amount of rainfall received by a watershed could lead to shifts in the amount of rainfall that contributes to the runoff. Also, the magnitude of the river/stream may impact the relationship such as a small stream being quite sensitive to any small changes upstream (chopping down some trees) which may be not known by the public. Overall, two main possibilities may explain the changed rainfall-runoff relationship. One is that a land use shift occurred upstream before the study period; as a result in any change either in climate or land use would impact rainfall-runoff relationship sensitively. However, no reference or information relating to the land use change upstream of these 10 discharge gauges has been found. Therefore, another possibility is the rainfall changes are especially unique such as influencing evaporation, this would, therefore lead to changes in rainfall-runoff linear relationship. Some references such as Goodrich et al. (1997), Risbey and Entekhabi (1996), De and Stankiewicz (2006) and Silvapalan et al. (2002) give a detailed studying on rainfall-runoff nonlinearity.

The times of changes in discharge time series gauged at 10 gauges are approximately 1981/2, 1988/9, 1996 which are quite close to the change times discussed in section 7.2 and 7.4. Therefore, the results of section 7.4 which further investigated the difference of different stable periods separated by the change years is also applicable for these 9 cases.

7.6.2 Investigation of the difference of rainfall-runoff relationships for different periods

Figures 7.52-7.61 are scatter diagrams between monthly precipitation and monthly mean runoff for the period before and after the change points. Comparing the relationship between monthly rainfall and monthly mean runoff for the different stable period for each flow gauge, except the paired rainfall runoff gauges at Karangahake, Ohinemuri River (Figure 7.59), the rainfall-runoff relationship are quite different to all of the remaining pairs. Therefore, it also confirmed that the double mass plots (section 7.6.1) could not be fitted as a straight line in the remaining nine cases.

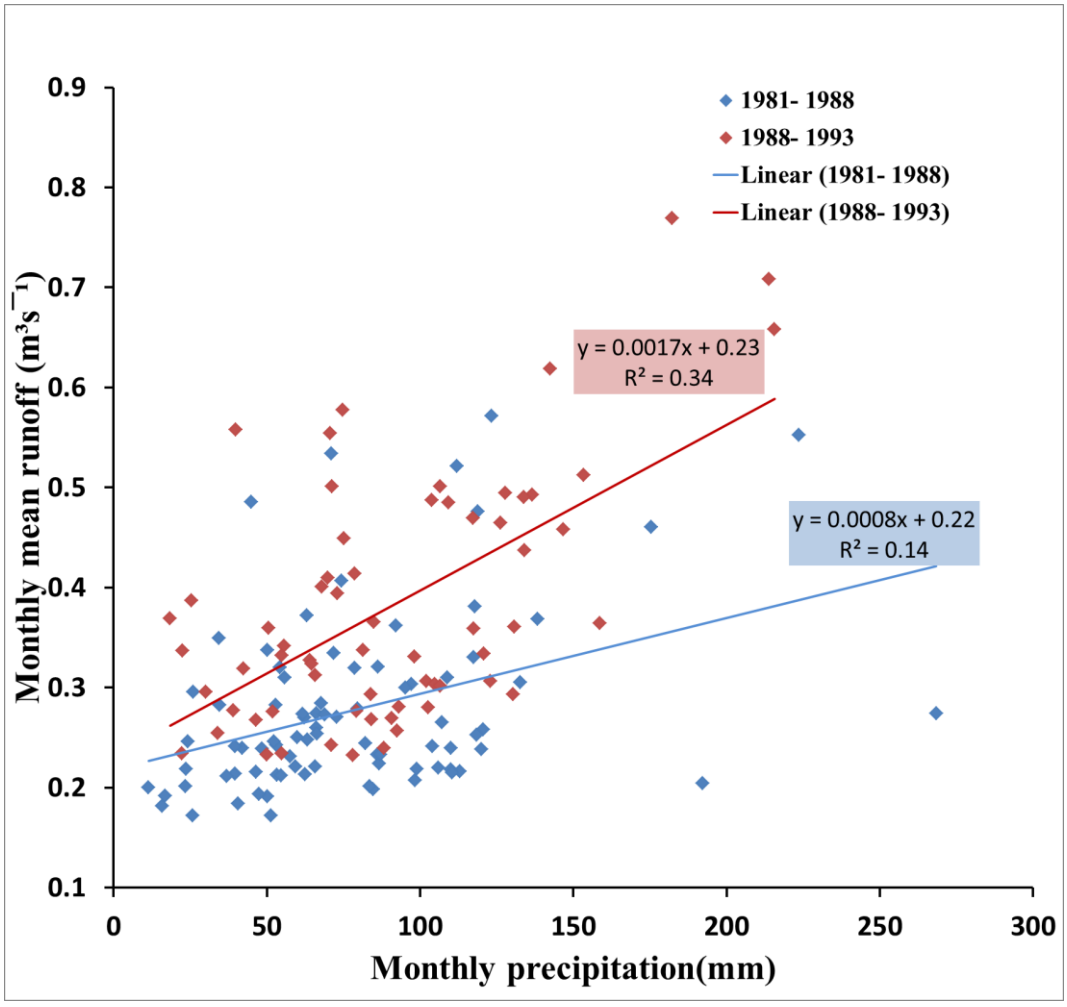

Figure 7.52: Scatter diagram between monthly precipitation at Sylvan Lodge, Torepatutahi Stream and monthly mean runoff at Butcher Road, Mangakara Stream for 1981-1988 and 1988-1993

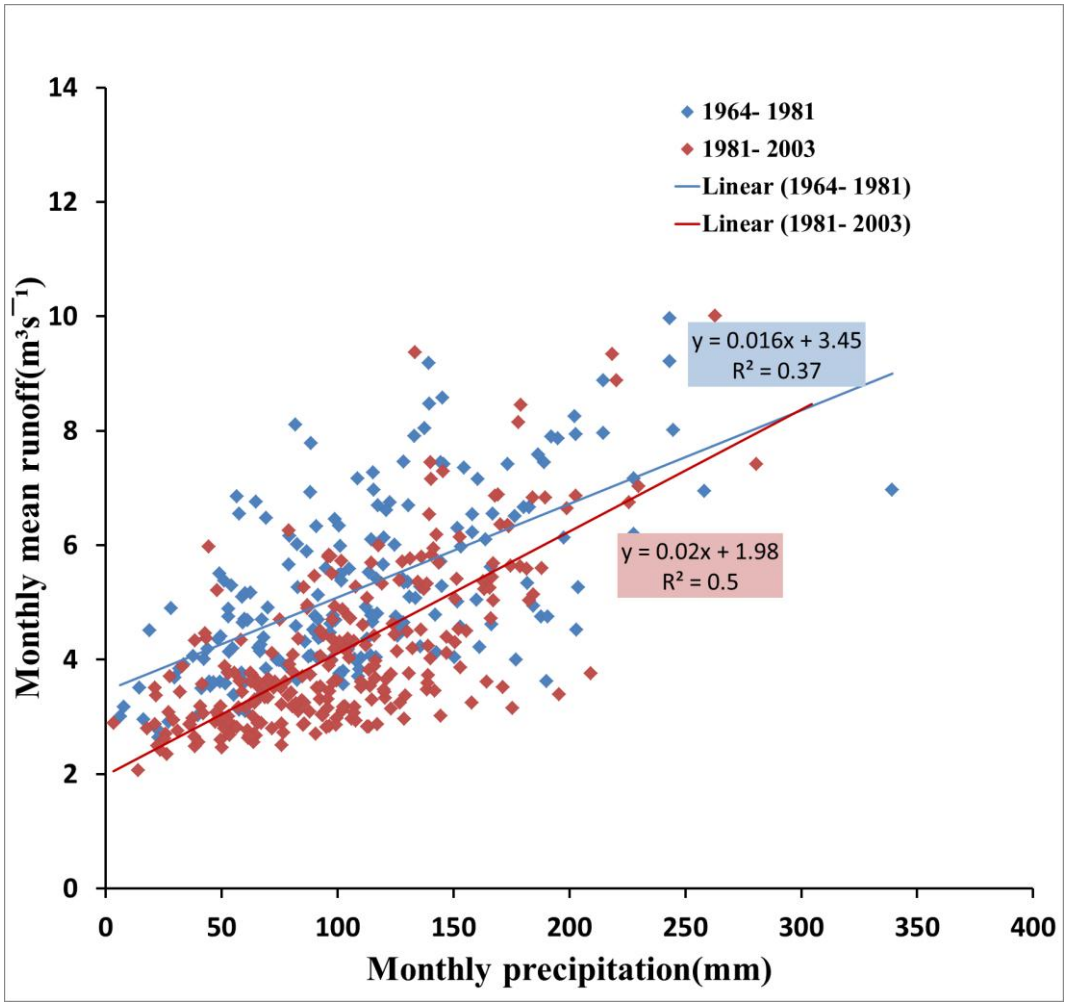

Figure 7.53: Scatter diagram between monthly precipitation at Ngakuru, Waikato River and monthly mean runoff at Ohakuri Road, Tahunaatara Stream for 1964-1981 and 1981-2003

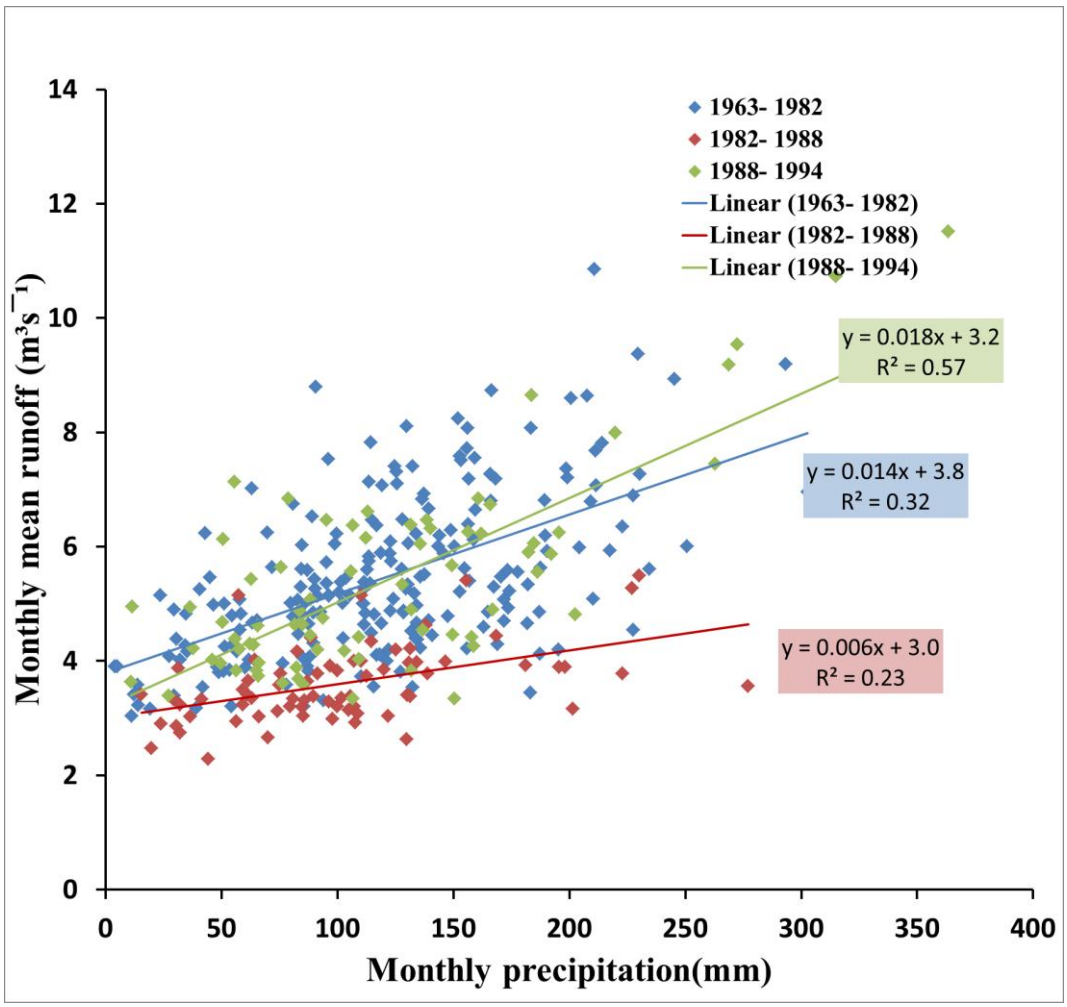

Figure 7.54: Scatter diagram between monthly precipitation at Arapuni Power Station, Waikato River and monthly mean runoff at Arapuni-Putaruru Road, Pokaiwhenua Stream for 1963-1982, 1982-1988 and 1988-1994

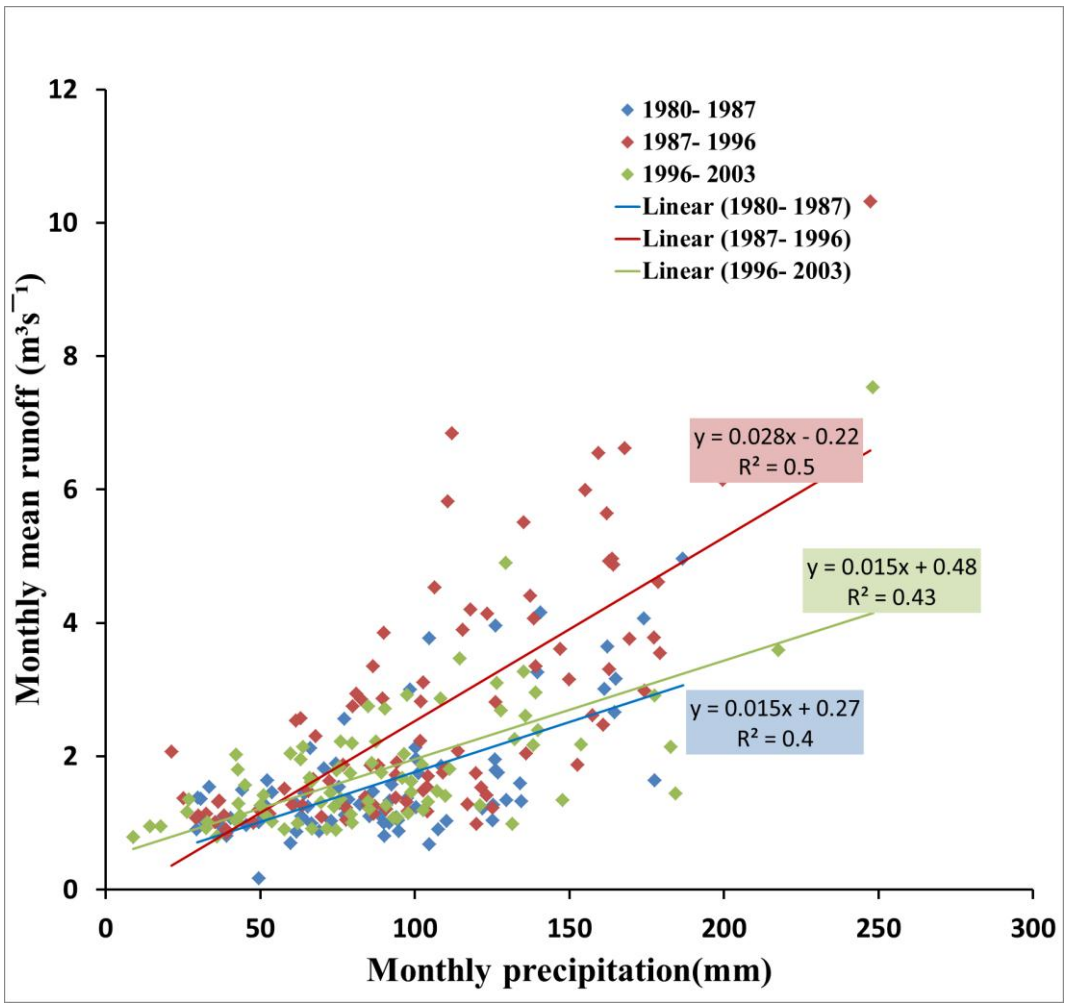

Figure 7.55: Scatter diagram between monthly precipitation at Horsham Downs 2, Waikato River and monthly mean runoff at Dreadnought Culvert SH1,Mangaonua Stream for 1980-1987, 1987-1996 and 1996-2003

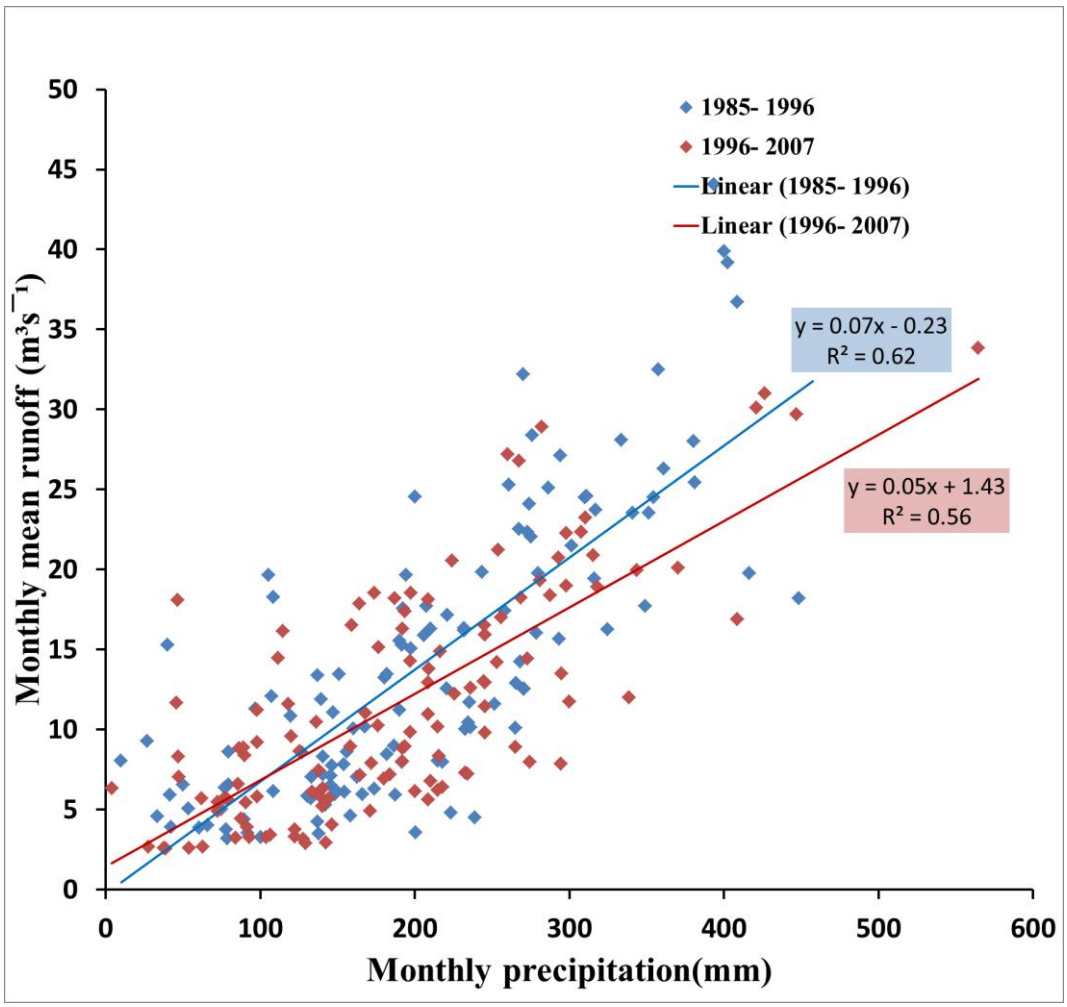

Figure 7.56: Scatter diagram between monthly precipitation at Ngaroma, Puniu River and monthly mean runoff at Otewa, Waipa River for 1985-1996 and 1996-2007

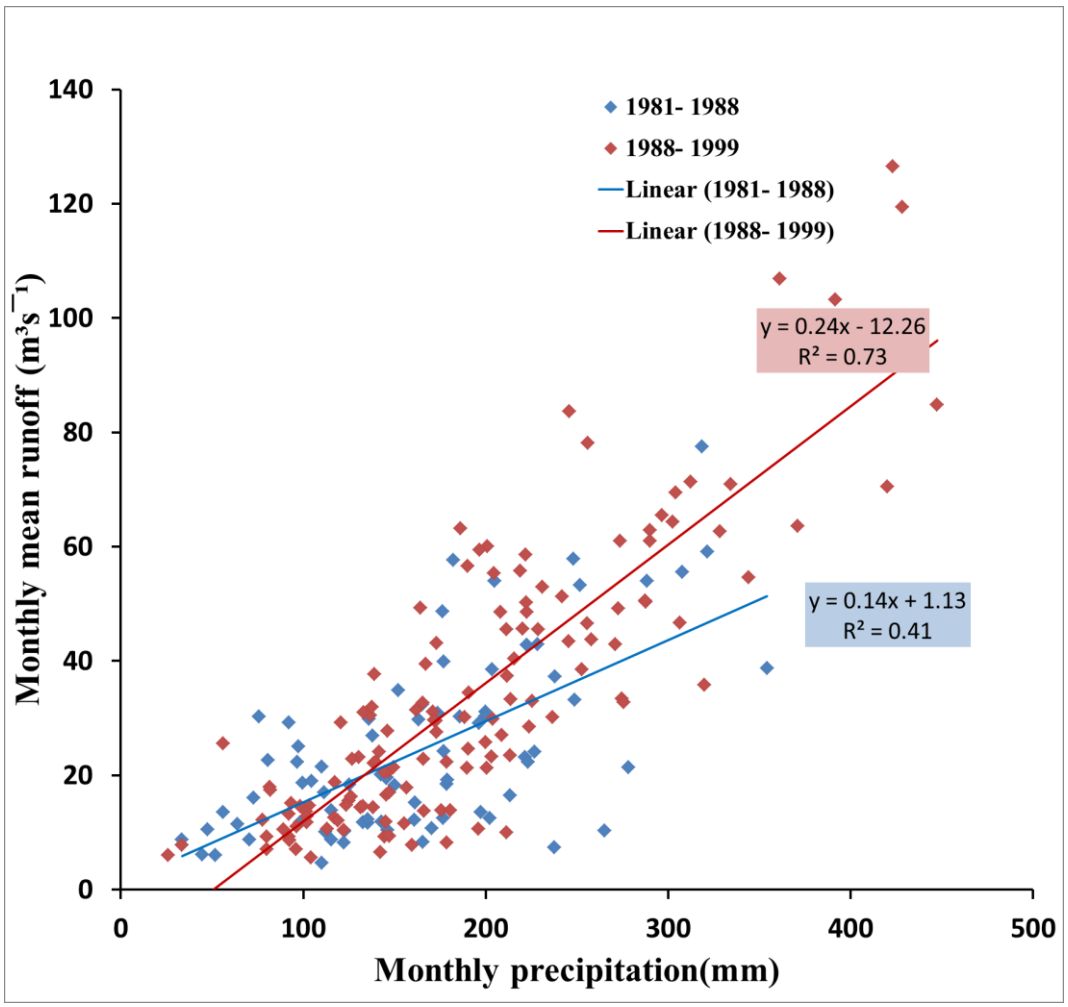

Figure 7.57: Scatter diagram between monthly precipitation at Ngutunui, Ngutunui stream and monthly mean runoff at SH31 Bridge Otorohanga, Waipa River for 1981-1988 and 1988-1999

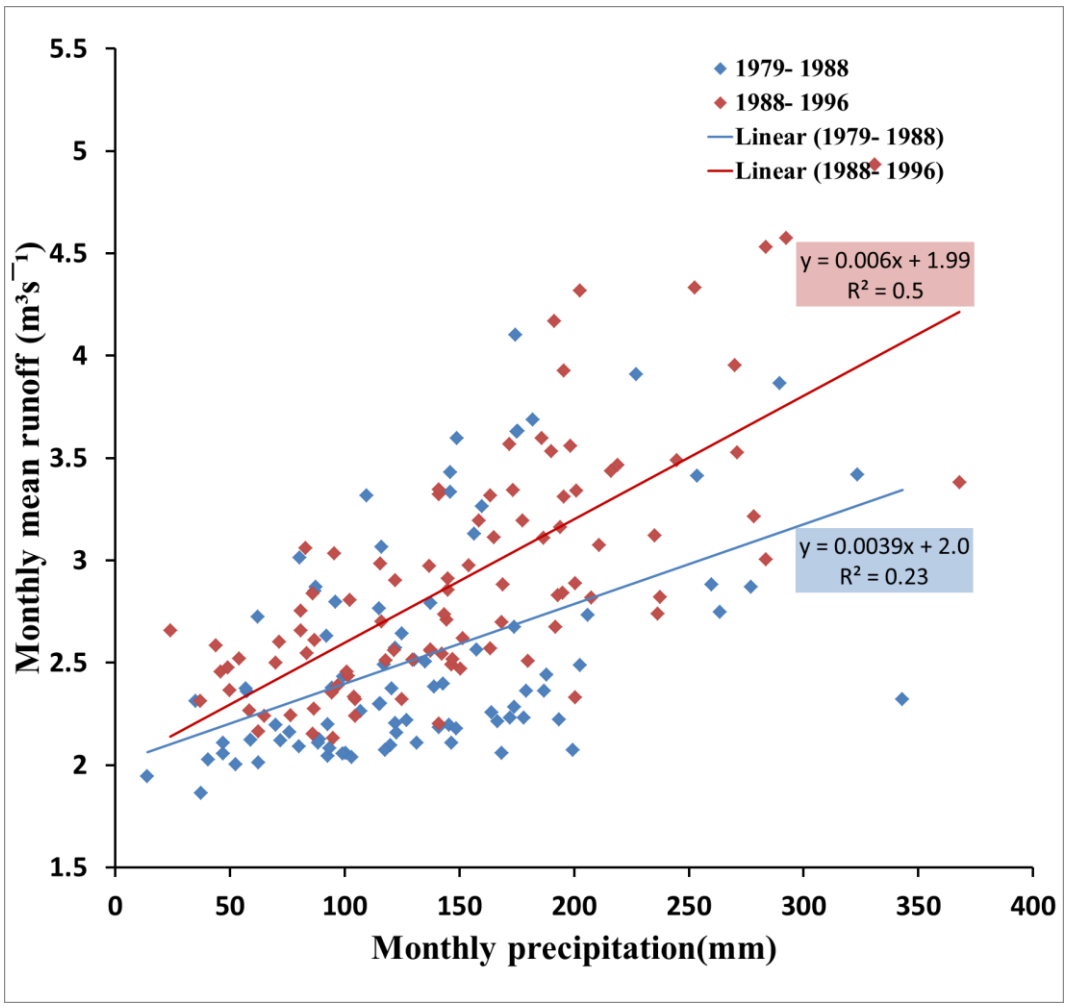

Figure 7.58: Scatter diagram between monthly precipitation at Kuhatahi ,Kuhatahi Stream and monthly mean runoff at Pinedale, Oraka Stream for 1979-1988 and 1988-1996

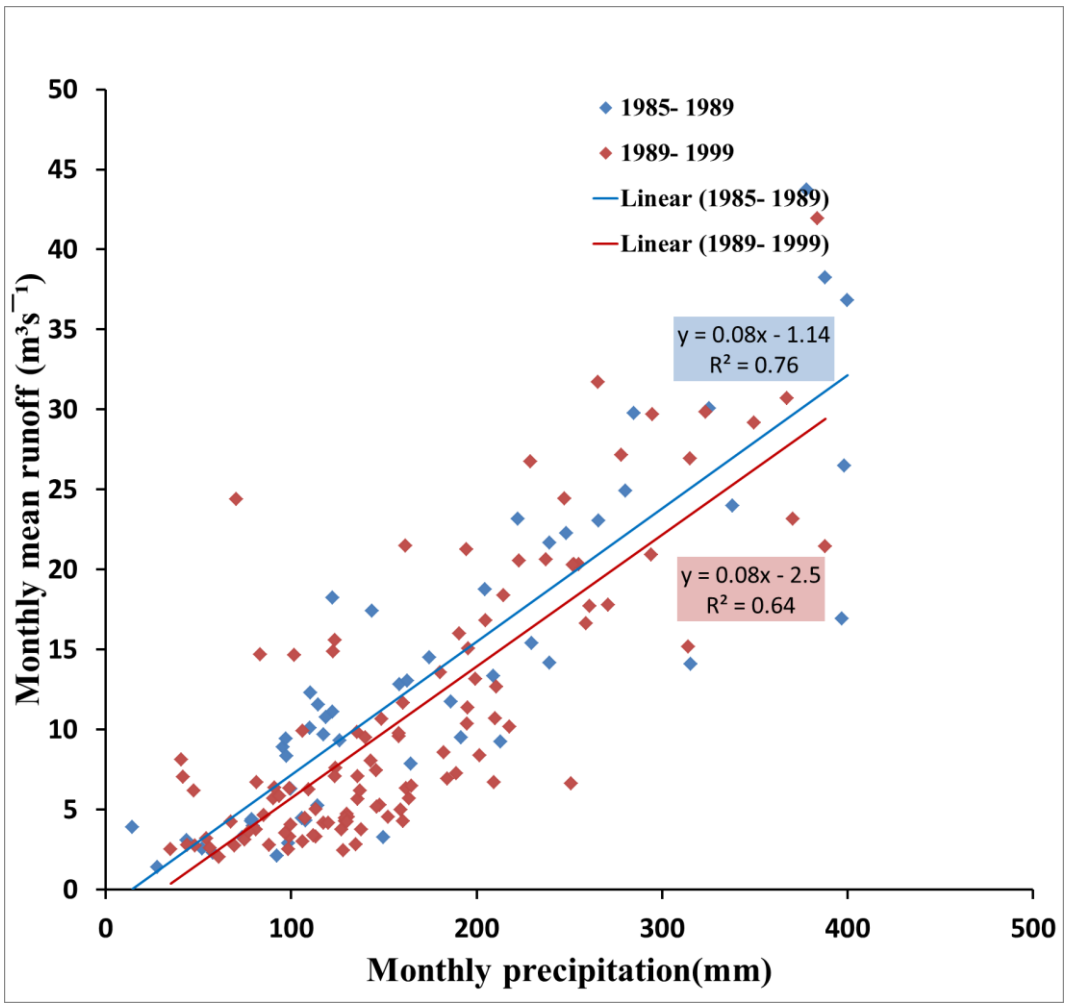

Figure 7.59: Scatter diagram between average monthly precipitation at Woodlands Road Waihi, Ohinemuri River and Waitawheta, Waitawheta River and monthly mean runoff at Karangahake, Ohinemuri River for 1985-1989 and 1989-1999

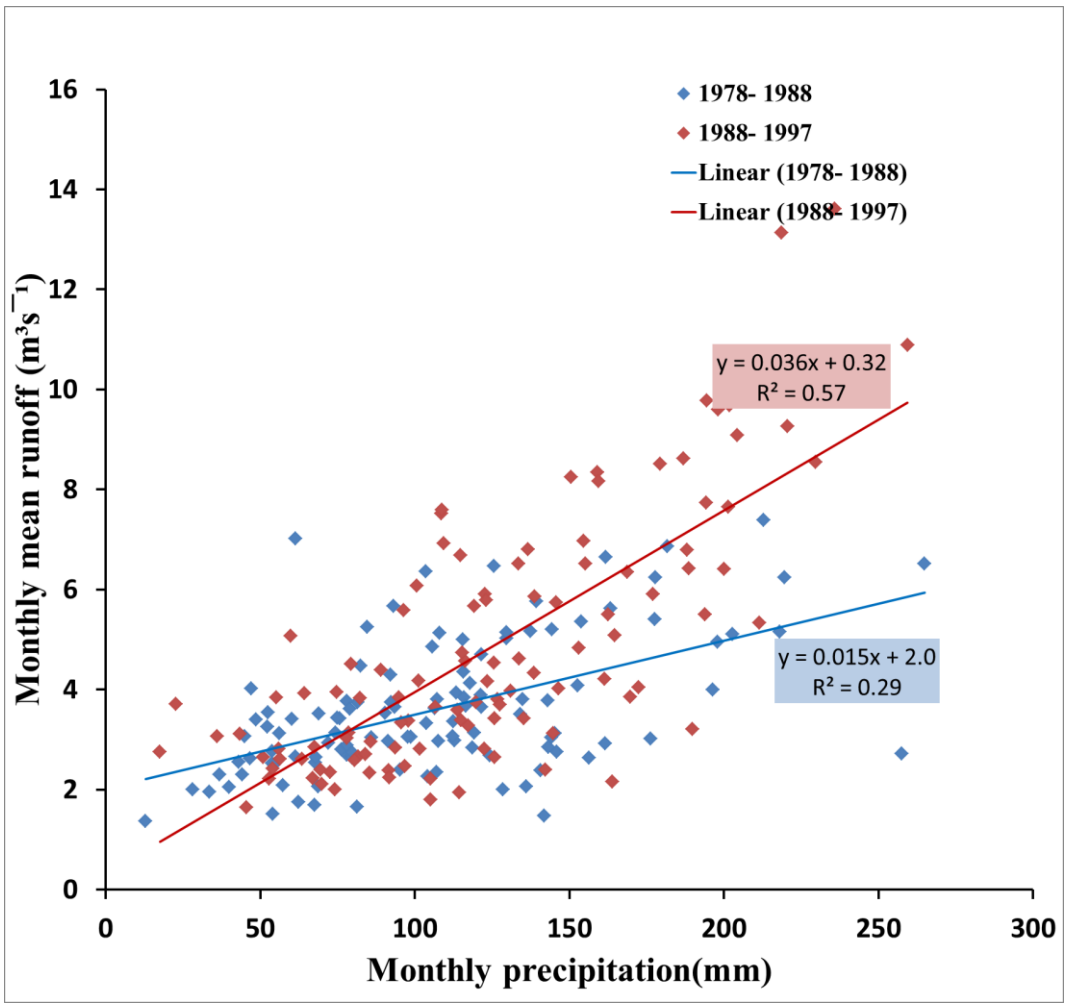

Figure 7.60: Scatter diagram between monthly precipitation at Power Station, Kuratau River and monthly mean runoff at SH41 Kuratau Junction, Kuratau River for 1978-1988 and 1988-1997

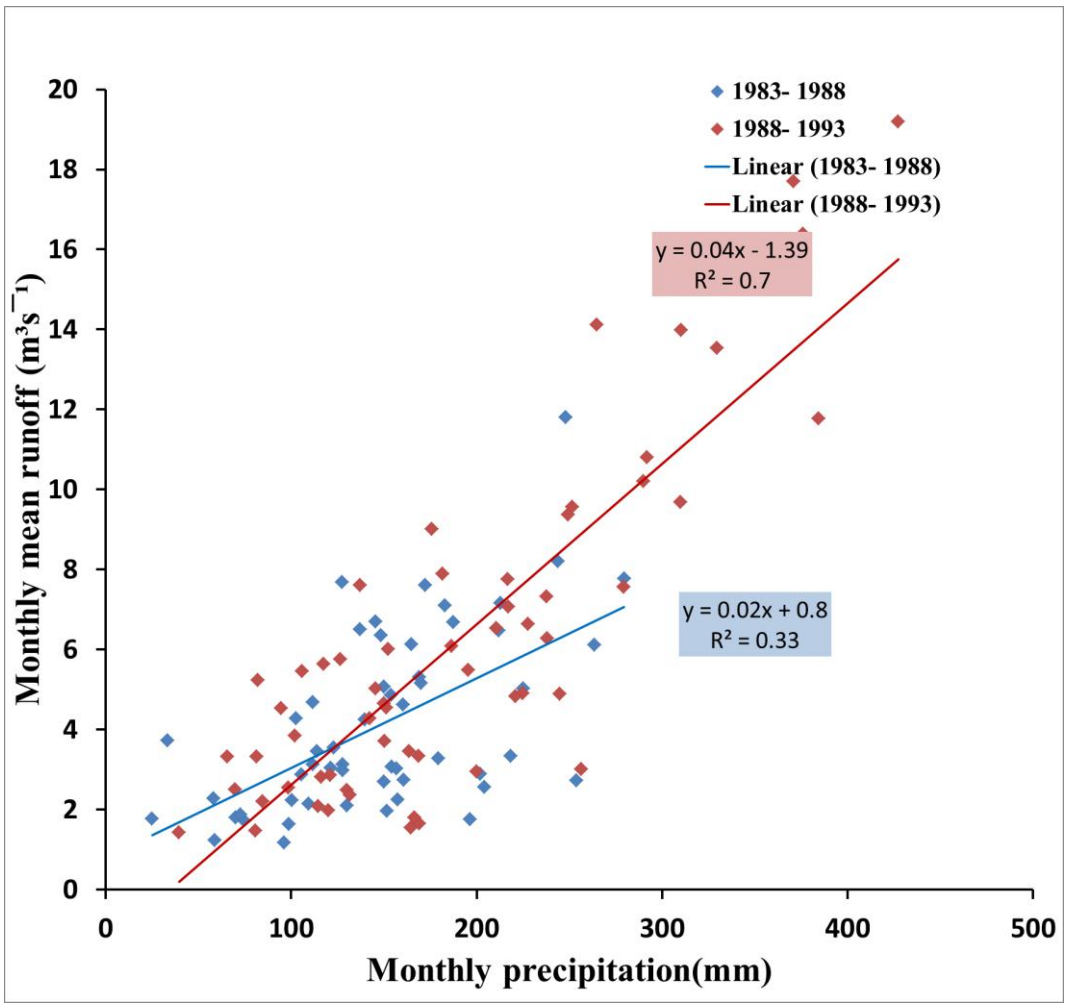

Figure 7.61: Scatter diagram between monthly precipitation at Mangakowhai at Airstrip and monthly mean runoff at Te Kuiti Pumping Station, Mangaokewa Stream

7.7 Relation of Rainfall and Runoff Shifts to Southern Oscillation Variations

Figure 7.62 plots the El Nino and La Nina years since 1950. From 1980 to 2000, the greatest El Nino years included 1982-1983 and 1998, the stronger La Nina events were in 1989-1990 and 1996-1997. There may be some relation here between increased rainfall and river flows in 1988 and 1994/1995 (Figure 7.1 and Figure 7.14), as they are close to the La Nina years. Similarly, the shift toward decreasing rainfall and runoff in 1981 and 1998 may have association with El Nino years. It may be that local sea surface temperatures also have an influence, not detected on the coarse scale of a whole-Pacific index like the Southern oscillation.

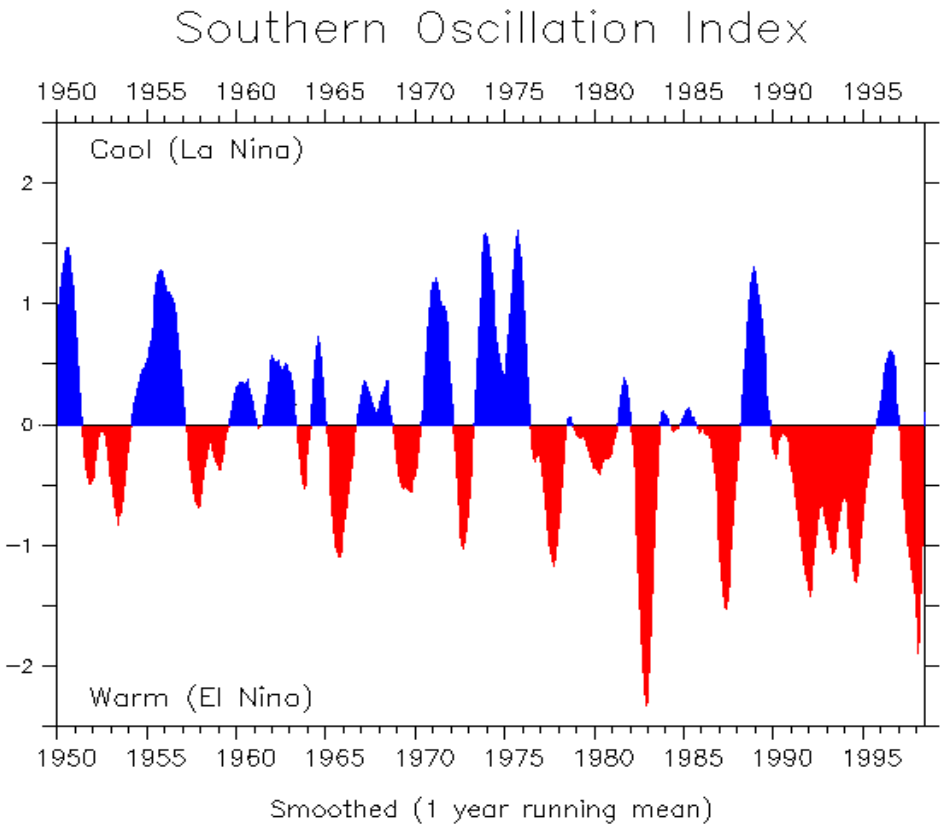

Figure 7.62: El Niño and La Niña years since 1950 (Source: NOAA)

7.8 Conclusion

Over the whole Waikato and part of the Whanganui regions, four rainfall shifts influenced river flow changes over a wide area and appear related to some degree to El Niño and La Niña events. Specifically, 1981 and 1998 are associated with a shift to decreased rainfall and streamflow, while 1988 and 1994/1995 were times of positive shifts. It appears that the main driver of the shifts is the changing frequency of high rainfall events. For the flow gauges, there was considerable variation in the medium and high flows, evidently driven by climatic fluctuations. Moreover, the extreme rainfall shifts may change a rainfall-runoff linear relationship by leading a change in the slope of the rainfall-runoff double mass plot in some specific flow gauges.

Chapter 8–Land Use Change Detection

8.1 Introduction

The variation of rainfall and runoff patterns in the study regions were estimated in Chapter 7 using the Least Square Regression method and the characteristics of the rainfall/runoff mass curves. This chapter is concerned with detecting signals of land use change from rainfall and river discharge time series. For each flow gauge record, when determining which changes are related to upstream land management changes, it is important to enable some degree of anticipation as to how land use changes in the study catchment might impact on the catchment. Therefore, the objectives of this chapter are to:

1. Compare the derived change points from Chapter 7 in each paired rainfall and runoff series to select the flow gauges containing the change points which may be driven by upstream land use change and then match the signals of land use changes to literature; and
2. Investigate the impact of land-use change on river discharge characteristics in the Waikato and the upper Whanganui river catchments.

8.2 Upstream Land-use Change Detection

The change points detected by the LSR method for each paired rainfall and runoff series are compared. The factors that drive the shifts in streamflow are investigated on the basis that discharge change points due to land management impacts are identified as flow changes in the absence of rainfall changes and conversely, change points due to climate variation are identified as discharge changes with concurrent rainfall changes. Additionally, the effects of land use change on streamflow are investigated by using the figures showing the average monthly mean streamflow, flow duration curves, and rainfall runoff scatter plots.

In total, 10 of the 44 given flow gauges were recognized to have the signals of upstream land use change (Figure 8.1). Four (3 are studied in Chapter 9) of the 10

flow gauges are in the Wanganui catchments and the rest are in the Waikato region.

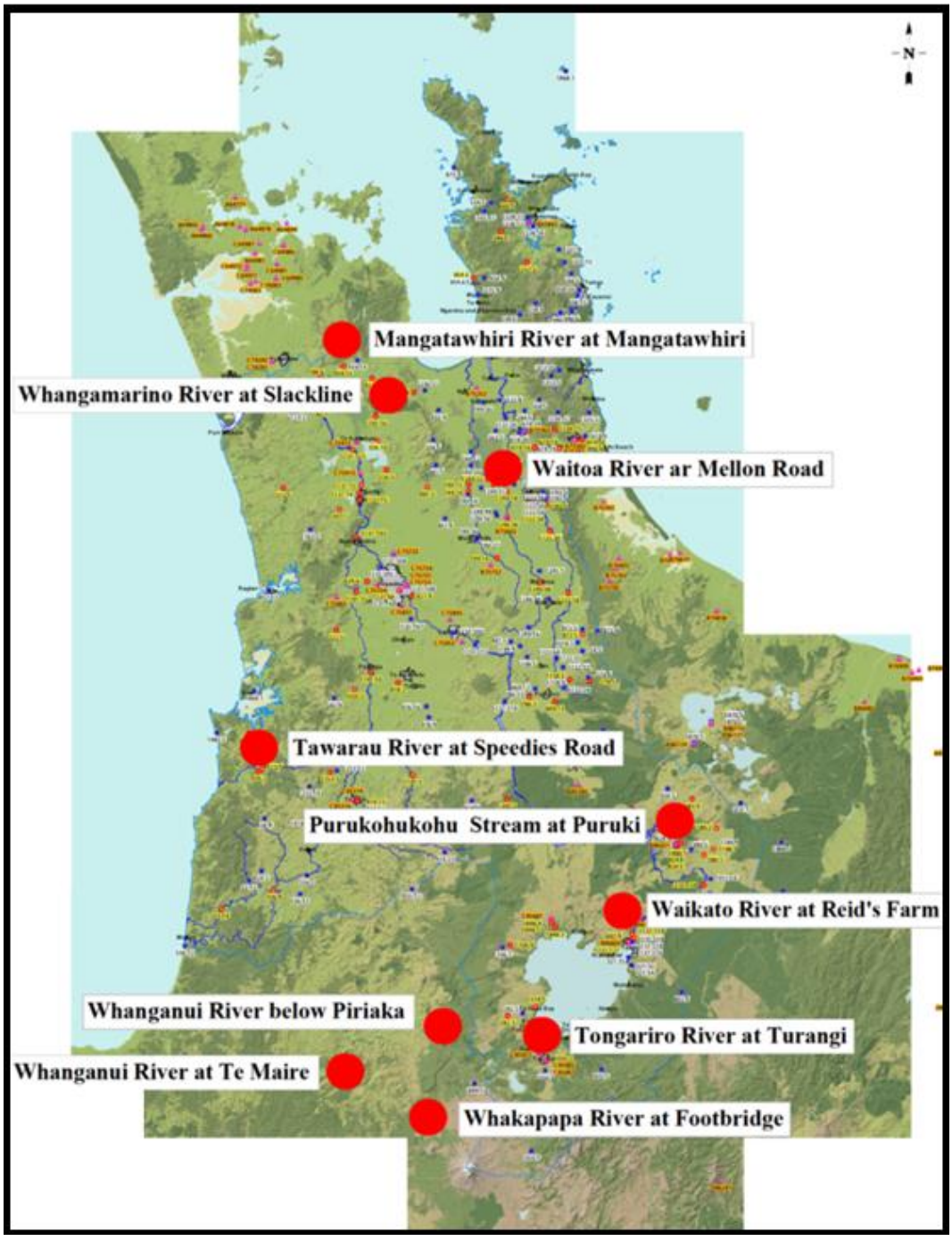

Figure 8.1: Location of the runoff gauges showing the signals of upstream land-use change

8.2.1 Gauge stations with signals of upstream land use change

The river discharges gauged at seven rivers/streams were found to be consisted with land-use change. There were three in the Wanganui catchments (Tongariro River, Whakapapa River and Whanganui River) and four in the Waikato region (Waikato River, the Purukohukohu Stream, the Mangatawhiri River, the Waitoa River, the Tawarau River and the Whangamarino River). A more detailed study of the Whakapapa River and the Wanganui River is presented in Chapter 9. The seven flow gauges were categorised into two groups: one being the flow time series containing apparent signals of land use change, meaning the change points in the flow time series are different from those in the rainfall time series (Group 1); the other is the flow time series not containing clear signals of land use change. In other words, the change points in rainfall and runoff time series are the similar. However, the slope of the rainfall-runoff double mass plot changed frequently as the rainfall and runoff change (Group 2).

Group 1

Purukohukohu Stream at Puruki

The small Purukohukohu catchment is a typical river catchment impacted by forest establishment. Compared to larger river catchments, the impact of vegetation change on the Purukohukohu catchment is more evident because of the dominating influence of hillslope flows (Davie and Fahey, 2005). In the Purukohukohu experimental basin, the catchment was converted to pinus radiata in 1973.

Purukohukohu Stream, with around 0.06 m^3s^{-1} mean monthly flow over the study period 1969 to 2003. For the discharge time series gauged in the Purukohukohu Stream at Puruki (Figure 8.1), the flow cumulative mass plot shows the anticipated progressive slope decrease rather than a sudden shift, reflecting progressive forest growth impacting from about 1975 (Figure 8.2). The cumulative rainfall (gauged at Ngakuru, Waikato River) mass plot (Figure 8.3) is approximately linear, quite different from the changes in the slope of the cumulative runoff mass plot.

The land use impact here (as opposed to rainfall shifts) is evident in the similar pattern of the double mass plot (Figure 8.4), with the changes in gradient denoting change in the rainfall-runoff relation.

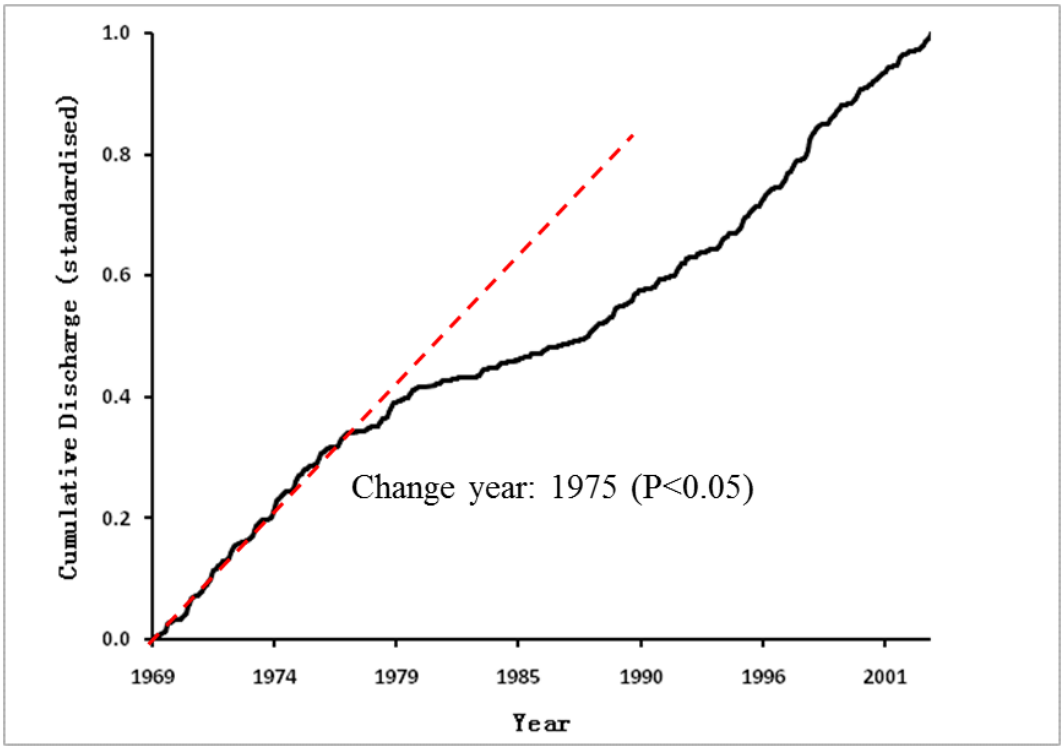

Figure 8.2: Cumulative mass plot of monthly mean runoff at Puruki, Purukohukohu Stream

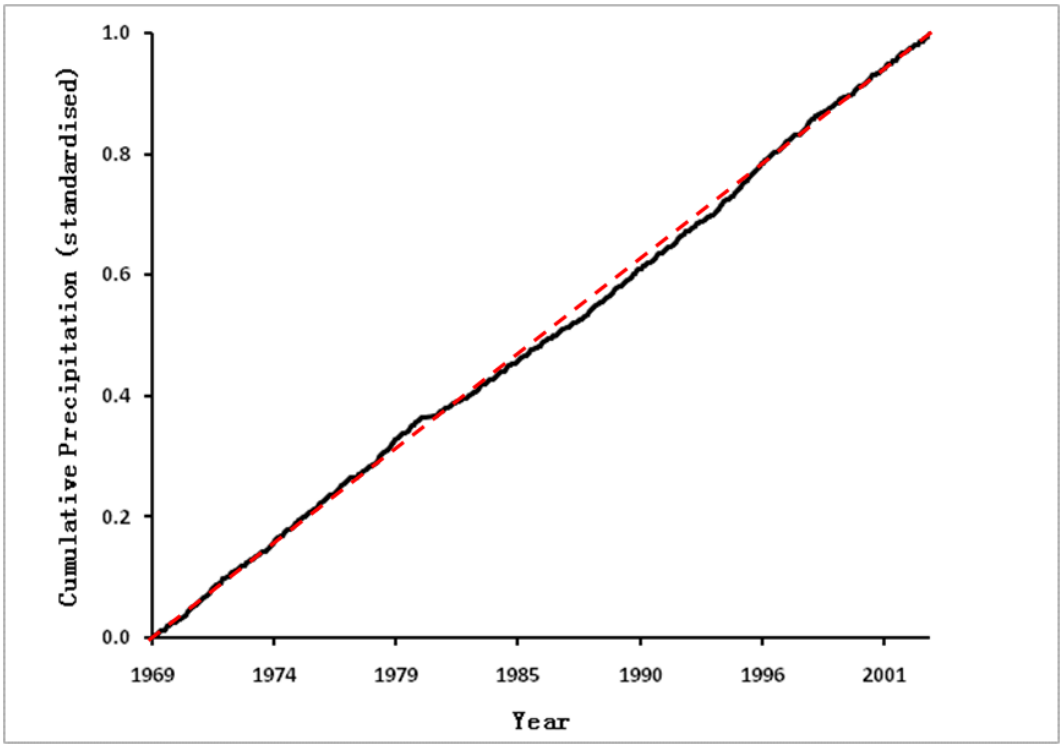

Figure 8.3: Cumulative mass plot of monthly precipitation at Ngakuru, Waikato River

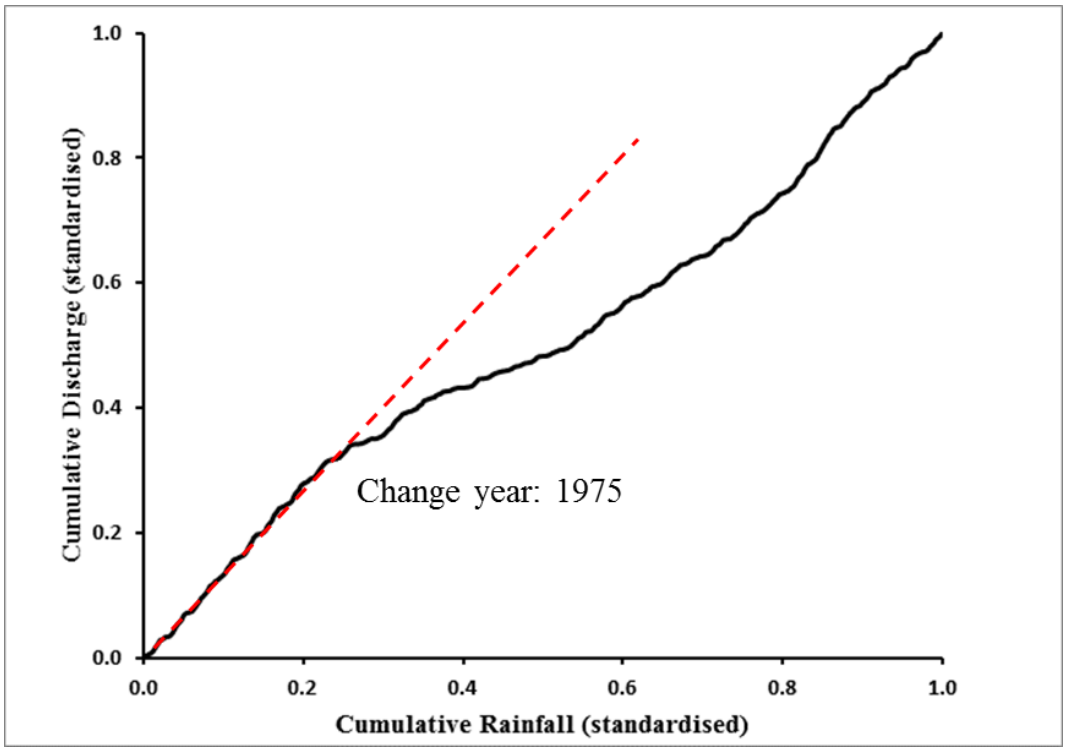

Figure 8.4: Double mass plot of monthly precipitation at Ngakuru, Waikato River and monthly mean runoff at Puruki, Purukohukohu Stream

Tongariro River at Turangi

In the Tongariro River at Turangi (Figure 8.1), the average monthly mean flow was 39.6 m^3s^{-1} for the period 1957 to 2003. For this flow time series, the 1973 change point is evident (Figure 8.5). However, the rainfall (gauged in Tongariro River at Tongariro Hatchery) cumulative mass plot (Figure 8.6) presents a straight line without clear change points. The change point in 1973 is also shown in the rainfall runoff double mass plot (Figure 8.7). Hence, it can be sure that land use shift happened in around 1973 in upstream Tongariro River at Turangi, reflecting the Tongariro diversions.

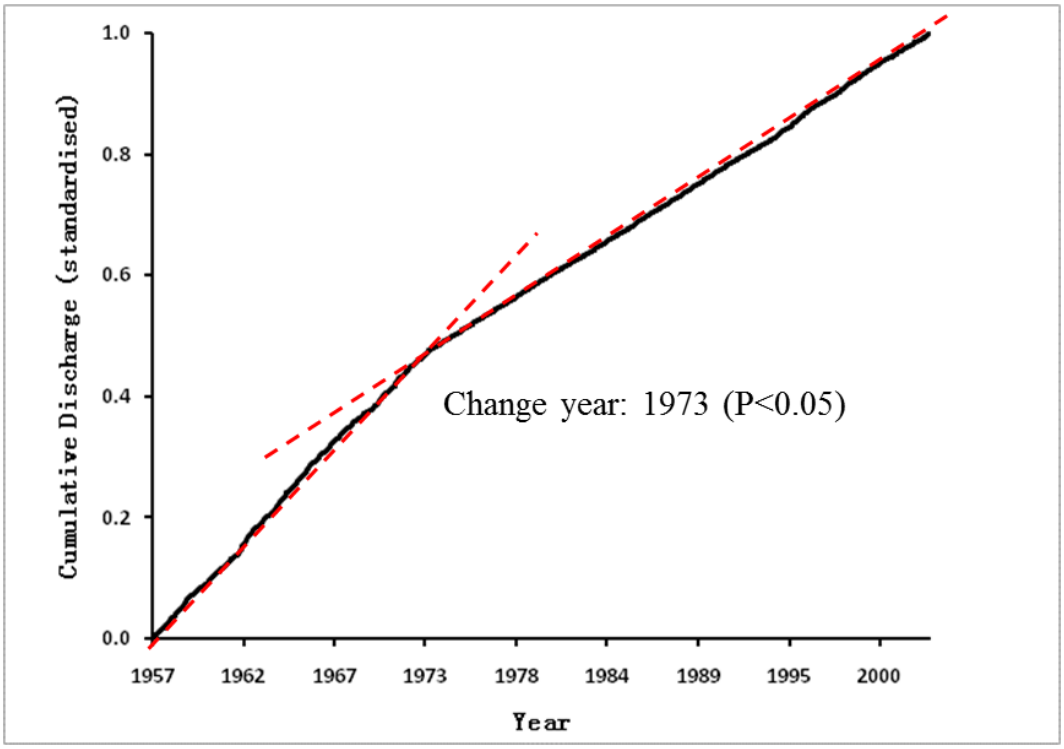

Figure 8.5: Cumulative mass plot of monthly mean runoff at Turangi, Tongariro River

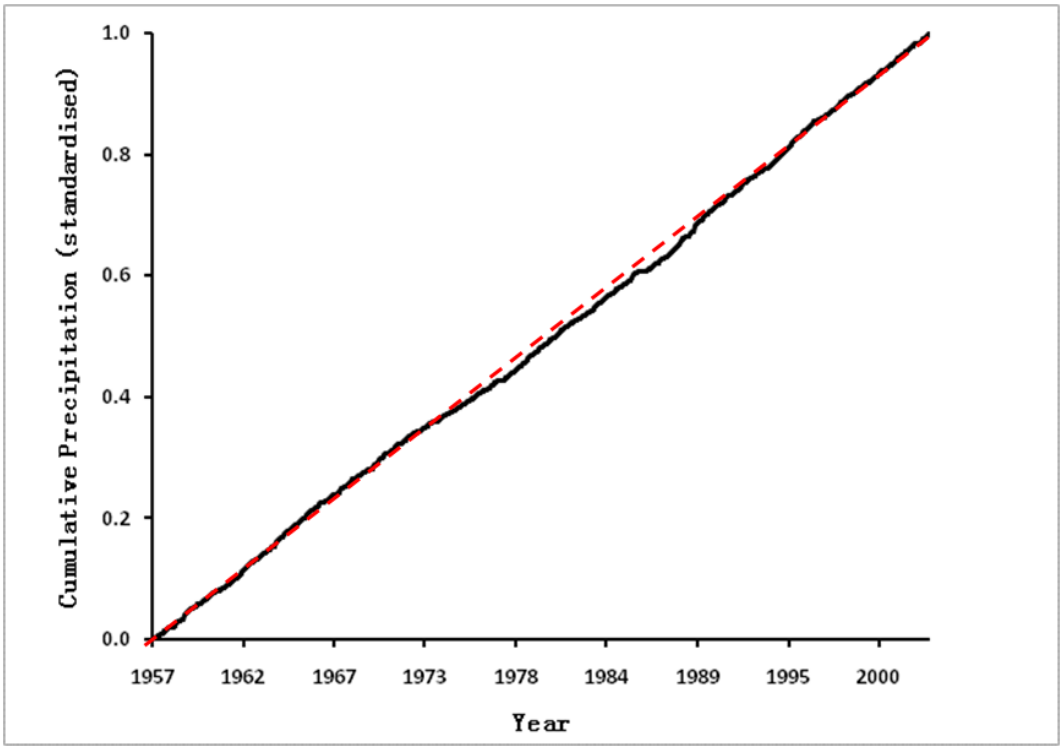

Figure 8.6: Cumulative plot of monthly precipitation at Tongariro Hatchery, Tongariro River

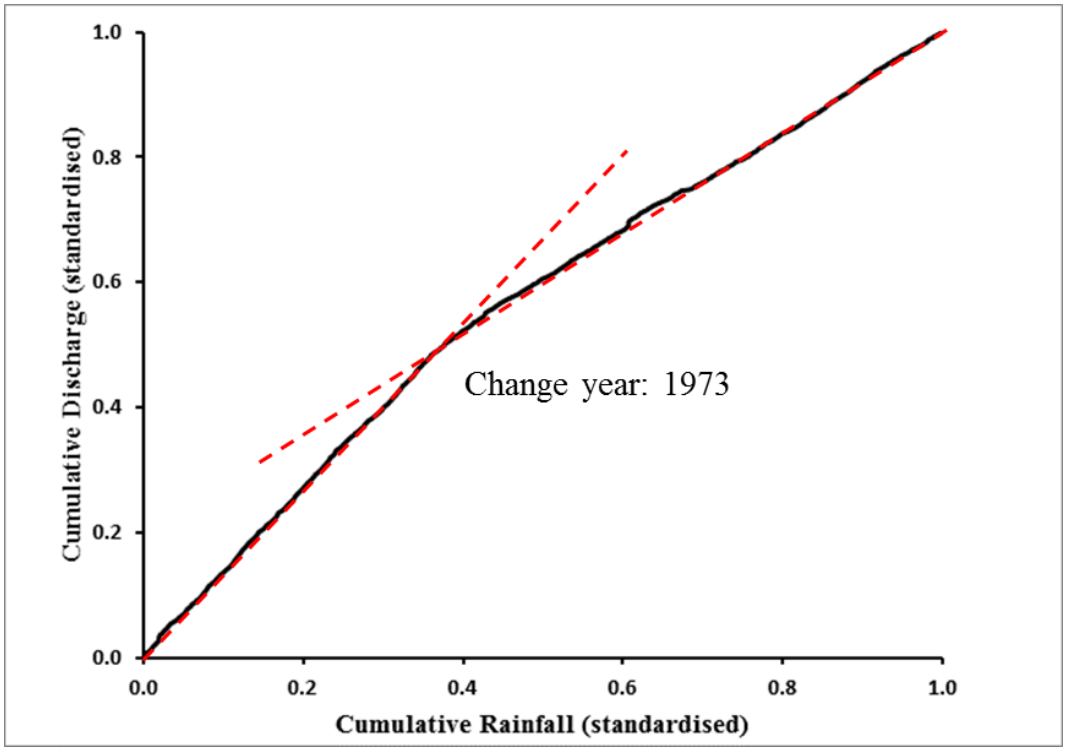

Figure 8.7: Double mass plot of monthly precipitation at Tongariro Hatchery, Tongariro River and monthly mean runoff at Turangi, Tongariro River

Waikato River at Reid's Farm

For monthly mean runoff series at Reid's Farm, Waikato River (Figure 8.1) for the period from 1969 to 1984, the break point in 1975 is evident with an around 19 percent increase in the mean (Figure 8.8). The mean monthly mean discharge for the period before 1975 was around 121 m^3s^{-1}, for the period 1975 to 1979 was 144 m^3s^{-1}, and for the period after 1979 was 154 m^3s^{-1}. For the monthly rainfall gauged in Reporoa, Waikato, the slope of the cumulative rainfall mass plot (Figure 8.9) remains unchanged for the whole study period. Therefore, the change point show in the runoff time series was not detected from the rainfall time series, representing the runoff change point 1975 might be driven by the impact of upstream land use change.

The rainfall runoff double mass plot (Figure 8.10) similarly showed a notable breakpoint around 1975. This change point appears in the cumulative mass and double mass plots which confirmed that the runoff upstream of Reid's Farm, Waikato River was impacted by the upstream land use changes.

With respect to land-use shift in the upstream of Waikato River at Reid's Farm, the Tongariro power scheme that drained approximately 20 % more water to Lake Taupo and operated in 1973 could be the most influential one. The commissioning year of the scheme offers the reason for the increase in runoff of Waikato River at Reid's Farm since 1975, while the two year lag is largely a transition period during which the drained water recharged the ground water.

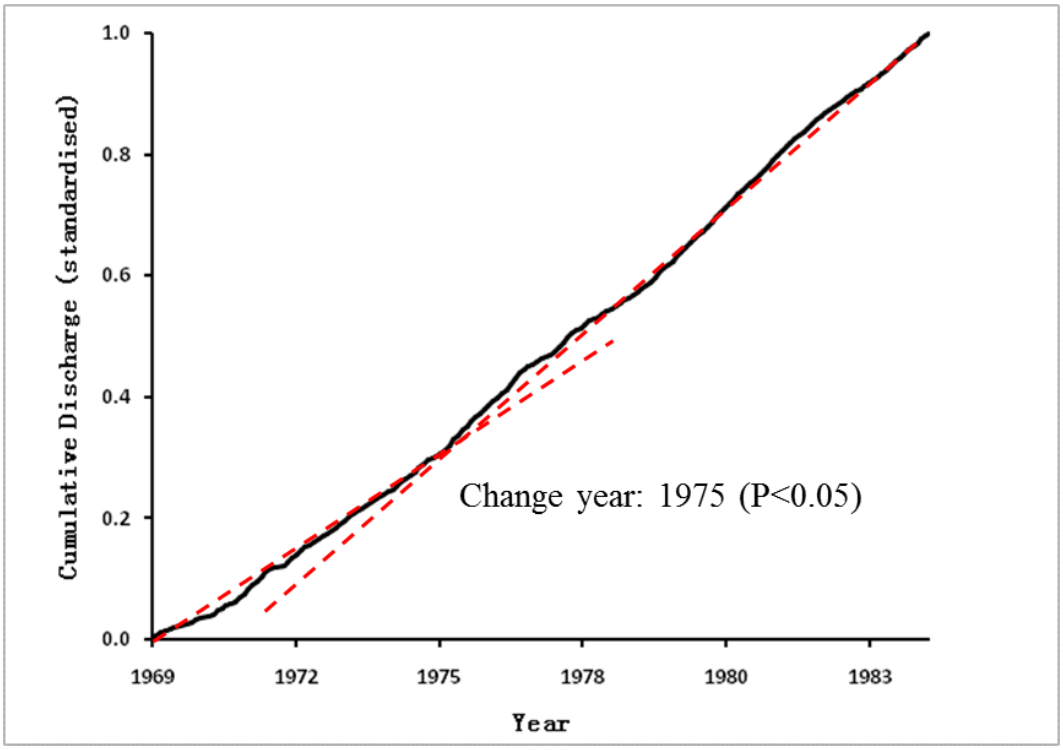

Figure 8.8: Cumulative mass plot of monthly mean runoff at Reid's Farm, Waikato River

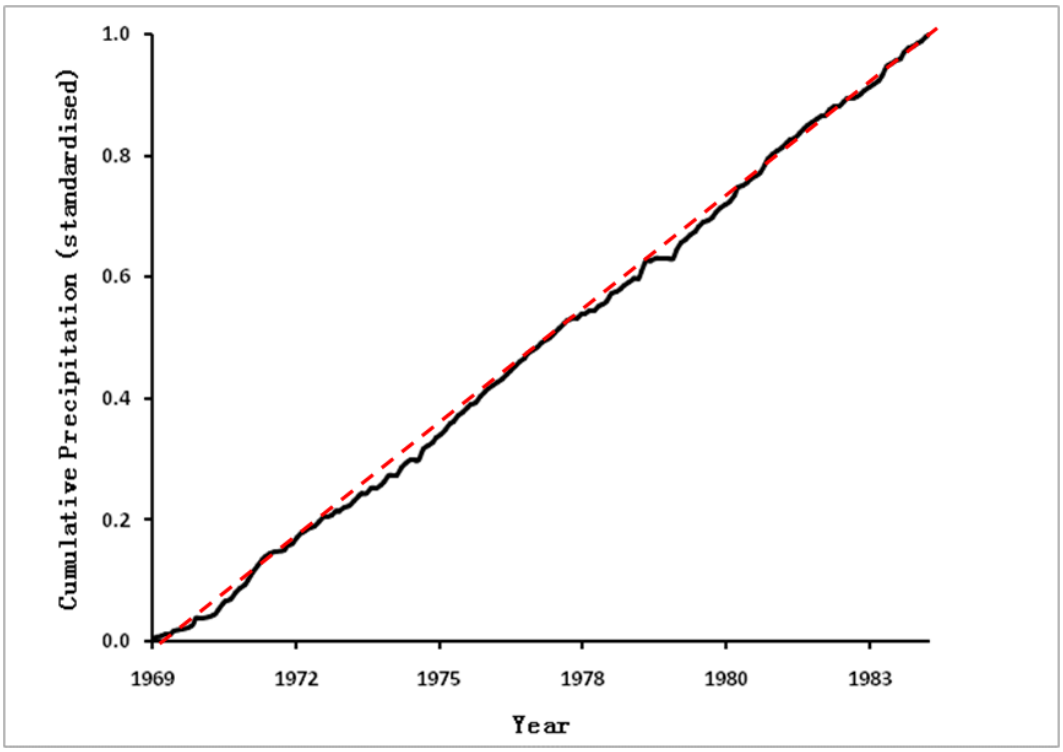

Figure 8.9: Cumulative mass plot of monthly precipitation at Tahorakur, Waikato

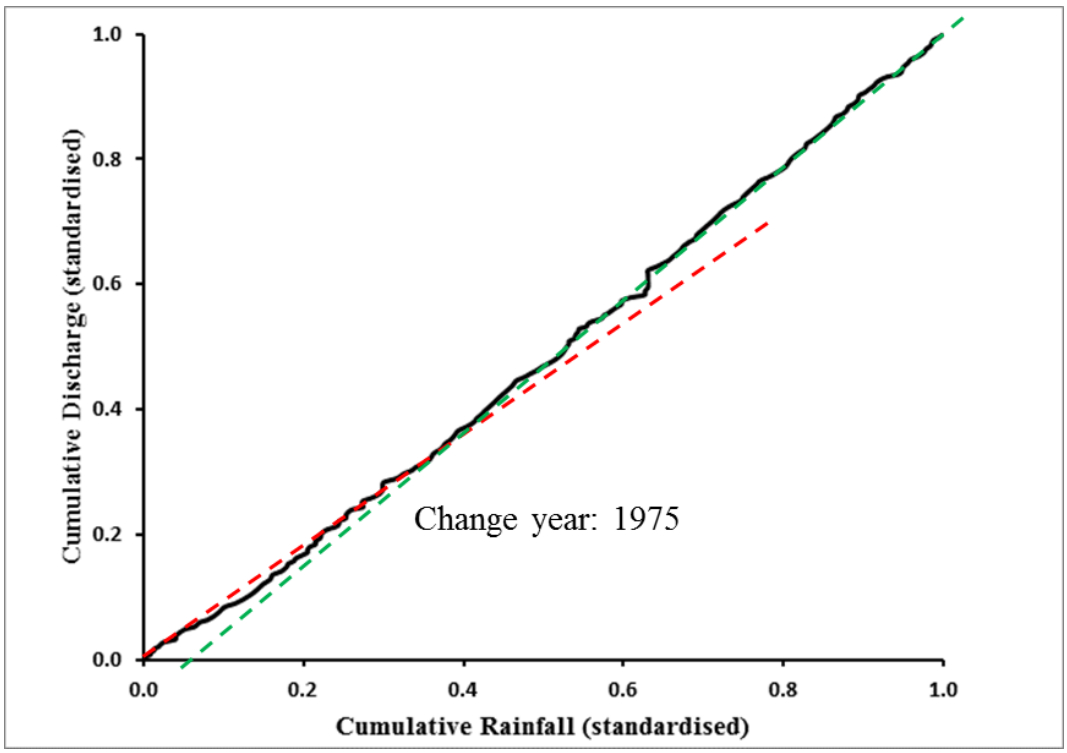

Figure 8.10: Double mass plot of monthly precipitation at Tahorakur, Waikato and monthly mean runoff at Reid's Farm, Waikato River

Mangatawhiri River at Mangatawhiri

The Mangatawhiri River is a major tributary of the Lower Waikato River and dischargeinto the Waikato River north of Mercer. It drains a total catchment area of approximately 18.4 km². In the small Mangatawhiri River gauge at Mangatawhiri (Figure 8.1), the average monthly mean flow was 1.86 m^3s^{-1} from 1969 to 2002. In the cumulative flow mass plot (Figure 8.11), there are multiple gradual change points from 1974 to 2002 such as the 1980 and 1987 change points. However, within the same period (1974 to 2002), the cumulative rainfall (gauged in Mangatawhiri River at Mangatawhiri) mass plot (Figure 8.12) is almost straight, representing stable rainfall in the Mangatawhiri area. In the double mass plot (Figure 8.13), there are several notable change points indicating rainfall-runoff relationship changed over the study period. They are similar to the change points in flow mass plot. Therefore, in such a small river, any small changes in the upstream may lead to an effect. The bumpy double mass plot could

due to the sensitivity of the small river to changes like climate changes and land use changes.

Mangatawhiri River is a tributary of Waikato River. In 1965, the upper reaches (the Mangatangi stream) of Mangatawhiri River were dammed to provide water for Auckland City. The reason for the bumpy double mass plot might be impacted by the construction of the Mangatangi reservoir.

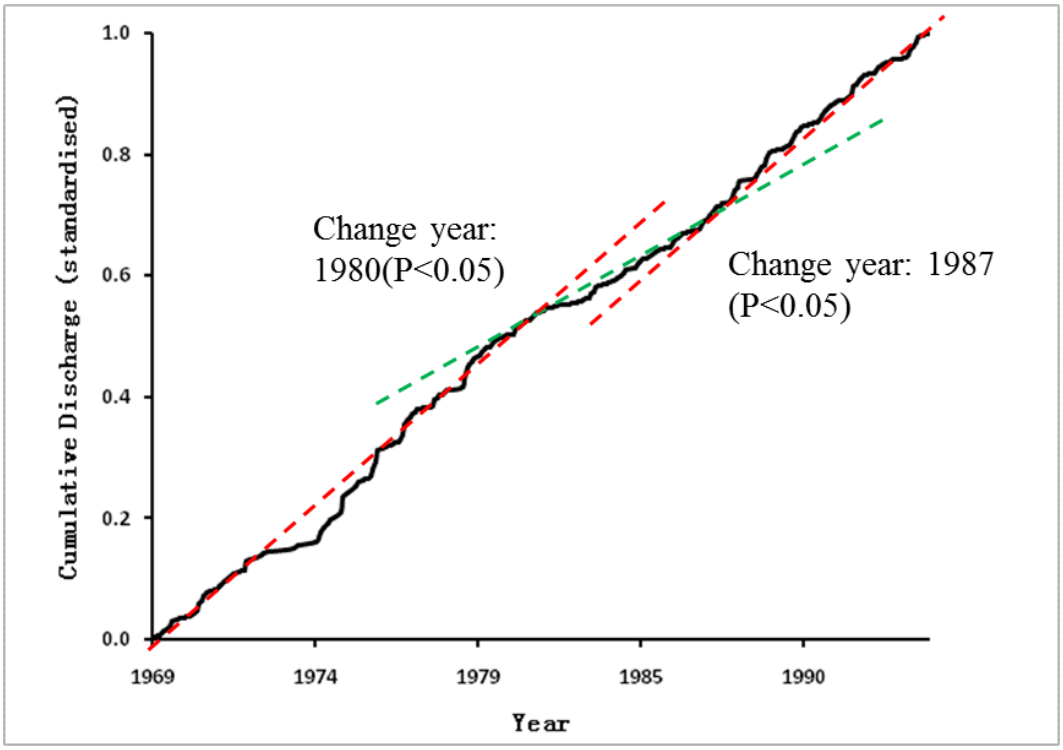

Figure 8.11: Cumulative mass plot of monthly mean runoff at Mangatawhiri, Mangatawhiri River

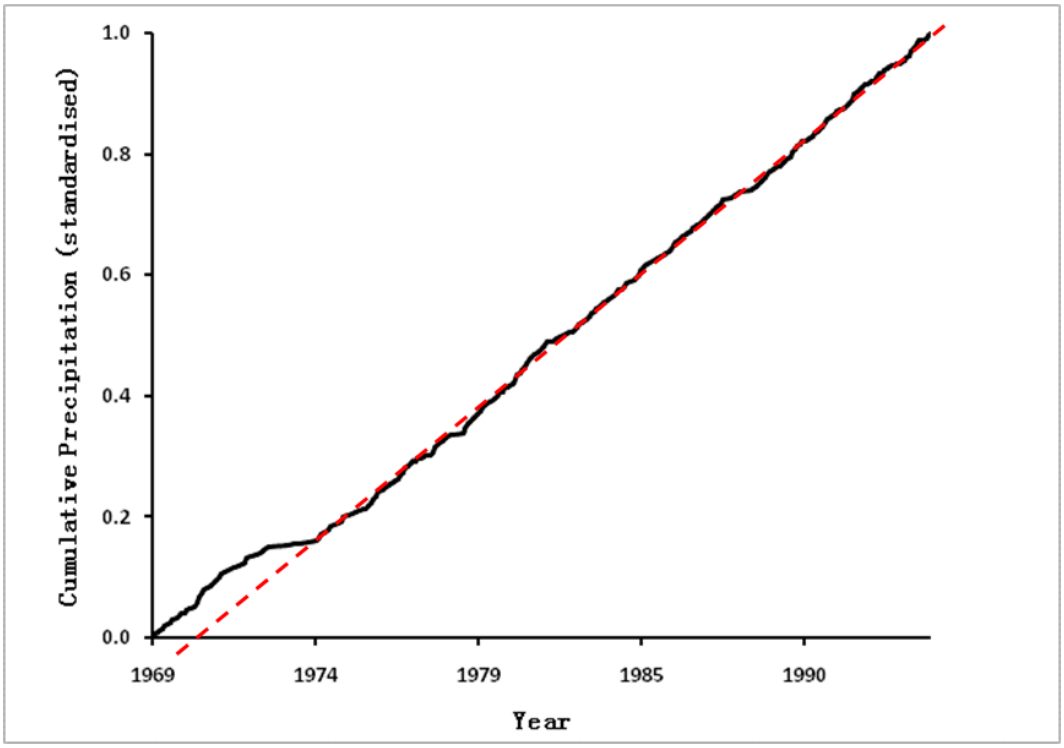

Figure 8.12: Cumulative mass plot of monthly precipitation at Mangatawhiri, Mangatawhiri River

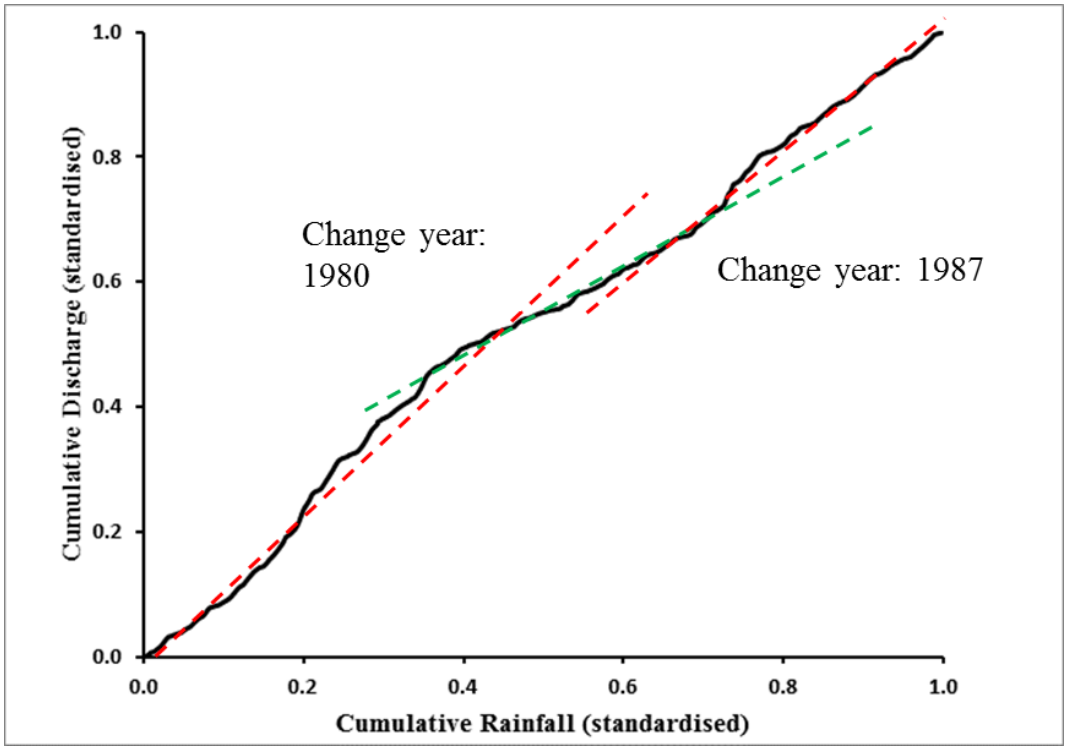

Figure 8.13: Double mass plot of monthly precipitation at Mangatawhiri, Mangatawhiri River and monthly mean runoff at Mangatawhiri, Mangatawhiri River

Waitoa River at Mellon Road

In the Waitoa River at Mellon Road (Figure 8.1), the average monthly mean flow was 4.87 m^3s^{-1} for the period 1986 to 2003. The slope of the flow cumulative mass plot (Figure 8.14) changed around 1989 and 1996. However, the rainfall (gauged in the Waihou River at Elstow) cumulative mass plot (Figure 8.15) presents an almost straight line. The change point in 1989 and 1996 are also shown in the rainfall runoff double mass plot (Figure 8.16). Therefore, the change point 1989 and 1996 in the cumulative flow mass plot and the double mass plot present in the rainfall mass curve represents land use change which occurred upstream.

There are several stopbanks which belong to the Piako River Scheme in upstream Waitoa River at Mellon Road. Therefore, the changed rainfall-runoff relationship may be impacted by the flood protection system.

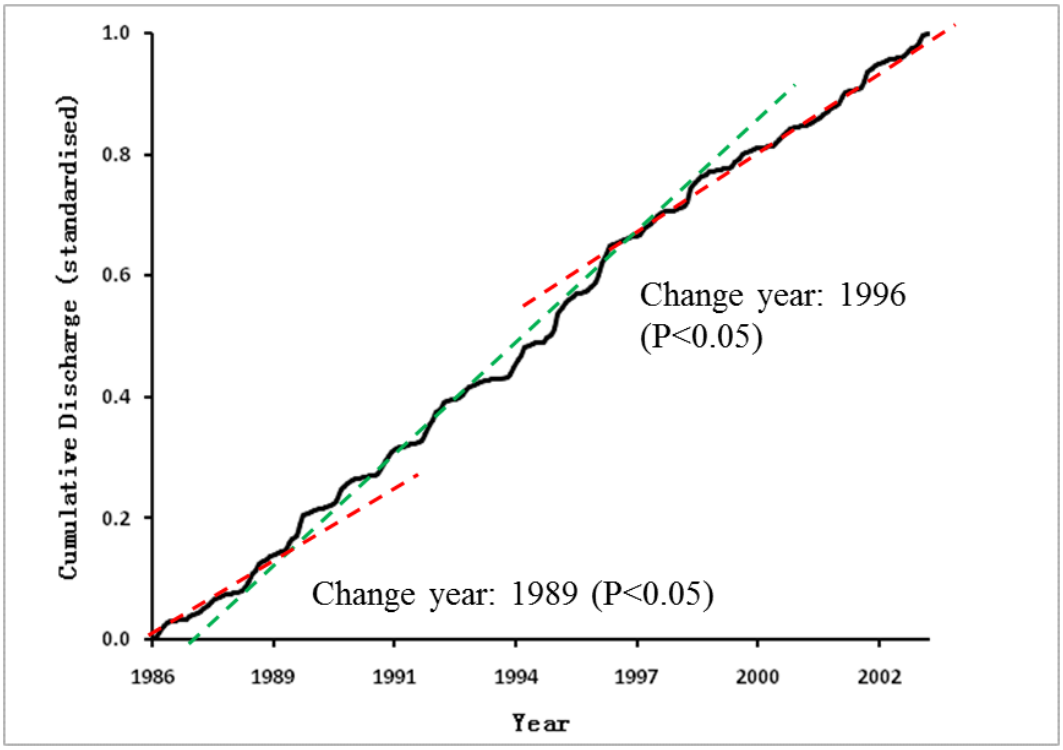

Figure 8.14: Cumulative mass plot of monthly mean runoff at Mellon Road, Waitoa River

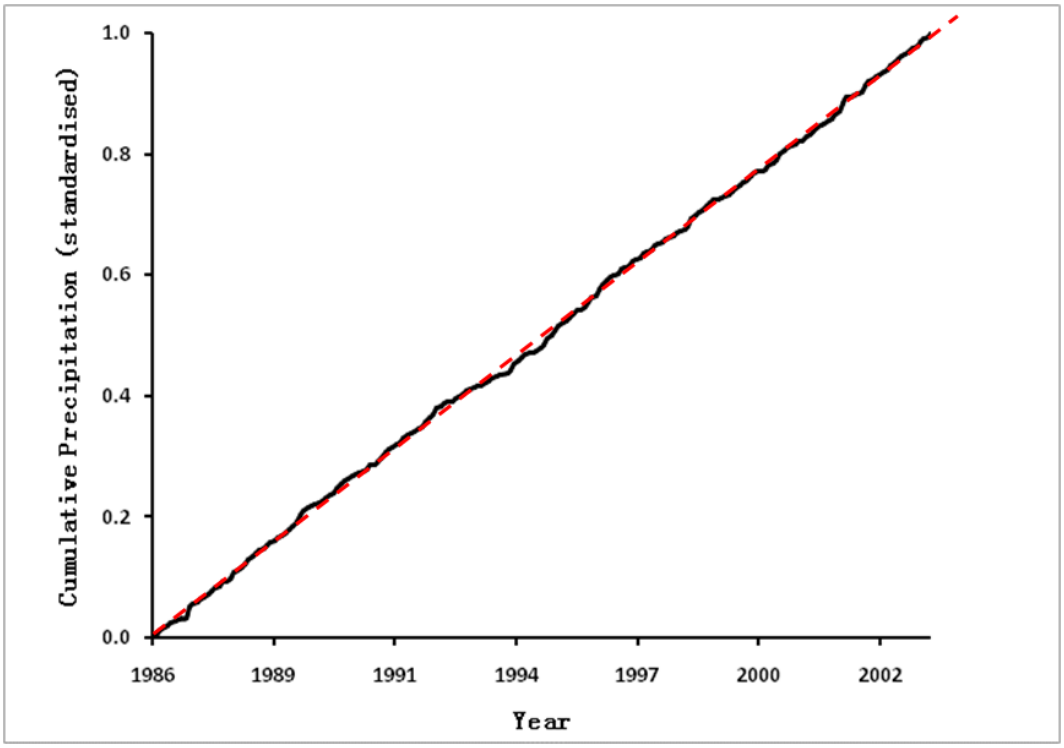

Figure 8.15: Cumulative mass plot of monthly precipitation at Elstow, Waihou River

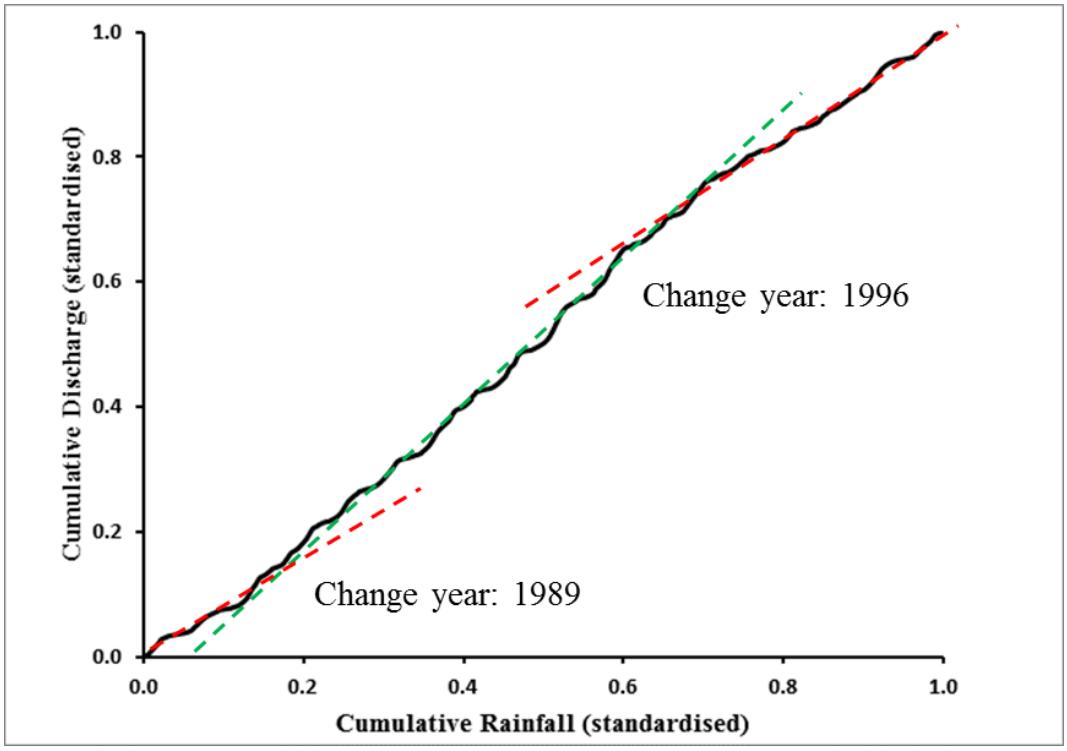

Figure 8.16: Double mass plot of monthly precipitation at Elstow, Waihou River and monthly mean runoff at Mellon Road, Waitoa River

Tawarau River at Speedies Road

In the Tawarau River at Speedies Road (Figure 8.1), the average monthly mean flow was 6.2 m^3s^{-1} from 1980 to 2003. The data for the period 1988 to 1992 are missing as shown by horizontal portion of the cumulative runoff plot (Figure 8.17) and the cumulative rainfall plot (Figure 8.18). In the cumulative mass plot (Figure 8.17), the break points 1981, 1988, 1994 and 1998 are notable. The rainfall (gauged in Waitomo Stream at Waipuna Road) cumulative mass plot presents an almost straight line (Figure 8.18). The double mass plot (Figure 8.19) indicates rainfall and runoff relationship changed in 1981, 1994 and 1998.

The reason for the changed rainfall runoff relationship in 1994 and 1998 is probably impacted by both climate change and land-use change which happened before the study period.

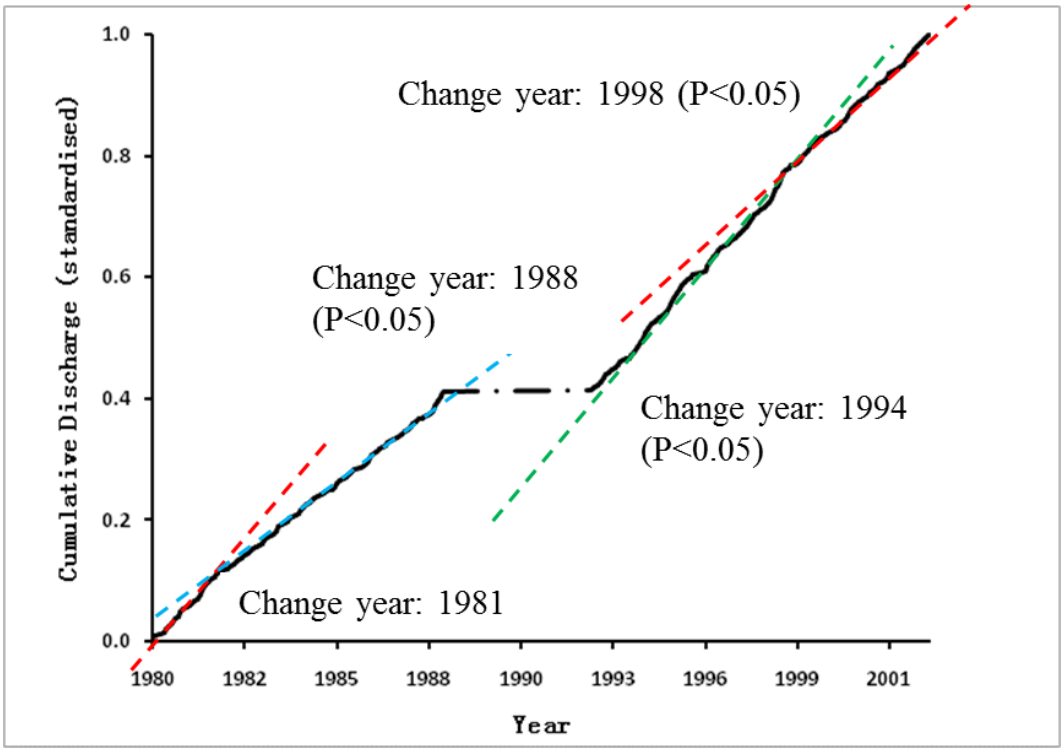

Figure 8.17: Cumulative mass plot of monthly mean runoff at Speedies Road, Tawarau River

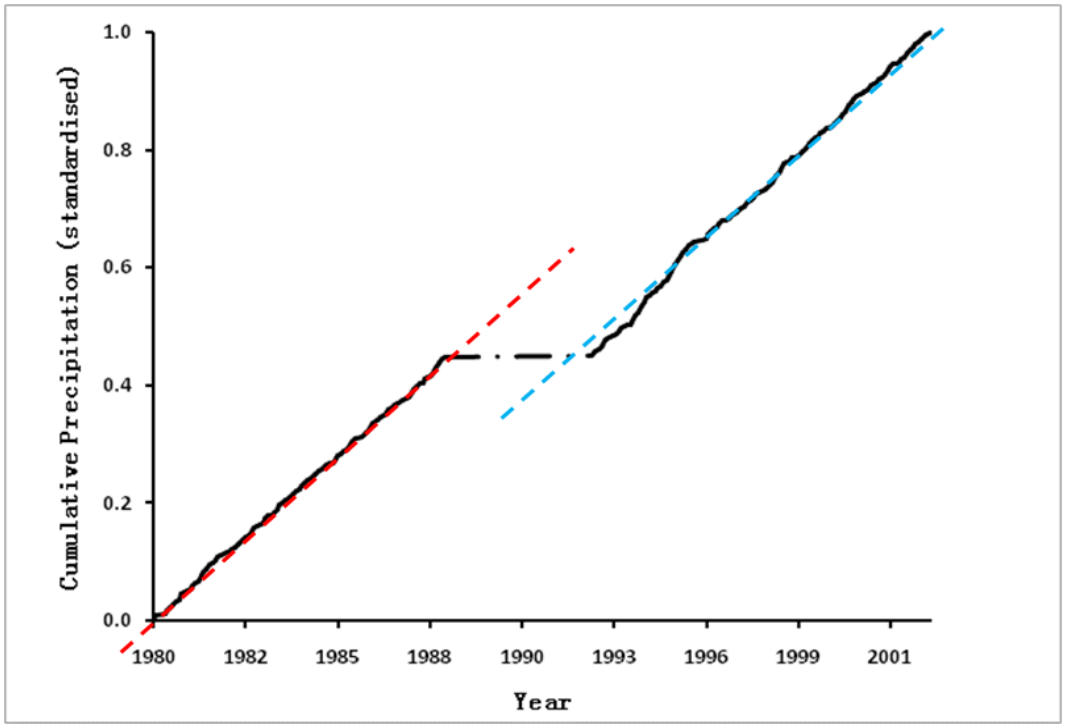

Figure 8.18: Cumulative mass plot of monthly precipitation at 823 Waipuna Road, Waitomo Stream

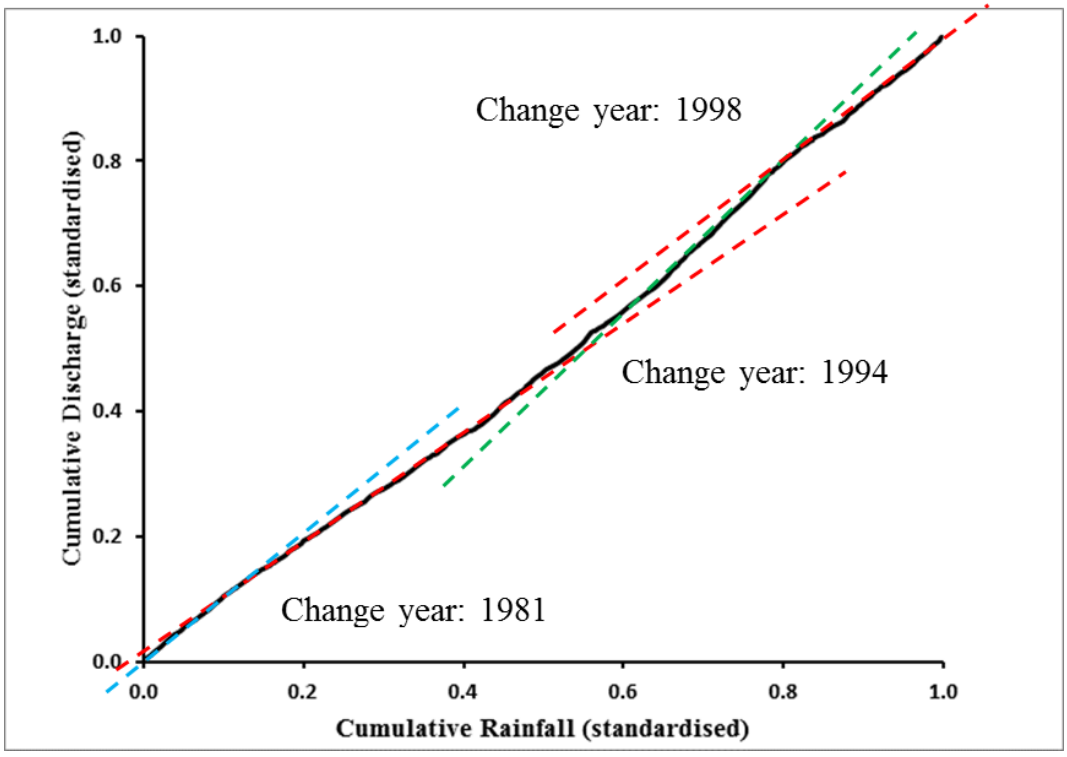

Figure 8.19: Double mass plot of monthly precipitation at Waipuna Road, Waitomo Stream and monthly mean runoff at Speedies Road, Tawarau River

Group 2

Whangamarino River at Slackline

The Whangamarino River (Figure 8.1), with an average monthly mean flow 1.86 m^3s^{-1} from 1979 to 1992, is a small river. The break point 1984 is evident in the flow cumulative mass plot (Figure 8.20). In the cumulative precipitation (recorded in Waitakaruru River at Hauraki Plains) mass plot (Figure 8.21), the 1984 change point is also clear. Therefore, comparing the change points in rainfall and runoff cumulative mass curve, upstream land-use did not change. In the double mass plot (Figure 8.22), the change-point 1984 is evident indicating rainfall-runoff relationship changed. Moreover, the double mass plot is characterized by a flexuous curve.

The Whangamarino River is a lowland river and belongs to the Lower Waikato-Waipa Flood Control Scheme system which was constructed in the 1960s. It works by catching the discharge from Lake Waikere when Waikato River condition is suitable. Therefore, the reason for the same change points in the cumulative and double mass plots may be driven by the flood control system in the Whangamarino River.

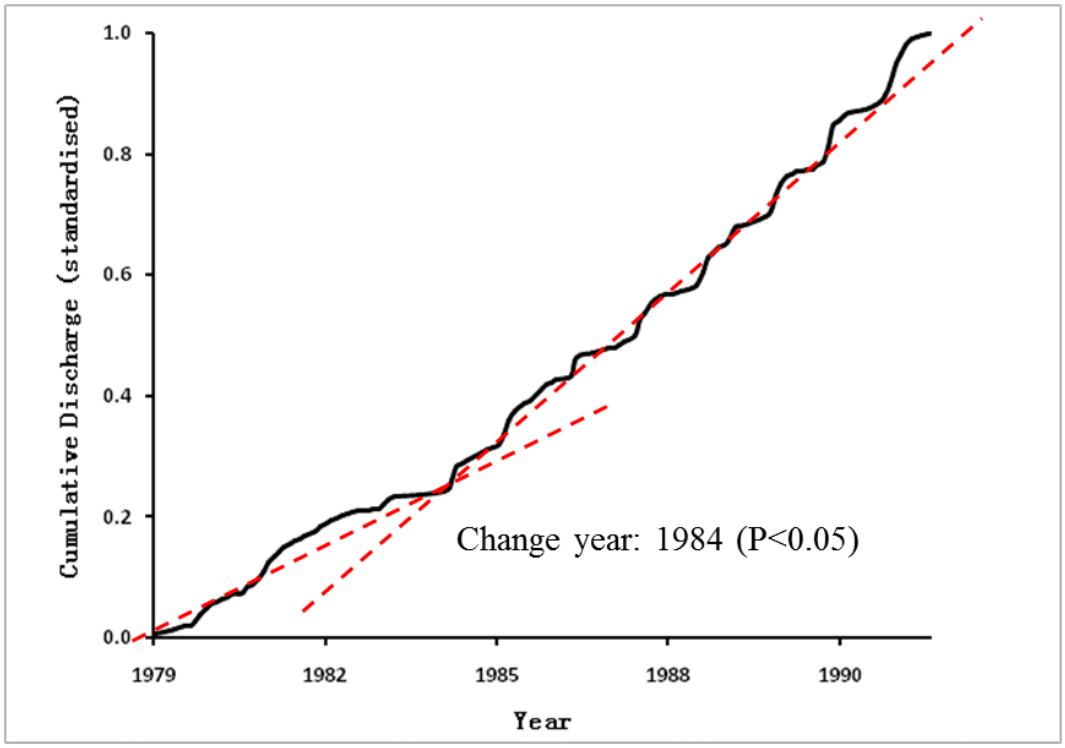

Figure 8.20: Cumulative mass plot of monthly mean runoff at Slackline, Whangamarino River (1293_16)

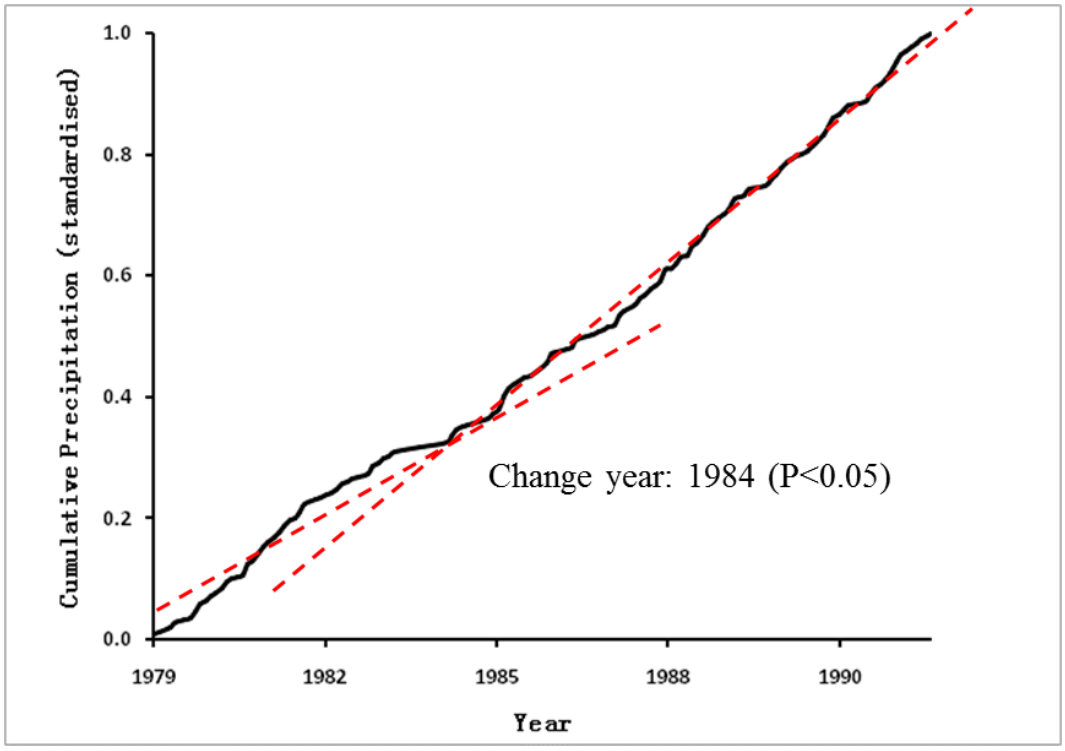

Figure 8.21: Cumulative mass plot of monthly precipitation at Hauraki Plains, Waitakaruru River

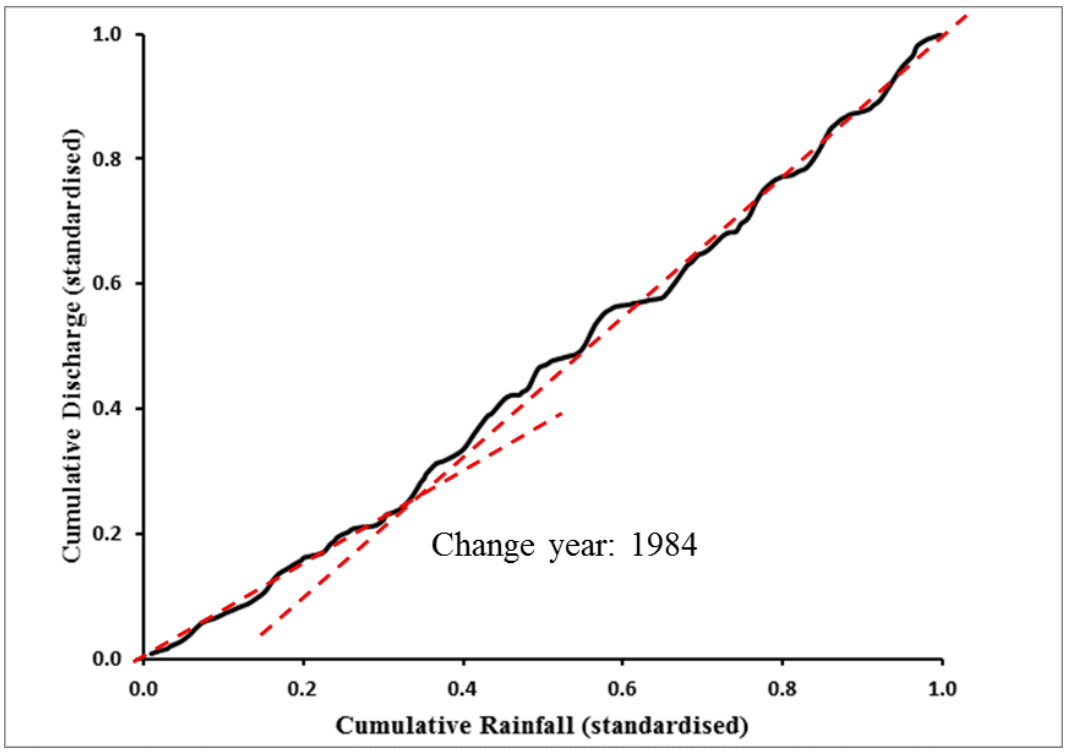

Figure 8.22: Double mass plot of monthly precipitation at Hauraki Plains, Waitakaruru River and monthly mean runoff at Slackline, Whangamarino River

8.2.2 Investigation of the effect of human activities on runoff

To further understand the impact of land use changes on runoff as well as the inter-annual variability of runoff in the 7 runoff gauges discussed in section 8.2.1, flow duration curves and the average mean monthly discharge diagrams were applied.

Purukohukohu Stream at Puruki

Figure 8.23 indicates the difference of streamflow for the period before and after 1975 at gauge site Purukohukohu Stream at Puruki. Comparing the flow over the two periods, the Q10 discharge decreased from 0.020 m^3s^{-1} to 0.012m^3s^{-1} (38% reduction), the Q50 discharge dropped from 0.007 m^3s^{-1} to 0.004 m^3s^{-1} (42% reduction); and the Q90 discharge decreased from almost 0.0013 m^3s^{-1} to 0.0008 m^3s^{-1} (44% reduction). Although the Purukohukohu Stream is a very small stream, the forest establishment impacted on the characteristics of flow, especially low

flow, greatly and similar impacts are likely to apply to forestry development in the Whanganui catchment.

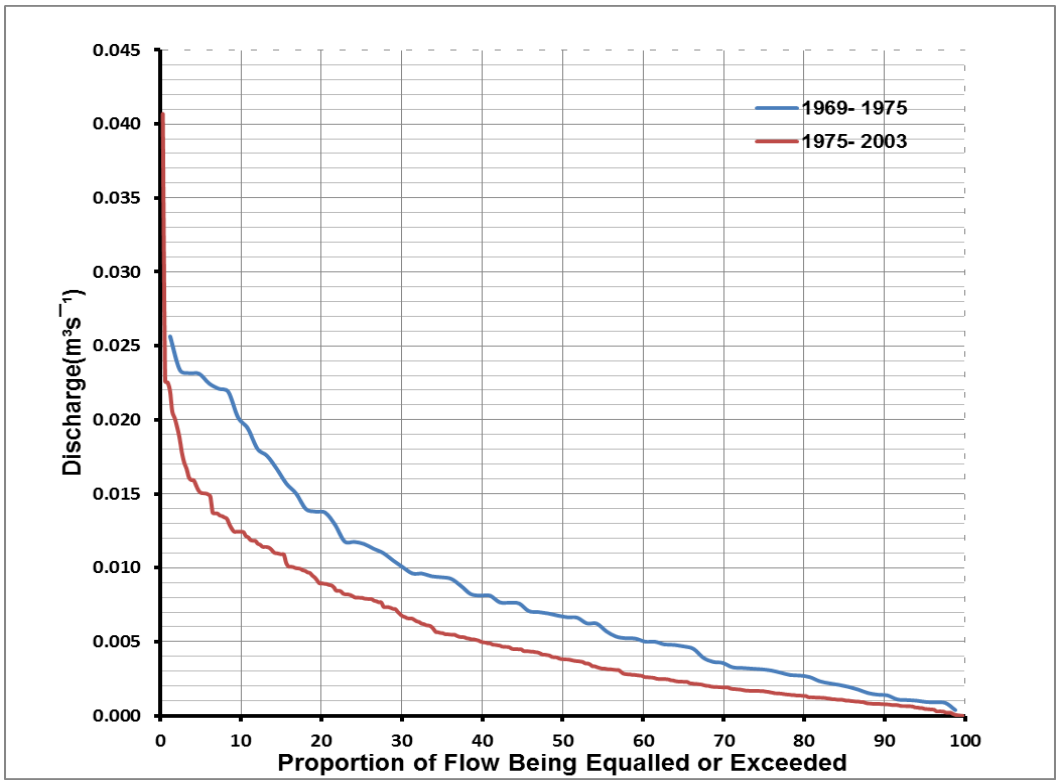

Figure 8.23: Flow duration curves for Purukohukohu Stream at Puruki

From Figure 8.24, it is noticeable that the flow seasonality with high flow in winter months is clear for the period 1969 to 1975. However, the stream flow seasonality for the period 1975 to 2003 was offset by the water abstractions, with winter months experiencing lower flow. Comparing the mean values for the two periods, the average monthly mean flow decreased significantly from 1973 for all months of the year.

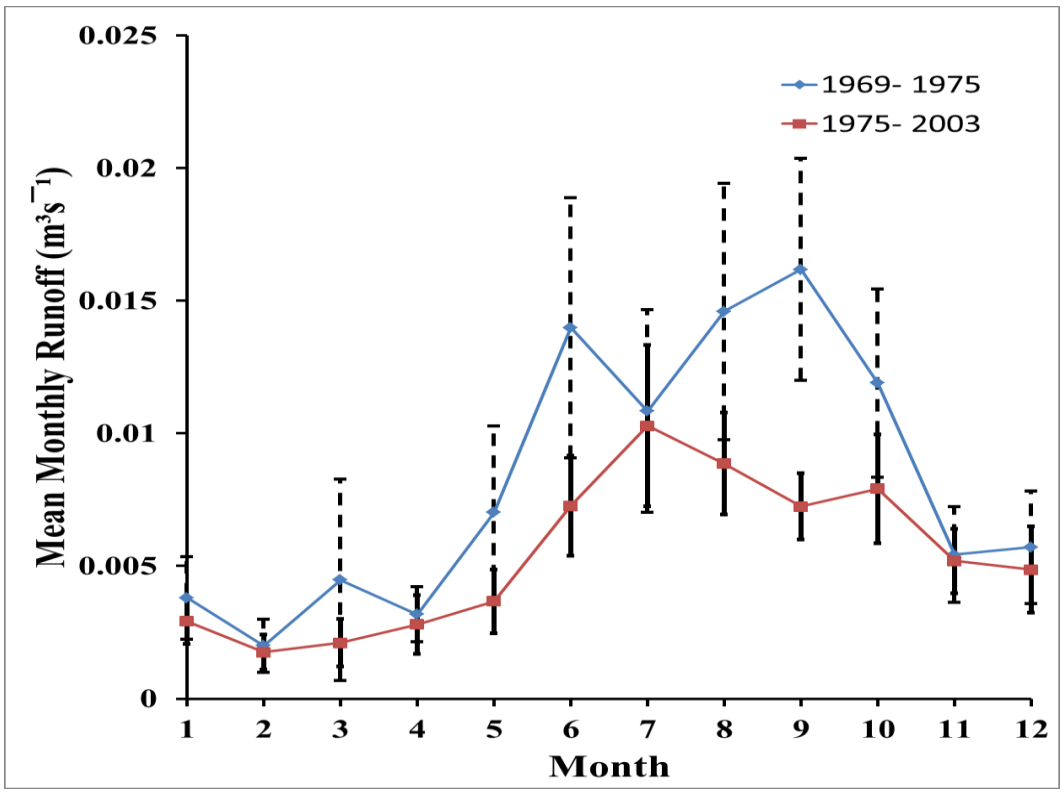

Figure 8.24: Mean monthly streamflow at Puruki Purukohukohu Stream. Vertical line ranges are ±2 standard errors about the mean flows.

Tongariro River at Turangi

For the gauge site on the Tongariro River at Turangi (Figure 8.25), the reduction in streamflow for the period 1973 to 2002 compared with the period 1957 to 1973 is obvious. Comparing the flow over these two periods, the Q10 discharge decreased from 77.2 m^3s^{-1} to 40.5 m^3s^{-1}, with an around 48 percent decline; the Q50 discharge dropped from 52.0 m^3s^{-1} to 29.8 m^3s^{-1}, with an around 43 percent decline; the Q90 discharge decreased from 33.6 m^3s^{-1} to 26.6 m^3s^{-1}, with an around 21 percent reduction.

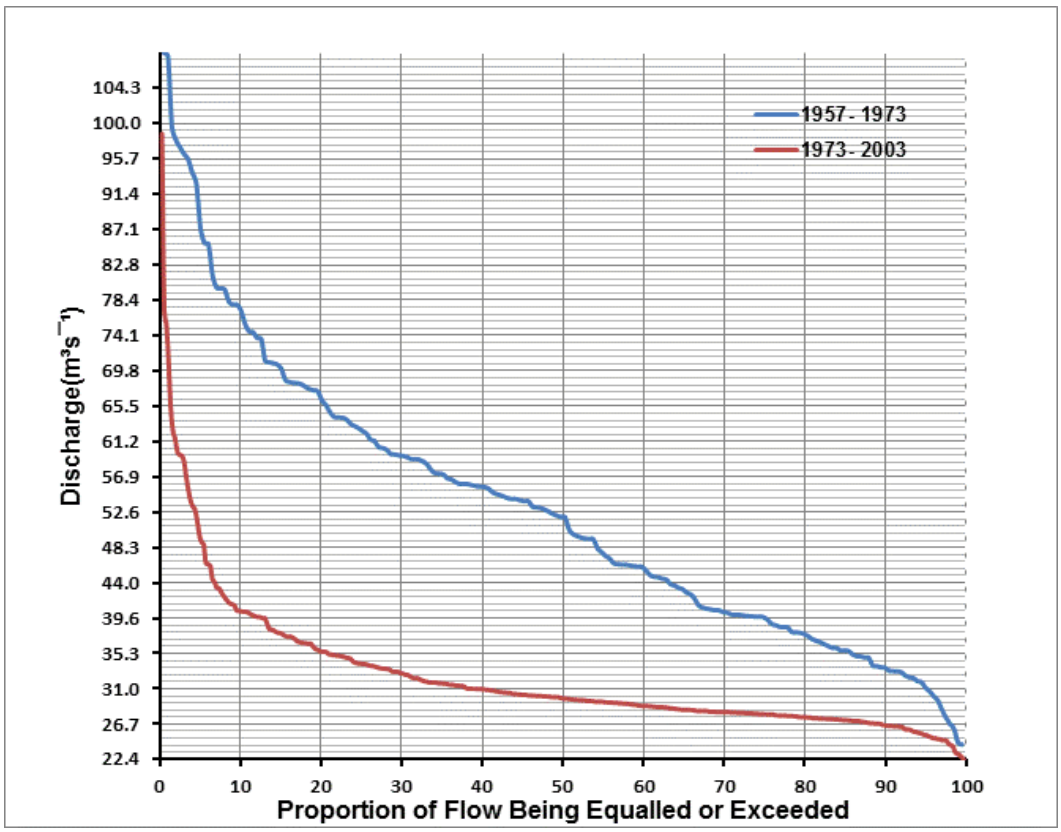

Figure 8.25: Flow duration curves for the Tongariro River at Turangi

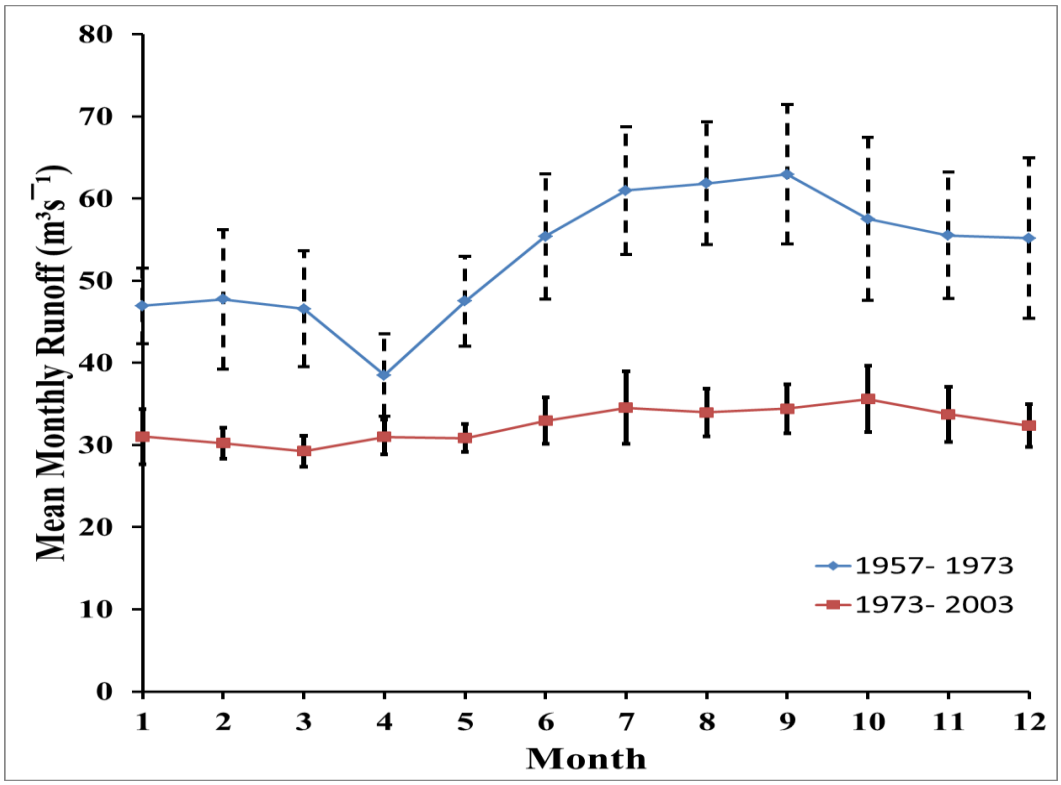

Figure 8.26: Mean monthly streamflow at the Tongariro River at Turangi. Vertical line ranges are ±2 standard errors about the mean flows.

The streamflow seasonality with high flow in winter months is shown for the period 1973-2003 for the Tongariro River at Turangi (Figure 8.26). The significant changes in the monthly mean flow over the two periods happened in the four seasons, but especially obviously in late winter and early spring. The 1973 change point decreased the average monthly flow in each month, particular in August and September, and shifts the nature of stream flow seasonality are unclear.

Waikato River at Reid's Farm

The discharge in the Waikato River at Reid's Farm reflects the influence of a wide range of river catchments upstream of Lake Taupo. Comparing the flow duration curves over the periods 1969 to 1975, and 1975 to 1984 (Figure 8.27), the Q10 discharge increased from 172 m^3s^{-1} to almost 199 m^3s^{-1}, with a 20 percent increase; the Q50 discharge increased from 120 m^3s^{-1} to 148 m^3s^{-1}, with a 24 percent increase; the Q90 discharge increased from almost 77 m^3s^{-1} to 101 m^3s^{-1}, with a 31.3 percent increase.

The discharge seasonality at Waikato River at Reid's Farm is evident over the 1975 to 1984 period (Figure 8.28). The most obvious and significant increase in the monthly mean flow is from February to April. Therefore, the 1973 diversions of the Tongariro increased the average monthly flow in each month, particularly significant in late summer and early autumn, but did not shift the nature of streamflow seasonality.

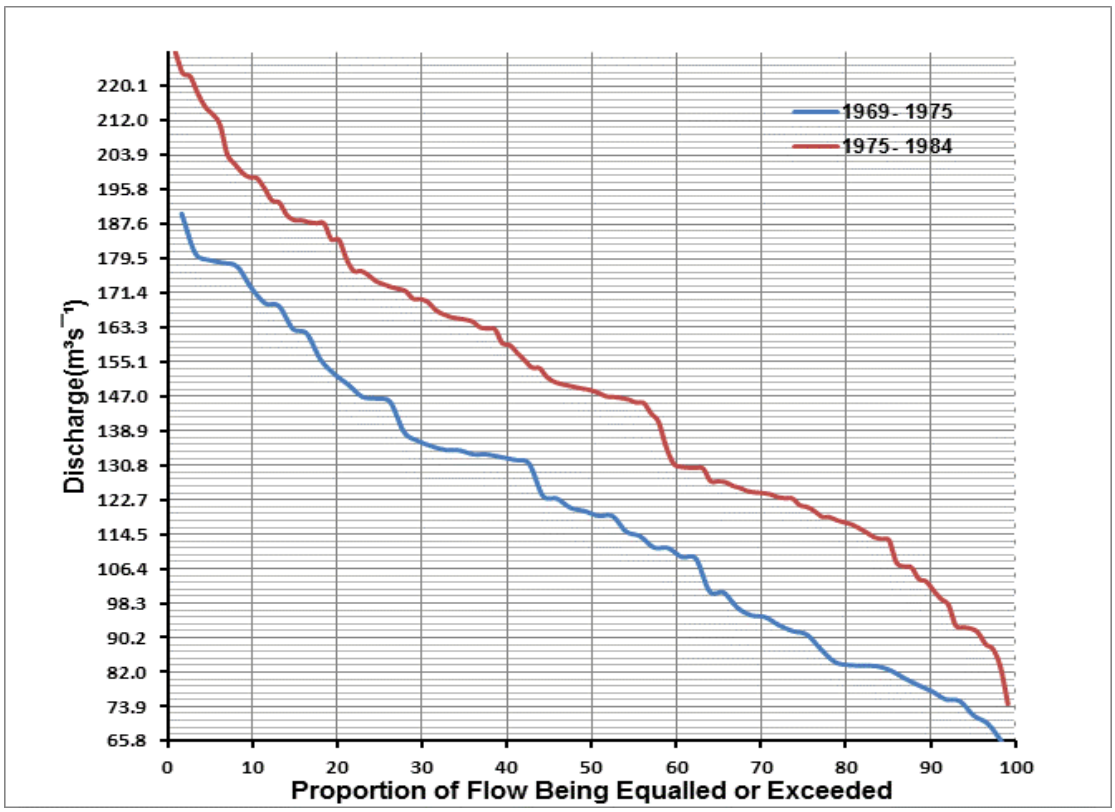

Figure 8.27: Flow duration curves for the Waikato River at Reid's Farm

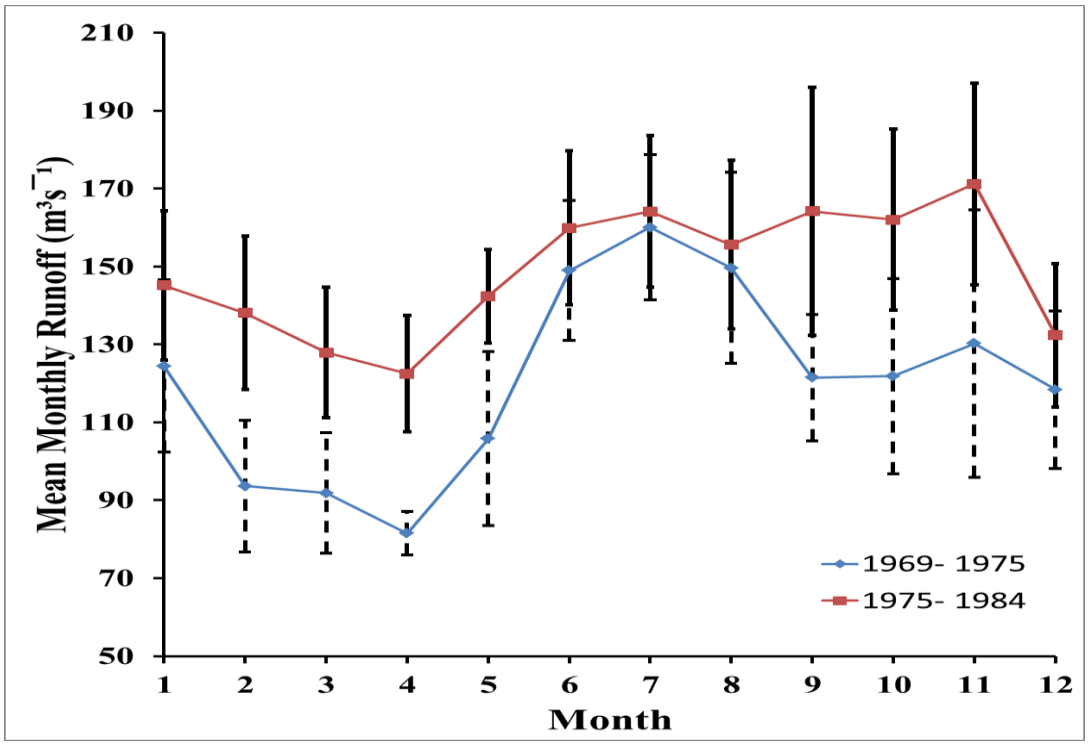

Figure 8.28: Mean monthly streamflow at the Waikato River at Reid's Farm. Vertical line ranges are ±2 standard errors about the mean flow.

For the rest gauge station, land use shift happened before the study period. Although the change points in the paired rainfall and runoff time series are similar in some gauges, the rainfall-runoff relationship was not uniform, indicating the changes in the relationship may be driven by the operation of the land use or by the impact of both climatic variation and land use. The flow duration curves for the period before and after the year when the rainfall-runoff relationship changed were created to identify the difference of flow as shown in Figure 8.29-8.32. For all of the seven gauge stations, the change impacted medium and high flows, with little change in the lower flows, indicating the land use within the study period was stable without obvious impact on the baseflow.

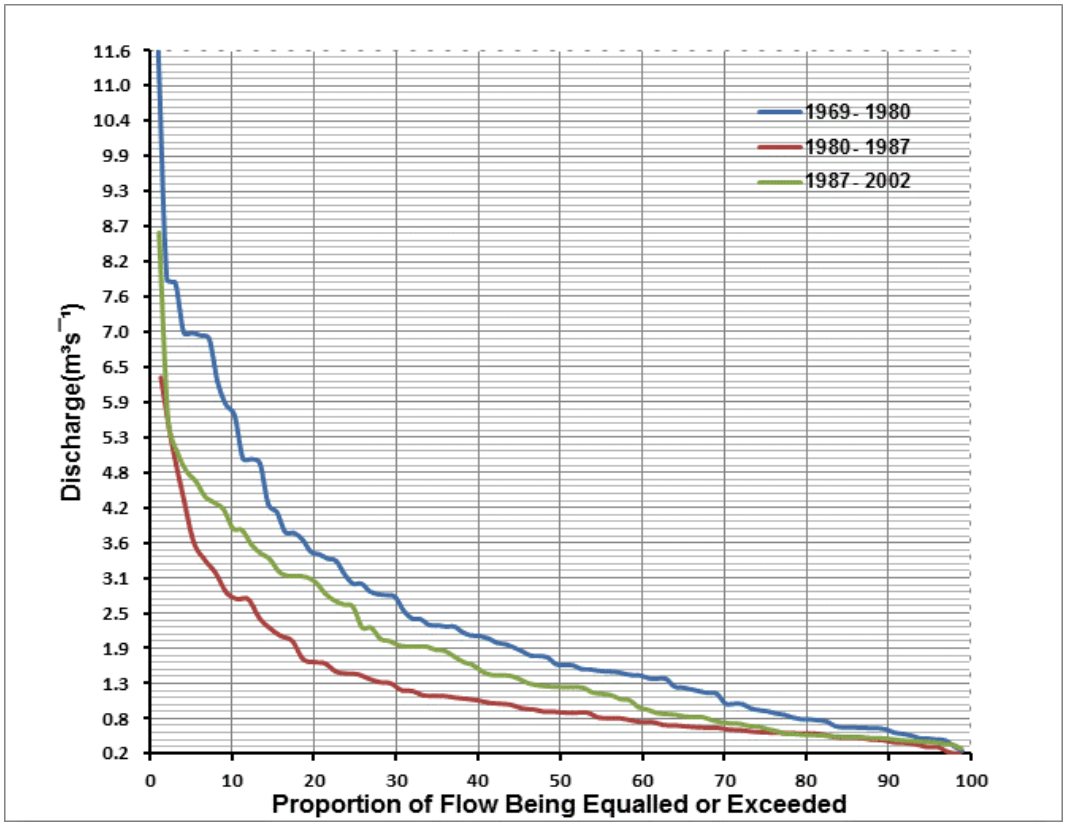

Figure 8.29: Flow duration curves for the Mangatawhiri River at Mangatawhiri

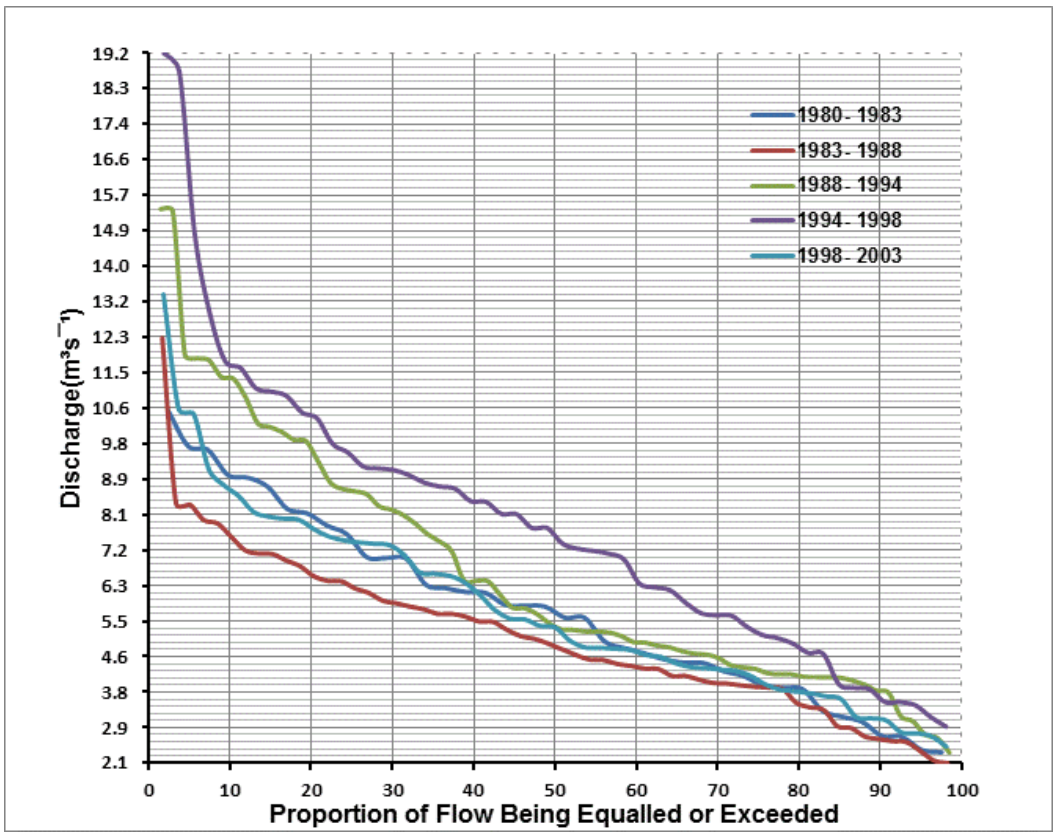

Figure 8.30: Flow duration curves for the Tawarau River at Speedies Road

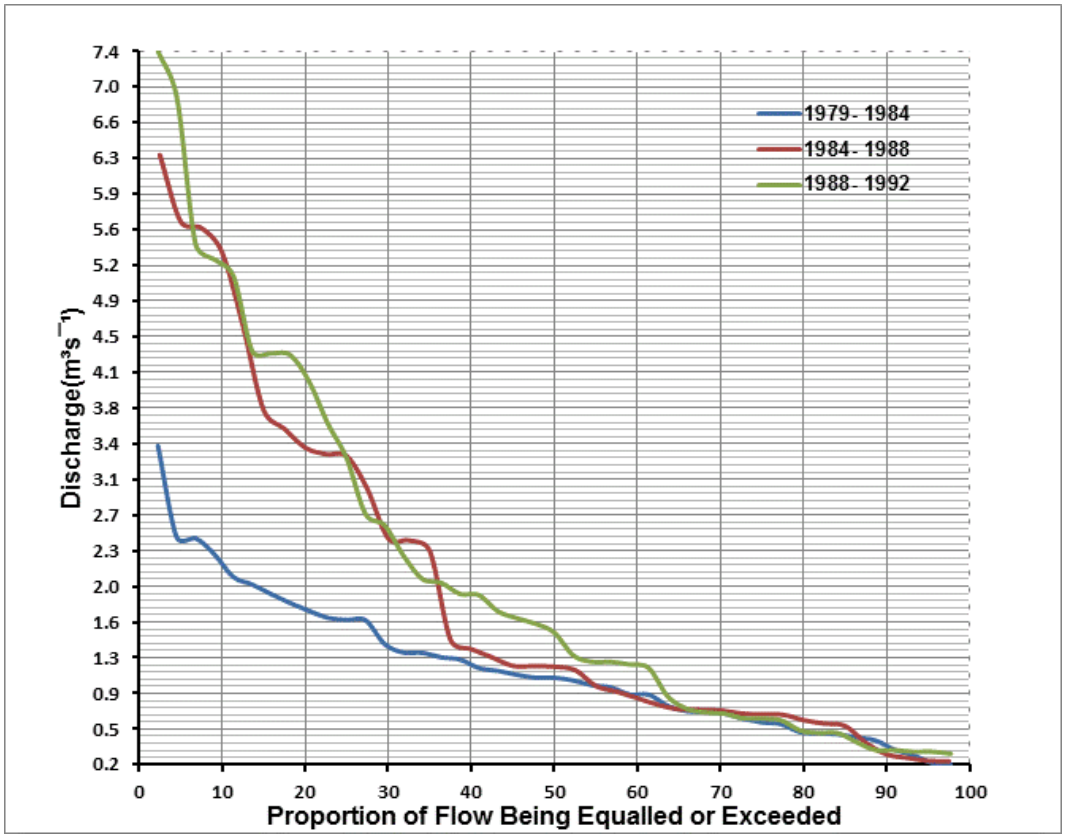

Figure 8.31: Flow duration curves for the Whangamarino River at Slackline

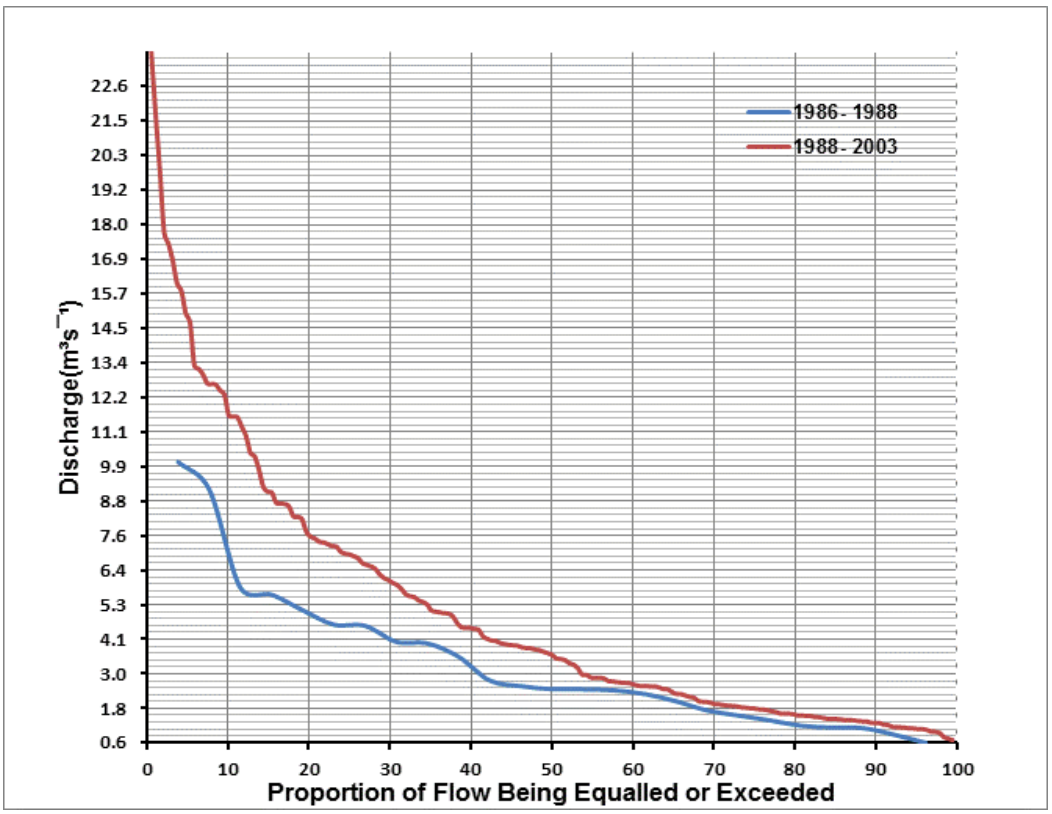

Figure 8.32: Flow duration curves for the Waitoa River at Mellon Road

8.3 Conclusion

For the rest of the flow gauges in the Waikato and the upper Whanganui catchments (total 24), no signals of upstream land use change were detected. The rainfall runoff double mass plots for the 24 flow gauge sites are presented in Appendix G. However, this does not mean that for all of the 24 flow gauges no land-use change happened in the upstream. Limited by the analysis period of the time series, some flow records do not show obvious signals of land use change such as the flow series gauged in the Waikato River at Hamilton, Ngaruawahia Cableway and Rangiriri Bridge which have been already impacted by upstream land-use change. In total, the flow time series for the seven rivers were found to have signals of land use change, some of them are obvious and some of them are evident. In the Purukohukohu Stream, the afforestation decreased the medium flow (Q50) by around 44 percent. With the diversion of the power scheme, the Tongariro River low flow (Q90) declined by 21 percent. The water diverted from the Tongariro Power Scheme to the Lake Taupo increased the high (Q10),

medium (Q50) and low flows (Q90) in the Waikato River at Reid's Farm by around 20, 24 and 31 percent, respectively. Upstream of the Mangatawhiri River, the Tawarau River, the Whangamarino River and the Waitoa River, different kinds of land use such as dam, flood control system and afforestation occurred before the study period. The cumulative rainfall and runoff mass plots for these rivers contain similar change points representing the impact of climate variations on river discharge; however, the rainfall-runoff double mass plots indicate the signals of changed rainfall-runoff relationship which is driven by upstream land use change. Moreover, there was considerable variation in the medium and high flows at these sites, probably driven by climatic fluctuations.

Chapter 9– A Specific Study in the Wanganui Catchment

9.1 Introduction

This chapter presents river discharge changes evidently derived from land use change in the Whanganui catchments. The Whanganui catchments focus here on the impact of Tongariro Power Scheme (Figure 9.1). The scheme operates to take water from tributaries of the Rangitikei, Whangaehu, Whanganui and the Tongariro Rivers to provide water to the Tokaanu and Rangipo power stations and finally release water to Lake Taupo. Briefly, the scheme contains the Eastern Diversion taking water from Whangaehu River to Rangipo Dam, Tongariro Diversion that diverts water from Rangipo Dam to Lake Rotoaira. The Western Diversion diverts water from Whakapapa River to Lake Rotoaira, which functions as a head pond for the Tokaanu Power Station, releasing water to Lake Taupo.

The impact of the Tongariro Power Scheme diversion on the river discharge mean value as well as its characteristics was analysed primarily. Rather than a simple before-after land use study, a land use impact example within the Whanganui catchment was carried out by means of a two-catchment comparison of river hydrology: the Ongarue catchment (already significantly converted to farmland), and the upper Whanganui prior to establishment of the Tongariro Power Scheme (largely in native vegetation).

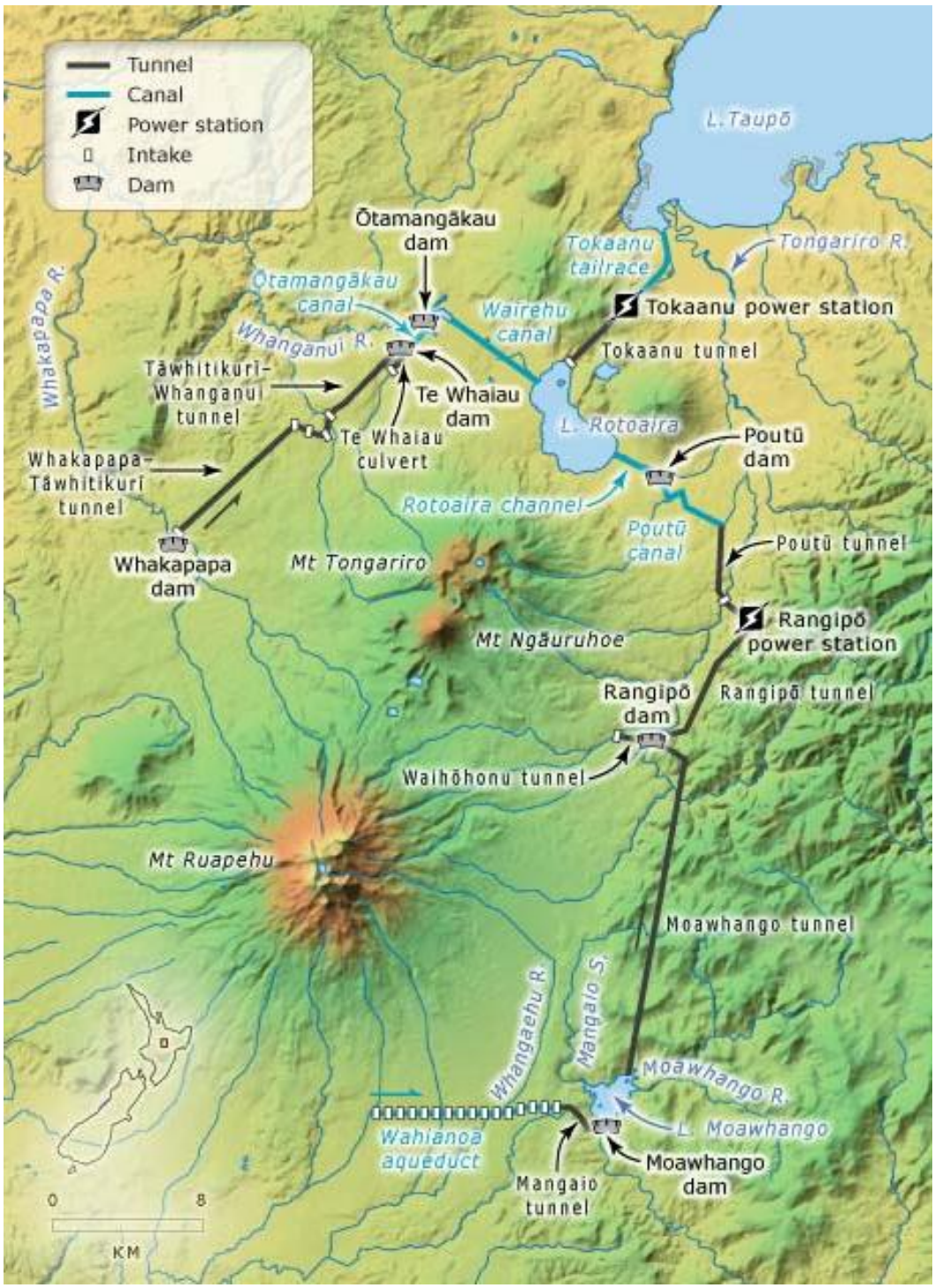

Figure 9.1: Overview of the Tongariro Power Scheme (Source: http://www.teara.govt.nz/en)

9.2 Impact of Hydro-power Diversion

In the Tongariro Power scheme, seven river discharge gauges, as well as four rainfall gauges that have a comparatively longer record period running from around 1960 to 2010, were available for this study. More details of the gauges are described in Appendix A-c (rainfall gauges) and Appendix A-d (flow gauges). The location of the rainfall/runoff gauges are shown in Figure 4.2.

9.2.1 Hydropower diversion effect on the mean river discharge

In this section, three flow gauge sites located downstream of hydropower diversions were selected for flow reduction quantification: Whakapapa River at Footbridge, the Whanganui River below Piriaka and the Whanganui River at Te Maire. The runoff mass plots and double mass plots were plotted and analysed to estimate the degree of the hydropower diversion impact on the average mean monthly discharge. All of the change points in the cumulative rainfall/runoff mass plots were detected by the least square regression method and are statistically significant.

Whakapapa River at Footbridge

For the discharge time series gauged in the Whakapapa River at Footbridge, the flow cumulative mass plot (Figure 9.2) is straight before 1972, with the anticipated abrupt change of slope representing an approximately 75 percent reduction in monthly mean flow. The evident increased discharge after 1990 may represent a change in diversion procedure from a modification in water right specification as the double mass plot with rainfall shows an almost identical plot (Figure 9.3).

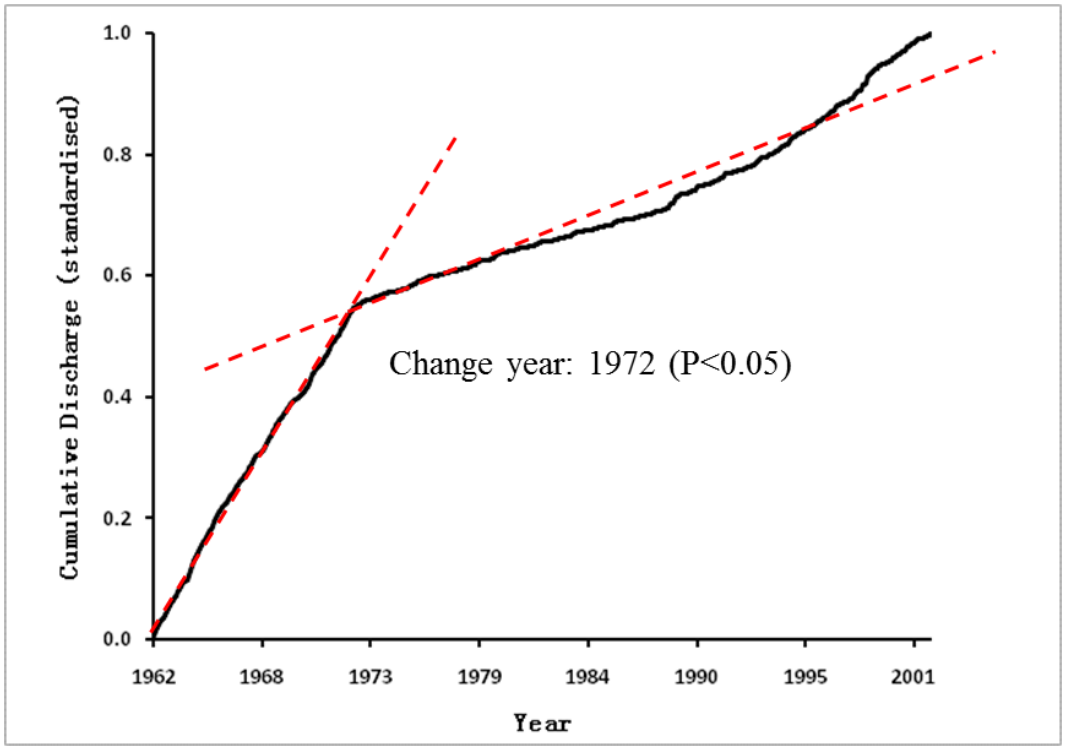

Figure 9.2: Cumulative mass plot from monthly mean runoff at Footbridge, Whakapapa

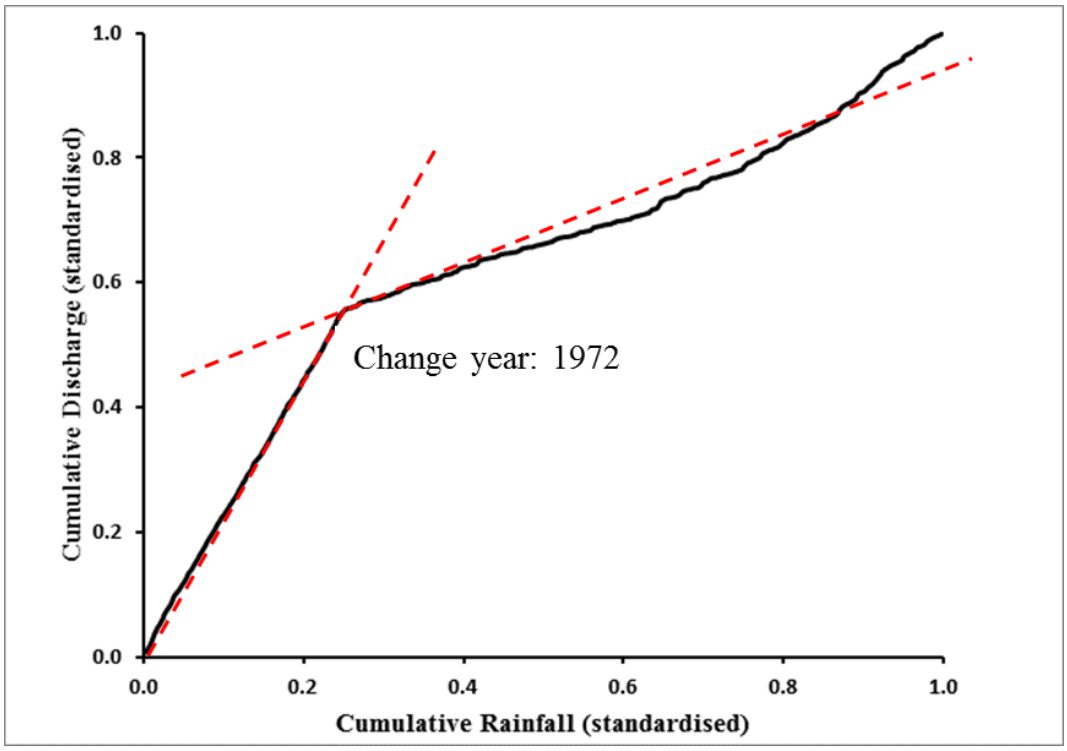

Figure 9.3: Double mass plot of monthly precipitation at Tongariro Hatchery, Whanganui River and monthly mean runoff at Footbridge, Whakapapa

Whanganui River at Below Piriaka

For the flow time series gauged in the Whanganui River below Piriaka from 1970 to 2002, the 1973 change point is also evident (Figure 9.4) (the 1975 change point was significant through permutation test), but in later years there is also some evident decline in discharge around 1987. This may be related to drier years in the late 1980s as the rainfall-runoff relation appears constant (Figure 9.5).

Whanganui River at Te Maire

The 1974 break point in the slope of flow cumulative mass plot for the Whanganui River discharge at Te Maire is clear (Figure 9.6), though less evident due to the increased distance from the diversion point. The 1974 change point is also evident in the rainfall runoff double mass plot (Figure 9.7). Again, the post-diversion river discharge variations appear related to rainfall variations because the rainfall-runoff mean relation remains unchanged (Figure 9.7).

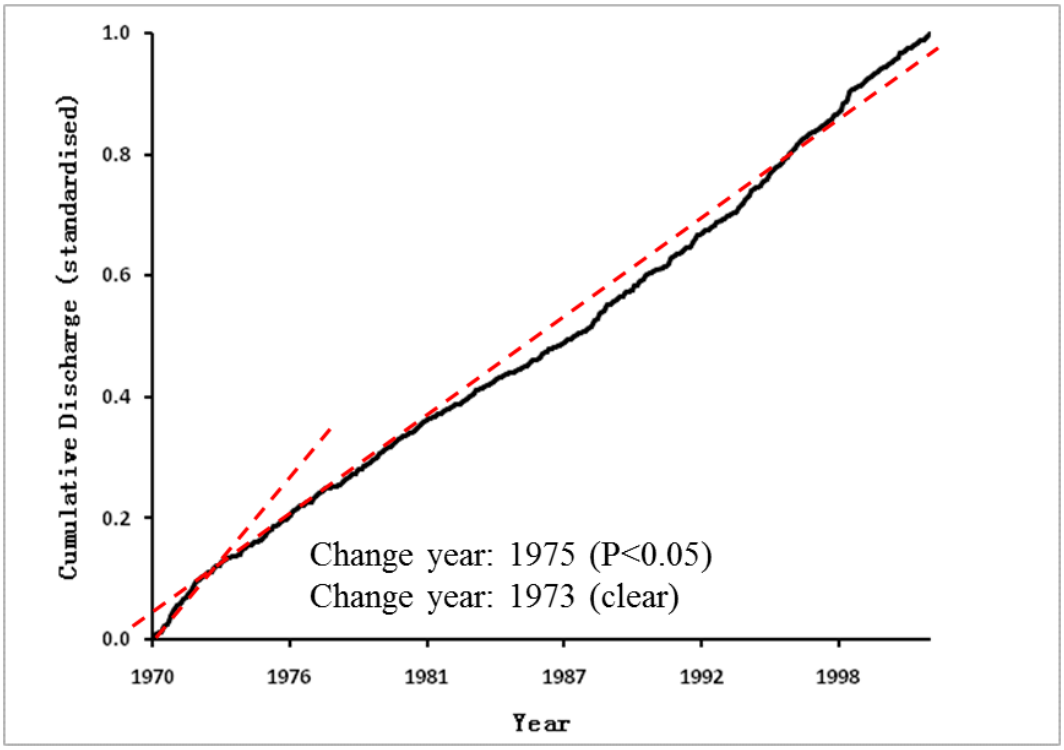

Figure 9.4: Cumulative mass plot of monthly mean runoff below Piriaka, Whanganui River

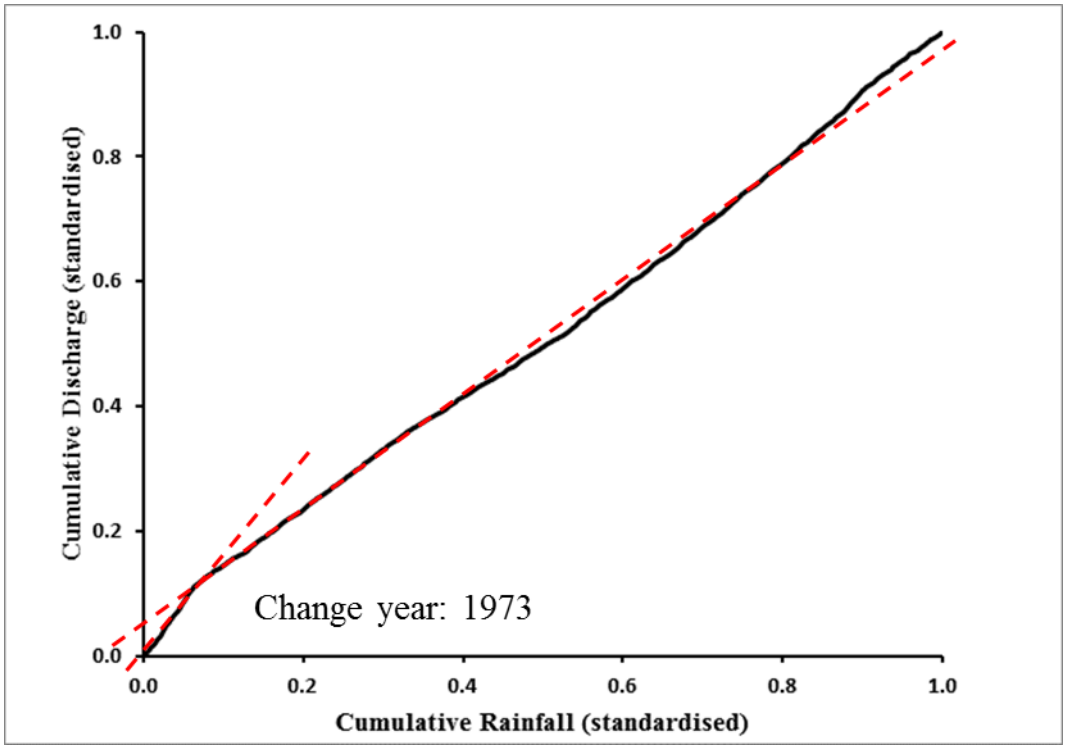

Figure 9.5: Double mass plot of monthly precipitation at TePorere, Whanganui River and monthly mean runoff below Piriaka, Whanganui River

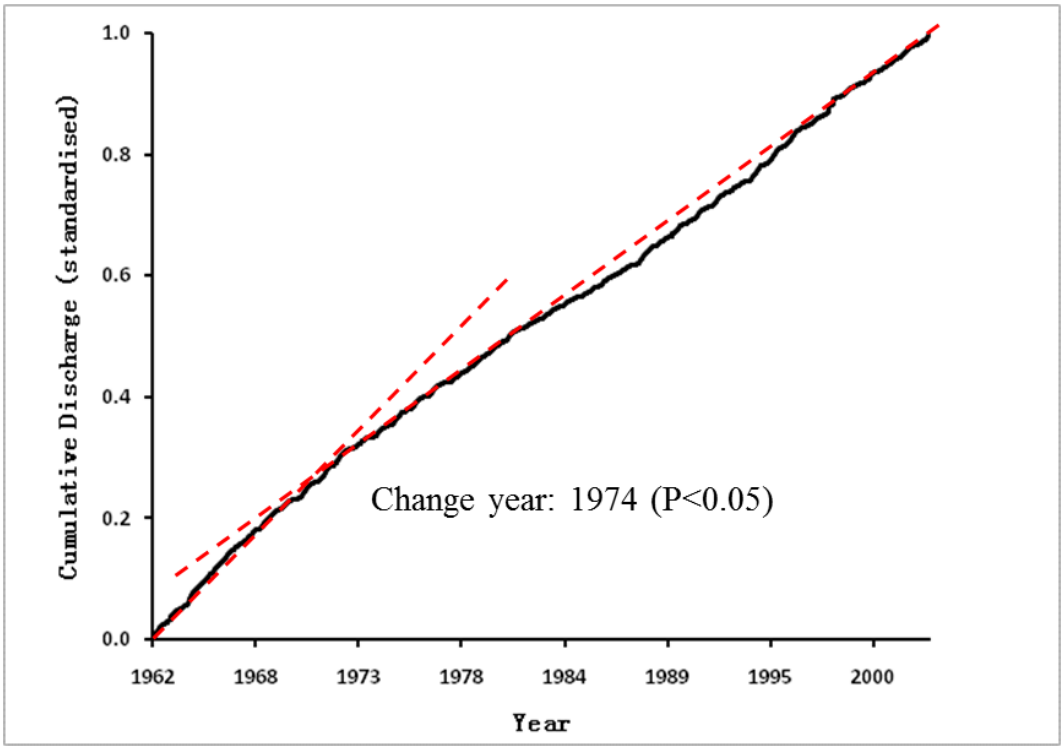

Figure 9.6: Cumulative mass plot of monthly mean runoff at TeMaire, Whanganui River

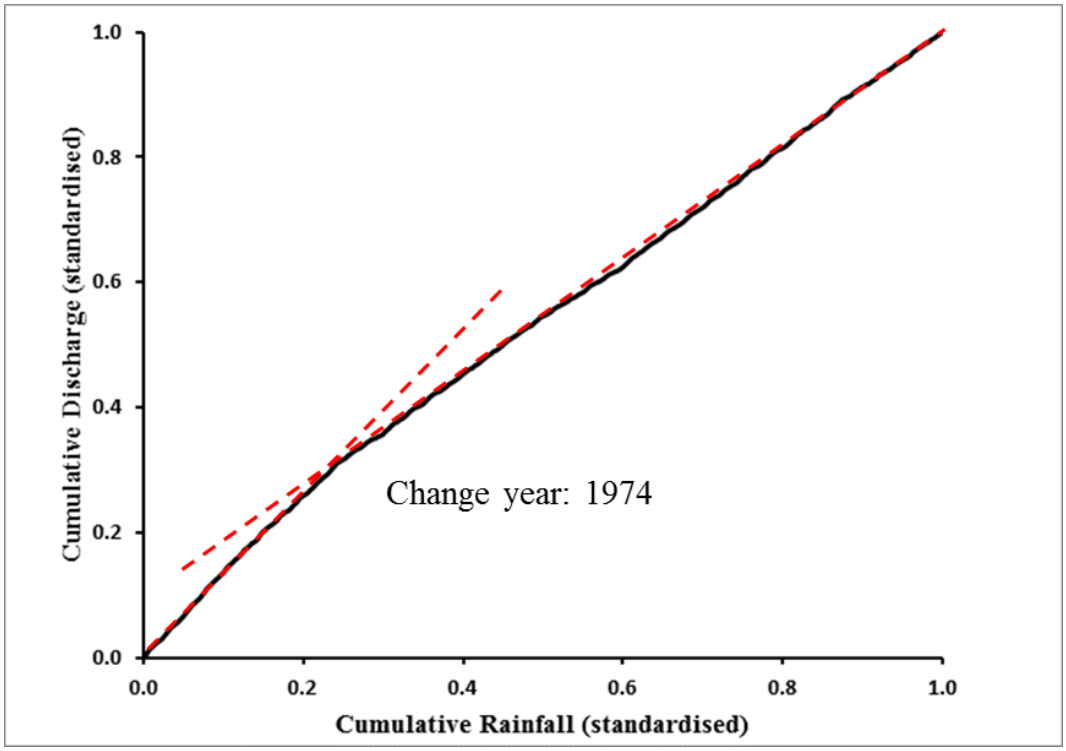

Figure 9.7: Double mass plot of monthly precipitation at Taumarunui, and monthly mean runoff at TeMaire, Whanganui River

9.2.2 The effect of the Tongariro hydropower diversions on river discharge characteristics

The different characteristics of river discharge in the period before and after 1973 at the three gauge sites (Whakapapa River at Footbridge, Whanganui River below Piriaka and Whanganui River at Te Maire) are described here in terms of flow duration curve differences and mean discharge differences.

Flow Duration Curves

Flow duration curves were plotted on a pre- and post-1973 basis for the three flow gauge sites (Figures 9.8-9.10). In particular, comparison was made of high flow (Q10), median flow (Q50) and low flow (Q90) which represent the flow equal or exceeding ten, fifty and ninety percentage of the time respectively were compared.

For the gauge site Whakapapa River at Footbridge (Figure 9.8), the reduction in streamflow for the period 1973 to 2002 compared with the period 1966 to 1973 is obvious. Comparing the flow over these two periods, the Q10 discharge decreased from 19.7 m^3s^{-1} to 8.8 m^3s^{-1}, with an around 55 percent decline; the Q50 discharge dropped from 13.7 m^3s^{-1} to 3.6 m^3s^{-1}, with an around 73 percent decline; the Q90 discharge decreased from 9.4 m^3s^{-1} to 0.96 m^3s^{-1}, with an around 89 percent reduction.

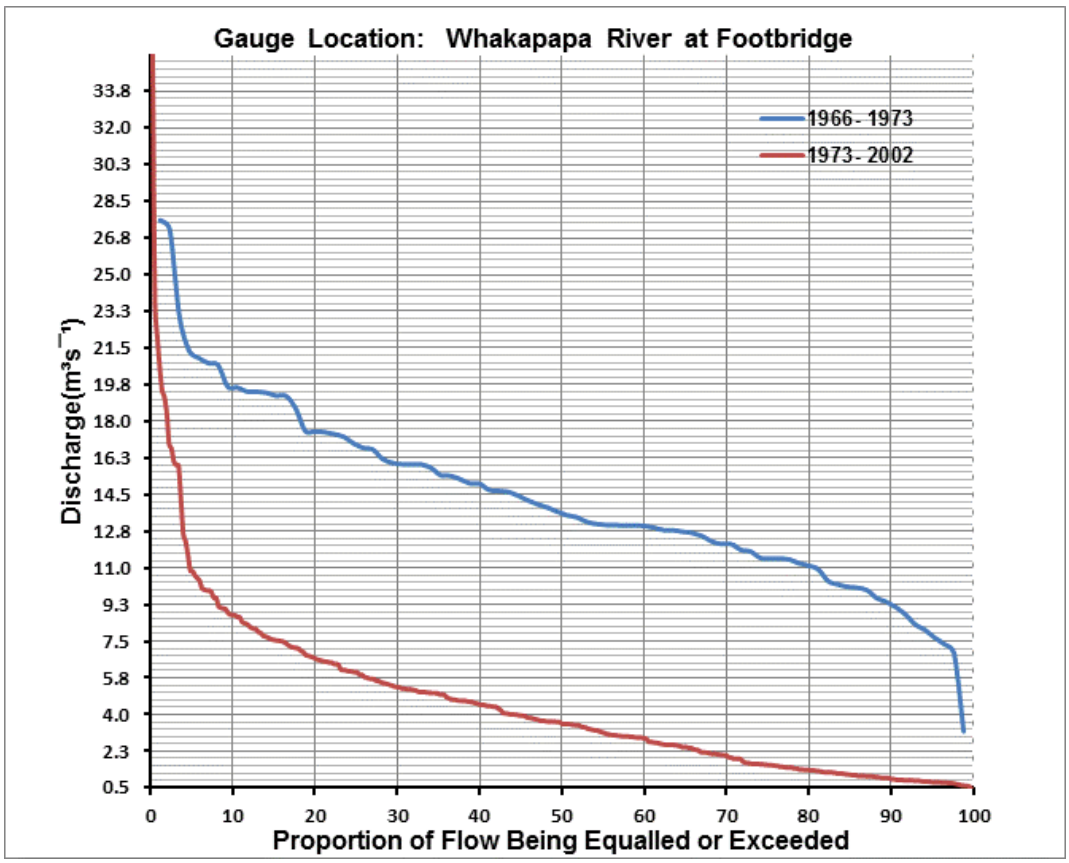

Figure 9.8: Flow duration curves for the Whakapapa River at Footbridge

Figure 9.9 indicates the difference of streamflow for the periods before and after 1973 at gauge site Whanganui River below Piriaka. However, because there was only a three year flow record before 1973, the flow duration curve for the period before 1973 may be not representative. Comparing the flow over these two periods, the Q10 discharge decreased from 67 m^3s^{-1} to 44.7 m^3s^{-1}, with an around 33 percent decline; the Q50 discharge dropped from 35.8 m^3s^{-1} to 22.7 m^3s^{-1}, with an around 36 percent decline; the Q90 discharge decreased from almost 21 m^3s^{-1} to 12 m^3s^{-1}, with an around 42 percent reduction.

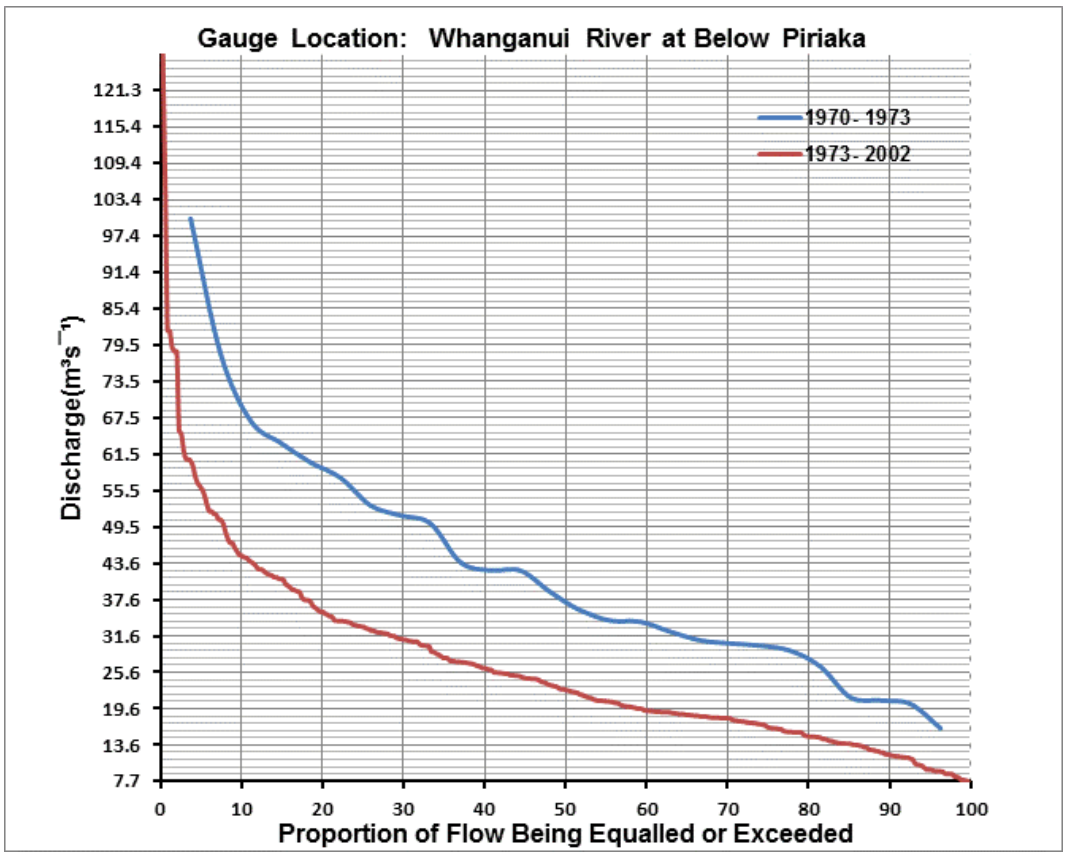

Figure 9.9: Flow duration curves for Whanganui River below Piriaka

The discharge furthest downstream in the Whanganui River at Te Maire reflects the influence of a wide range of river catchments including the Ongarue and the upper Whanganui River catchments. Comparing the flow duration curves over the period 1962 to 1973, and 1973 to 2002 (Figure 9.10), the Q10 discharge decreased from 162 m^3s^{-1} to almost 130 m^3s^{-1}, with a 19 percent decline; the Q50 discharge dropped from 89.8 m^3s^{-1} to 60.8 m^3s^{-1}, with a 32 percent decline; the Q90 discharge decreased from almost 39 m^3s^{-1} to 28.7 m^3s^{-1}, with a 26 percent reduction.

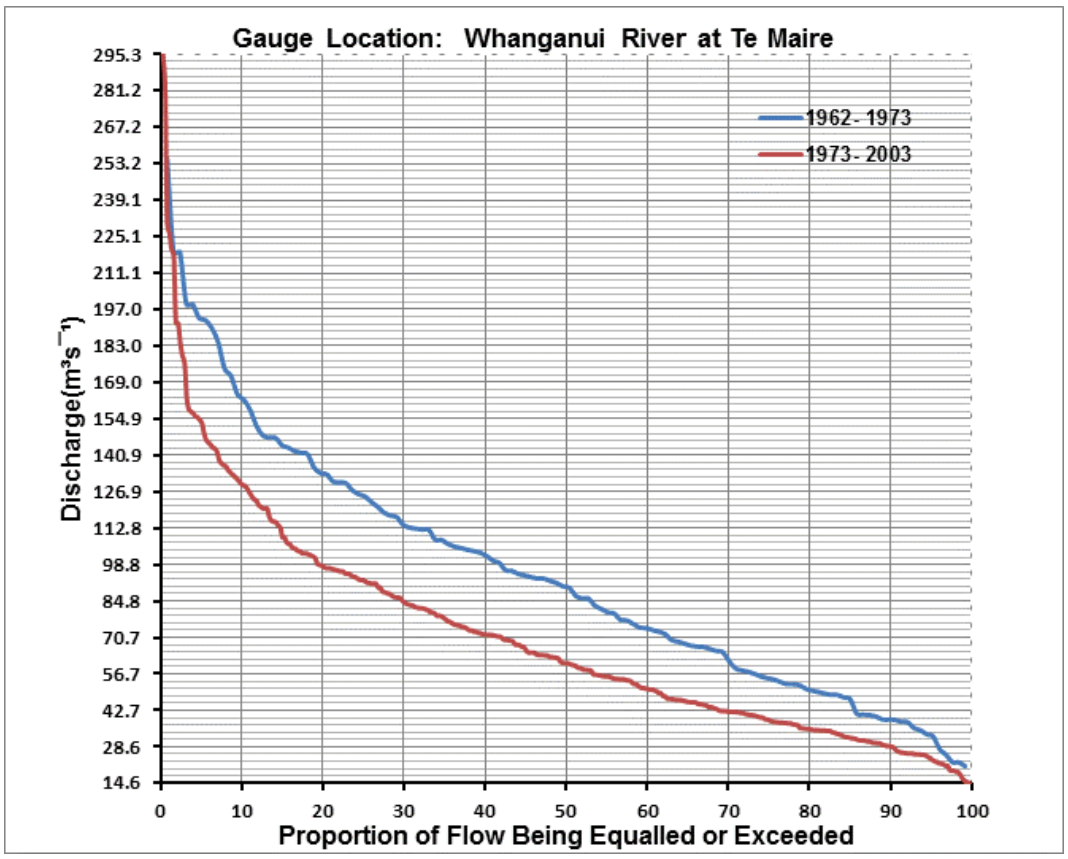

Figure 9.10: Flow duration curves for Whanganui River at Te Maire

Average monthly mean streamflow

To indicate pre- and post-diversion streamflow differences, average monthly mean streamflow graphs were constructed for the three flow sites. Two-standard error bars were plotted to illustrate the statistical significance of differences between respective monthly means in the two data sets. The error bars show 95 percent confidence intervals for the means, with separation of the respective intervals indicating significant differences ($p < 0.05$).

For the gauge site Whakapapa River at Footbridge (Figure 9.11), it is noticeable that the flow seasonality with high flow in winter months is clear for the period 1966 to 1973. However, the stream flow seasonality for the period 1973 to 2002 was offset by the water abstractions with winter months experiencing lower flow. Comparing the mean values for the two periods, the average monthly mean flow decreased significantly from 1973 for all months of the year.

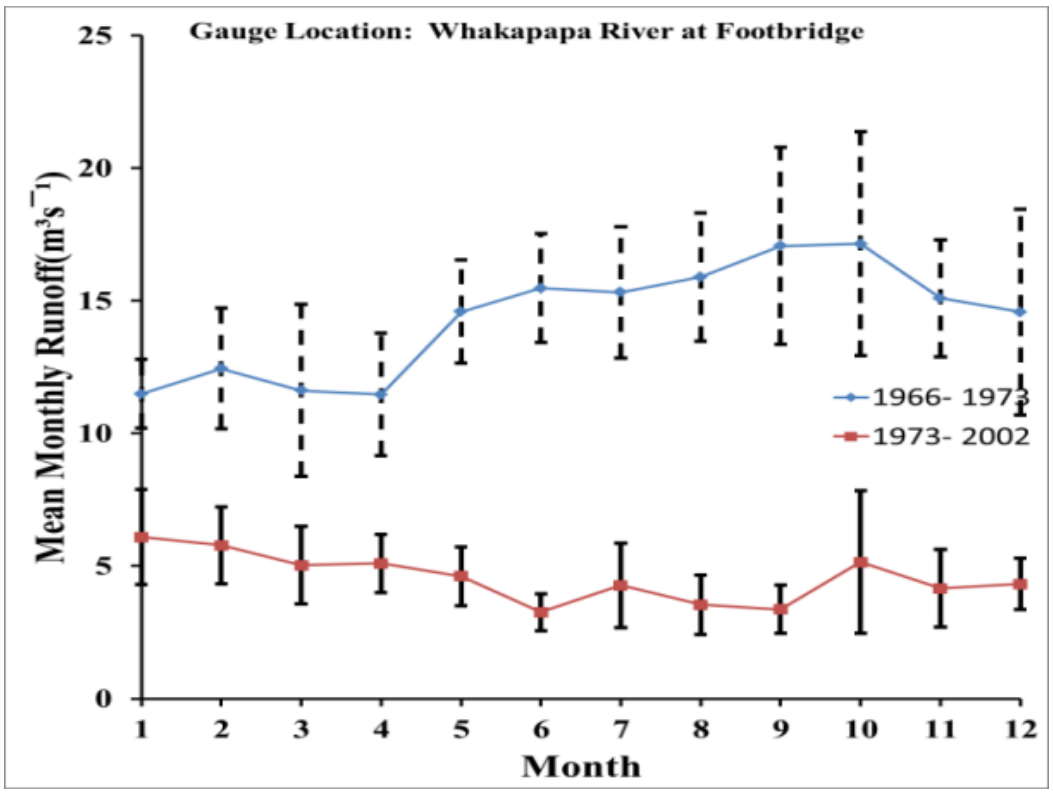

Figure 9.11: Average monthly mean streamflow at Footbridge, Whakapapa River. Vertical line ranges denote ±2 standard errors about the mean flow.

In contrast to the gauge site on Whakapapa River at Footbridge, the streamflow seasonality with high flow in winter months is shown for the period 1973-2002 for the Wanganui gauge site below Piriaka (Figure 9.12). The most obvious and significant change in the monthly mean flow over the two periods is in late winter and early spring. The 1973 diversions decreased the average monthly flow in each month, particular in August and September, but did not shift the nature of stream flow seasonality because of the distance downstream from the diversion point.

Similar to the gauge site below Piriaka, discharge seasonality at Te Maire is also evident over the period 1973 to 2002 (Figure 9.13). The most obvious and significant decline in the monthly mean flow is in September. Similarly, the 1973 diversions reduced the average monthly flow in each month, particularly significant in September, but did not shift the nature of streamflow seasonality.

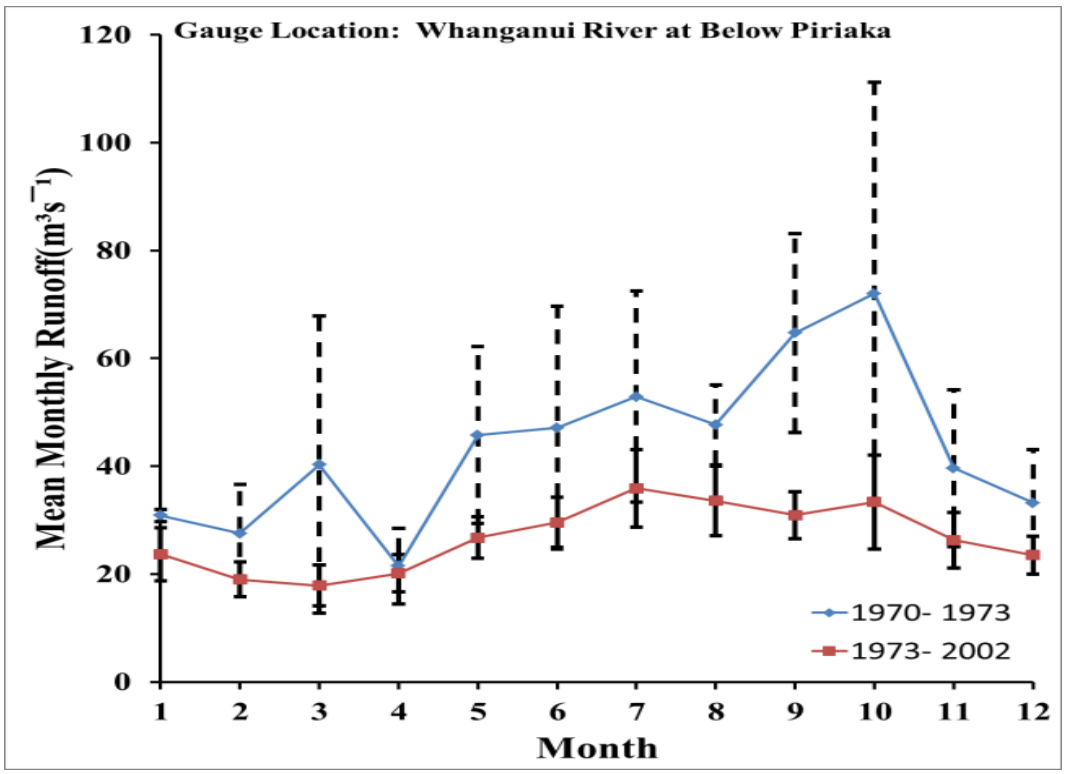

Figure 9.12: Average monthly mean streamflow below Piriaka, Whanganui River. Vertical line ranges are ±2 standard errors about the mean flow.

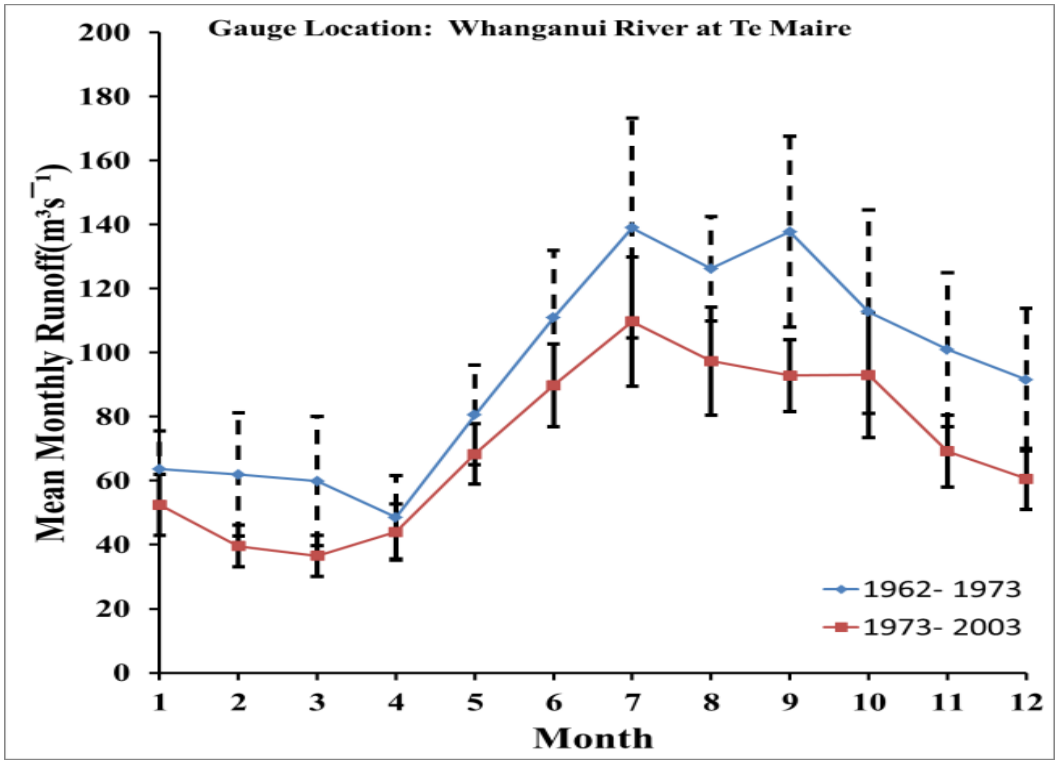

Figure 9.13: Average monthly mean streamflow at Te Maire, Whanganui River. Vertical line ranges are ±2 standard errors about the mean flow.

Conclusion

In summary, the 1973 diversions to hydropower from the western diversion produced a significant reduction in runoff from 1973 in the Whakapapa River at Footbridge, a less significant decrease in runoff of the Whanganui River below Piriaka and the further downstream gauge site at Te Maire. The reduced impact is essentially the effect of increased distance downstream from the diversion points.

9.3 Catchment Comparison within the Whanganui Region

This section presents an example of land use impact within the Whanganui catchments by way of comparison of two catchments with different land cover: the Ongarue catchment (considerable extent of farm pasture land), and the upper Whanganui catchment prior to establishment of the Tongariro Power Scheme (largely a natural flow regime with native vegetation). Before the diversions of the Tongariro Power Scheme in 1973, there was no significant forest clearance in the Whanganui catchment above Piriaka. However, in the Ongarue catchment, much forest had been already been converted to farmland many years before the period of river discharge record.

9.3.1 Catchments comparison based on monthly data

The relationship of recorded mean monthly streamflow in the Whanganui River (Piriaka and Te Maire) and the Ongarue River at Taringamutu are presented here. For convenience, the study period before 1973 is referenced as the pre-hydro period. Flow duration curves are shown in Figure 9.14 for the period before 1973.

Although rescaling by catchment area will be required for confirmation, there is some suggestion that the baseflow of the Ongarue River is less than might be expected, perhaps arising from decreased groundwater storage and larger quickflow events as a consequence of forest clearance.

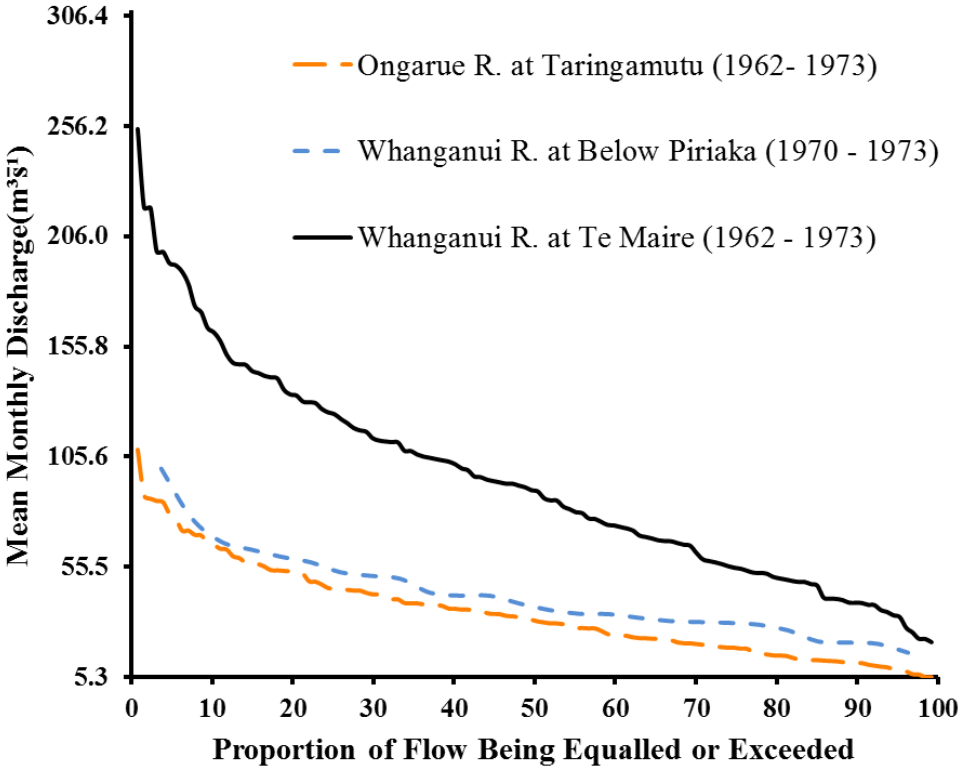

Figure 9.14: Flow duration curves for flow gauge sites: Ongarue River at Taringamutu,; Whanganui River below Piriaka; and Whanganui River at Te Maire

A plot of monthly mean discharges is shown in Figure 9.15 for the respective sites, with the error bars defining 95 percent confidence intervals for the mean.

However, the comparison based on the monthly mean discharge data could not provide robust evidence for the impact of land use conversion from forest to farmland on river discharge. A proper comparison requires a rescaling to specific discharge units. However, the rescaling of the data unit is not enough for a useful comparison because the period of river discharge record for the Wanganui River below Piriaka is short, only two years. Therefore, the following study will focus on an analysis based on a longer period record comparison.

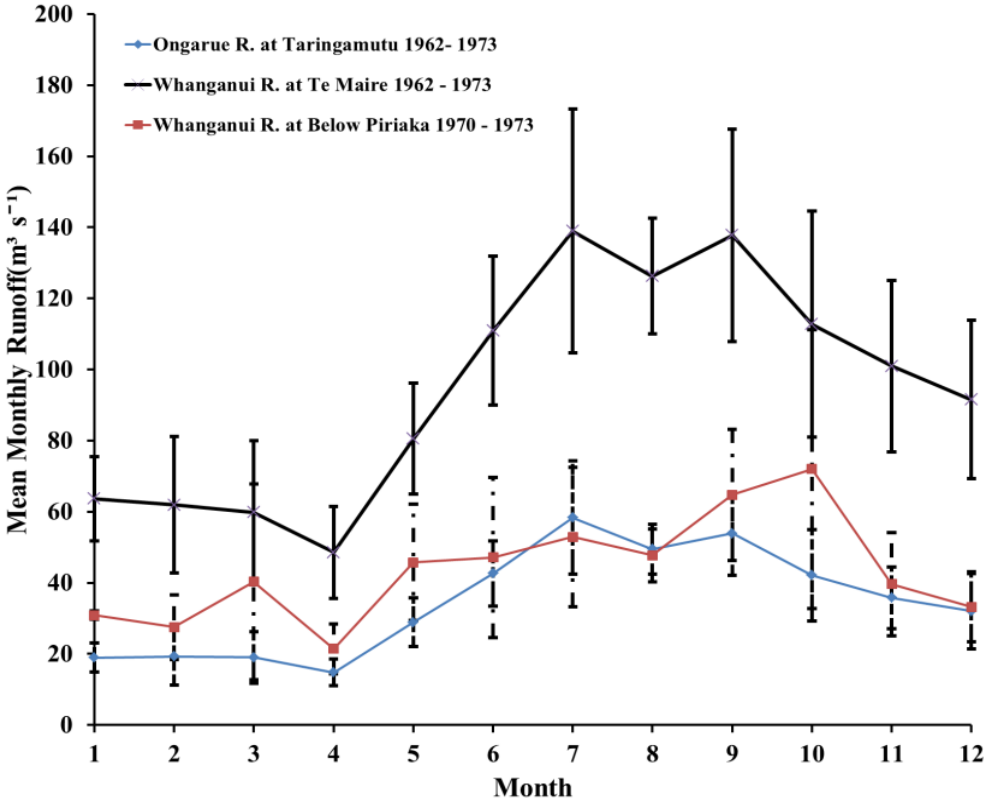

Figure 9.15: Mean monthly streamflow at Taringamutu, Ongarue River; below Piriaka, Whanganui River; and Te Maire, Whanganui River. Vertical line ranges are ±2 standard errors about the mean flow.

9.3.2 Catchments comparison based on daily data

To study the impact of different types of land use on the river hydrology in the Ongarue and the upper Wanganui catchments, the daily average flow records were considered due to the limitations in length of monthly data available for paired catchment studies. The western diversion of the Tongariro Power Scheme takes water from six rivers and streams from the Whakapapa River to the Whanganui River, into Lake Rotoaira through Lake Otamangakau.

Minimum flows which have been in effect since September 1992 for the Whakapapa and Whanganui Rivers were set to balance the water use. According to the minimum flow rules, the minimum flow for the Whakapapa River and the Whanganui River at Te Maire has been set at $3m^3s^{-1}$ and $29m^3s^{-1}$, from 1 December each year to the next 31 May. Therefore, to meet the rules, especially during summer, occasionally the operation of the Tongariro Power Scheme has to cease the diversions or return the abstracted waters to their natural state such as

the release of the western diverted water in Whanganui River at Otamangakau. The Wanganui River at Otamangakau (Figure 9.16) valve measurement site was established when the Te Maire minimum flow rules came in to effect (1992).

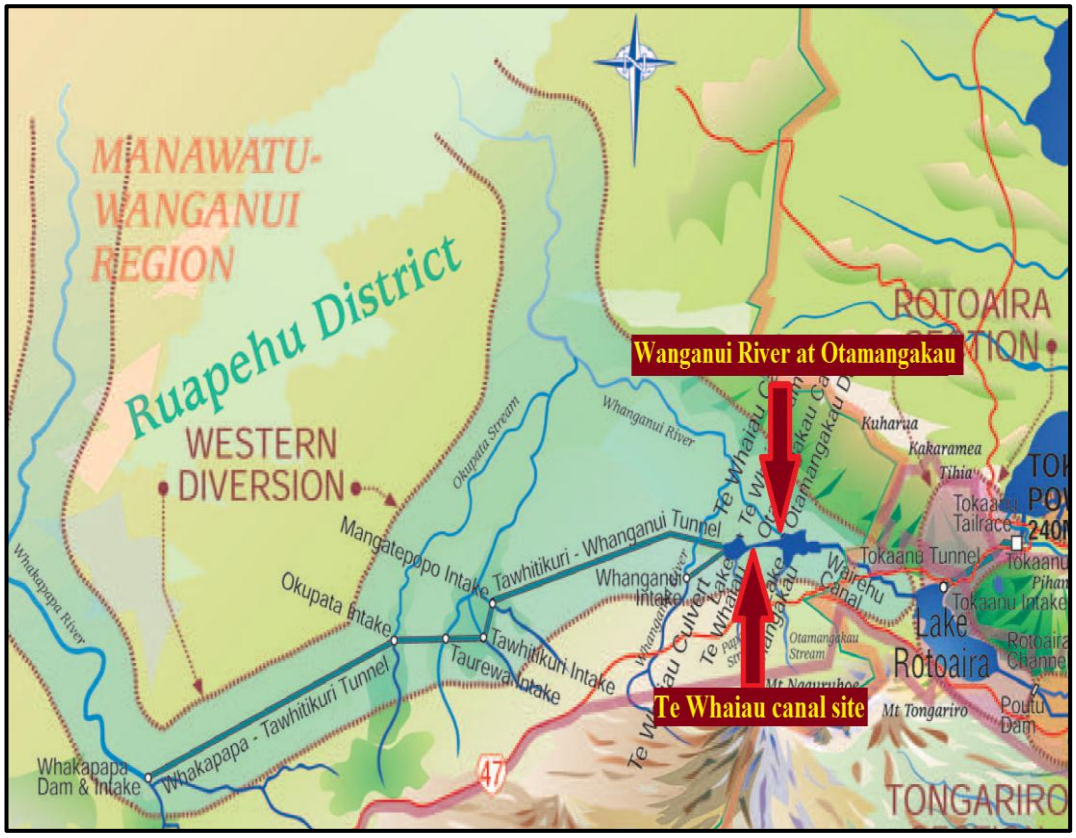

Figure 9.16: Western diversion of the Tongariro Power Scheme

9.3.2.1 Available daily data for the comparison

Three river flow gauge sites are available for the upper Wanganui River part. The Whanganui at Te Whaiau canal site (Figure 9.16) is the water in the pipe bridge. This record ran for a couple of years in the 1970s (data started from 9/11/1972 to 16/11/1973) and was then disestablished until the late 1990s (data available from 12/05/1999 to 29/04/2011). The Wanganui River at Otamangakau (Figure 9.16) valve measurement site was established when the Te Maire minimum flow rules came in to effect (1992). The period of the available data for the gauge site the Whanganui River at Otamangakau was from 24/04/1993 to 29/04/2011. The flow

record of the Whanganui River below Piriaka ran from 1970 till now (available data record: 2/12/1970 to 30/04/2011).

In the Ongarue River part, the gauge site at Taringamutu was established from the early 1960s (available data record: 5/08/1962 to 1/05/2011).

The upstream river catchment area for the upper Whanganui River below Piriaka and the Ongarue River at Taringamutu (as shown in Figure 9.17) are approximately 7.897×10^8 square metres and 10.504×10^8 square metres respectively.

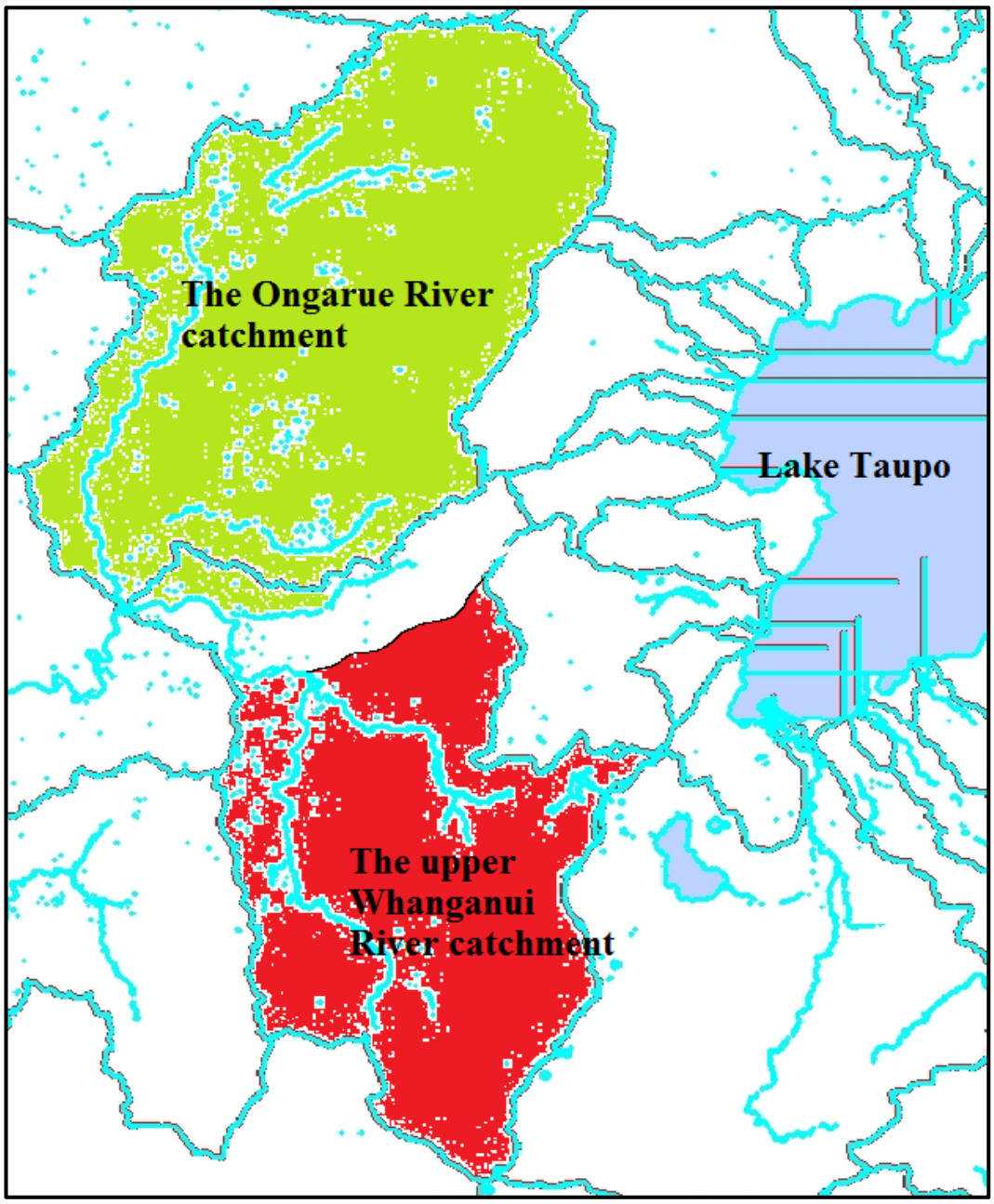

Figure 9.17: Catchment boundary for the upper Wanganui River and the Ongarue River

9.3.2.2 Catchment comparisons

Because the overlapping period of the available data gauge in the Whanganui River below Piriaka and the Ongarue data at Taringamutu which started from the 1970 is only two years before the diversion of the Tongariro Power Scheme. The catchment comparison directly using the two gauge records is limited and not credible. Therefore, to give a more catchment-specific comparison, the daily

records for a longer period were considered. Moreover, the flow gauge in the Whanganui River below Piriaka could not represent the river discharge of the upstream due to the impact of the hydropower diversion.

Therefore, considering both a longer period comparison and the comparison based on the natural flow of the two river catchments, the flow gauged in the Whanganui River below Piriaka was transformed to the non-hydropower impacted (natural) river discharge utilizing the available flow record in the Whanganui at Te Whaiau canal site and the Whanganui River at Otamangakau. Briefly, the natural river discharge in the Whanganui River below Piriaka is equal to the sum of the impacted river discharge at this gauge site and the flow diverted by the power scheme in the upstream. The diverted river flow is equal to the flow gauged in the Whanganui at Te Whaiau canal site minus the flow returned to the Whanganui River (the Whanganui River at Otamangakau). The overlapping period of the four data sets is from 12/05/1999 to 29/04/2011 which was utilised for the catchment comparison analysis.

Finally, the discharge in the Ongarue River and the natural river discharge in the upper Whanganui River were transformed to specific discharge. The hydrographs for these two rivers have been created as shown in Figures 9.18 and 9.19.

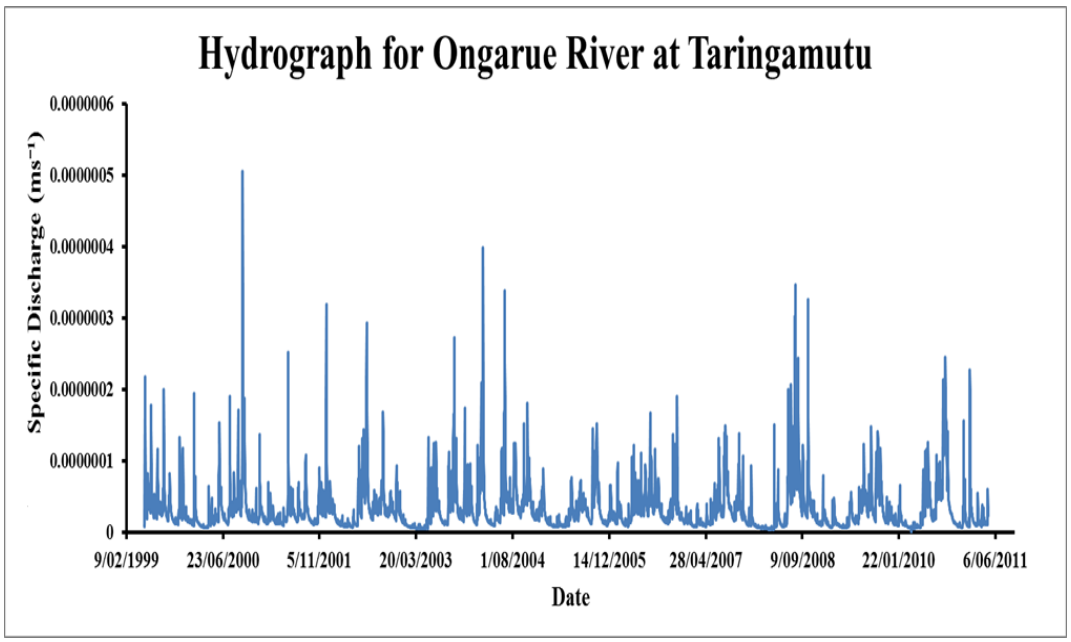

Figure 9.18: Daily hydrograph for the Ongarue River at Taringamutu

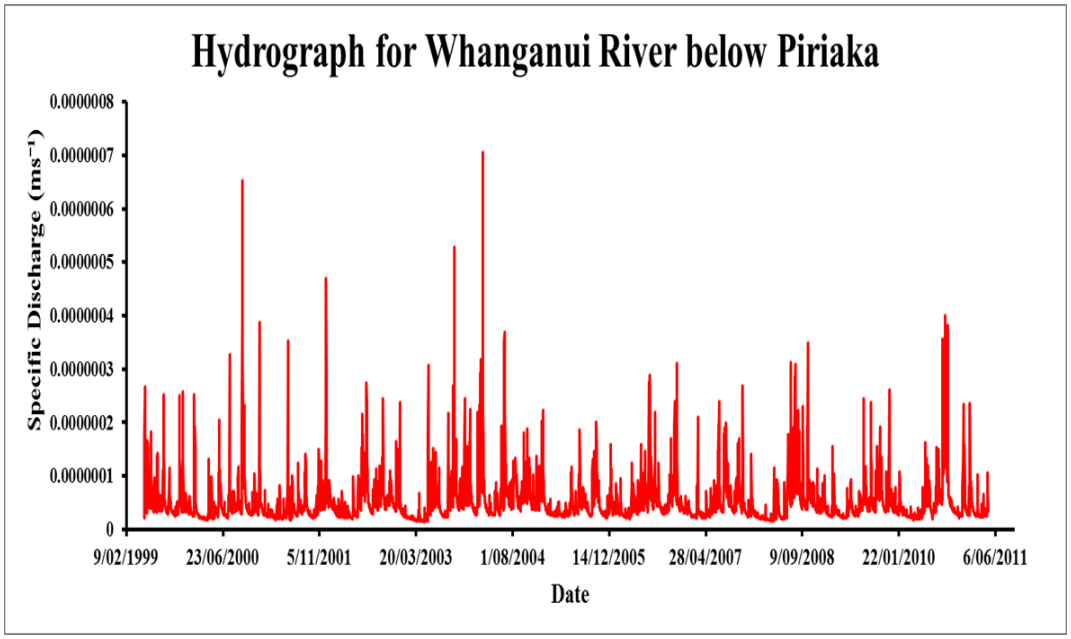

Figure 9.19: Daily hydrograph for the upper Wanganui River below Piriaka

Flow Duration Curves

The flow duration curves (Figure 9.20) have been plotted for the upper Whanganui and the Ongarue river catchments with the large areas of native forest and farmland respectively. The flow duration curves depict the high, median and

low flow in the two river catchments as well as the relationship of the two catchments with different types of land cover.

The catchment area of the upper Whanganui River below Piriaka is around 789.7 km^2 which equals to approximately 75 % of the catchment area of the Ongarue River at Taringamutu (1050.4 km^2).

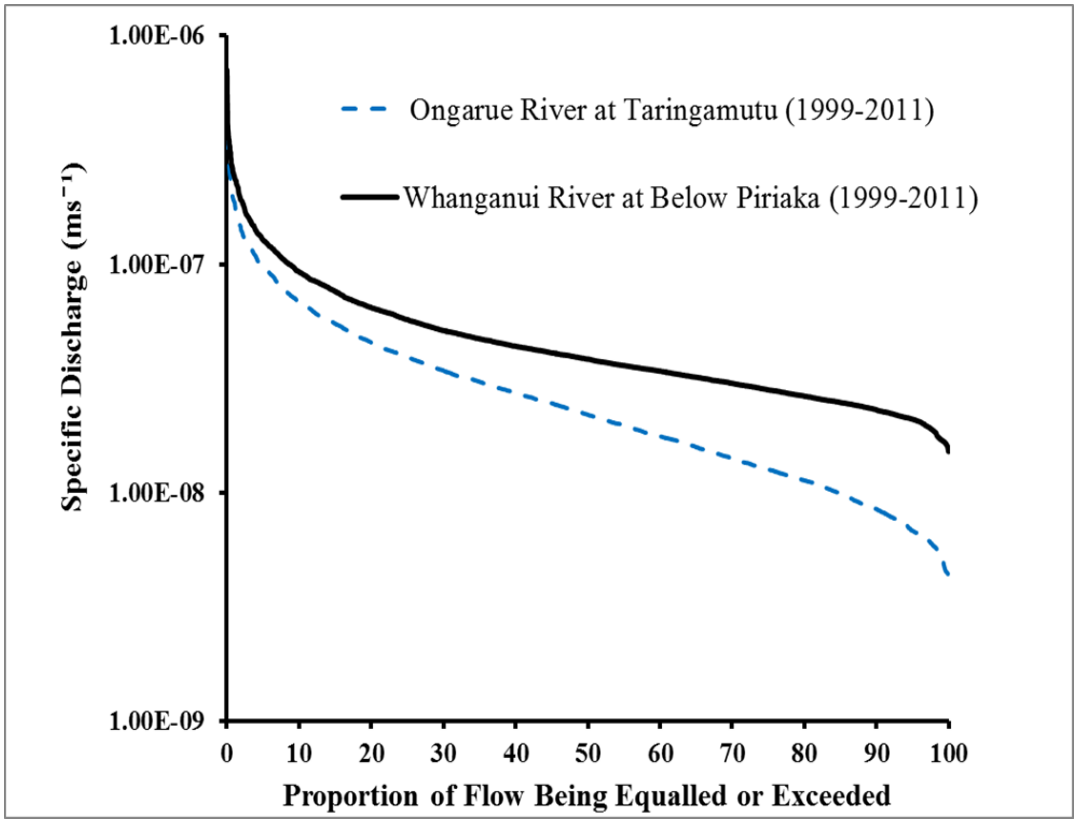

Figure 9.20: Specific discharge flow Duration Curves for the upper Wanganui River below Piriaka and the Ongarue River at Taringamutu

The flow duration curves (Figure 9.20) indicate that there is a different relationship between the two rivers with respect to the high (10%), median (50%) and low (90%) flows which equals to 9.3×10^{-8} ms^{-1}, 3.8×10^{-8} ms^{-1} and 2.3×10^{-8} ms^{-1} in the upper Whanganui River and 6.9×10^{-8} ms^{-1}, 2.2×10^{-8} ms^{-1} and 0.85×10^{-8} ms^{-1} in the Ongarue River. On average, the specific discharge for the upper Whanganui River is higher than 75 % of the flow for the Ongarue River and the difference increased as the increase of the proportion of flow was equalled or exceeded (Figure 9.21). This implies that the replacement of native forests by

farmland in the Ongarue River catchments has led to a rapid decrease in flow, especially a large decrease in low flows.

The ratio relationship is defined here as ratio of the specific discharge (equalled or exceeded different proportion of the time) of the upper Whanganui River over the specific discharge (equalled or exceeded different proportion of the time) of the Ongarue River.

The ratio relationship of the specific discharge variability of the two rivers is summarized in Figure 9.21. There is a general increase in the ratio relationship with respect to the high and median flow (1 % to 50 %), and a sharp increase in the ratio relationship with respect to the low flows (50 % to 99 %).

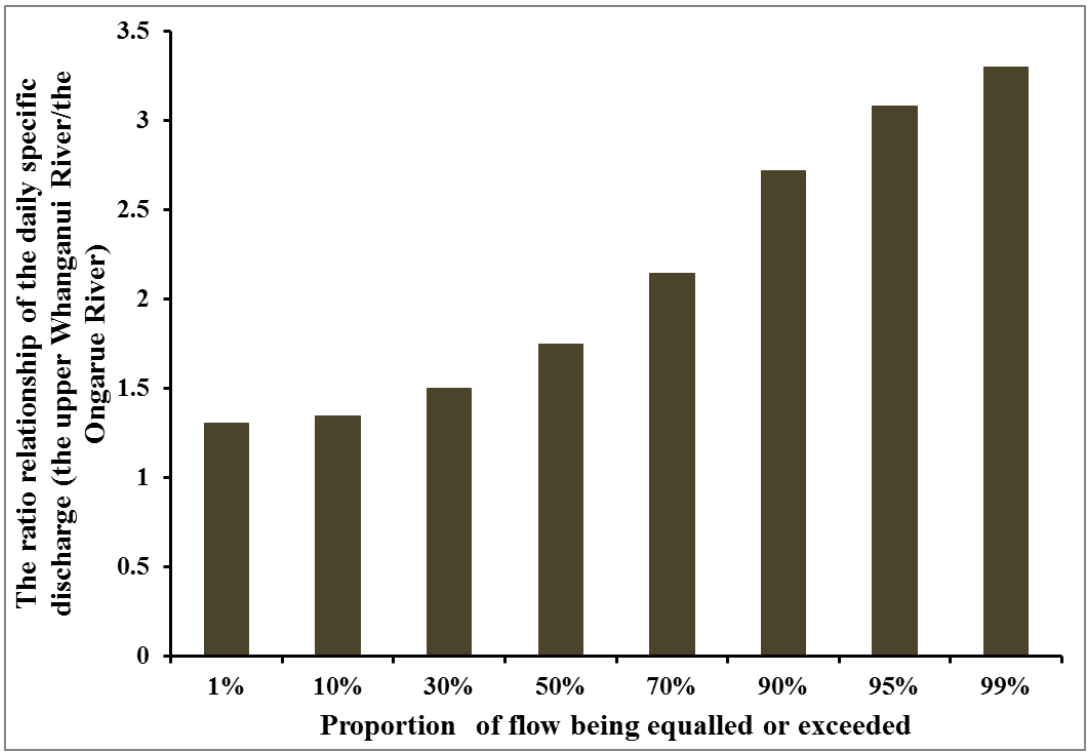

Figure 9.21: The ratio relationship of the daily specific discharge between the Ongarue River and the upper Whanganui River (upper Whanganui River /Ongarue River)

Minimum and Maximum Specific Discharge Histograms

The maximum and minimum daily specific discharge was found for each month. With respect to the maximum and minimum specific flow values, we plotted the

discharge histograms to compare the magnitude distribution of the maximum and minimum daily specific flow of each month over the two river catchments.

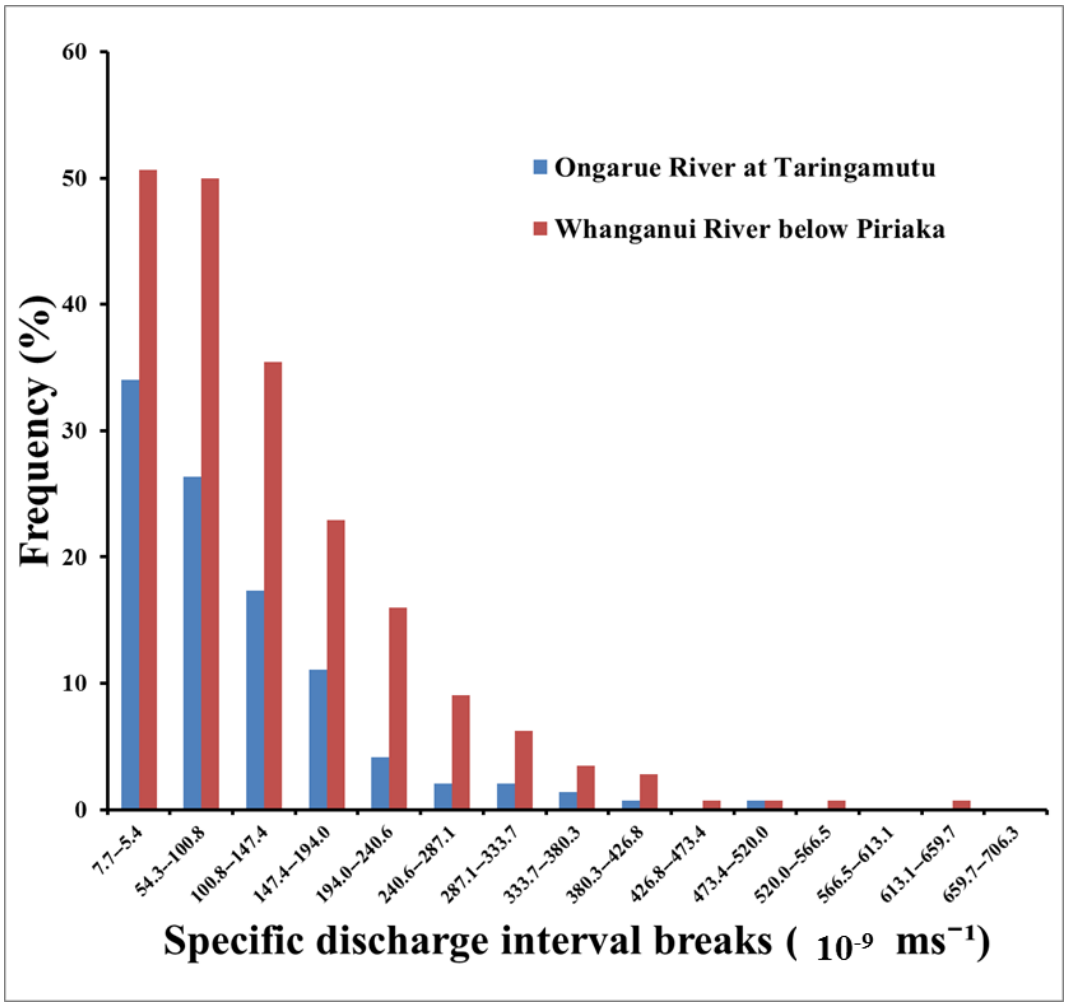

Figure 9.22: Histogram of the monthly maximum value of mean monthly flow

From the histogram of maximum specific flow of each month shown in Figure 9.22, it can be seen that 34 percentage for the Ongarue River catchment and 50 percentage for the upper Whanganui River catchment of the maximum flow lie between 7.7 $\times 10^{-9}$ ms^{-1} and 5.4 $\times 10^{-8}$ ms^{-1}. For any same discharge magnitude, the upper Whanganui catchment experienced larger proportion of the maximum daily specific flow. With the increase of the magnitude of the maximum flow, the frequency of maximum flow for the Ongarue River becomes lower than that for the upper Whanganui River, especially as there is no maximum flow for the Ongarue River within the range between 5.2×10^{-7} ms^{-1} to 7.06×10^{-7} ms^{-1}. Thus it

appears that the farmland may have reduced the frequency of maximum flow more compared with the native forest. However, this result is opposite to the normal idea of forest decreases peakflow greatly than farmland.

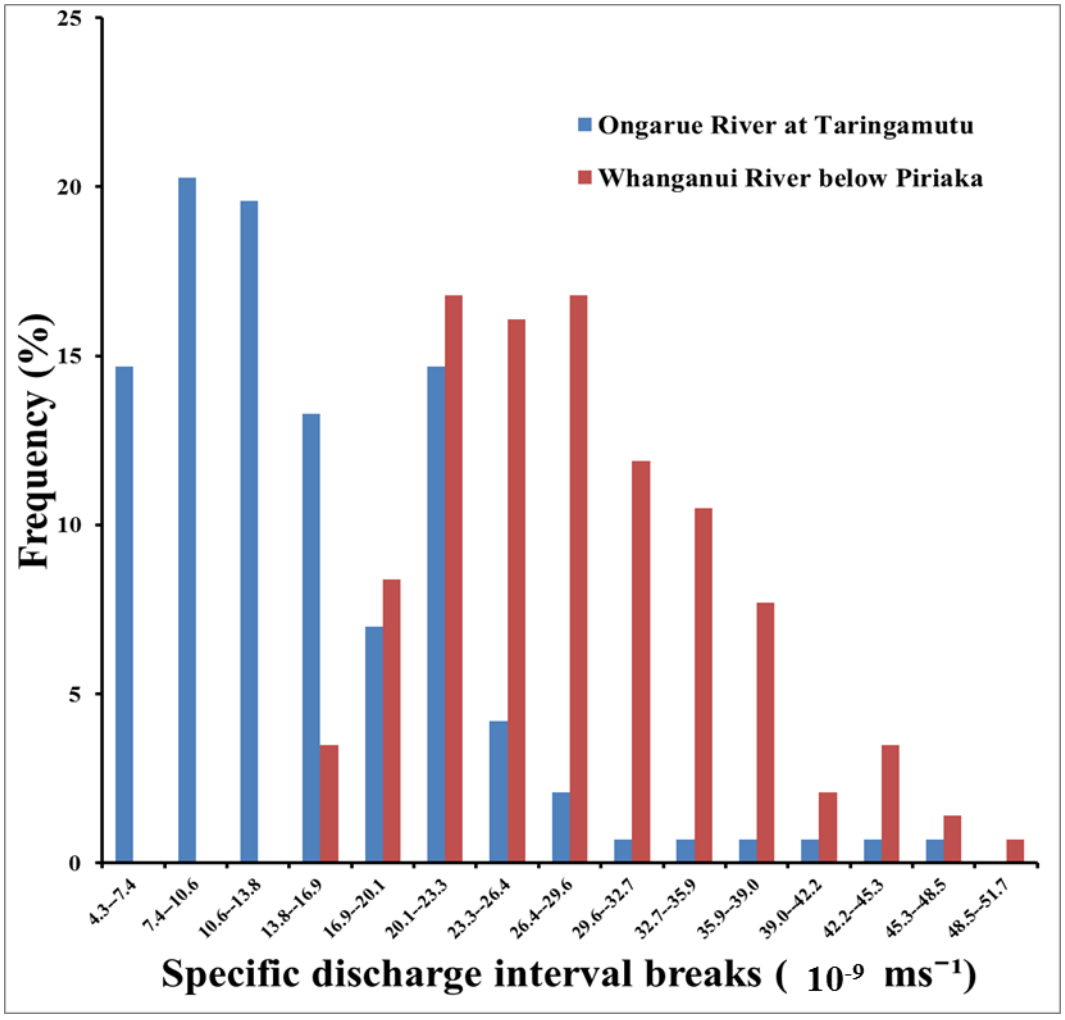

Figure 9.23: Histogram of the monthly minimum value of mean monthly flow

The frequency and magnitude of low flow events are key parameters of a river. From the histogram (Figure 9.23) which shows a typical low flow frequency analysis, the magnitude of the minimum flow with around 15 percentage frequency for the Ongarue River is larger than that for the upper Whanganui River. From the distribution of the minimum flows, it can be implied that the baseflow in the Whanganui River catchment is higher than that in the Ongarue River catchment indicating the land use of farmland reduced the baseflow more greatly than the native forest.

Briefly, the significantly converted to farmland in the Ongarue catchment decreased the magnitude and frequency of high flows and low flows more greatly than the native vegetation in the upper Whanganui catchment. As discussed previously, although these result are quite different from the normal experience of forest can reduce peakflow/lowflow through evaporation more greatly than pasture, it reflects the local characteristics of river discharge in the upper Whanganui and Ongarue catchments such as some geological characteristic of the Ongarue catchment makes more water recharge to groundwater. More studies needed to be carried out for these interesting results.

9.4 Conclusion

With respect to the Whanganui catchment, long-term flow records at seven river gauge sites in the northeast of the Whanganui catchments were examined to monitor the effects of land use impacts, as well as climatic variation. Not unexpectedly, the hydro diversion change point in 1973 is clearly evident in the flow records at Whakapapa River at Footbridge, Whanganui River below Piriaka, as well as Whanganui River Te Maire. Since 1973, the flow at all these sites gauges decreased to greater or lesser extent with the expected dramatic reduction in low flow (Q90) of around 89 % in the Whakapapa River (a main tributary of Whanganui River). However, Q90 impacts were lower in the Whanganui River at Piriaka and Te Maire (42% and 26%, respectively), reflecting the greater distances from diversion points.

For the non-hydro flow gauges - Whanganui River at Te Porere, the Tongariro River at Waipakihi and the Ongarue River at Taringamutu - no upstream land use shift was detected for the time of available records. However, there was considerable variation in the medium and high flows at these sites, evidently driven by climatic fluctuations.

With respect to the comparison of the Ongarue and the upper Whanganui catchments, the specific flow of the Whanganui catchment is more than 75 % of the specific flow of the Ongarue river catchment, especially higher for the median and low flows, which is also proved by the minimum and maximum flow

histograms. It appears that farmland in the Ongarue catchment reduce more river discharge than the native forest in the upper Whanganui catchment, especially reduce the low flows. These results are totally opposite to the hydrological common knowledge of forest impact on river discharge is greatly more than pasture's impact. Therefore, more studies are suggested to be carried out to analyse the reasons.

Chapter 10 – Conclusions

Local climate may alternate in the scale of decades with similar climatic regime characteristics in the transition period. Any climate variation could lead to a corresponding variation in precipitation and river discharge regimes. Moreover, land use change within a river catchment may result in different degrees of changes in the downstream discharge mode in terms of water quality and quantity. The impact of climatic and land use changes in the upstream may not significant, but is worthwhile to quantify as it could change the water-related parameters dramatically. The objective of this research was to investigate the impact of climate variation and land use change on river discharge for the Waikato and the upper Whanganui catchments.

Both the Whanganui and Waikato catchments contain regions with similar climatic change points which can be combined to provide a more robust framework for future water right specifications in both regions. Mainly, over the whole Waikato and part of the Whanganui regions, four rainfall shifts (1981, 1988, 1994/5 and 1998) influenced river flow changes over a wide area and appear related, to some degree, to El Nino and La Nina events. Specifically, 1981 and 1998 are associated with a shift to decreased rainfall and streamflow, while 1988 and 1994/1995 were times of positive shifts. It appears that the main driver of the shifts is the changing frequency of high rainfall events. Interestingly, the rainfall shifts can change the rainfall-runoff linear relationship by leading a change in the slope of the rainfall-runoff double mass plot in some specific flow gauges but not in all gauges. Overall, of the 44 flow gauge sites, 10 indicate the changed rainfall-runoff relationship due to the climatic factor.

The signals of upstream land management changes were determined as the changes due to land use change show in the flow time series but there is an absence of same changes in the related rainfall time series. In both the Whanganui and Waikato catchments, land use changes have been occurring, particularly with respect to the consequences of hydropower diversion, flood control systems as well as forest planting. In total, 10 of the 44 flow gauge sites in seven rivers were found to have signals of land use change, some of them are obvious and some of

them are evident. In the Purukohukohu Stream, the afforestation decreased the medium flow (Q50) by around 44 percent. The diversion of the power scheme in the Tongariro River decreased the low flow (Q90) by 21 percent. Upstream in the Mangatawhiri River, the Tawarau River, the Whangamarino River and the Waitoa River, different kinds of land use such as dams, flood control systems and afforestation occurred before the study period. The cumulative rainfall and runoff mass plots for these rivers contain similar change points representing the impact of climate variations on river discharge; however, the rainfall-runoff double mass plots indicate signals of changed rainfall-runoff relationship which is driven by upstream land use change. Moreover, there was considerable variation in the medium and high flows at these sites, probably driven by climatic fluctuations.

For the rest of the flow gauges (total 24), no signals of upstream land use change were detected. However, this does not mean no land use change happened upstream of all the 24 flow gauges. Limited by the analysis period of the time series, some flow records do not show obvious signals of land use change such as the flow series gauged in the Waikato River at Hamilton, Ngaruawahia Cableway and Rangiriri Bridge which had been already been impacted by upstream land use change.

In respect of the Whanganui catchment, long-term flow records at seven river gauge sites in the northeast of the Whanganui catchments were examined to monitor the effects of land use changes, as well as climatic variation. Not unexpectedly, the hydro diversion change point in 1973 is clearly evident in the flow records at Whakapapa River at Footbridge, Whanganui River below Piriaka, as well as Whanganui River, Te Maire. Since 1973, the flow at all these site gauges decreased to a greater or lesser extent with the expected dramatic reduction in low flow (Q90) of around 89 percent in the Whakapapa River (a main tributary of Whanganui River). However Q90 impacts were lower in the Whanganui River at Piriaka and Te Maire (42% and 26%, respectively), reflecting the greater distances from diversion points. For the non-hydro flow gauges (Whanganui River at Te Porere, the Tongariro River at Waipakihi and the Ongarue River at Taringamutu) no upstream land use shift was detected for the

time of available record. However, there was considerable variation in the medium and high flows at these sites, evidently driven by climatic fluctuations.

Thus, in the Waikato and the Whanganui catchments, climatic variation leads to the approximately concurrent changes in both rainfall and runoff time series. However, the extreme changes in the rainfall regime, especially high rainfall events, can change the rainfall-runoff linear relationship which should be considered and the reasons for this might be further investigated.

With respect to the comparison of the Ongarue and the upper Whanganui catchments, the specific flow of the Whanganui catchment is more than 75 % (75 % is the ratio of the area of the upper Whanganui catchment over the area of the Ongarue catchement) of the specific flow of the Ongarue river catchment, especially higher for the median and low flows. It appears that farmland in the Ongarue catchment reduce more river discharge than the native forest in the upper Whanganui catchment, especially reduce the low flows. These results are totally opposite to the hydrological common knowledge of forest impact on river discharge is greatly more than pasture's impact. Therefore, more studies are suggested to be carried out to analyse the reasons.

References

Aitken, A. P. (1973). Assessing systematic errors in rainfall-runoff models. *Journal of Hydrology*, 20 (2), 121-136.

Berndtsson, R. (1987). On the use of cross-correlation analysis in studies of patterns of rainfall variability, *Journal of Hydrology*, 93, 113-134.

Brown, A.E., Zhang, L., McMahon, T.A., Western, A.W. and Vertessy, R.A. (2005). A review of paired catchment studies for determining changes in water yield resulting from alterations in vegetation. *Journal of Hydrology*, 310 (1-4), 28-61.

Chandler, R.E. and E.M. Scott (2011). *Statistical Methods for Trend Detection and Analysis in the Environmental Sciences*. Chichester, England, John-Wiley.

Chang, H. and Jun, I. W. (2010). Spatial and temporal changes in runoff caused by climate change in a complex large river basin in Oregon. *Journal of Hydrology*, 388(3–4), 186–207.

Changnon, S. A and Demissie, M. (1996). Detection of changes in streamflow and floods resulting from climate fluctuations and land-use drainage changes. *Climatic Change,* 32 (4), 411–421.

Chescheir, G.M., Skaggs, R.W., and Amatya, D.M. (2009). *Quantifying the Hydrologic Impacts of Afforestation in Uruguay: A Paired Watershed Study*. XIII World Forestry Congress, Buenos Aires, Argentina.

Chiew, F.H.S. and McMahon, T.A. (1993). Detection of trend or change in annual flow of Australian rivers. *International Journal of Climatology*, 13 (1993), pp. 643–653.

Collins, R. (2002). Management strategies to mitigate faecal contamination inferred from Analysis of data from the Waikato region. Ministry of

Agriculture and Forestry Technical paper. (No: 2002/15). Wellington, New Zealand: Niwa.

Coulibaly, P. and Burn, D.H. (2004). Wavelet analysis of variability in annual Canadian stream flows. *Water Resources Research*, 40(3), p. W03105, 1-14.

Cuo, L., Lettenmaier, D. P., Alberti, M. and Richey, J. E. (2009). Effects of a century of land cover and climate change on the hydrology of the Puget Sound basin. *Hydrological Processes,* 23, 907-933.

Davie, T.J.A. and Fahey, B.D. (2005). Forestry and water yield–the New Zealand example. *NZ Journal of Forestry*, 49(4), 3-8.

De, Wit. M. and Stankiewicz, J., (2006). Changes in surface water supply across Africa with predicted climate change. *Science,* 311(5769): 1917–21

Derryberry, D.R., Schou, S.B., and Conover, W.J. (2010). Teaching Rank-Based Tests by Emphasizing Structural Similarities to Corresponding Parametric Tests. *Journal of Statistics Education* [Online], 18(1)

Feng G. L, Gong, Z. Q. and Zhi, R. (2010). Latest Advances in Climate Change Detection Techniques. *ACTA METEOROLOGICA SINICS,* 24 (1), 1-16.

Galeano, P. (2007). The use of cumulative sums for detection of change points in the rate parameter of a Poisson process. *Computational Statistics and Data Analysis*, 51, 6151-6165.

Gao, P., Mu, X.M., Wang, F. And Li, R. (2011). Changes in streamflow and sediment discharge and the response to human activities in the middle reaches of the Yellow River. *Hydrology and Earth System Sciences*, 15(1), 1-10.

Gong, D.Y. and Ho, C.H. (2002). The Siberian High and climate change over middle to high latitude Asia. *Theoretical and Applied Climatology*, 72, 1–9.

Goodrich, D. C., Lane, L. J., Shillito, R. M. and Miller, S. N. (1997). Linearity of basin response as a function of scale in a semiarid watershed. *Water Resources Research,* 33(12), 2951–2965.

Ha, K.J. and Ha, E. (2006). Climatic change and interannual fluctuation in the long term record of monthly precipitation for Seoul, *International Journal of Climatology*, 26, 607- 618.

Hannart, A. and Naveau, P. (2009). Bayesian multiple change-points and segmentation: application to homogenization of climatic series. *Water Resources Research*, 45, W10444. doi: 10.1029/2008WR007689

Jiang, S.H., Ren, L. L., Yong, B., Singh, V. P., Yang, X. L. and Yuan, F. (2011). Quantifying the effects of climate variability and human activities on runoff from the Laohahe basin in northern China using three different methods. *Hydrological Processes*, 25: 2492–2505. doi: 10.1002/hyp.8002.

Kalteh, A. M. and Hjorth, P. (2009). Imputation of missing values in a precipitation-runoff process database. *Hydrology Research*, 40(4), 420-432.

Kiely, G. (1999). Climate change in Ireland from precipitation and streamflow observations. *Advances in Water Resources*, 1999, 23, 141-151.

Kim, H.S., Croke, B.F.W., Jakeman, A.J., Chiew, F.H.S. (2009, July). *Towards model adequacy for identifying the impacts of climate and land use on catchment hydrology*. Paper presented at the 18th World IMACS Congress and MODSIM09 International Congress on Modelling and Simulation. Cairns, Australia.

Kundzewicz, Z. W. and Robson, A. J. (2004). Change detection in river flow records—review of methodology. *Hydrological Sciences, Journal,* 49(1), 7–19.

Labat, D., Ronchail, J., Callede, J., Guyot, J.L., De Oliveria, E. and Guimaraes, W. (2004). Wavelet analysis of Amazon hydrological regime variability. Geophysical Research Letter, 31, L02501.

Lee, D.T.L. and Yamamoto, A. (1994). Wavelet analysis: Theory and applications. *Hewlett-Packard Journal*, 45(4), 44–54.

Levi, B.G. (2008). Trends in the hydrology of the western US bear the imprint of manmade climate change. *Physics Today*, April, 16-18.

Li, Z., Liu, W., Zhang, X. And Zheng, F. (2009). Impacts of land use change and climate variability on hydrology in an agricultural catchment on the Loess Plateau of China. *Journal of Hydrology*, 377, 35–42.

Lin, Y. P., Hong, N. M., Wu, P. J., Wu, C. F. And Verburg, P. H. (2007). Impacts of land use change scenarios on hydrology and land use patterns in the Wu-Tu watershed in Northern Taiwan. *Landscape and Urban Planning*, 80, 111–126.

Liu, P., Guo, S., Xiong, L. and Chen, L. (2010). Flood season segmentation based on the probability change-point analysis technique. *Hydrological Processes*, 55(4), 540-554.

Lo, P. R., Barca, E. and Passarella, G. (2010). A methodology for treating missing data applied to daily rainfall data in the Candelaro River Basin (Italy). *Environ Monitor Assess*, 160, 1.

Lorrey, A., Fowler, A. M. and Salinger, J. (2007). Regional climate regime classification as a qualitative tool for interpreting multi-proxy palaeoclimate data spatial patterns: A New Zealand case study. *Palaeogeogr Palaeoclimatol Palaeoecol, 253*, 407-433.

Massei, N., Laignel, B., Rosero, E., Motelay-Massei, A., Deloffre, J., Yang, Z.-L. And Rossi, A. (2009). A wavelet approach to the short-term to pluridecennal variability of streamflow in the Mississippi river basin from

1934 to 1998. *International Journal of Climatology*, 31, 31-43. doi: 10.1002/joc.1995

McFadgen, B., (2001). Report on some implications of climate change to Department of Conservation activities. Science and Research Unit, Department of Conservation, Wellington.

Ministry for the Environment (2008). Climate Change Effects and Impacts Assessment. A Guidance Manual for Local Government in New Zealand. 2nd Edition. Prepared by Mullan B, Wratt D, Dean, S (NIWA); Allan S, Morgan, T (MWH New Zealand Ltd); Kenny G. and MfE.

Mullan, A.B., Salinger, M.J., Thompson, C.S. and Porteous, A.S. (2001). The New Zealand climate: present and future. In RA Warrick, GJ Kenny, JJ Harman (eds), *The Effects of Climate Change and Variation in New Zealand: An Assessment Using the CLIMPACTS System*. Chapter 2. IGCI, University of Waikato, 11-31.

National Aeronautics and Space Administration (NASA) (2011). Global Climate Change: The Current and Future Consequences of Global Change. Retrieved from 19/02/11. http://climate.NASA.gov/effects

National Institute of Water and Atmospheric Research (NIWA) (2001). Overview of New Zealand Climate. Retrieved from 19/02/11. http://www.niwa.co.nz/education-and-training/schools/resources/climate/overview

National Institute of Water and Atmospheric Research (NIWA) (2005). Past Climate variations over New Zealand. National Institute of Water and Atmospheric Research, Wellington. Retrieved from 19/02/11. http://www.niwa.co.nz/our-science/climate/information-and-resources/clivar/pastclimate

Pereira, V. R., Teixeira Filho, J., and Fabbro, I. M. D. (2009). *Land use conversion and the hydrological functions effects during the dry season in*

Atibainha watershed, Brazil. Paper presented at the EFITA conference 09, Wageningen.

Perreault, L., Bernier, J., Bobée, B. and Parent, E. (2000). Bayesian change-point analysis in hydrometeorological time series. Part 1. Normal model revisited. *Journal of Hydrology,* 235, 221–241.

Perreault, L., Bernier, J., Bobée, B. and Parent, E. (2000). Bayesian change-point analysis in hydrometeorological time series. Part 2. Comparison of change-point models and forecasting. *Journal of Hydrology*, 235, 242–263.

Perreault, L., Haché, M., Slivitzky, M. and Bobée, B. (1999). Detection of changes in precipitation and runoff over eastern Canada and U.S. using a Bayesian approach. *Stochastic Environmental Research and Risk Assessment*, 13, 201–216.

Perreault, L., Parent, E., Bernier, J., Bobée, B. and Slivitzky, M. (2000). Retrospective multivariate Bayesian change-point analysis: a simultaneous single change in the mean of several hydrological sequences. *Stochastic Environmental Research and Risk Assessment*, 14, 243–261.

Radziejewski, M., Bardossy, A. and Kundzewicz, Z. W. (2000). Detection of change in river flow using phase randomization. *Hydrol. Sci. J.* 45(4), 547–558.

Renwick, J.A., Mladenov, P., Purdie, J., McKerchar, A. and Jamieson, D. (2010). The effects of climate variability and change upon renewable electricity in New Zealand**.** Climate Change Adaptation in New Zealand: Future scenarios and some sectoral perspectives, 136

Risbey, J.S. and Entekhabi, D. (1996). Observed Sacramento basin streamflow response to precipitation and temperature changes and its relevance to climate impact studies. *Journal of Hydrology*, 184, 209–223.

Ryan, Sandra, E., Porth, Laurie, S. (2007). A tutorial on the piecewise regression

approach applied to bedload transport data. Gen. Tech. Rep. RMRS-GTR-189. Fort Collins, CO: U.S. *Department of Agriculture, Forest Service, Rocky Mountain Research Station*. P.41

Searcy, J.K. and Hardison, C.H. (1960). Double-mass curves. U.S. Geological Survey. *Water-Supply Paper* ,1541-B.

Sen, Z., Habib, Z. (2001). Monthly spatial correlations rainfall and interpretations for Turkey. *Hydrological Sciences Journal.* 46 (4), 525–535.

Sivapalan, M., Jothityangkoon, C. and Menabde, M. (2002). Linearity and nonlinearity of basin response as a function of scale: discussion of alternative definitions. *Water Resources Research*, 38 (2), 1012.

Storey, L.P. (2009). Effect of climate and land use change on invasive species: a case study of tradescantia fluminensis (vell.) in New Zealand. Unpublished doctoral dissertation, University of Waikato, Hamilton, New Zealand.

Subramanya, K. (2008). *Engineering Hydrology* (3rd ed). New Delhi, India: Tata McGraw Hill.

Tabari, H. and Talaee, P.H. (2011). Temporal variability of precipitation over Iran: 1966-2005. *Journal of Hydrology*, 396(3-4), 313-320.

Tripathi, S., and Govindaraju, R. S. (2009). Change detection in rainfall and temperature patterns over India, Paris, France: Sensor-KDD Challenge organized as part of the 3rd International Workshop on Knowledge Discovery from Sensor Data (Sensor-KDD 2009).

Ummenhofer, C. C., England, M. H., McIntosh, P. C., Meyers, G. A., Pook, M. J., Risbey, J. S., Gupta, A. S. and Taschetto, A.S. (2009). What causes Southeast Australia's worst droughts? *Geophysical Research Letters*, 36, L04706.

Vogel, R.M. and Fennessey, N.M. (1995). Flow Duration Curves II: A Review of Applications in Water Resources Planning. *Water Resources Bulletin*, 31(6), 1029-1039.

Wang, L.H. and Cai, H.Y. (2010). Wavelet Change-point Estimation for Long Memory Nonparametric Random Design Models. *Journal of Time Series Analysis*, 31, 86-97.

Westmacott, J.R. and Burn, D.H. (1997). Climate change effects on the hydrologic regime within the Churchill-Nelson river basin. *Journal of Hydrology*, 202, 263-279.

Xu, H., Taylor, R.G. and Xu, Y. (2010). Quantifying uncertainty in the impacts of climate change on river discharge in sub-catchments of the River Yangtze and Yellow Basins, China. *Hydrology and Earth System Science Discussi*ons, 7, 6823-6850.